Synthesis and reactions of Janus-type bis(NHCs), tuned by phosphorus bridges

Dissertation

zur

Erlangung des Doktorgrades (Dr. rer. nat.)

der

Mathematisch-Naturwissenschaftlichen Fakultät

der

Rheinischen Friedrich-Wilhelms-Universität Bonn

vorgelegt von

Nabila Rauf Naz

aus

Chawinda, Pakistan

Bonn, 2020

Angefertigt mit Genehmigung der Mathematisch-Naturwissenschaftlichen Fakultät der Rheinischen Friedrich-Wilhelms-Universität Bonn

1. Gutachter: Prof. Dr. Rainer Streubel
2. Gutachter: Prof. Dr. Robert Glaum

Tag der Promotion: 25.01.2021
Erscheinungsjahr: 2021

To see the world in a grain of sand,

and to see heaven in a wild flower,

hold infinity in the palm of your hands,

and eternity in an hour.

William Blake

Some results of this PhD thesis were previously published.

(1) N. R. Naz, G. Schnakenburg, A. Mikeházi, Z. Kelemen, L. Nyulászi, R. T. Boeré, R. Streubel, *Chem. Commun.*, **2020**, *56*, 2646–2649, DOI: 10.1039/c9cc08468a.
(2) N. R. Naz, G. Schnakenburg, Z. Kelemen, D. Gál, L. Nyulászi, R. T. Boeré, R. Streubel, *Dalton Trans.*, 2021, **50**, 689-695. DOI: 10.1039/D0DT03915B.

Conference contributions

• Nabila Rauf Naz and Rainer Streubel. Syntheses and reactions of tricyclic P-functional bis-NHCs. Oral talk, European workshop on phosphorus chemistry (EWPC 17) 2020 Rennes (France)

• Nabila Rauf Naz and Rainer Streubel. Synthesis and reactivity of novel tricyclic bis-NHCs having tunable P-linkers. Oral talk, Conjugated oligomers and polymers Functional π-Systems and Beyond (KOPO) 2019.

• Nabila Rauf Naz, Rainer Streubel. Synthesis and reactivity of a tricyclic1,4-diphosphinine diselone and bis(NHCs) thereof. Oral talk, MHC-10Deutsch-Österreichischer Mitarbeiterwokshop (MHC) 2019.

• Nabila Rauf Naz and Rainer Streubel. Tricyclic bis (NHCs) with variable p-linkers. Poster presentation, Stable carbene symposium (SCS) 2018.

• Nabila Rauf Naz, Rainer Strubel. P-TEMPO phosphane tungsten and manganese complexes. Chemistry at Spin Centers: Women in Science Conference (SFB 813) 2016

Die vorliegende Arbeit wurde im Zeitraum von Oktober 2016 bis März 2020 im Arbeitskreis von Prof. Dr. R. Streubel am Institut für Anorganische Chemie der Rheinischen Friedrich Wilhelms-Universität in Bonn angefertigt.

Acknowledgements

I believe, a few words will not be enough to express my gratitude and convey mydeep appreciation, thanks and acknowledgement to my supervisor Prof. Dr. RainerStreubel. I thank him with great pleasurefor giving me the opportunity to be co-workerin his research group, for all the support, valuable guidance and constant encouragement during the last three years of my work.

I am also thankful to Prof. Dr. Robert Glaum, Prof. Dr. Menche and Prof. Dr. Diana Imhof for refereeing my thesis.

I would like to thank Prof. Dr**.** László Nyulásziand Dr. Zsolt Kelemen, Department of Inorganic and Analytical Chemistry, Budapest university of Technology andEconomy, Budapest, Hungary for the fruitful collaboration helpful theoretical calculations.

I also express my gratitude to Prof. Dr. René T. Boeré, Department of Chemistry and Biochemistry the University of Lethbridge Lethbridge, Alberta, Canada for his help to conduct and understand the electrochemistry of our compounds and for sharing his valuable knowledge.

I am very much grateful to Dr. Gregor Schnakenburg, Ms. Charlotte Rödde for the single crystal X-ray diffraction measurements.

I specially convey my gratitude to Prof. Dr. Amir Waseem, Prof. Dr Zai ur Rehman, Institute of Inorg/Ana Chemistry, Qauid e Azam University, Islamabad Pakistan for their valuable guidance during my MPhil research.

I would like to thank our central analytical department, as without their support it would not be possible to carry out the the research work properly. I am grateful to Dr.Claud Schmidt, Ms. Karen Procknicki and Ms. Hannelore Spitz (NMR spectroscopy), Dr. Marianne Engeser and her colleagues (Mass spectrometry), Dr. Sabine Rings and Ms. Anna Martens (Elemental Analyses) and all members in Chemical Store, Glass Blowing section, Mechanical and Electrical workshops.

I would like to convey my special thanks to the people around me who made my entire stay in Bonn, a pleasant experience for me. First of all, I am extremely thankful to Dr. Tobias Heurich and Dr. Abhishek Koner for the valuable introductory guidance in the early days of my PhD and beyond. I am also extremely thankful to Dr. Andreas Kyri and Dr. Jose Manuel Villalba Francofor all those valuable discussions and a sourse of inspiration

ambitious researchers.Besides, I also thank the rest of my lab colleagues (especially Shahryar Kermanshahian, Mridhul Ram, Robert Kunzmann, Niklas Volk, Philip Junker) for the friendly atmosphere.

I wish to thank friends and family, especially my MOTHER for her love and encouragement, without whom I would never have enjoyed so many opportunities in my life. Last but not least my best friend, my beloved sister Shaista andleeb, whose utmost support, love and incouragement kept my spirits always high.

Contents

Abbreviations

Xa, a′= a mixture of two isomers (*cis*, *trans*); where **X**= compound number and **a,a′**are two isomers

Å	Ångström (1·10-10 m)	eV	electron volt
°	angle in degree	FWHM	full width at half maximum
Ar	aromatic substituent	G	Gram
ATR	Attenual Total Reflexion	H	height or hour
Au	Atomic unit	HMDS	Hexamethyldisilazide
Br	broad signal	KHMDS	Potassium hexamethyldisilazide
calc.	Calculated	HMQC	Heteronuclear Multiple Quantum Correlation
°C	degree Celsius	Hz	Hertz
C_6D_6	deuerated benzene	iPr	*iso*-propyl
$CDCl_3$	deuterated chloroform	IR	Infrared
Et_2O	diethyl ether	M	metal or molar weight in g/mol
EA	elemental analysis	LDA	Lithium diisopropylamide
EI	electron impact ionization	Me	methyl (CH_3)
eq.	Equivalent	mg	Milligram
K	Kelvin	cm	centimeter
MLn	bearing n ligands	min	minutes
Mmol	Millimole	mL	Millilitre
MS	mass spectrometry	THF	Tetrahydrofuran
m/z	mass to charge ratio	TfOH	trifluoromethanesulfonic acid
N	Normal	THF-d8	deuterated tetrahydrofuran
^{n}Bu	n-butyl	TMEDA	Tetramethylethylenediamine
Nm	Nanometre	toluene-d8	deuterated toluene
NMR	nuclear magnetic resonance	$\tilde{\nu}$	wave number
%	Percent	Vs	very strong
PE	petroleum ether (40/60)	VT-NMR	Variable Temperature NMR
Ph	phenyl (C_6H_5)	W	Weak

ppm	parts per million	X	halogen or leaving group
Q	Quartet	quin	Quintet
L	Ligand	R, R´, R´´	organic substituent
M	Medium	r.t.	room temperature
M	Multiplett	S	Singlet
ESI	electrospray ionization	Et	Ethyl
D	Days	Ø	Diameter
Δ	chemical shift in ppm	Δδ	chemical shift difference

1. Introduction

Carbenes are a class of compounds that possess a neutral divalent and dicoordinate carbon atom with six valence shell electrons. Carbenes have been proposed for over 170 years,[1] though not in isolated form. There are twoelectronic states of carbene species: singlet carbenes and triplet carbenes (Figure 1.1). Singlet carbenes usually favour low oxidation state metals, with strong π-acceptor ligands (e.g. CO, CN^{-}, NO ligands), while triplet carbenes are typically found in metal complexes with metals in high oxidation state and with π-donor ligands (e.g. Cp, OR, halide ligands). Carbene complexes may be used as both electrophilic and nucleophilic reagents in carbon–carbon bond-forming reactions. The intrinsic electrophilic nature of the carbene carbon atom allows for the addition of C-nucleophiles and is also evident in Michael reactions in which an α,β-unsaturated carbene complex acts as an organometallic acceptor. [1b-d] N-Heterocyclic carbenes (NHCs) are those withat least one α-N-center and a carbene atom embedded in a ring, having effective electronic donation from the lone pair of the π-donating substituents into the empty p-orbital of the carbene atom.[2] Therefore,they have been sometimes regarded as subclass of singlet carbenes. NHC metal interactions can be differentiated from those of singlet and triplet carbene ligands due to their single σ-bond [2] to the metal compared to the double bonds usually present in singlet and triplet carbene metal complexes. [3]

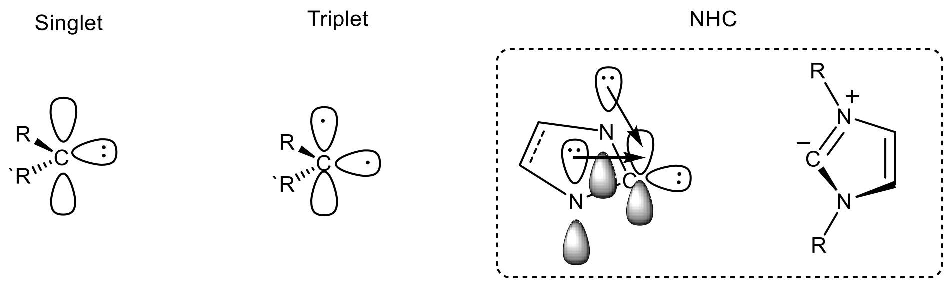

Figure 1.1. Simplified frontier orbital demonstration of singlet, triplet and N-heterocyclic carbenes.

1.1 N-Heterocyclic carbenes

N-heterocyclic carbenes (NHCs) were proposed as transient species more than a half century ago[4] but the first N-heterocyclic carbene complex was proposed by Chugaev *et al*. in 1915, though the correct structure was not determined until the 1970s.[5] Well-defined NHC metal complexes were synthesized by Wanzlick in 1962,[6] by introducing strong electrondonating groups next to the carbene in order to increase the stability and form a nucleophilic carbene. Öfele later discovered the first mono-dentate transition metal NHC complex.[7] Wanzlick independently Preparerамercury bis(carbene) compound.[8] However, in each case they were unable to isolate the free carbene.The first free organic carbene was isolated by Bertrand,[9] but the reactivity shed some doubt on its nature for several years. NHCs and their complexes remained a curiosity until Arduengo *et al.*[10a] isolated the first stable imidazol-2-ylidene, namely 1,3-bis(adamantyl)imidazol-2-ylidene **I** (Scheme 1) in 1991. This discovery initiated wide-ranging research into NHCs and their metal complexes.[10b-j]

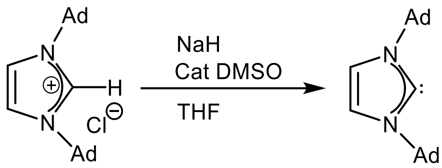

I

Scheme 1.1. Synthesis of the first isolated free NHC **I**.[10a]

Today, there are numerous ways to generate free NHCs from different starting materials (Scheme 1.2). For example, it is possible to desulfurize thioureas with potassium in hot THF; the by-product, K_2S, is insoluble in THF and easy to remove.[11,12] Vacuum pyrolysis can also be used and removes volatile by-products such as C_6F_5H.[13] NHC–CO_2 adducts can simply be heated to form the free NHC in situ, and can be used in systems when the activation of the catalyst needs to be delayed.[14] Another technique treats imidazolium chloride salts with $Hg(TMS)_2$ to give the free carbene, TMS-Cl and elemental mercury.[15]

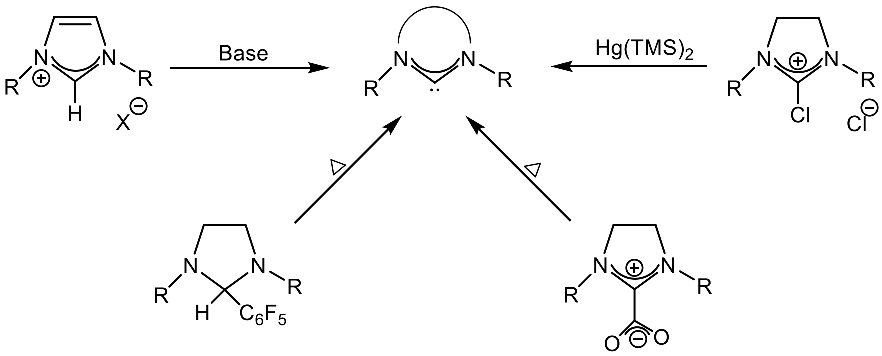

Scheme 1.2. Different routes to generate symmetrical free NHC.

1.2. N-heterocyclic selones

Selone is the structural analogue of a ketone where selenium replaces oxygen. Synthesis of the first *N*-heterocyclic selone was reported by Warner, in 1963 [16] wherein *o*-phenylene-diamine **II** was refluxed in CCl_4 solvent with carbon diselenide to form 2-isoselenocyanatoaniline

III. The intermolecular reaction between isoselenocyanate and amino group produced selone **IV** in 85% yield (Scheme 1.3).

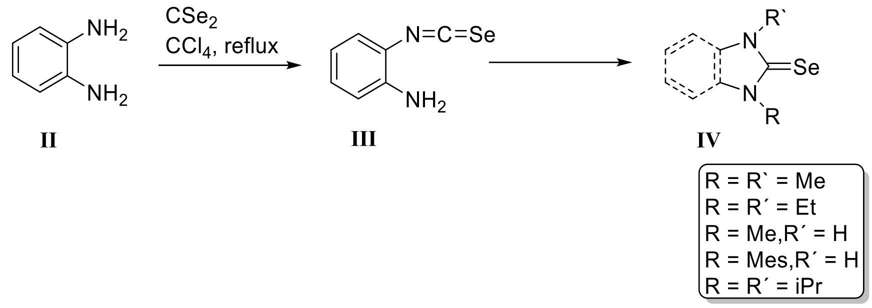

Scheme 1.3. First report by Warner on the synthesis of N-heterocyclic selone **IV**.[16]

There are numerous reports where selones have been synthesized by the reaction of *N*,*N′*-alkyl-imidazolidine based salts with elemental selenium in the presence of a base.[17] The precursor imidazolium salts were prepared by two different routes; a) nucleophilic substitution at the nitrogen atoms of the imidazole,[18] followed by the quaternization at the *N′*-position,[19] or b) multi-component reactions for the generation of the *N*,*N′*-substituted heterocycles.[20] On the contrary, Nolan and coworkers synthesized stable selone compounds by the reaction of base with imidazolium salt, followed by their reaction with elemental selenium.[21]

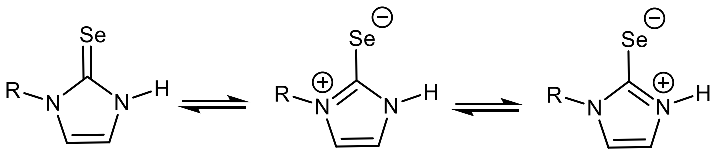

Figure 1.2. Resonance structures of N-heterocyclic selones.

Selones are considered to be a resonance hybrid of three majorcannonical structures as exemplified in Figure 1.2.[22] According to calculations by Parkin and coworkers, the combined zwitterionic resonance structures with C–Se single bond **VI**, **VII** provided greater contribution than that of the C=Se resonance structure**V**. It is further supported by the C-Se bond distance of 1.884,[23] which is significantly longer than that found for an isolated double bond, such as in CSe_2 (1.698 Å).

To select a carbene for a specific application, comprehensive assessment of its properties is of crucial importance. Specifically, a number of methods have been utilized over the past years to tune the electronic properties of ligands.[24,25] The ^{77}Se NMR chemical shifts are very sensitive to the relative position of a given adduct within the two limiting structures: π-acidic NHCs feature a higher degree of C-Se double-bond character leading to NMR signals shifted to lower field in comparison with less π-acidic NHCs.[26] Ganter and co-workers incorporated ^{77}Se NMR spectroscopy as an efficient method for the assessment of the π-acceptor strengths of selones.[27] For instance, in selone **IV**, the aromatic ring is fused with imidazole which causes a decrease in aromaticity making the lone pair of nitrogen more accessible for back donation to carbene carbon, which in turn reduces the back-donation from selenium in the C-Se bond. Hence, Se in compound **IV** (67 ppm) is more shielded than compound **VIII** (87 ppm). In compound **IX**, owing to the wider NCN angle, the vacant p-orbital of the carbene carbon atom is lowered in energy which consequently nurtures π-back-bonding from the selenium atom.[28] Consequently, the six-membered compound **IX** is shifted by another 90 ppm to lower field. The increasing π-acidity of the carbenes contained in the adducts **X** (472 ppm) and **XI** (593 ppm) is due to the presence of an electron-withdrawing carbonyl group in the former and the acyclic nature of the carbene in the latter, leading to an enhanced conformational flexibility and reduced interaction of the nitrogen lone pair with the vacant p orbital on the carbene C atom.[29,30] The diamidocarbene **XII** is known as a very electron poor carbene with a strong π-acceptor character and it consequently appears at the lowest field (856 ppm).[31,32]

Table 1.1. Correlation of the ^{77}Se chemical shifts (ppm) of selones with π-acceptance character.

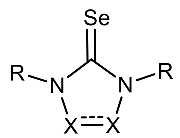

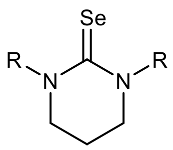

IX

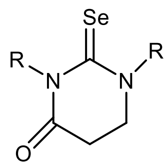

X

	X	R	^{77}Se NMR
VI	-	^{i}Pr	67 ppm
VIII	X = CH	R = Dipp	87 ppm
IX	-	R = Mes	184 ppm
X	-	R = Mes	472 ppm
XI	X = ^{i}Pr	R = ^{i}Pr	593 ppm
XII	X = CO	R = Mes	856 ppm
XIII	X = CH	R = ^{t}Bu	183 ppm
XIV	X = CH	R = adamantyl	197 ppm

Nolan and co-workers further incorporated computational studies to explore the link between the shielding of the selenium center and the electronic properties of the NHCs.[33] It is apparent that the Se resonance, δ_{Se} is synchronized to the energy gap between a filled lone pair orbital on Se and the empty π* orbital corresponding to the Se-NHC bond.Unsaturated imidazol-2-ylidenes with secondary alkyl *N*-substituents exhibit the lowest δ_{Se} (<0 ppm), while unsaturated *N*,*N′*-diarylimidazol-2-ylidenes and *N*,*N′*-dialkyl-4,5-dihydroimidazol-2-ylidene show Se resonance in the range 30–100 ppm. Saturated *N*,*N′*-diaryl species exhibit higher δ_{Se} (110–190 ppm). Interestingly, **XIII** and **XIV**, with quaternary *N*-alkyl substituents, exhibit very high chemical shifts (δ_{Se} = 183 and 197 ppm, respectively). While saturated NHCs are known to be more π-accepting than unsaturated NHCs, this difference amongst *N*,*N′*-dialkylimidazol-2-ylidenes was very captivating. Remarkably, structurally similar unsaturated bis(aryl) NHCs led to quite different values of δ_{Se} (23 and 34).[34]

According to Bertrand, ^{31}P NMR chemical shifts of carbene–phenylphosphinidene adducts allow the determination of the relative π-acceptor properties of carbenes. Such compounds can be represented by two canonical structures: a typical phosphaalkene featuring a formal P=C double bond **A**, whereas **B** corresponds to a carbene–phosphinidene adduct featuring a P-C dative bond with two lone pairs of electrons at phosphorus.[33b] The main feature of these compounds is the very high-field ^{31}P{^{1}H}NMR chemical shift of the phosphorus center (δ = −53.5 to −10.4 ppm) in comparison with the chemical shift usually displayed by typical, non-inversely polarized phosphaalkenes (δ=230–420 ppm) [33c,d] An increase of the π-accepting property of the carbene favors the back-donation of the lone pair of the phosphorus atom to the vacant p orbital of the carbene center, therefore increasing the contribution of resonance form **A**. Consequently, the ^{31}P{^{1}H}NMR chemical shift of carbene–phosphinidene adducts provide a straightforward method to evaluate the π-acceptor property of the carbene: the more π-accepting the carbene is, the further downfield the chemical shift of the phosphorus nucleus will be.[29]

1.3. Backbone functionalized mono(NHCs)

More recently, targets in NHC chemistry became more sophisticated, *i.e.*, to build advanced ligands possessing structural diversities and catalytic functionalities,[35] applicable in coordination chemistry,[36] homogeneous catalysis,[37] and organocatalysis.[38] Therefore, modification of electronic properties of NHCs, most often imidazole-based, became a primary issue and various concepts were followed, *i.e.*, N-substituent design or annellation with the imidazole ring,[39] but also to exert electronic influence[40] via NHC backbone substituents[41].In case of the latter, the initial focus was on mono(NHCs) bearing substituents derived from heteroatoms such as Cl,[42] N,[39b, 44] Si,[45] B,[46] and P[47] (Figure 1.3).

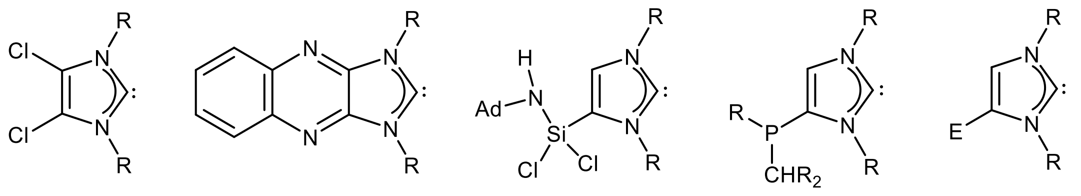

Figure 1.3. Backbone-functionalized mono(NHC)s (R = alkyl or aryl groups, X = Cl, Br).

A high yieldsynthetic approach was employed by Streubel and co-workers to develop a series of P-functional imidazole-2-ylidenemetal complexes via oxidative desulfurization of the P-functional thiones **XX**. H_2O_2 was used to produce phosphanoyl-imidazolium salts**XXI** followed by de-pronoation to generate NHC *in situ* which was trapped by treatment with metal precursor (Scheme 1.4).[49] Following the same synthetic protocol, bis(phosphanoyl) NHC complex was obtained and convertedto heterobimetalliccomplex.[50] Adaptation of this strategy not only prompted to combine two chemically andelectronically different environments in a single molecule,[51] but also lead to multifunctional ligand systems to create homo- andheterobimetallic complexes.[52, 53]

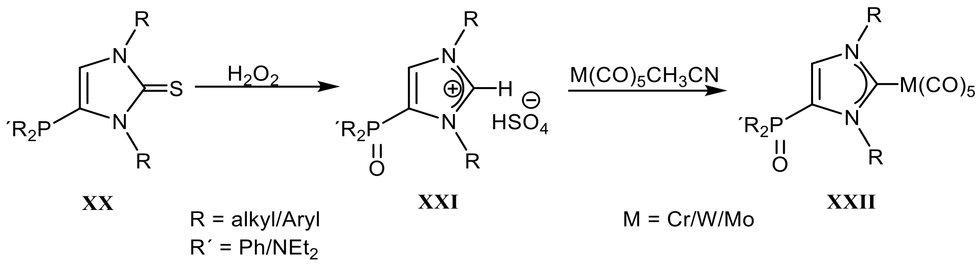

Scheme 1.4. Synthesis of the backbone-phosphanoyl substituted NHC metal complexes **XXII**.[49]

1.4. Diverse structural designs of NHCs

The design of poly(NHC) ligands [36]has increased the architecturalvariability and coordination modes in organometallic chemistry (Figure 1.4).Bis(NHCs)of type **XXIII** are linked via two *N*-centers and a varying carbon chain between the two NHCs . These bidentate bis(NHCs) have been prepared and their coordination properties aschelating ligands have been studied.[54-63] Iridium bis(NHC) complexes were synthesized by Crabtree and co-workers and used as catalyst for the reduction ofaldehydes.[57] Similarly, tetrakis(imidazole-2-ylidenes) **XXIV**were formed and theirstructural and spectroscopic properties have been investigated.[64-70] Different heteroatom such as P, O, S, and N atoms in the linker **XXV**offers tris-chelating coordination mode of these ligands that has providedpincerand tripodalbis(NHC) complexes.[71-74]The first example of an anionic N-heterocyclic dicarbene **XXVI** was reported by Robinson and co-workers, in which one of the sites of the imidazole-2-ylidene backbone has been deprotonated, giving rise to an NHC capable of coordinating through the C_2 and C_4 positions simultaneously (Figure 1.4).[75]

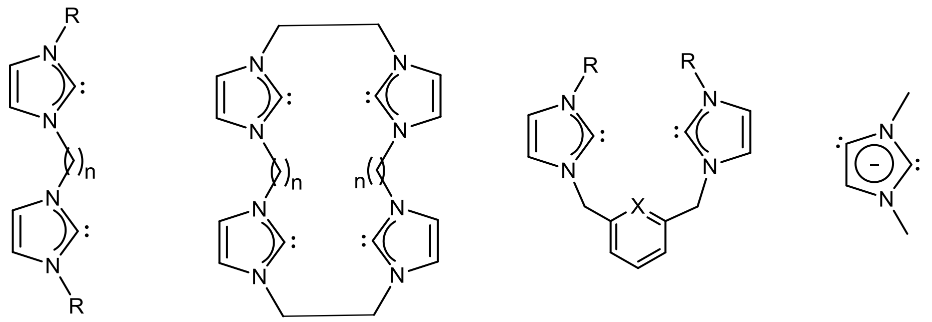

XXIII[53-64] **XXIV**[64-70] **XXV**[71-74] **XXVI**[75]

Figure 1.4. Bis, tetrakis and hetarene-bridge functionalized NHCs.

1.5. Janus-type bis(NHCs)

Contrary to mono(NHCs), knowledge about [a,d]benzannulated “ditopic” Janus-type bis(NHCs) **XXVII**, first reported by Bielawski et al.,[76] remains scarce. The benzobis(imidazolium)salt was deprotonated to create the bis(NHC) **XXVII**, while its metalcomplexes **XXXI** were produced by reacting it with suitable metal precursors. Similarly, they also studied the influence of the electronic properties on the NHC ligand by introducing a reducible redox-active functionality, such as a naphthoquinone **XXVIII**.[81] In its neutral form, the NHC was predicted to be a relatively weak donor (or nucleophile) due to conjugation between the lone pairs of electrons on the nitrogen atoms of the imidazolylidene and the carbonyl groups of the quinone moiety. The nucleophilic characteristics may also be enhanced by the formation of negative charge experienced by the carbene upon reduction.[35]In 2012, Peris *et.al* reported the preparation of a new ditopic bis(carbene) that shares redox-active characteristics, the pyracene bis(NHC) **XXIX**. Depending upon the steric bulk of *N*-substituents, these benzobis(NHCs) form monomeric,[76] dimeric[77] and polymeric[78] units.The reactions of benzo-bis(imidazolium) salts with suitable metal precursors allowed thesynthesis of organometallic polymers.[79,80]

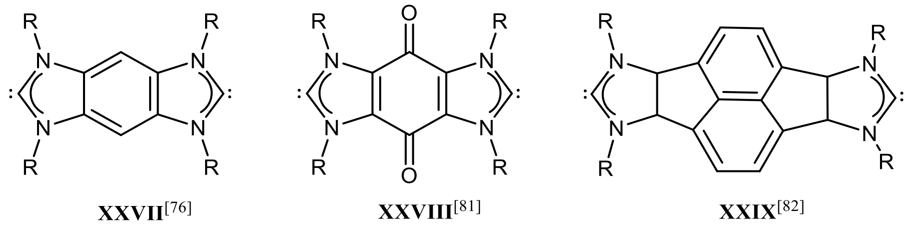

Figure 1.5. Examples of Janus-type ditopic bis(NHCs).

Coordination properties of such and related NHCs were investigated by Bielawski and Peris to build novel organometallic architectures.[83] Homobimetallic bis(NHC) complex **XXXI** was obtained by reacting bisimidazolium salt **XXX** with Ag_2O.[76] Hahn and co-workers quickly realized the huge potential of derivatives of **XXVII** to create molecular squares and quadrilaterals in supramolecular assemblies.[84] Besides the synthesis of homobimetallic Janus-type bis(NHC) complexes, Peris and his coworkers also synthesized heterobimetallic bis(NHC) complexes.[83b] They proposed monometalation of **XXXII** by its reaction with a base (NaOAc) followed by the addition of complexes $[MCl_2(Cp^*)]_2$ (M = Rh, Ir) and KI; the latter was added to the reaction mixture in order to support the formation of only one halogen containing species. The metalation of **XXXII** with rhodium occurred selectively at the C^2 position of the deprotonated imidazolium group (Scheme 1.5).

The differences in reactivity observed for Ir^{III} and Rh^{III} in this monometalation was due to rather labile $Rh–C^{NHC}$ bonds as compared to the more inert $Ir–C^{NHC}$ bonds.[85] Thus, it was assumed that any undesirable M–benzimidazolylidene complex can rearrange to the more stable $C^{NHC}{\wedge}C^{phenyl}$ chelate complex for M = Rh, while such a rearrangement is less likely for M = Ir.[83b]

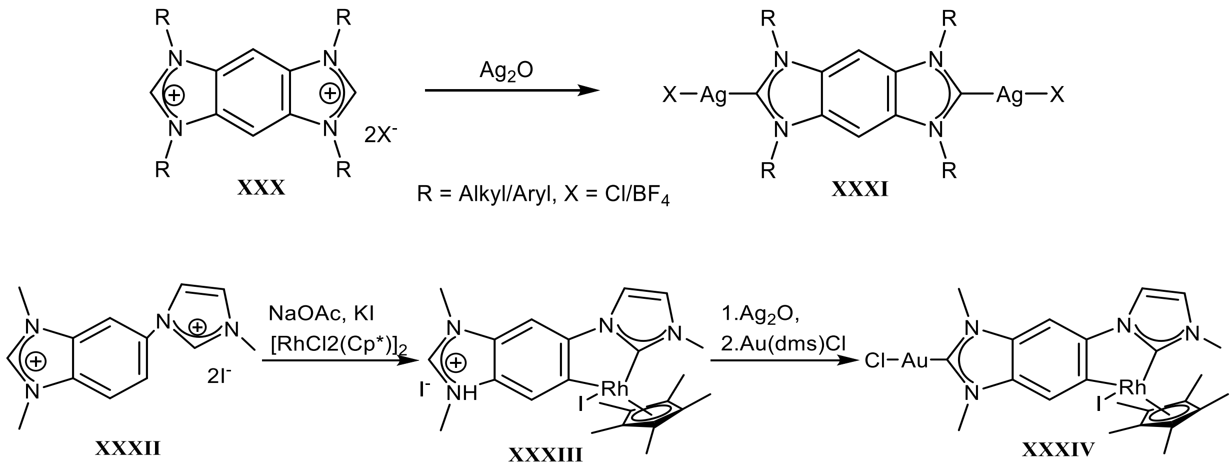

Scheme 1.5. Synthesis of the homo and heterobimetallic bis(NHC) metal complexes **XXXI**[76]**,** **XXXIV**[83b]**,** respectively.

A new design of bis(NHCs) having a P^V-center incorporated as linker (Scheme 1.6)was developed by Streubel and co-workers. The bis(imidazolium) salt **XXXV** was accessed via oxidative-desulfurization of the bis(imidazolyl)phosphane. Reacting **XXXVI** with two equivalents of potassiumhexamethyldisilazide (KHMDS) gave access to the free bis(NHC)**XXXVI**, while treating **XXXV** with two equivalents of KO^{t}Bu and AgOTf(PPh_3) lead to the bis(NHC) silvercomplex **XXXVII**.[86]

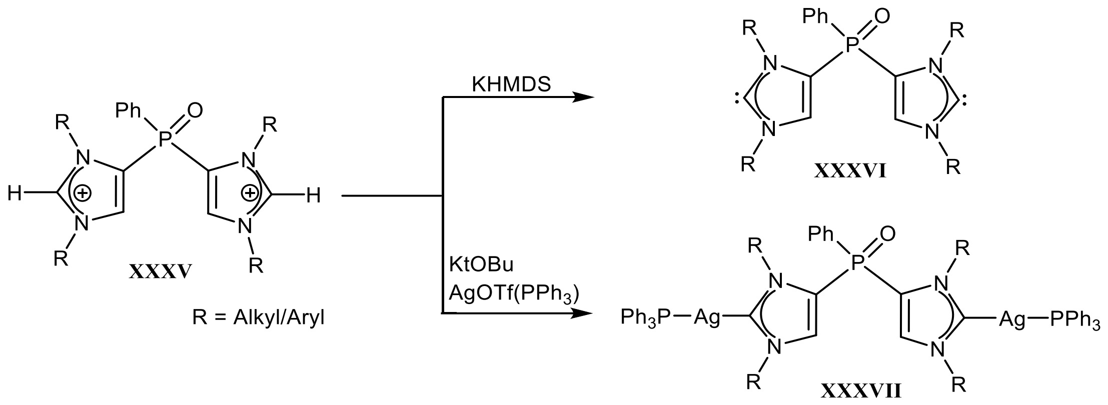

Scheme 1.6. Synthesis of the P^V bridged bis(NHC) **XXXVI** and its metal complexes **XXXVII.**[86]

There are very few examples of NHC ligands acting as bridging ligands in dinuclear complexes, where one metal is bound at the carbene carbon atom and another one is bound at the unsubstituted ring-nitrogen.[87] Such structures are probably promising candidates as catalysts for unique trans-formations through obliging action of the two metal centers.[88] It has been shown that N-deprotonation of platinum or palladium complexes bearing protic NH,NR(NHC) ligands leads to homodinuclear complexes **XXXVIII** (Figure 1.6) with a head to-tail (H−T) orientation of the bridging ligands.[89] Similar dinuclear complexes of type **XXXIX** have been obtained by treatment of an iron(II)−di-NHC complex with PhLi (Figure 1.6)[90].The formation of homodinuclear head-to-head (H–H) complexes **XXXX** has been proposed for the reaction of $[Ir(cod)(\mu\text{-}Cl)]_2$ with lithium *N*-benzylimidazolate.[91]

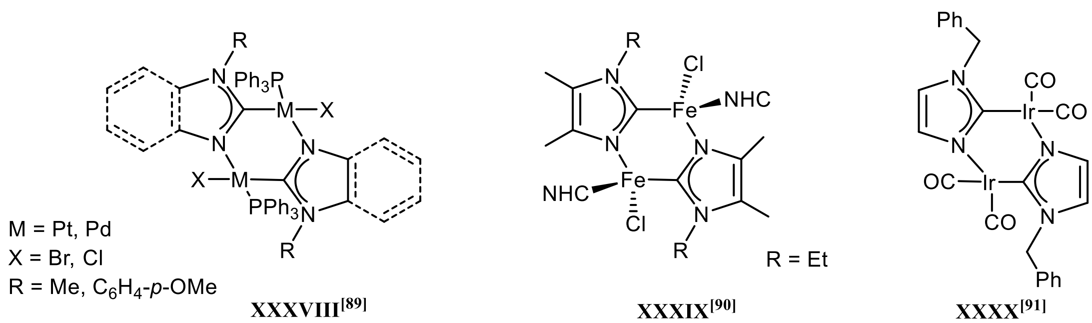

Figure 1.6. Literature known dinuclear NHC complexes with C, N-bridging ligands..

1.6. Backbone-functionalized anionic NHCs

It has been reported that the incorporation of an anionic functionality confers higher stability to resulting NHC complexes compared to related neutral donor substituents.[92] Especially backbone-functionalized NHCs having anionic heteroatom substituents facilitates π-electron interaction with the heterocyclic ring, which then may also lead to electronic tuning of the donor properties of the carbene center.[53] Only a small number of anionic NHCs of possessing low-coordinate moieties such as enolate**XL**,[93] borate**XLI**,[94] amido**XLII**[95] have been reported (Figure 1.7). The first anionic NHC-4-olate**XL** was synthesized by Lavigne and co-workers where they perposed deprotonation of starting material 4-hydroxyimidazolium chloride with LiHMDS (2eq.).[93] Later, Tamm and co-workers introduced a weekly coordi-natinganionic functionality $B(C_6H_5)_3$ at the NHC backbone to generate **XLI**. Zwitterionic gold complexes of the obtained NHC were obtained via reacting with suitable gold complexes and their catalytic studies towards skeletal rearrangement of enyne were commenced.[94] Backbone arylimino-substituted NHC ligands **XLII** was postulated by Braunstein and coworkers via reacting imidazolium precursors with LiHMDS and tmeda (N, N,N',N'-tetramethylethylene-diamine).[95]

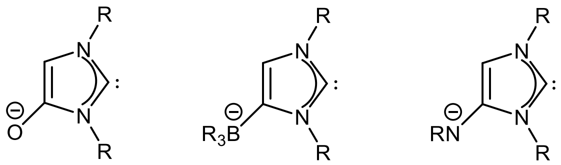

XL[93] **XLI**[94] **XLII**[95]

Figure 1.7. Literature known NHCs (R = alkyl or aryl groups; shown without the counter cations).

A novel zwitterionic compound **XLIV** was reported by Streubel and co-workers, in 2013 and proposed a reaction of the imidazole-2-thion-4-yl-substituted phenylphosphanes **XLIII** with four equivalents of potassium (Scheme 1.7). Subsequent deprotonation of **XLIV** resulted into anionic NHC derivative **XLV**.[96] Synthesis of the anionic bis(NHC) **XLVII** was reported, by reduction of a bis(imidazole-2-thione-4-yl)phosphane**XLVI** using a large excess of potassium metal. But **XLVII** could neither be isolated nor structurally con-firmed.[97]

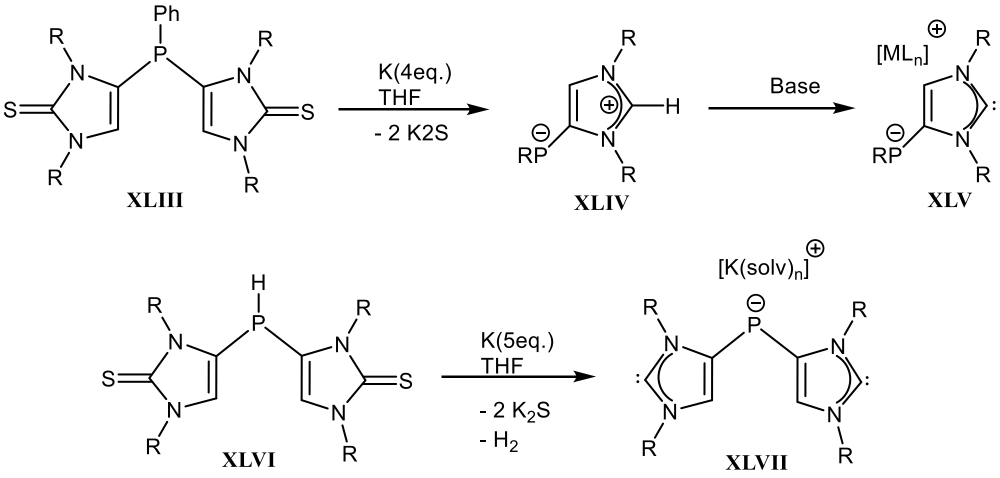

Scheme 1.7. Synthesis of anionic NHCs **XLV**[96] and **XLVII**[49].

1.7 Diphosphinines

Concerning diphosphinines, there are three possible regioisomers, *i.e.* 1,2-diphosphinine, 1,3-diphosphinine and 1,4-diphosphinine (Figure 1.8). Due to a limited stability and high reactivity, chemistry of these compounds are still largely unexplored.

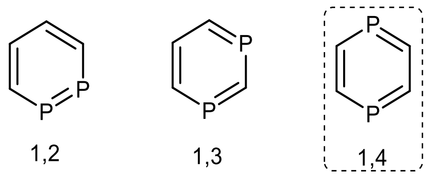

Figure 1.8. Regioisomers of diphosphinines.

Here, I will focus on 1,4 diphosphinines as they constitute an important part of this thesis. The first monocyclic $1\lambda^3$, $4\lambda^3$-diphosphinine **XLX** [97] was reported by Kobayashi and co-workers using a stepwise protocol. They proposed to start with a $RhCl_3$ catalyzed addition of MeOH to the 1,4-diphosphabarrelene **XLVIII** to give **XLIX**. The latter eliminated the alkene **XLXI** under thermal conditions andafforded the 1,4-diphosphinine **XLX** having four electron withdrawing CF_3 groups (Scheme 1.8). Owing to the limited stability, this compound could neither be isolated nor fully characterized and was only handled as *n*-hexane solution. Noteworthy, the^{31}P-NMR resonance of **XLX** was reported at a very low field (287.0 ppm).

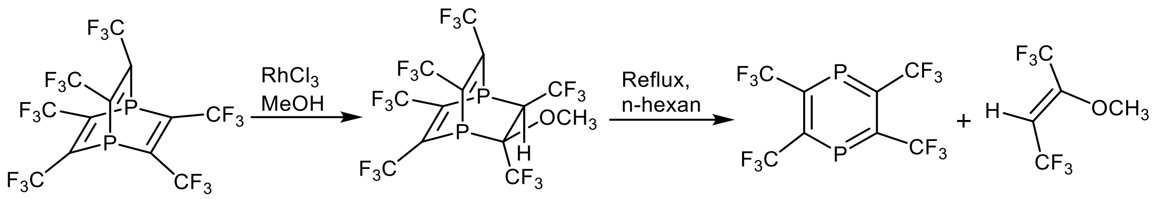

XLVIII XLIX XLX XLXI

Scheme 1.8. Synthesis of the first example of a 1,4 diphosphinine (**XLX**).[97]

The facile access of imidazole-2-thione-based tricyclic 1,4-diphosphinines **XLXVI**[101] by Streubel and co-workers, has revived this research area, recently (Scheme 1.9). By treating imidazole-2-thiones with ^{n}BuLi *in situ* generates the lithiated salt in the first step, which undergo a reaction with organochlorophosphane $(Et_2N)_2PCl$ to get access to compound **XLXIV**. After extracting it with pentane, it was scrambled with PCl_3 to afford compound **XLXV** via substitution reaction. Later on, reaction with a suitable base and subsequent intramolecular nucleophilic substitution lead to the formation of tricyclic compound **XLXVI**. Multigram synthetic protocol was used to access 1,4-diphosphinines **XLXVI** via reduction of the 1,4-dihydro-1,4-dichloro-1,4-diphosphinines **XLXV** with ${}^{n}Bu_3P$ (Scheme 1.9).[101]

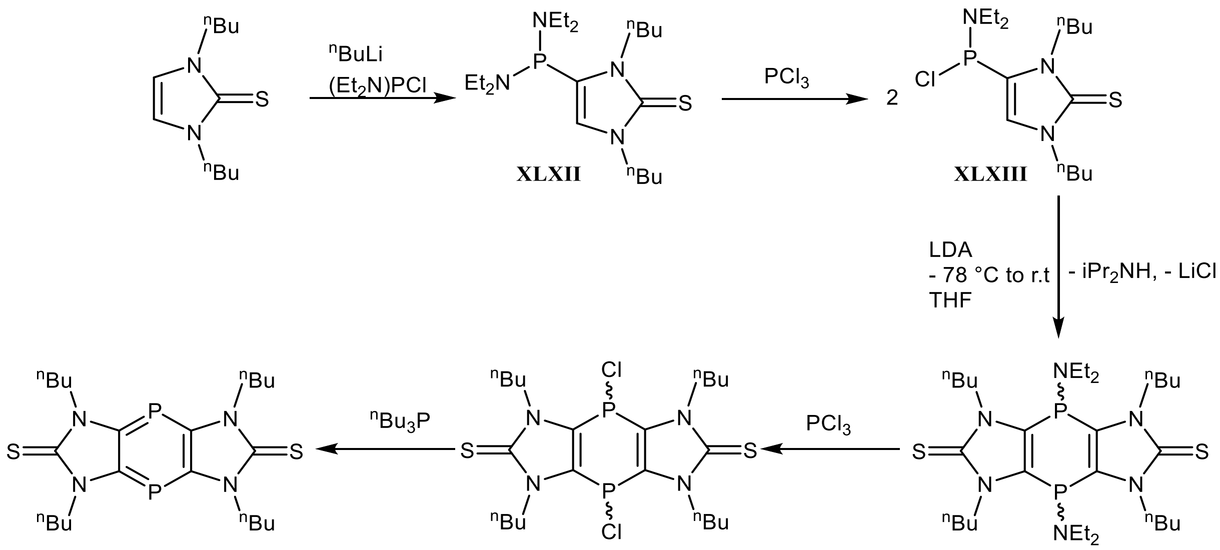

XLXII XLXIII XLXVI XLXV XLXIV

Scheme 1.9. Reported synthetic protocol of first tricyclic imidazole-based 1,4 diphosphinine **XLXVI**[101].

Initially, the chemistry of **XLX** was studied by Kobayashi and co-workers, *e.g.*, by heating compound **XLX** with carbon tetrachloride at 130°C causes formation of diphosphanorbornadiene derivative **XLXVII**[98] by a pathway, possibly similar to the reaction between $PPh_3$and CCl_4;[99a] but more recent studies suggest that a 1,4-addition of a C-Cl bond occurs first[99b]. Compound **XLX** was also used as a diene in several thermal [4+2]-cycloaddition reactions to afford diphospha-barrelenes **XLXVIII**.[98] Similarly, when it was heated with an episulfide, 2,3,5,6-tetrakis-(trifluoro-methyl)-7-thia-1,4-diphosphanorbornadiene **XLXIX** via a formal [4+1]-cycloadditionreaction was obtained. Photoisomerization was performed to get access to **XLXX** and provide insight into valence bond isomerization.[100] Interestingly, derivatives **XLXIV** retain a high degree of aromaticity (NICS(1) value −9.5) and redox-active functionalities making it a very remarkable starting point for the formation of multifunctional ligands.[101] Early reactivity studies demonstrated that **XLXIV** can react with dichalcogenides PhCh-ChPh (Ch =S, Se) in [4π+2σ]-cycloaddition reactions, followed by inversion at the phosphorus center (Scheme 1.10).[102] In another reaction, compound **XLXVI** could be subjected to oxidative hydrolysis in moist air to get access to tricyclic bis(phosphinic) acid **XLXXII**.[103] After the first report on a thiazole-2-thion-based 1,4 diphosphinine **XCXIX** by the Streubel group had appeared, nucleophilic addition reactions were carried out using a base KHMDS to synthesize compound **XLXXIII**. Compound **XLXXIII** could be isolated and fully characterized.[104] Similarly, dianionic compound **XLXXIV** was obtained selectively via two-fold reduction of compound **XCXIX** in THF.[105]

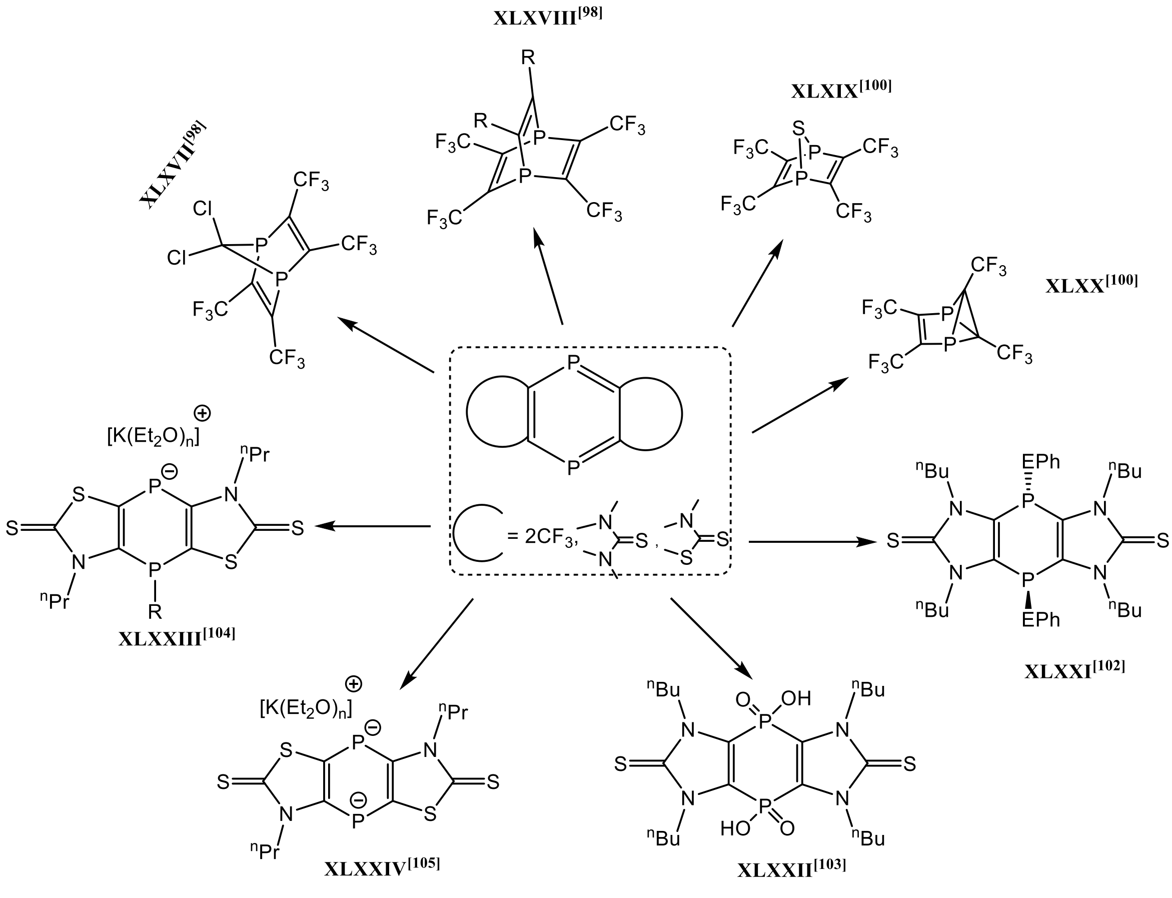

Scheme 1.10. Reactivity studies of three different 1,4-diphosphinines (R = alkyl groups).

With this background it is particularly interesting to synthesize hitherto unknown bis(NHCs) having bridging *P*-functionalities bound to the backbones of two NHCs, thus being able to study their co-ordination properties and, in the long run, applications in materials chemistry.

2. Aims of the PhD Thesis

The main aim of this PhD Thesis was to synthesize new classes of P-functional Janus-type bis(NHCs) such as **XLXXV**and **XC** (Figure 2.0) using imidazole-2-selone-derived tricyclic 1,4-dihydro-1,4-diphosphinines.

Figure 2.0. Examples of targeted P-functional bis(NHCs).

Furthermore, initial studies on synthesis and reactivity in coordination chemistry:

- Of $P^{V/V}$-functional tricyclic bis(NHCs)
- Of $P^{III/III}$-functional tricyclic bis(NHCs)
- Of anionic tricyclic bis(NHCs)

3. Syntheses of 1,4-dihydro-1,4-diphosphinines

In previous studies by Majhi, a successful synthetic approach was developed to get access to imidazolium salts via oxidative desulfurization of imidazole-2-thiones. Later on, they were used as starting precusors for imidazole-2-ylidenes.[86] Following the same approach, Koner had tried to synthesize bis(NHCs) using imidazole-2-thione-based tricyclic 1,4-dihyro-1,4-diphosphinines. He has shown that when compound **XCI** was treated with 10 molar equivalent of aqueous H_2O_2 in methylene chloride a clean conversion to compound **XCII** occurred (Scheme 3.1) but, unfortunately, this showed limited stability during the purification process. The latter might be due to the formation of hydrogen sulphate in the bis(imidazolium) salt.[103]

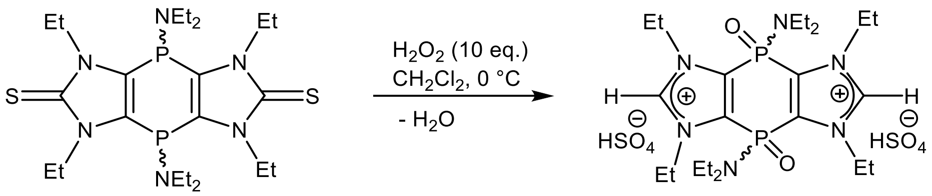

Scheme 3.1. Oxidative desulfurization to the bis-imidazolium salt **XCII**.[103]

Keeping in view to get access to a series of tricyclic P-functional bis(NHCs), having a heteroatom functionality that could be redox-active and/or possesses further, different donor centers in the same ligand, we decided to prepare 1,4 dihydro-1,4 diphosphinine diselones.

3.1 Syntheses of P-functional imidazole-2-selones

As imidazole-2-selone **1** had been synthesized before in rather good yields, we decided to use it as precursor following the literature protocol: preparation of the corresponding imidazolium salt and its treatment with elemental selenium.[106,107] To the best of our knowledge, there was no report on the synthesis of a backbone-phosphanylated imidazole-2-selone so far. Furthermore, we employed a similar synthetic strategy as reported by Sauerbrey,[49,108] to achieve the synthesis of C^4-phosphanyl-substituted imidazole-2-selones **2** and **3**. Imidazole-2-selone **1** was reacted with *n*-butyl lithium at - 90 °C with subsequent addition *insitu* of chlorophosphanes such as ($Ph(NEt_2)PCl$ and $(Et_2N)_2PCl$) to get the 4-phosphanylated imidazole-2-selones **2** and **3** (Scheme 3.2). Crude products were purified via column chromatography and obtained as light yellow oils in excellent yields {92% (**2**), 83% (**3**)}. $^{31}P\{^1H\}$ NMR spectroscopic analysisof **2** and **3** confirmed that only one major product was formed in each case, showing resonances at chemical shifts at 72.5 ppm (**2**) and 32.9ppm (**3**). In the ^{1}H NMR spectrum the *C*^{5}-H proton appeared at higher field at 6.7 (for **2**) and 6.6 ppm (for **3**) compared to the precursor backbone protons.

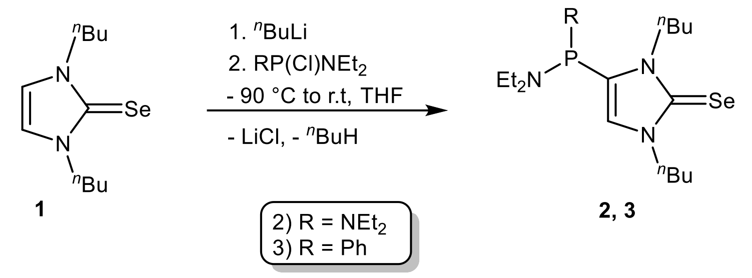

Scheme 3.2. Synthesis of *C*^{4}-phosphanylated imidazole-2-selones **2, 3**.

The ^{77}Se NMR spectrum showed a singlet at 36.6 ppm (for **2**), but no coupling to the phosphorus, which was comparatively deshielded to imidazole-2-selone **1** (δ = - 12.2 ppm, Δδ = 24:4). Furthermore, **2** and **3** were characterized via IR spectroscopy and mass spectrometry.

3.2. Syntheses of amino(chloro)phosphanyl substituted imidazole-2-selones 4, 5

Aiming to employ the chlorophosphanyl substituted imidazole-2-selones in low-coordinate phosphorus chemistry containing bis(NHC)units later, the synthesis of such derivatives was required. Therefore, scrambling reactions were performed using **2** and **3** and PCl_3 to get access to backbone chloro(organo)phosphanyl substituted imidazole-2-selones **4** and **5** following the reported protocol by Streubel and coworkers.[101,109] Reactions were performed at – 80 °C in diethyl ether (**4**)/dichloromethane (**5**) (Scheme 3.3) and monitored by ^{31}P NMR spectroscopy. The ^{31}P{^{1}H} NMR spectra of **4** and **5** showed singlet resonance signals at 105.8 ppm (**4**) and 48.9ppm (**5**) being significantly downfield-shifted compared to **2** and **3,** respectively. After purification, both compounds (**4, 5**) were isolated as light yellow oils in very good to excellent yields {80 % (**2**), 87% (**3**)}. Both compounds were characterized by multinuclear NMR, IR and MS analysis.

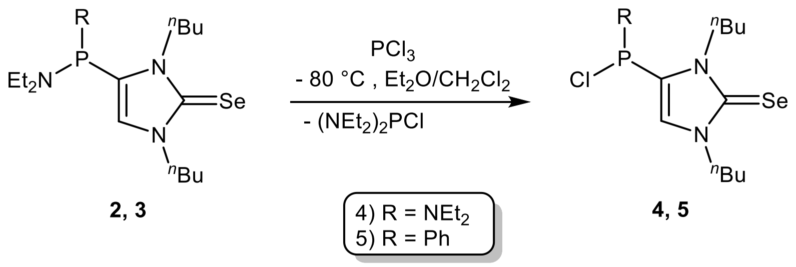

Scheme 3.3. Synthesis of the *C*^{4} chloro(organo)phosphanyl substituted imidazole-2-selones **4**, **5**.

The ^{31}P NMR resonances of compounds **4, 5** are very close to the related known *P*-chloro derivativesof imidazole-2-thiones.[101] However, the signals appeared significantly downfield-shifted as compared to **2, 3**.

3.3. Syntheses of imidazole-2-selone-derived tricyclic 1,4-dihydro-1,4-diphosphinines

Six-membered heterocyclic compounds having two σ^3 λ^3-phosphorus centers are generally known as 1,4-dihydro-1,4-diphosphinines. The first example **XCIII** was reported by Mann in 1964, proposing a stepwise ring closure reaction for its formation (Figure 3.1).[110] After simplification of the synthetic protocol, Märkl could successfully synthesize Mono-heterocylic compound **XCIV** with different substituents at the *P*-center.[111] Later on, different structural motifs were introduced in place of benzene rings resulting in compounds **XCV**[112], **XCVI**[113]. The N-heterocyclic tricyclic framework in **XCVII** was reported by Kostyuk and co-workers, using a reaction of the corresponding 1,4-dichloro-1,4-diphosphinine with dimethyamine.[114]

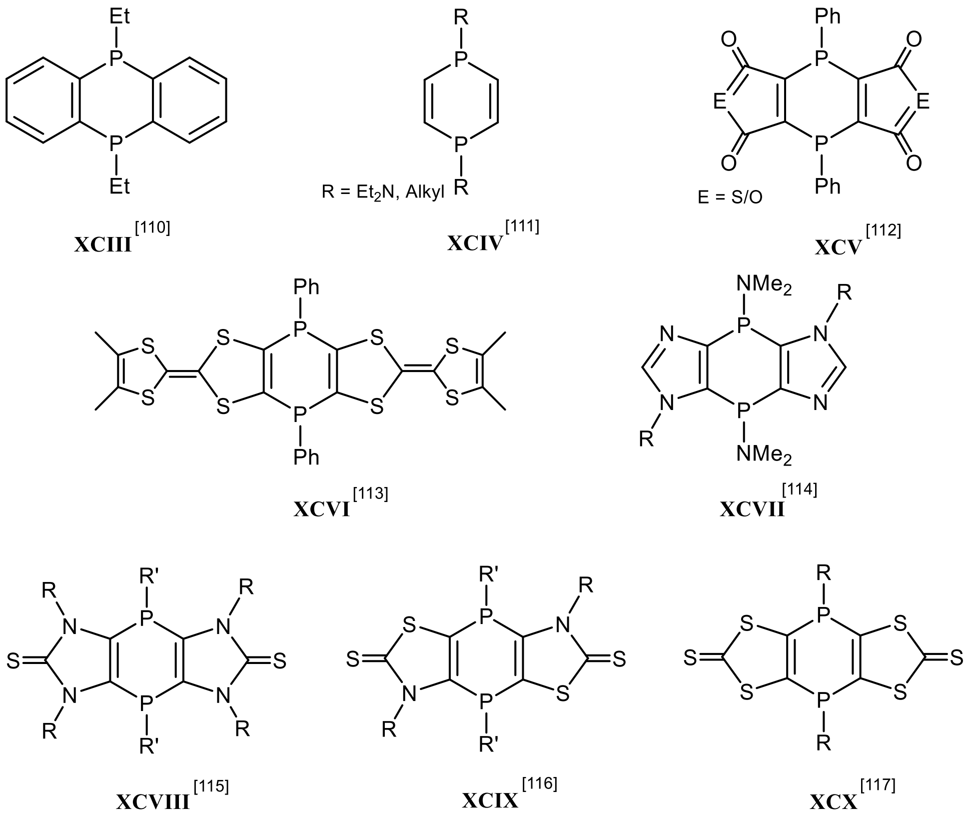

Figure 3.1. Literature known examples of 1,4-dihydro-1,4-diphosphinines.

Recently, Streubel and co-workers came up with imidazole-2-thione (**XCVIII**)[115] thiazole-2-thione- (**XCIX**)[116] and dithia-2-thione- (**XCX**)[117] derived 1, 4 dihydro-1,4-diphosphinines via backbone deprotonation of the *C*^{4}-organo(chloro)phosphanyl-2-thione followed by an *in situ* use for cyclization and lithium chloride elimination. As mentioned beforehand, the initial studies of the oxidative desulfurization of tricyclic 1, 4-dihydro-1,4-diphosphinine dithiones failed,[103] we considered synthesizing and employing the corresponding diselones instead.

Following the similar synthetic methodology reported by Koner[101] and Begum[116], 1,4 dihydro-1,4-diphosphinine diselones **6**$^{cis/trans}$**, 7**$^{cis/trans}$ were synthesized by deprotonationofchloro(organo)-phosphanyl imidazole-2-selones followed by intermolecular nucleophilic substitution reaction with **4** and **5**, respectively,in THF at – 80 °C (Scheme 3.4). The resulting crude products were subjected to column chromatography with diethylether to remove LiCl. After work up, light yellow colored solids were obtained for **6**$^{cis/trans}$**, 7**$^{cis/trans}$in good yields (53 % for **6**$^{cis/trans}$ and 48 % for **7**$^{cis/trans}$).

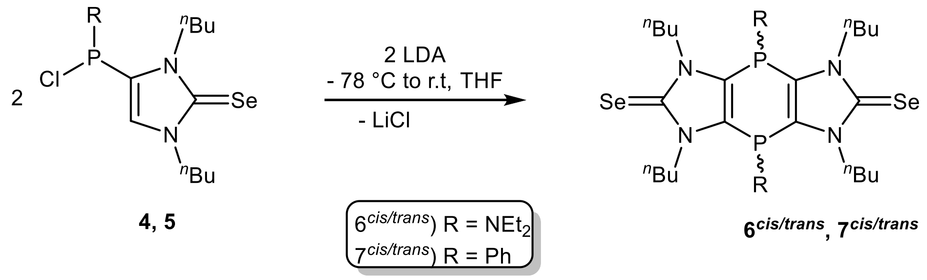

Scheme 3.4. Synthesis of the1,4-dihydro-1,4-diphosphinine-bis(imidazole-2-selones) **6**$^{cis/trans}$**, 7**$^{cis/trans}$.

The ^{31}P NMR spectrum showed a clean conversion into the corresponding isomeric mixtures of tricyclic compounds with resonances of **6**$^{cis/trans}$ (0.9 and 3.7 ppm) and **7**$^{cis/trans}$ (- 53.9 and -54.9ppm), which are comparable with those of the previously reported imidazole-2-thione derived tricyclic compound **LXXIV** (R = ^{n}Bu, R' = NEt$_2$; δ^{31}P = 0.2, 3.6 ppm) [101] and (R = ^{n}Bu, R' = Ph; δ^{31}P = -54.9, -56.2 ppm).[115a] In the^{77}Se NMR spectrum two resonances were observed corresponding to *cis* and *trans* isomers at 35.9, 37.9 ppm (**6**$^{cis/trans}$). Nevertheless, we tried to separate the isomeric mixture of compounds **6**$^{cis/trans}$ using low temperature column chromatography (- 20 °C). Compounds **6**$^{cis/trans}$ were subjected to a long silica column (Φ= 6 cm, h = 12 cm) and a mixture of *n*-pentane and diethyl ether (1: 0.3) was used as eluent to get a *cis/trans* mixture as first fraction. However, usage of pure diethyl ether led to a separation of only one isomer, that appeared at 0.9 ppm in the ^{31}P{^{1}H} NMR spectrum and which was assigned to **6**^{cis}. Apparently, the *trans* isomer is less soluble in polar solvents due to a smaller dipole moment (compared to the *cis* isomer). Therefore and from now onwards, we will describe the signal appearing at 3.7 ppm as**6**^{trans}. The mixtures of both diastereomers (**6**$^{cis/trans}$, **7**$^{cis/trans}$) were characterized by MS, IR, EA and some of which by single crystal X-ray diffraction studies.[118]

Molecular structures of **6**^{cis} and **7**^{cis} are given in Figure 3.2, and selected structural parameters are given in Table 3.1. In both cases, the *cis* isomers crystallized preferentially and were obtained by slow evaporation of their methylene chloride/diethyl ether solution at – 4 °C. X-ray crystallographic measurements revealed monoclinic crystal systems for both **6**^{cis}and **7**^{cis} with space group $P2_1/n$.

C-Se bond lengths of **6**^{cis}, **7**^{cis} are intermediate between the values of carbon and selenium atom single and double bonds {(C-Se) =1.94 and (C=Se) = 1.74}, thus suggesting that selenium possesses a significant negative charge and, hence, can behave as a nucleophile.[119]

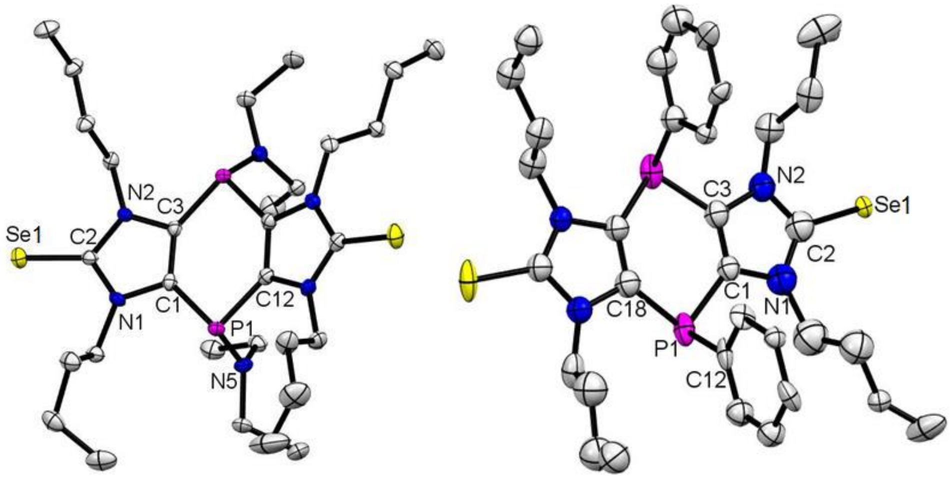

Figure 3.2. Displacement ellipsoids plot (50% probability) of molecular structure of **6**^{cis} (left) **7**^{cis} (right); hydrogen atoms have been omitted for clarity.

The N1-C2-N2 bond angle which is slightly more acute than inthe corresponding tricyclic imidazole-2-thione compounds,[101]which is an important feature regarding the *C*^{2}center chemistry discussed later. The bond lengths and bond angles of both **6**^{cis} and **7**^{cis} are otherwise very close to those of literature known similar compounds [103, 119] and, hence, shall not be discussed further.

Table 3.1. Selected bond lengths (Å) and angles (°) of **6**^{cis}and **7**^{cis}.

	6^{cis}	**7**^{cis}
C2-Se1	1.828(13)	1.857(13)
C1-P1	1.816(14)	1.836(11)
C2-N1		1.405(17)
	1.374(17)	
P1-N5	1.669(12)	-
P1-C12	-	1.820(12)
N1-C2-N2	104.9(11)	107.9(11)
C1-P1-C12	95.2(6)	-
C1-P1-C18	-	94.3(5)

4. Synthesis and transition metal complexes of a {P(O)NEt$_2$}-functional Janus-type bis(NHC)

The access to Janus-type bis(NHC) chemistry seemed within reach after having synthesizedthe tricyclic 1,4-dihydro-1,4-diphosphinine compounds **6***cis/trans*. Especially, as the two C=Se functions in compounds **6***cis/trans* offer a promising starting point to investigate the synthesis of annulated bis(NHCs) **XLXX** having tunable P-linkers (Figure. 4.1). This would represent a unique variation of the Bielawski-type bis(NHCs) **XXXI**.[76,78] So, as an initial studies we decided to introduce $P^{V/V}$ moeities on the backbone of two NHCs. It might increase the acidity of the C^2-proton, thereby facilitating a selective deprotonation to get access to corresponding stable and rigid bis(NHCs).

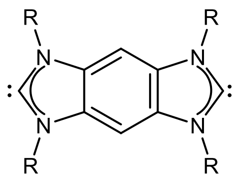

XXXI[76, 78]

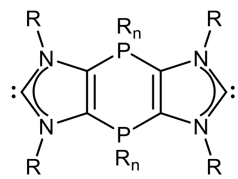

XLXX

Figure 4.1. Examples of tricyclic Janus-type bis(NHCs) **XXXI**[76, 78] (known) and **XLXX**(unknown).

4.1. Oxidative deselenization of 1,4-dihydro-1,4-diphosphinines

To achieve oxidative deselenization[120], a previously reported approach[86]was applied here to compounds **6***cis/trans*. Using hydrogen peroxide in methylene chloride followed by anion exchange with $BaCl_2.2H_2O$,the bis(imidazolium) chloride salts **8***cis/trans* (Scheme 4.1) were obtained after purification as white hygroscopic solid (78 %).

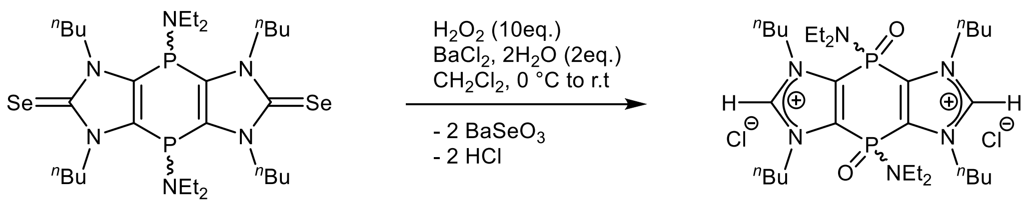

6*cis/trans*   **8***cis/trans*

Scheme 4.1. Synthesis of tricyclic $P^{V/V}$-functional bis(imidazolium) salts **8***cis/trans*.

The change of the P^{III} to the P^{V} oxidation state was monitored by ^{31}P NMR spectroscopy, and high-field shifted resonances were observed at - 6.2 and - 5.9 ppm (*cis/trans)* with a 1:0.9 isomeric ratio. The deselenization and, hence, the formation of bis(imidazolium)chloride was firmly established through the ^{1}H NMR spectrum;two characteristic triplets revealed the C^2-protonsat δ = 11.1and11.8 ppm of the *cis* and *trans* isomers.[76, 50, 121, 103] Further confirmation on the formation of bis(imidazolium) salts **8**$^{cis/trans}$came through the ^{13}C{^{1}H} NMR spectrum showing the C^2-carbon resonance at δ = 147.3 ppm, while the selone C^2carbon resonance had disappeared.[50, 121, 122]

The bis(imidazolium) salts werealso confirmed by positive ESI mass spectrometry showing m/z 689.3351 (theor. 689.3366),which was assigned to $[C_{30}H_{58}Cl_2N_6O_2P_2]^+$. The δ_P values for this bis(imidazolium) salts were found to be markedly highfield-shifted compared to the acyclic backbone bis(diphenyl)phosphinoyl-substituted imidazolium salt (δ_P = 23.7 ppm),[121a]thus revealing a more potent and more effective electronic communication between the phosphorus nuclei and the attached donor centers.

Single crystal X-ray diffraction analysis was performed using crystals obtained from a 1:0.8 mixture of compounds **8**$^{cis/trans}$via slow evaporation of saturated methylene chloride, water and isopropanol solution (1: 0.4: 0.8) at low temperature (- 20 °C). The compound **8**^{trans} crystallizes triclinic in the space group P-1. The selected structural parameters of compound **8**^{trans} are given in figure 4.2. Bond lengths and angles were found to be in the common range for imidazolium salts[76,121a,123] and *P*-oxide derivatives of imidazoles.[124, 125]The large N1-C2-N2 bond angle (109.67°) is typical for annulated imidazolium compounds as are the endocyclic imidazole bond lengths;[126] especially, the widening of the N1-C2-N2 bond angle (vs. 104.9(11)° in **6**^{cis}) is rather typical for imidazolium salts.[76, 121a]. It is interesting to note that each chloride anion show contacts with two C^2-H bonds of the nearest imidazolium ions with a distance of about 3.3 Å.[49]

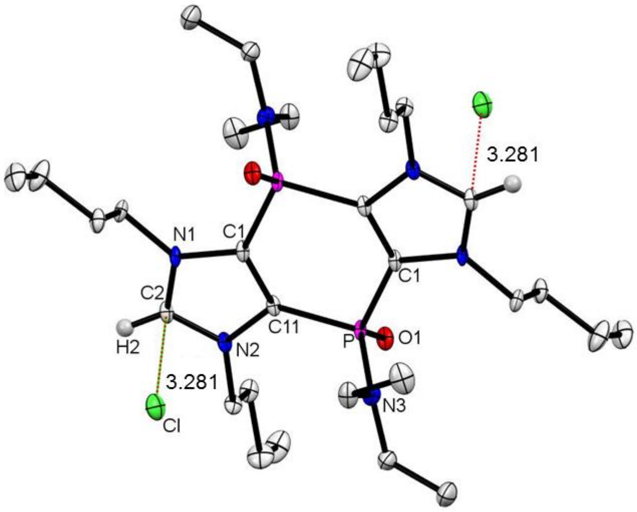

Figure 4.2. Displacement ellipsoids plot (50% probability) of the molecular structure of **8**^{trans}; hydrogen atoms, H_2O and *iso*propanol molecules have been omitted for clarity. Selected bond lengths [Å] and angles [°]: N1-C2 1.326(2), N2-C2 1.328(2), P-C1 1.7991(18), P-C1 1.8121(17), P-N3 1.6318(15), P-O1 1.4704(12), N1-C2-N2 109.67(15), C1-P-C11 99.22(8).

4.2. C^2-Deprotonation toform tricyclic {P(O)NEt_2}-functional bis(NHCs)

Starting from the bis(imidazolium) salts **8**$^{cis/trans,}$ the synthesis of the related bis(NHCs) was examined. Treating **8**$^{cis/trans}$ with 2.2 equivalent of KHMDS in THF at - 78 °C (Scheme 4.2) afforded the new bis(NHCs)**9**$^{cis/trans}$ as an isomeric mixture (ratio 1:0.7). After the removal of potassium chloride via filtering cannulation followed by drying *in vacuo*, a light yellow coloured solid was obtained in excellent yields (78%).The pure bis(NHCs) **9**$^{cis/trans}$ were characterized by NMR spectroscopy and the $^{31}P\{^1H\}$ NMR spectrum revealed slightly downfield-shifted resonancesat -2.3(*cis*) and -1.2 (*trans*) ppm – compared to bis(imidazolium) salts **8**$^{cis/trans}$ {δ =-6.2(*cis*) and-5.9 (*trans*) ppm}.

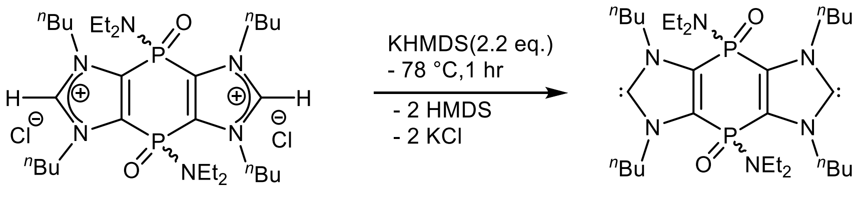

Scheme 4.2. Synthesis of tricyclic {P(O)NEt_2}-functional bis(NHCs) **9**$^{cis/trans}$.

The ^{1}H NMR spectrum of **9**$^{\textit{cis/trans}}$ showed that the C^2-protons of bis(imidazolium) salts **8**$^{\textit{cis/trans}}$ had disappeared. In addition, the $^{13}C\{^1H\}$ NMR spectrum(THF-d_8) exhibited diagnostic triplet signals at δ = 224.9 and 225.4ppm (t, $^3J_{P,C}$ = 2.4 Hz, $\underline{C^2}$) (*cis/trans*),which were indicative of the highly symmetric structure shown in scheme 4.2 and consistent with data of other known annulated and phosphonyl bis(NHCs) **XXXI**, **XXXVI**, **XCI** (Figure 4.3).[76,127,126a,128] Besides these NMR studies, the proposed constitution of **9**$^{\textit{cis/trans}}$ was also verified by HRMS (EI) as experimental and theoretical m/z values were in acceptable agreement (exp. 594.3926, theor. 594.3933), which was independently confirmed by elemental analysis.

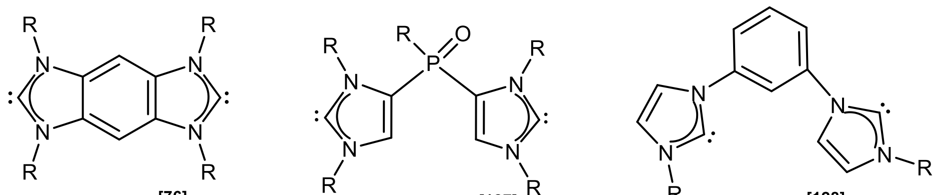

Figure 4.3. Literature reported bis(NHCs) **XXXI**,[76]**XXXVI**[127] and **XCXI**[128].

Further confirmation was obtained by X-ray diffraction analysis using a crystal of **9**$^{\textit{trans}}$obtained from a 1: 0.2 mixtureby slow evaporation of a saturated *n*-pentane/Et_2O solution (1:1) at room temperature. An ellipsoidal presentation of the molecular structure is shown in Figure 4.4, together with selected bond lengths and angles in the figure caption. Markedly, the molecular structure of **9**$^{\textit{trans}}$ possesses an N1-C3-N2 bond angle of 102.4(11)° that is slightly more acute than in (mono)(imidazole-2-ylidenes)(R = Ad or ^{t}Bu, 104.4° or 104.8°).[129)] This promising result strongly suggested that each carbene “face” of these Janus-type ligands could possess related reactivities and, hence, also affinities toward transition metals.

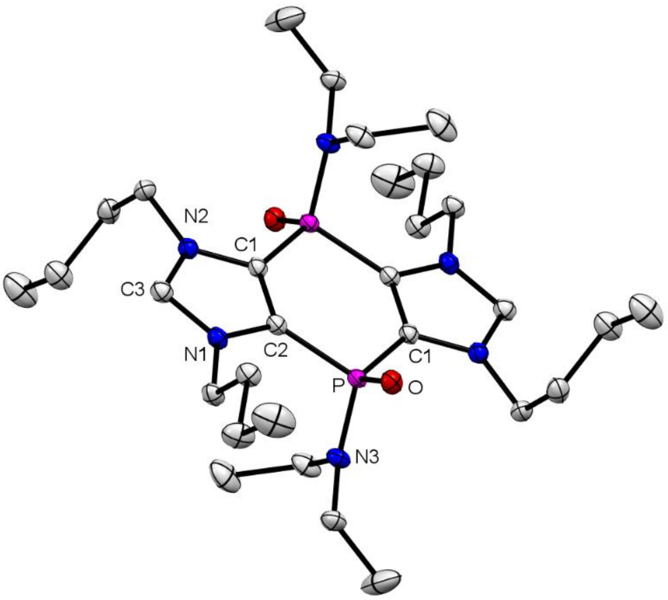

Figure 4.4. Molecular structure of **9**^{trans}. Ellipsoids are set at 50 % probability, and hydrogen atoms are omitted for clarity. Selected bond lengths [Å] and angles [°]: N1-C3 1.3686(17), N2-C3 1.3674(17), P-C1 1.7921(13), N1-C3-N2 102.40(11), C1-P-C2 101.11(6).

4.2.1. Theoretical investigations

All calculations were performed by Nyulászi and co-workers using the Gaussian 09 program package.[130] All investigated structures have been fully optimized at the M06-2X/6-31+G* level of theory (ultrafine integration grid was applied), followed by the subsequent calculation of the eigenvalues of the Hessian at the same level, to characterize the nature of the stationary point obtained. For transition states, IRC calculations have been performed to locate the corresponding minima. The energy of the orbitals was calculated at B3LYP/6-31+G*//M06-2X/6-31+G* and B3LYP/6-31G*//M06-2X/6-31+G*level of theory.Model compounds **9'** were calculated with N-methyl substituents of the imidazole units (instead of the *n*-butyl) to reduce the computational time. For the visualization of the molecular structures and the molecular orbitals, the MOLDEN program was used.[131]

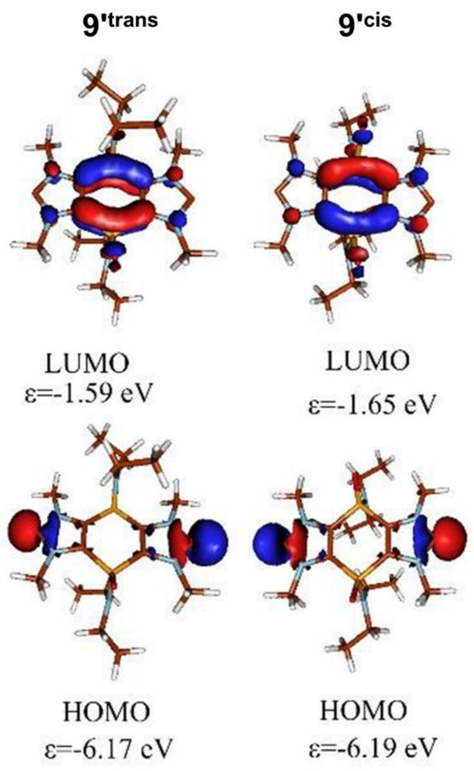

Figure 4.5. Kohn-Sham frontier orbitals of **9′** and their energies at B3LYP/6-31+G*//M06-2X/6-31+G* level of theory.

M06-2X/6-31+G* DFT calculations on **9′***cis/trans* [132] indicate a 0.5 kcal/mol preference for the *trans* isomer. For both isomers (**9′***cis/trans*), the π-type LUMO (Figure 4.5) is delocalized over the central ring and the HOMO (ε = -6.17 eV for the *trans* isomer and ε = - 6.19 eV for the *cis* isomer are antibonding combinations of the two weakly coupled in-plane carbene lone pairs (Figure 4.5). In accordance with the acute bond angle, they have strong *s*-character (51.7% at B3LYP/6-31+G**//M06-2X/6-31+G*, comparable to 53.0% in PH_3, see Figure 4.5). To assess the stability of the tricyclic carbenes, we investigated the isodesmic reaction (scheme 4.4) for **9′cis/trans**. [133] While for *N*-methyl-imidazole-2-ylidene 111.5 kcal/mol, for **9′***cis* 113.3, and for **9′***trans* 111.7 kcal/mol stabilization was obtained.

R`R``C: + $CH_4$ => R`R``CH_4 + CH_2(1), (Scheme 4.4)

The NICS(0) values of the imidazole units are -10.5 for the *cis* and -10.9 for the *trans* isomer, indicating slightly reduced aromaticity compared to the parent imidazole-2-ylidene (NICS(0) = -11.3 middle ring is about non-aromatic as indicated by the small positive NICS(0) values (0.5 for **9′***cis* and 0.1 for **9′***trans*). Also the 89.9(*cis*)/ 94.1 ppm (*trans*) measured ^{77}Se chemical shift of derivative $\mathbf{9}^{cis/trans}$=Se, is somewhat more negative than for 1, 3-diisopropyl-imidazole-2-selone (-3 ppm), and comparable to 1, 3-dipp-imidazole-2-selone (87.0 ppm).[134]

4.2.2. Cyclic voltammetric studies

To investigate the electrochemical properties of the bis(carbene)$\mathbf{9}^{cis/trans}$ in solution cyclic voltammetry (CV) in both THF (0.2 M [^{n}Bu$_4$N][PF$_6$]) and CH_2Cl_2 (0.4 M [^{n}Bu$_4$N][PF$_6$]) at gold ceramic screen printed electrodes (Au CSPE®) was used. Similar results were obtained in both solvents, but the behaviour in CH_2Cl_2 is better defined. For $\mathbf{9}^{cis/trans,}$ an irreversible oxidation process with $E_{p1}^{a} = -0.16\ V\ vs. Fc^{+/0}$(Fc = ferrocene) in CH_2Cl_2 (Figure 4.6), and $-0.45\ V$ in THF was observed (Figure 4.8). Scanning further positive indicates several closely-spaced subsequent oxidation processes with peaks with $E_{p2}^{a} = +0.18\ V$ and $E_{p3}^{a} = +0.42\ V$ (with which are associated strongly offset reduction processes $E_{p2}^{c} = -1.00\ V$ and $E_{p3}^{c} = -0.58\ V$) and continuous anodic current to the solvent limit (Figure. 4.7). In the cathodic region, a process is observable at the edge of the CH_2Cl_2 solvent limit with $E_{p4}^{c} = -2.36\ V$. In THF, this cathodic process has a defined return peak ($E_{p4}^{c} = -3.10$; $E_{p4}^{c1} = -2.72\ V$) (Figure 4.6).

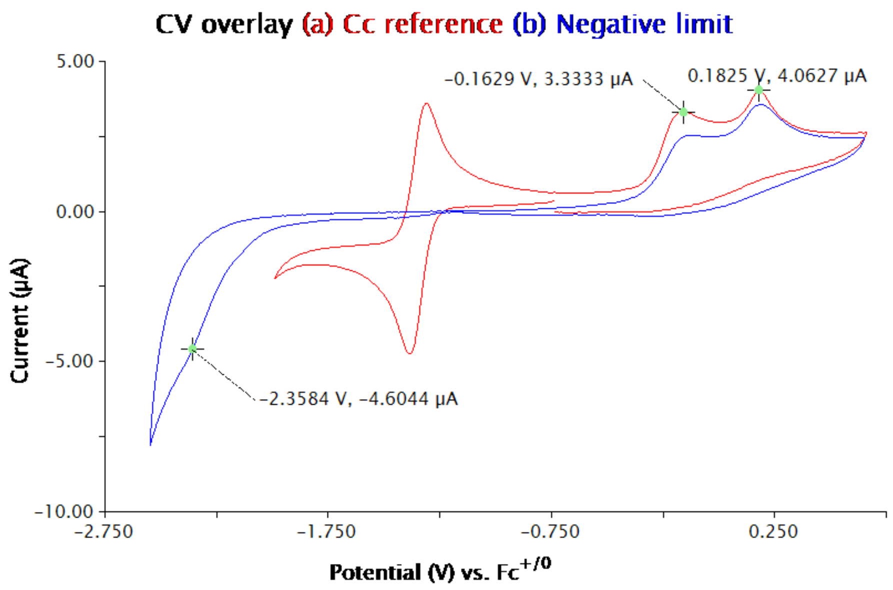

Figure 4.6. Cyclic voltammogram of a 1.0 mM solution of $\mathbf{9}^{cis/trans}$(0.4 M [^{n}Bu$_4$N][PF$_6$] in CH_2Cl_2) at 50 mVs^{-1} (a) also containing 1.0 mM [Cp_2Co][PF$_6$] as internal reference. (b) Before adding the cobaltocenium salt but including scans to the cathodic limit.

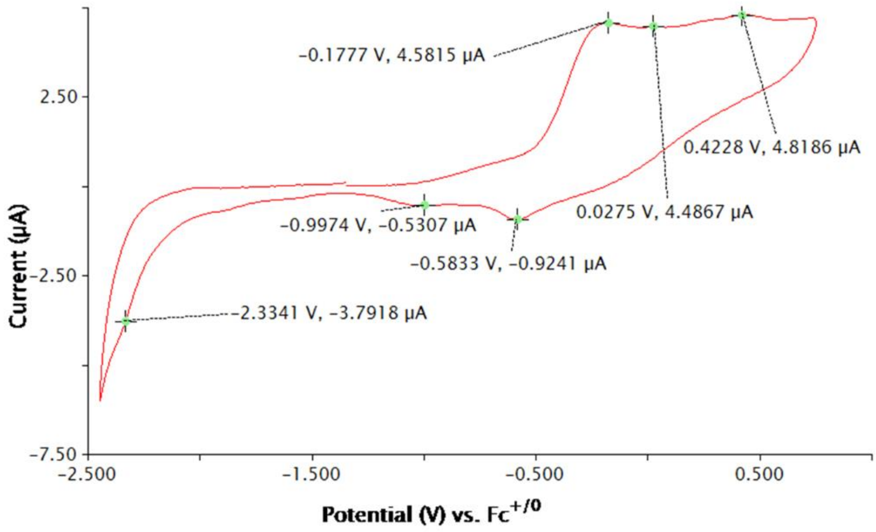

Figure 4.7. Cyclic voltammogram of a 1.0 mM solution of **9**$^{cis/trans}$(0.4 M [^{n}Bu$_4$N][PF$_6$] in CH_2Cl_2) at 200 mVs^{-1} scanned to the cathodic limit. Offset reduction processes at -1.00 and -0.53 V is connected to the anodic peaks at +0.03 and +0.42 V and are not observed with slower scan rates.

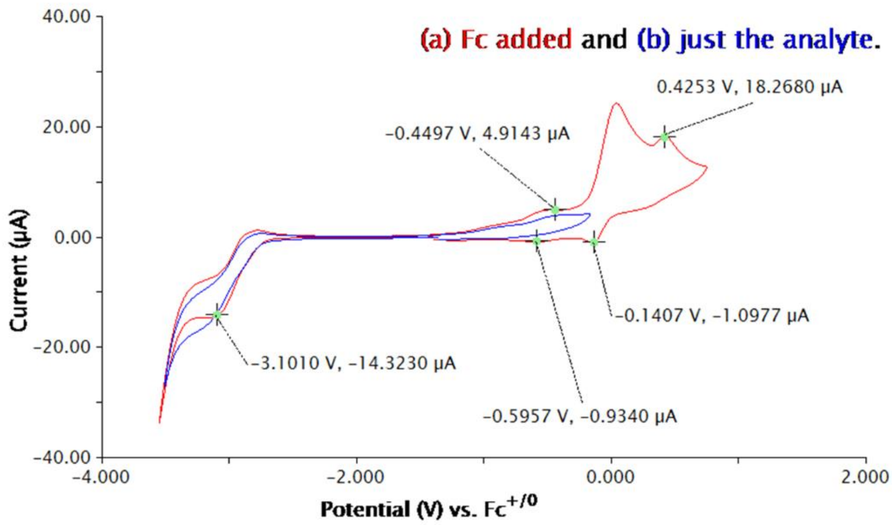

Figure 4.8. Cyclic voltammogram of a 1.0 mM solution of **9**$^{cis/trans}$(0.2 M [^{n}Bu$_4$N][PF$_6$] in THF) at 200 mVs^{-1} also containing 1.0 mM Cp_2Fe as internal reference.

4.3. Complexation of tricyclic {P(O)NEt$_2$}-functional bis(NHCs)

4.3.1. Synthesis of Ag(I) and Cu(I) bis(NHC) complexes 10a,b$^{cis/trans}$

New coinage metal(I) *P*-functional bis(NHC) complexes **10a,b**$^{cis/trans}$ were formed via deprotonation using the respective metal(I) oxides, a method described previously in the literature.[135, 136] Thus, treatment of metal oxides M_2O (M = Cu, Ag) with **8**$^{cis/trans}$(1:0.8) in CH_2Cl_2 solutions at ambient temperature led to the formation of Ag(I) (1:0.4), Cu(I) (1: 0.3) complexes in moderate to good yields (Scheme 4.5). These complexes **10a, b**$^{cis/trans}$ were fully characterized by multinuclear NMR spectroscopy [^{1}H, ^{31}P,^{13}C{^{1}H}]. The ^{31}P NMR spectrum revealed two signals corresponding to *cis* and *trans* isomers at δ = -3.9, - 3.3 ppm (Cu) and δ = - 4.1, - 3.6 ppm (Ag) slightly downfield shifted compared to the educt.

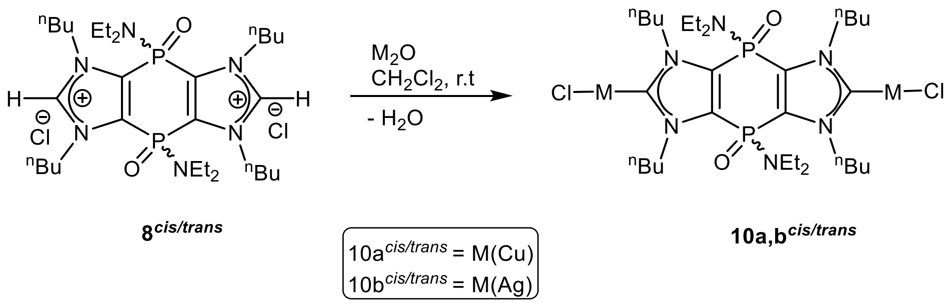

Scheme 4.5. Synthesis of tricyclic bis-NHC Ag(I) and Cu(I) complexes **10a,b**$^{cis/trans}$.

Further confirmation for **10a,b**$^{cis/trans}$ came from the ^{13}C{^{1}H} NMR spectrum as the C^2 imidazolium carbon at δ = 147.3 ppm was not observed. However, new signals at δ = 186.2 ppm for Cu(I) and 188.9 ppm for Ag(I) complexes were seen, which were assigned to the C^2 carbons (Table 4). The observed chemical shifts were in the typical range for the NHC silver(I) and copper(I) complexes, reported earlier.[137] The coordination of the bis(NHC) ligand to the metal ion (M = Cu, Ag) was confirmed by positive ESI mass spectrometry showing the following values m/z 798.25 $[C_{32}H_{59}Cu_2ClN_7O_2P_2]^+$ and 886.19 $[C_{32}H_{59}Ag_2ClN_7O_2P_2]^+$.

4.3.2. Synthesis of a Au(I) bis(NHC)complexes 10c$^{cis/trans}$

Various reports have shown that direct reaction of NHCs with Au(I) reagents to synthesize Au(I) NHC complexes should not be attempted as several hurdles and drawbacks could be envisaged, such as usage of inert conditions as well as (potential) competition of disproportionation and decomposition processes, thus leading to poor yields.[138] So, it was decided to treat the Ag(I) bis-NHC complex mixture **10b**$^{cis/trans}$ with [AuCl(SMe$_2$)] in methylene chloride to achieve the transmetallation reaction[136, 139] and formation of **10c**$^{cis/trans}$ (Scheme 4.6). After removing the silver chloride side product, compound **10c**$^{cis/trans}$ was isolated as an ivory-coloured solid in moderate yield (68 %).

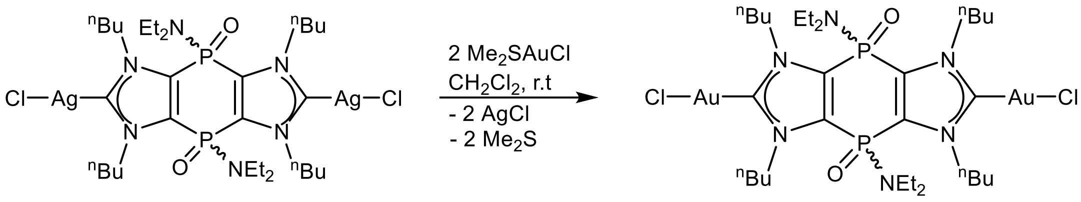

10b$^{cis/trans}$ **10c**$^{cis/trans}$

Scheme 4.6. Synthesis of the tricyclic bis(NHC) Au(I) complexes **10c**$^{cis/trans}$.

The formation of **10c**$^{cis/trans}$ was confirmed by observing slightly downfield shifted C^2-carbon resonance signals relative to **10b**$^{cis/trans}$ at δ = 181.8 (t, $^3J_{P,C}$ = 2.3 Hz), 181.4 (t, $^3J_{P,C}$ = 2.3 Hz) corresponding to two isomers in the $^{13}C\{^1H\}$ NMR spectrum. Also, positive ESI mass spectrometry showed the m/z value 1064.3221(theor. 1064.3220) which is in good agreement with $[C_{32}H_{59}Au_2ClN_7O_2P_2]^+$ and, hence, supported the composition of **10c**$^{cis/trans}$.

The molecular structure for compound **10c**^{trans}was determined by single-crystal X-ray diffraction. The C2-N1 and C2-N2 bond distances are in the typical range for the NHC-Au-Cl complexes.[76,140,141]The angle C2-Au1-Cl1 (176.4(3)°) is close tolinearity and, hence, typical for mono NHC gold(I) chloride complexes.[142] Interestingly, the solid-state structures reveal a coordination polymer formed via intermolecular aurophilic interactions, which is shown for two molecules in figure 4.9.

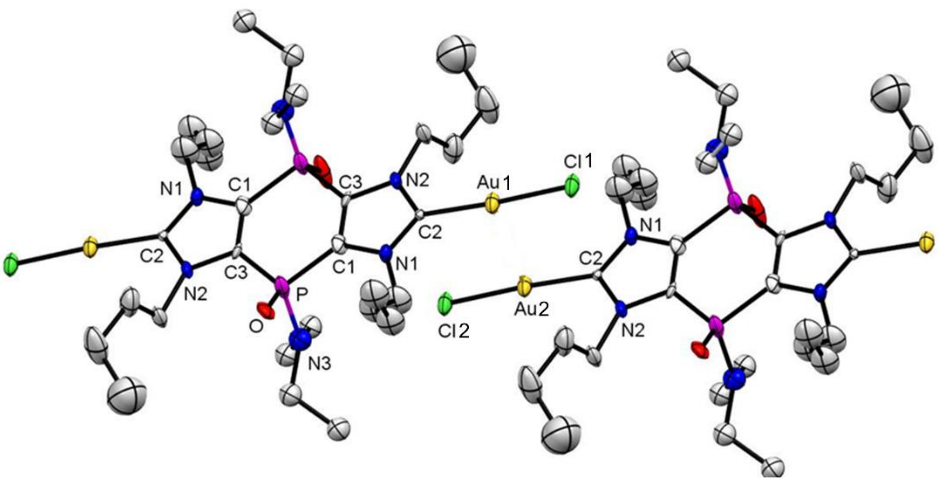

Figure: 4.9. Two next neighbouring molecules in thestructure of **10c*trans***. Ellipsoids are set at 50 % probability, and hydrogen atoms are omitted for clarity. Selected bond lengths [Å] and angles [°]:C2–N1 1.319(14), C1–P 1.772(13), Au···Au 3.221(3), N1–C2-N2 107.6(11)°, C1–P–C12 100.2(6)°, C2-Au-Cl1 176.4(3)°.

4.3.3. Syntheses of Rh(I) and Ir(I) bis(NHC) complexes 10d,e$^{cis/trans}$

After exploring the $P^{V/V}$ bis(NHCs) towards coinage metal(I) coordination, it was of great interest to study; further, the electronic properties of the tricyclic diphosphanoyl substituted bis(imidazole-2-ylidene) ligands using rhodium(I) and iridium(I) metal complexes. Therefore, the 1:0.7 mixture of bis(NHCs) **9**$^{cis/trans}$ was treated with 1 eq. of $[M(cod)Cl]_2$ (M = Rh, Ir, cod = 1,5-cyclooctadiene) in diethyl ether afforded the desired bis(NHC) complexes **10d**$^{cis/trans}$(1: 0.5) and**10e**$^{cis/trans}$ (1: 0.6) (Scheme 4.7). Products precipitated out of the reaction mixture, thus leading to yellow coloured solids, finally, confirmed by analytical data.

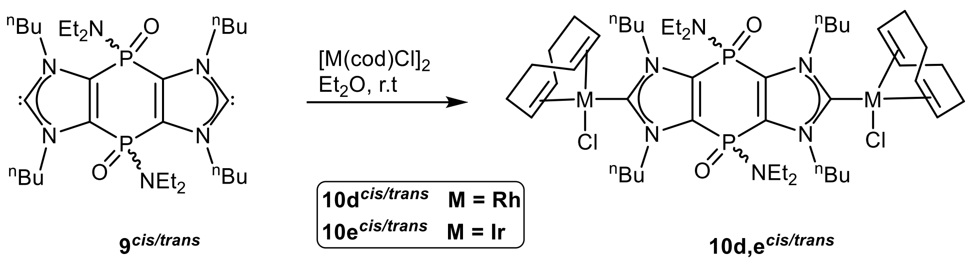

Scheme 4.7. Synthesis of tricyclic bis(NHC) Rh(I) and Ir(I) complexes **10d,e**$^{cis/trans}$

Mixtures of complexes **10d,e**$^{cis/trans}$ were fully characterized by NMR spectroscopy. In particular, informative are the $^{13}C\{^1H\}$ NMR signals easily assigned to the carbene (C^2) nuclei (Table 4) as they appear downfield-shifted with respect to those of Bielawski's complexes,[76] thus showing the electron-withdrawing effect of the P(V) centers of theP(O)NEt_2 groups. In addition, **10d**$^{cis/trans}$ showed chemical shifts of δ195.2 and 195.9ppm having $^1J_{Rh,C}$ = 52.1 Hz and $^3J_{P,C}$= 2.3 Hz.[143] Further confirmation was achieved by elemental and mass spectrometric analysis.

Table 4. ^{31}P NMR, ^{13}C NMR (C^2-nuclei) resonances and isomer ratio of **10a-e**$^{cis/trans}$**.**

	^{31}P NMR (ppm)	**$^{13}C\{^1H\}$ NMR (ppm)**	**Ratio**
10a$^{cis/trans}$	- 3.91 (*cis*), - 3.31 (*trans*)	186.1 (br)	1: 0.40
10b$^{cis/trans}$	- 4.10 (*cis*), - 3.62 (*trans*)	188.9 (br), 191.3 (br)	1: 0.16
10c$^{cis/trans}$	- 4.38 (*cis*), - 3.81 (*trans*)	181.8 (t, $^3J_{P,C}$ = 2.3 Hz), 181.4 (t, $^3J_{P,C}$ = 2.3 Hz)	1: 0.20
10d$^{cis/trans}$	- 4.60 (*cis*), - 3.75 (*trans*)	195.2 (ddd, $^1J_{C,Rh}$ = 52.1 Hz, $^3J_{P,C}$ = 1.8 Hz), 195.9 (ddd, $^1J_{C,Rh}$ = 52.1 Hz, $^3J_{P,C}$ = 1.7 Hz)	1 : 0.48
10e$^{cis/trans}$	- 4.28(*cis*), - 3.17 (*trans*)	191.1 (t, $^3J_{P,C}$ = 2.1 Hz), 191.8 (t, $^3J_{P,C}$ = 1.7 Hz)	1 : 0.61

5. Synthesis of (*P*-NEt$_2$) functional Janus type bis(NHCs) and its metal complexes

As Gates and co-workers had discovered the unusual reaction between asterically demanding NHC and a phosphaalkene to givethe first bifunctional 4-phosphanyl-NHC derivatives (**XCXII-XCXV)**.[1] This was later followed by Majhi to get more P^{III}-functional mono NHC derivatives (see chapter 8).[49]

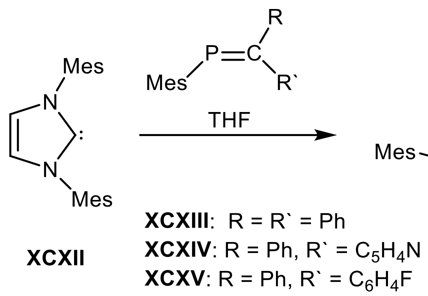

XCXII **XCXIII-XCXV**

Scheme 5.1. Formation of first P^{III} functional mono(NHC) derivatives by Gates.[144,145]

However, no example was reported concerning bis(NHC) having a phosphanyl bridged functionnality, so far.Toexamine relative nucleophilicities of *P*- and *S*-centers on imidazole-derived 1,4-dihydro-1,4-diphosphinines, theoretical studies[103] were performed to obtainmolecular electrostatic potential (MEP) values which showed that C=S-centers are more negative (= nucleophilic) than that of the *P*-centers. Moreover, the orbital coefficients for the HOMO of the molecules were found to be more located at the *S*-centers.

Thus, having access to neutral P$^{III/III}$-functional bis(NHC) and extend our studies towards ditopic and tetratopic complexes thereof, it was decided to adopt the synthetic strategy established for tetrathiafulvalene (TTF). The first step is the *S*-methylation of diathiole-2-thione using the electrophile methyl iodide (MeI), followed by reduction and deprotonation as shown in scheme 5.2, [146] without the dimerization step.

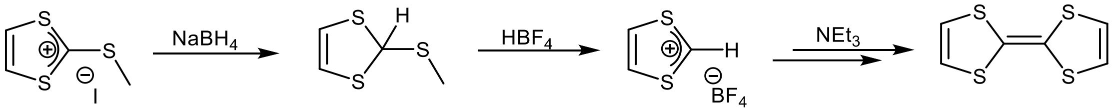

XCXVI **XCXVII** **XCXVIII** **XCXIX**

Scheme 5.2: Schematic synthetic protocol for TTF.[146]

5.1. Methylation of 1,4-dihydro-1,4-diphosphinine diselones 6*cis/trans*

In order to get access to $P^{III/III}$-functional Janus bis(NHCs), firstly, methylation of **6*cis/trans*** was carried out using methyl trifluoromethanesulfonate (MeOTf) in methylene chloride at room temperature (Scheme 5.3). The reaction was monitored by ^{31}P NMR spectroscopic analysis, revealing two signals belonging to *cis* and *trans* isomers (1: 0.7) and downfield-shifted resonances by almost 1 ppm compared to **6*cis/trans***.

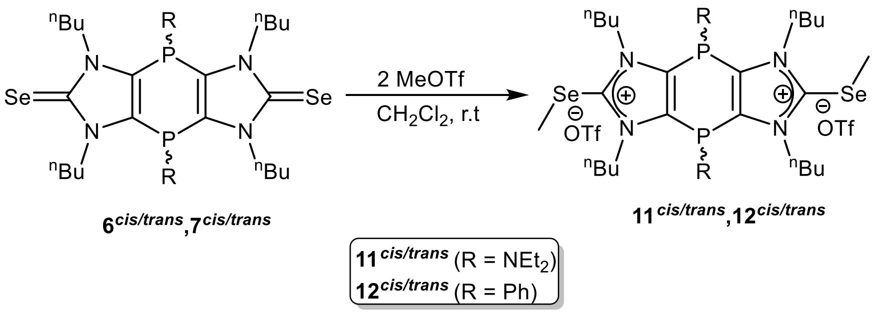

Scheme 5.3. Synthesis of tricyclic {P-NEt$_2$)-functional double methylated salts **11*cis/trans*** and **12*cis/trans***.

^{13}C NMR spectrum of **11*cis/trans*** showed new highfield-shifted singlets at δ = 142.6 ppm and 143.1 ppm belonging to two isomers, characteristic of C^2-carbon nuclei of imidazolium salts. Upon comparison of NMR data with reported similar compounds **XCXX**[103]and **XCXXI**[105] (Figure 5.1), it became evident that compounds **11*cis/trans*** were formed. Interestingly, ^{77}Se NMR data also showed a prominent downfield shift (δ = 115.1 (*cis*) ppm, 119.1 (*trans*) ppm) compared to the educt, indicating the delocalized cationic charge next to the selenium atoms. Further support came from the ESI-MS experiment, which exhibited an ion peak at m/z 376.1, assigned to the cation $[C_{32}H_{62}N_6P_2Se_2]^{+2}$in **11*cis/trans***. Compound **12*cis/trans*** was also synthesized using the same protocol and fully characterized.

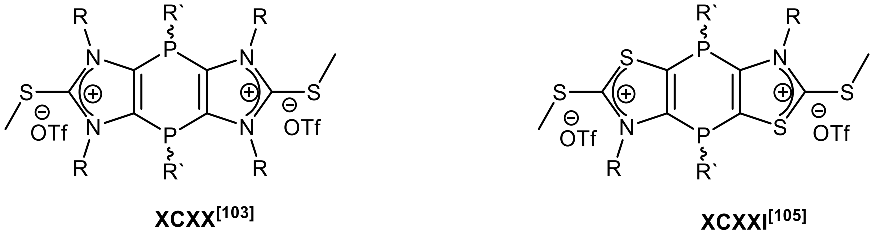

Figure 5.1. Literature known based *S*-methylated 1,4-dihydro-1,4-diphosphinines.[103,105]

Se-methylation in **12**$^{cis/trans}$ was confirmed by X-ray crystallographic measurement using single crystals grown from a saturated methylene chloride solution at –20 °C. Surprisingly, the *trans* isomer of the mono-methylated product **12**$^{cis/trans}$ (Figure 5.2) had crystallized; the monoclinic crystal system with the space group Pc was present. Close inspection of the packing pattern revealed that the Se-Me group is anti-periplanar oriented with respect to the plane of the tricycle. The C2-Se1 bond length is slightly elongated than reported similar compound **XCX** (C2-S1 1.7881(2) Å) as well as C14-Se2. All n-butyl and phenyl groups are *trans* to each other. Upon comparison to literature known thione dervatives, Se1-C8 bond length is significantly longer than in **XCX** (C2-S7 1.8114(1) Å).

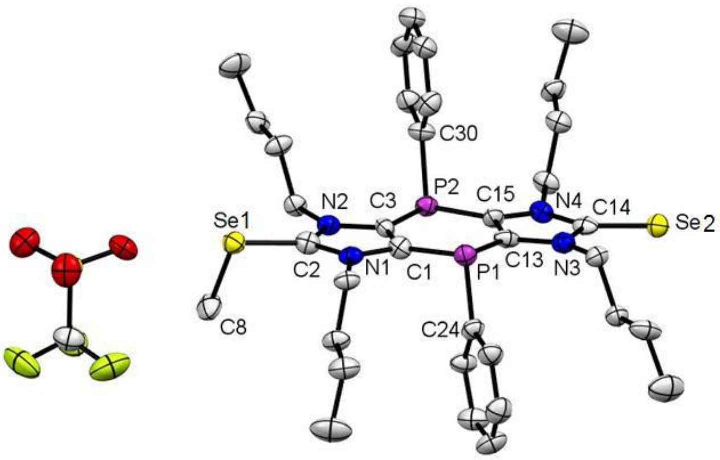

Figure 5.2. Molecular structure of **12**^{trans}. Ellipsoids are set at 50 % probability and hydrogen atoms are omitted for clarity. Selected bond lengths [Å] and angles [°]:N1-C2 1.345(16), C2-Se1 1.888(18), C14-Se2 1.818(13), Se1-C8 1.953(12), P2-C3 1.823(12), P2-C15 1.832(12);N1-C2-N2 106.2(11)°, N3-C14-N4 104.7(10)°.

5.2. Reductive deselenization of bis(*Se*-methylated) salts 11$^{cis/trans}$

A variety of methods have been employed for the reductive cleavage of selenides, including the use of Raney nickel,[148] lithium triethylborohydride,[149] and lithium in ethylamine.[148f] However, these reagents serve efficiently for a small range of substrates, as they are also capable of reducing many other functionalities. Later, tin hydride reagents were used for free-radical deselenizations with excellent selectivity in the presence of many other types of functionalities.[150,151] However, it does suffer from some limitations such as expensive reagents, elevated and inert conditions, and “hectic” isolating procedures.[152] Nevertheless, the first attemptswere made for the reductive deselenization of ketene diseleno-acetalusing nickel boride. The reaction required only afew minutes without the need for an inert atmosphere.[148b, 153]The precise mechanism of the nickel boride mediated deselenization reaction was speculative with the finding that a transient Ni(0) or nickel hydride species on the nickel boride surface plays a key role in the process.

By keeping background knowledge of reductive deselenization and synthetic protocol of TTF in mind, we decided to reduce compound **$11^{cis/trans}$**selectively using reducing agent ($NaBH_4$) sodium borohydride in methanol at 0 °C (Scheme 5.4). Upon addition of $NaBH_4$, a strong odour was observed due to the formation of volatile compound HMeSe as a side product. The reaction was monitored by ^{31}P NMR spectroscopy depicting a very slight downfield shift of resonance signals at δ = 5.4(*cis*) ppm and 5.8 (*trans*) ppm.

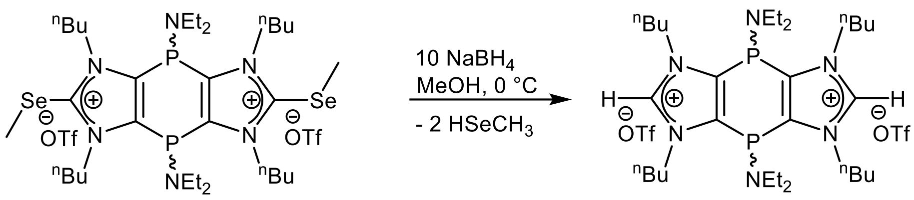

$11^{cis/trans}$ **$13^{cis/trans}$**

Scheme 5.4. Synthesis of tricyclic {P-NEt_2)}-functional bis(imidazoium) salts **$13^{cis/trans}$**.

To get further insight in the reaction mixture, it was isolated using column chromatography and subjected for ^{1}H NMR measurements. On comparison of proton NMR spectrums of educt and product, all the signals belong to *n*-butyl and bis-diethyl amino group are same in both spectra.

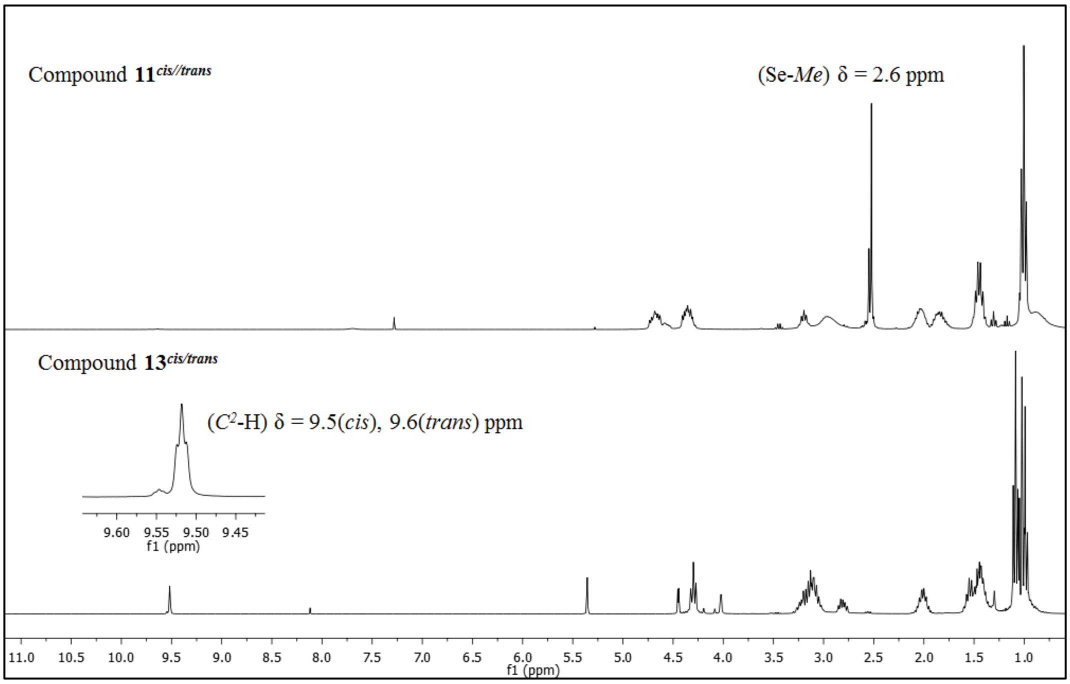

Figure 5.3. ^{1}H NMR spectrums of **11**$^{cis/trans}$ (bottom, $CDCl_3$, 25 °C) and **13**$^{cis/trans}$ (top) (CD_2Cl_2, 25 °C).

However, the two singlets belongs to Se-*Me* protons appeared at δ = 2.5 and 2.6 chemical shift values in the bottom spectrum, vanished in the top spectrum, as shown in figure 5.3. Furthermore, two new characteristic signals showing triplet pattern at δ = 9.5, 9.6 ppm ($^4J_{P,H}$ = 1.8 Hz) appeared in the top spectrum, corresponding to *cis* and *trans* imidazolium protons which supporting the formation of bis(imidazolium) salts **13**$^{cis/trans}$. Table 5.1 depicts a relative study of ^{1}H NMR chemical shift of C^2-H protons, revealing the effect of heteroatom functionality on its acidic properties [154]. Two phosphanoyl group substitution causes a downfield shift of Δδ = 2.5, whereas two phosphanyl groups causes downfield shift of Δδ = 0.6 compared to C^2unsubstituted imidazolium salts **XCXXII** reported by Belawski and co-workers.[155] Similar chemical shift changes are also observed in the ^{13}C{^{1}H} NMR spectrum for imidazole ring C^2 nuclei between phosphanoyl and phosphanyl substituted imidazolium salts, probably due tothe electron-withdrawing nature of the phosphanoyl group(s). The constitution of compound**13**$^{cis/trans}$ was further confirmed by HRMS (pos. ESI) m/z {theor.(exp.)565.428 (565.429)} and elemental analysis.

Table 5.1. Comparison of ^{1}H and $^{13}C\{^{1}H\}$ NMR chemical shifts (ppm) of (C^{2}-*H*) between **XCXXII**,[76,78] $\mathbf{8}^{cis/trans}$ and $\mathbf{13}^{cis/trans}$

	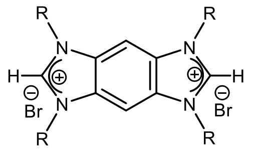 **XCXXII**	$\mathbf{13}^{cis/trans}$	$\mathbf{8}^{cis/trans}$
$\delta^{1}H$	9.1 (s)	9.5 , 9.6 ($^{4}J_{P,H}$ = 1.8 Hz)	11.1, 11.8(br)
$\delta^{13}C\{^{1}H\}$	147.0 (s)	140.9 (br,C^{2})	147.3 (br,C^{2})

5.3. Deprotonation of bis(imidazolium) salts ($\mathbf{13}^{cis/trans}$)

Low-coordinate phosphanyl bridged Janus-type bis(NHCs) $\mathbf{14}^{cis/trans}$ were selectively formed by deprotonation of bis(imidazolium) salts $\mathbf{13}^{cis/trans}$ using KHMDS as strong base in THF (Scheme 5.5). Reaction was monitored by ^{31}P NMR spectroscopy showing a slight downfield shift at δ = 6.6 (*cis*) and 6.9 (*trans*) in 1: 0.3 ratio.The identification of signals at δ = 220.3(*cis*), 220.4(*trans*) ppm (t, $^{3}J_{P,C}$ = 3.5 Hz) in the $^{13}C\{^{1}H\}$ NMR spectrum is consistent with the presence of the C^{2} nuclei of the $P^{III/III}$-functional bis(NHCs) $\mathbf{14}^{cis/trans}$.

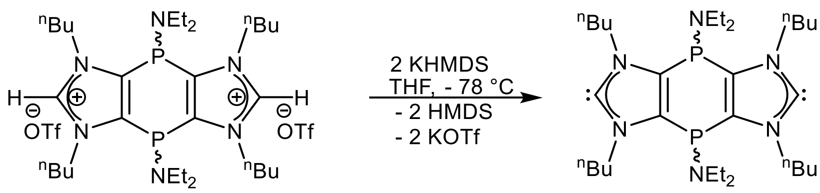

$\mathbf{13}^{cis/trans}$ $\mathbf{14}^{cis/trans}$

Scheme 5.5. Synthesis of tricyclic {P-NEt_2)}-functional bis(NHCs)$\mathbf{14}^{cis/trans}$.

These values are very well in agreement with reported annulated bis(NHCs) [155, 156] and relatively highfield shifted than $P^{V/V}$-functional bis(NHCs) $\mathbf{9}^{cis/trans}$. In addition, the absence of C^{2}-H protons in the ^{1}H NMR spectrum supported the formation of $\mathbf{14}^{cis/trans}$. EI mass spectrometry also confirmed the composition of $\mathbf{14}^{cis/trans}$ showing HRMS with *m/z* 563.4118/563.4116(theor./exp.) for [$C_{30}H_{56}N_{6}P_{2}$] monocation.

Attempts to confirm the formation of compound $\mathbf{14}^{cis/trans}$ by means of X-ray crystallographic measurements brought a surprising result. The crystals, obtained by slow evaporation of saturated solution of diethyl ether and *n*-pentane mixture (1:1) at - 20 °C, were analysed by X-ray crystallography. The results showed an unexpected solid state structure for its *cis* isomer (Figure 5.4). One KHMDS moleculecoordinated to one carbene center while two hydrogen atoms were bound to the other carbene center. Furthermore, another KHMDS molecule is coordinated to one imidazole ring via a η^4 coordination mode. The selected bond parameters are given in the figure caption. Despite being monomeric, the C14-K2 distance of 2.905(5) Å falls in the typical range of K-C carbene interactions found in the literature for the polymeric potassium imidazol-2-ylidene complexes{*e.g*C(3)-K distance of 3.066(6) Å by Majhi[96]}.[157] The N1-C3 and C3-N2 bond distances are larger than C14-N3 and C14-N4 (Figure 5.4). Similarly, P2-C2 bond length of 1.820(4) Å slightly lengthened than the P1-C13 1.804(5) Å, which is different from the situation in **9***trans*. The most evident change in the geometry of imidazole ring was observed from the N3-C14-N4 bond angle of 102.7(4)° and N1-C3-N2 of bond angle 101.1(3) are comparable to literature known examples {102.40(11)° (in **9***trans*) and 102.1(5)°[158]}.

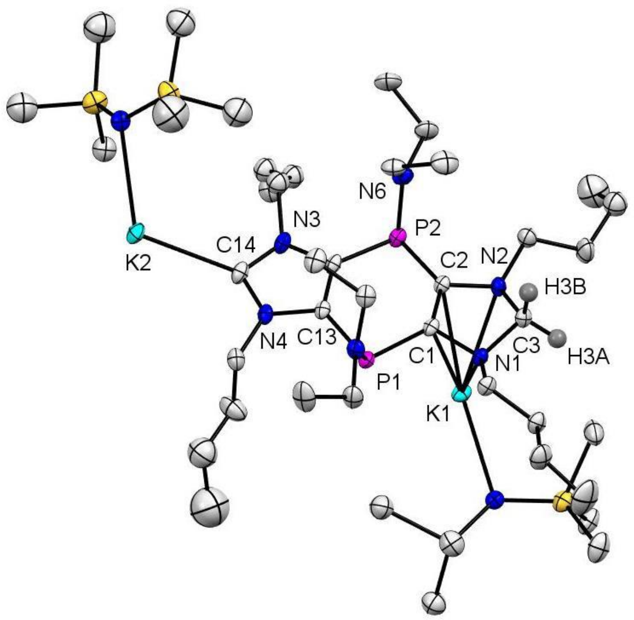

Figure 5.4. Molecular structure of **14***cis*. Ellipsoids are set at 50 % probability, and hydrogen atoms are omitted for clarity. Selected bond lengths [Å] and angles [°]:N1-C3 1.450(6), C3-N2 1.460(6), C14-N31.355(7), C14-N4 1.357(6), C14-K2 2.905(5), P1-C13 1.804(5) P2-C2 1.820(4);N1-C3-N2 101.1(3) °, N3-C14-N4 102.7(4)°.

5.3.1. Theoretical investigations

The main results of the theoretical investigations of Nyulászi and co-workers [118] are the following. As for **9′***cis/trans*, the energy difference between the two isomers of **14′***cis/trans* is small (0.8 kcal/mol). However, in the case of **14′** the *cis* isomer is the more stable one. The inversion barrier of the phosphorus center is high (44.2 kcal/mol); thus, isomerization cannot be expected at room temperature. The stabilization energy in reaction (*1*) of **14′** (111.1 kcal/mol for *cis* and 109.2 kcal/mol for *trans*) is also close to those of the parent imidazole-2-ylidene and **9′**. The aromaticity of the imidazole ring decreased somewhat according to the NICS(0) values (-9.2 for *cis* and -9.5 for *trans*) compared to **9′**$^{cis/trans}$. On the other hand, the aromatic character of the middle ring increased slightly, which was indicated by the negative (although small) NICS(0) values (-0.5 for **14′**^{cis} and -0.9 for **14′**^{trans}. Oxidation of P^{III} centers was shown to increase antiaromaticity in phospholes.[159] This is due to the increased involvement of σ* orbitals, which are significantly lower in energy for the P^{V} system.[160]

In accordance, the shape and the localization of HOMO and the LUMO of **7′**$^{cis/trans}$ are similar to **3′**$^{cis/trans}$, their energy levels (especially that of the LUMO) are somewhat stabilized (Figure. 5.5). Interestingly, the stabilization of the LUMO of **9′**$^{cis/trans}$ with respect to **14′**$^{cis/trans}$ has not too much effect on the electron acceptor property of the NHC since the carbene atoms are not involved in the LUMO.

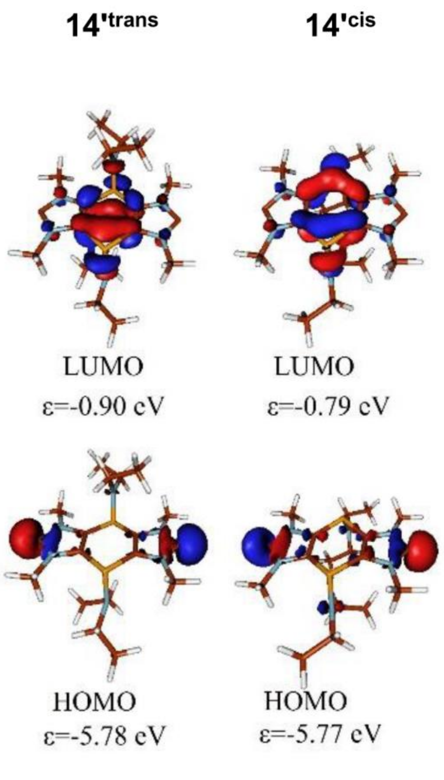

Figure 5.5. Kohn-Sham frontier orbitals of **14′** and their energies at B3LYP/6-31+G*//M06-2X/6-31+G* level of theory.

Indeed, the 35.9 (*cis*) / 37.9 (*trans*) ^{77}Se chemical shift of **7**$^{cis/trans}$ is closer to that of 1,3-diisopropyl-imidazole-2-selone (-3 ppm, than in the case of **9**$^{cis/trans}$ (89.9/94.1 ppm – see above), showing that the P^{V} substitution increases somewhat the electron acceptor ability of the carbene, however, these values are still within the known range of imidazole-2-ylidenes.[161]

5.3.2. Cyclic voltammetric studies

The electrochemical behaviour of the bis(NHCs) **14**$^{cis/trans}$, similarily to **9**$^{cis/trans}$, was also investigated by cyclic voltammetry (CV) in both THF (0.2 M [$^{n}Bu_4N$][PF_6]) and CH_2Cl_2 (0.4 M [$^{n}Bu_4N$][PF_6]). For **14**$^{cis/trans}$, the first oxidation in CH_2Cl_2 displays a return peak ($E_{p1}^{a} = -0.30$; $E_{p1}^{c} = -0.42\ V; \Delta E = 120\ mV; E_m = -0.36\ V$; Figure 5.6) but scanning even slightly more positive wipes the return wave and shows several other anodic peaks with a continuous anodic current to the limit (Figure 5.7). In THF, there is no evidence of a return peak and $E_{p1}^{a} = -0.61\ V$ (Figure5.8). In the anodic region, **7**$^{cis/trans}$ appear irreversible with $E_{p4}^{c} = -1.93\ V$ in CH_2Cl_2 but in THF, there is an observable return peak ($E_{p4}^{c} = -2.75$; $E_{p4}^{a} = -2.592\ V; \Delta E = 160\ mV; E_m = -2.67\ V$).

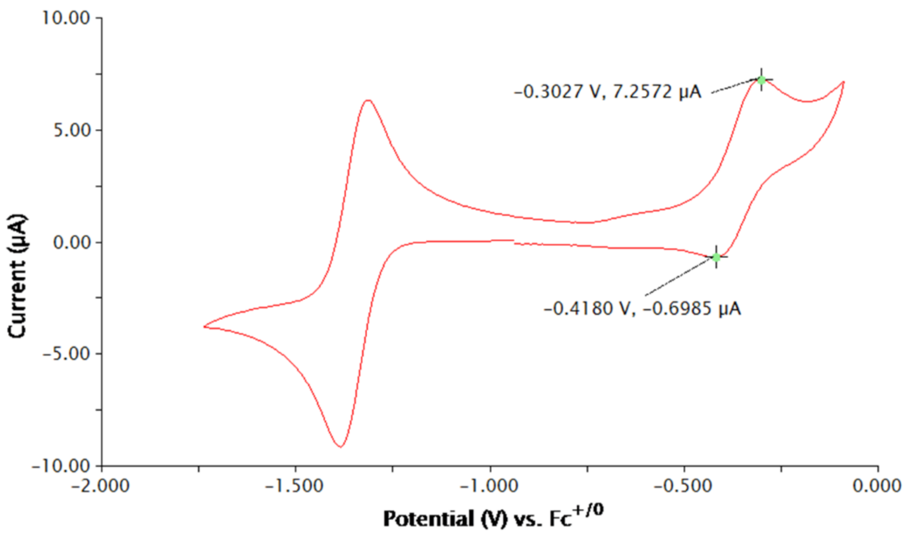

Figure 5.6. Cyclic voltammogram of a 1.0 mM solution of **14**$^{cis/trans}$ (0.4 M [$^{n}Bu_4N$][PF_6] in CH_2Cl_2) at 50 mVs^{-1} also containing 1.0 mM [Cp_2Co][PF_6] as internal reference.

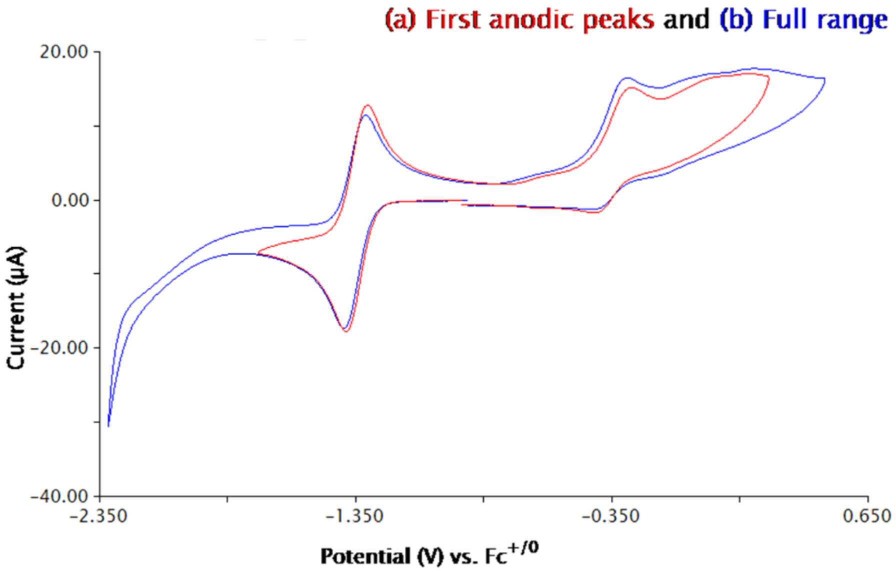

Figure 5.7. Cyclic voltammogram of a 1.0 mM solution of **14**$^{cis/trans}$ (0.4 M [^{n}Bu$_4$N][PF$_6$] in CH_2Cl_2) at 50 mVs^{-1} also containing 1.0 mM [Cp$_2$Co][PF$_6$] as internal reference (a) through the anodic peaks and (b) scanned to include the onset of a cathodic process.

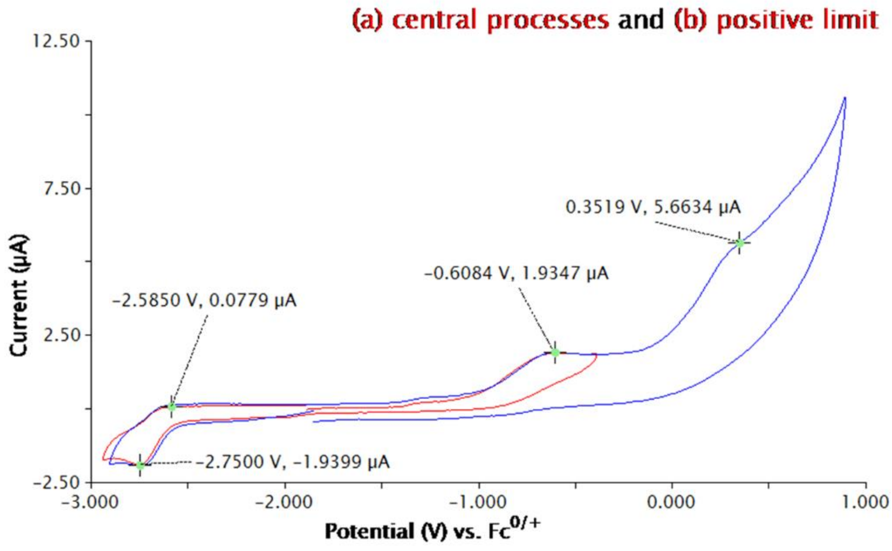

Figure 5.8. Cyclic voltammogram of a 1.0 mM solution of **14**$^{cis/trans}$ (0.2 M [^{n}Bu$_4$N][PF$_6$] in THF) at 200 mVs^{-1} (a) through the first cathodic and first anodic peaks and (b) scanned to the anodic limit.

In none of these experiments are distinct processes from the *cis* and *trans* isomers observable. Moreover, the irreversible nature of the (first) oxidations is evidenced by a scan-rate and strong solvent dependencies of the potentials, as previously observed for voltammetry of carbenes [162,163].As suggested first by Clyburne, imidazolium-based cations are electroactive. Their cathodic reduction yields the NHC and dihydrogen. The electrogenerated NHC is electroactive as well, and it is involved in a mono oxidative process.The oxidation of that carbene leads to various products, of which the dication dimer has been observed in some cases, i.e. a C-centered radical coupling mechanism. In addition, the carbenes slowly react with solvent/electrolyte over the course of the experiment, which could complicate the coulometry of these species.[162, 163] The unprecedented results from voltammetry of these dicarbenes – previously only voltammetry of metal complexes of some dicarbenes were reported [164] – are in broad agreement with the DFT calculations.

Thus, in either solvent, **14***cis/trans* are more easily oxidized than **9***cis/trans* in accordance with the higher energy of their HOMO orbitals. Similarly, the numerous, closely spaced anodic processes can be understood in the light of the existence of numerous filled MOs close in energy to the HOMO that has either carbene α (C) or ring π character.

5.4. Complexation of tricyclic (P-NEt$_2$)-functional bis(NHCs)

5.4.1. Synthesis of coinage metal (I) bis(NHC) complexes

Low-coordinate P-functional bis(NHCs) were also examined for their coordination properties, especially the C^2vs phosphane-type reactivity of **13***cis/trans* towards coinage metal oxides, as shown in Scheme 5.6. The treatment of a methylene chloride solution of **13***cis/trans* with stoichiometric amounts of Cu_2O and Ag_2O led to the formation of bis(NHC)**15a***cis/trans* and **15b***cis/trans*. $^{31}P\{^1H\}$ NMR data are very similar to the respective bis(imidazolium) salts **13***cis/trans*, given in Table 5.2.

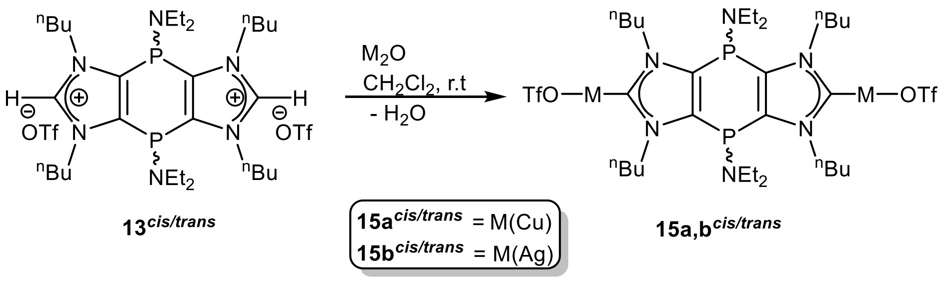

Scheme 5.6. Synthesis of tricyclic bis(NHC) Ag(I) and Cu(I) complexes **15a,b***cis/trans*.

However, Au(I) bis(NHC) complexes were synthesized using[AuCl(SMe$_2$)]as reagent and compounds**15b***cis/trans* in methylene chloride (Scheme 5.7). After removal of the solvent and drying, the^{31}P NMR spectrum revealed slight highfield-shifted resonances for the isomeric mixture, as given in Table 5.2. Pos-ESI-MS spectrum of the obtained yellow-brownsolid showed the HRMS (pos-ESI) for **15c***cis/trans* ($[C_{33}H_{59}Au_2F_3N_7O_3P_2S]^+$ *m/z* = theor. (exp.) 1148.3315 (1148.3311)

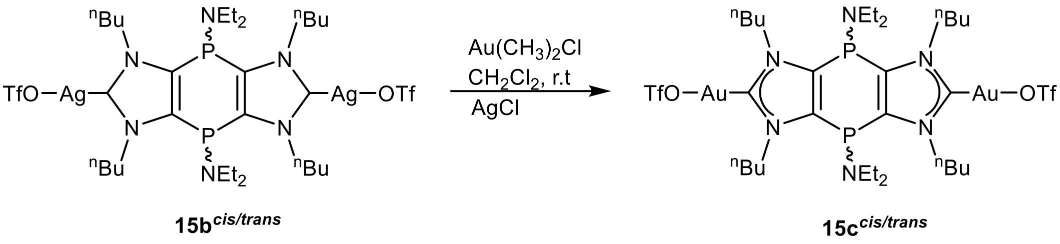

Scheme 5.7. Synthesis of tricyclic bis(NHC) Au(I) complexes **15c***cis/trans*.

The obtained products **15a-c***cis/trans* displayed signals at δ = 4.2 (*cis*), 5.0 (*trans*), δ = 3.3 (*cis*) and 3.7 (*trans*) and δ = 2.4 (*cis*) and 3.1 (*trans*), respectively, in the ^{31}P NMR spectrum (Figure. 5.9). The identification of signals at δ = 171.0 ppm (br; **15a***cis/trans*), δ = 179.1 ppm (br; **15b***cis/trans*) and δ = 172.1 and 172.3 (t, $^{3}J_{P,C}$ = 2.6 Hz; **15c***cis/trans*) in the ^{13}C{^{1}H} NMR spectrum (Figure. 5.9) is consistent with the presence of the C^2 nuclei of the bis(NHC) derivatives **15a-c***cis/trans*.

It is evident from the ^{13}C{^{1}H}) NMR spectra (Figure. 5.9) that the C^2centers resonate more in the downfield region compared to bis(imidazolium) C^2 nuclei in all the three cases. For **15b***cis/trans*,due to the dynamic behaviour as well as the poor relaxation of the quaternary C^2 carbon resulting quite broaden C^2 signal, thus, could not observe $^{1}J_{Ag,C}$ satellites.[165] Besides NMR spectroscopy, **15a-c***cis/tran* were characterized via IR spectroscopy and mass spectrometry, as well aselemental analysis.

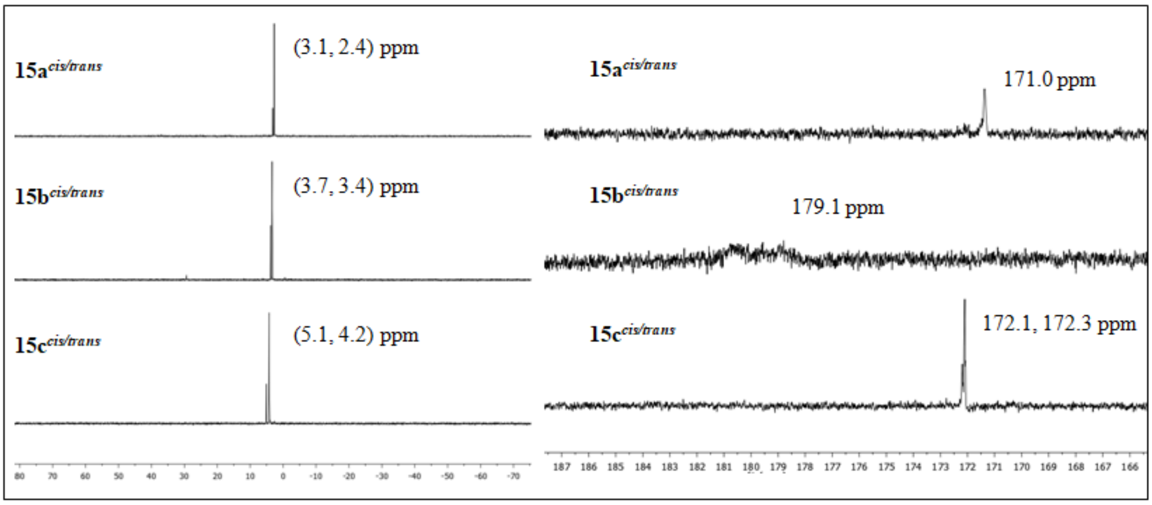

Figure 5.9. ^{31}P{^{1}H} NMR spectrum (left) and ^{13}C{^{1}H} NMR spectrum (right, C^2 nuclei) of **15a-c***cis/trans*.

5.4.2. Synthesis of Rhodium(I) bis(NHC) complex 15d$^{cis/trans}$

After getting access to coinage metals bis(NHC) complexes, and to enable a better comparison, we extended our studies to the synthesis of Rh(I) complexes of respective tricyclic phosphanyl substituted bis(NHC) ligands. In particular, ethereal solution of bis(NHCs)**14**$^{cis/trans}$was treated with $[Rh(cod)Cl]_2$, 1 eq.) at ambient conditions, afforded the desired bis(NHC) complexes **15d**$^{cis/trans}$ (Scheme 5.8). Again, a clean reaction occurred and the products were obtained in moderate yield (62 %).

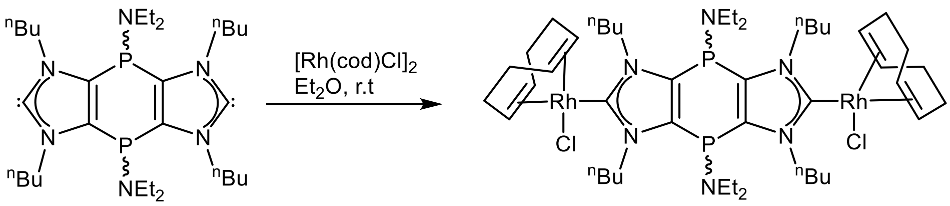

14$^{cis/trans}$ **15d**$^{cis/trans}$

Scheme 5.8. Synthesis of tricyclic bis(NHC) Rh(I) complexes **15d**$^{cis/trans}$.

The $^{31}P\{^{1}H\}$ and $^{13}C\{^{1}H\}$ NMR spectroscopic data confirmed that **15d**$^{cis/trans}$ coordinate through the carbene rather than the phosphane-type center. For comparison, C^2 resonances of tricyclic phosphanoyl bis(NHC) complexes **10d**$^{cis/trans}$ are shifted highfield with respect to the analogous Bielawski`s rhodium(I) complex **XCXIII**[78] ($\Delta\delta$ = 3.2). Interestingly, an even larger highfield shift in C^2 is observed for the bis(NHC) complexes **15d**$^{cis/trans}$ with respect to the reported complexes**XCXIII** ($\Delta\delta$ = 8.2). In addition, the bis(diethylamino)phosphanyl derivative **15d**$^{cis/trans}$ showed a chemical shift of δ = 190.3 ppm having $^{1}J_{Rh,C}$ = 50.7 Hz and $^{3}J_{P,C}$ = 3.6 Hz. Presumably, the trend in highfield shifts is a consequence of the electron-donating nature of $P(NEt)_2$ groups in **15d**$^{cis/trans}$ compared to the electron-withdrawing effect imparted by the $P(O)NEt_2$ in **10d**$^{cis/trans}$. However, in the $^{13}C\{^{1}H\}$ NMR spectrum,the same trend of resonance shifting towards higher field was also reported by Streubel *et.al* for the mono-phosphanyl substituted NHC complex.[49]

Table 5.2. Comparison of $^{13}C\{^1H\}$ NMR chemical shifts (ppm) between **XCXXIII**,[13] **10d*cis/trans*** and **15d*cis/trans***

	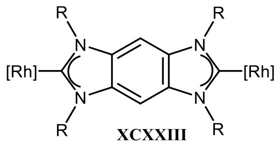 **XCXXIII**	**10d*cis/trans***	**15d*cis/trans***
$\delta^{13}C\{^1H\}$/ppm	198.0 (d, $^1J_{C,Rh}$ = 51.4 Hz)	195.20 (ddd, $^1J_{C,Rh}$ = 52.1 Hz, $^3J_{P,C}$ = 1.8 Hz), 195.88 (ddd, $^1J_{C,Rh}$ = 52.1 Hz, $^3J_{P,C}$ = 1.7 Hz)	190.3 (t, $^1J_{C,Rh}$ = 50.7 Hz, $^3J_{P,C}$= 3.6 Hz), 190.5 (t, $^1J_{C,Rh}$ =50.7 Hz)

5.4.3. Synthesis of hetero-dinuclear B/Rh(I)) complex 17$^{cis/trans}$

To gather more information on coordination properties of these neutraltricyclic phosphanyl substituted bis(NHCs) **14**$^{cis/trans}$ and to examine if these compounds can coordinate via C^2-centers as well as at the *P*-centers. To start this, compounds **15a-c**$^{cis/trans}$ were subjected to reactions with coinage (I) metal complexes, *e.g.*, [Au(Me_2S)Cl], [AgOTf(PPh_3)] etc., to synthesize tetratopic bis(NHC) complexes. But none of the metal complexes showed selective reactivity. Instead, reaction mixtures precipitated out as dark-coloured solids, insoluble in organic solvents (CH_2Cl_2, THF). Later, these precipitates were dissolved in methanol, and their $^{31}P\{^1H\}$ NMR spectra measured, but only showing unselective product formations. It might be due to the weak binding of coinage metal centers with phosphorus, thus leading to different product mixtures.

Therefore, the strategy to approach hetero-dinuclear bis(NHC) complexes using *P*-NEt_2-bridged bis(NHC) derivatives was changed. In the first step, compounds**13**$^{cis/trans}$ was treated with borane dimethyl sulfide (DMS) in methylene chloride at room temperature, and the reaction progress monitored by $^{31}P\{^1H\}$ NMR spectroscopy (Scheme 5.9).The $^{31}P\{^1H\}$ NMR spectrum of the reaction mixture showed complete consumption of the starting material after 3h. Compound **16**$^{cis/trans}$ could be isolated from the reaction mixture by washing the residues with *n*-pentane to obtain an orange powder in excellent yield (88 %).

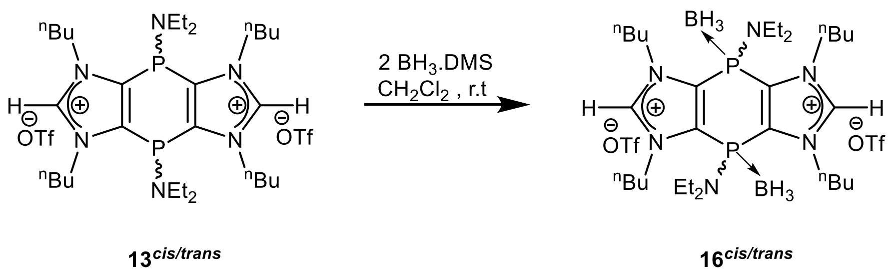

Scheme 5.9. Synthesis of tricyclic P-borane bis(NHC) complexes **16**$^{cis/trans}$.

The $^{31}P\{^1H\}$ NMR spectrum of **16**$^{cis/trans}$ showed a considerably downfield-shifted and broad (FWHM 78.5 Hz) resonance signals at 35.2(*cis*) ppm and 37.3(*trans*) ppm with 1: 0.1 isomeric ratio (Figure 5.10).

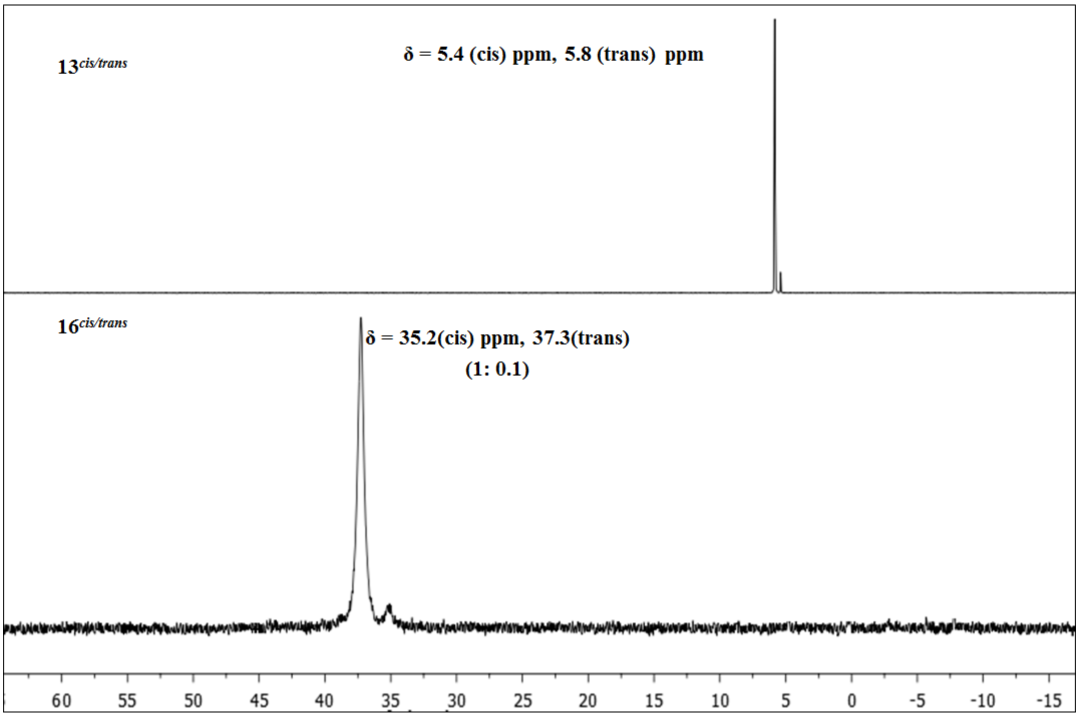

Figure 5.10. Comparison of $^{31}P\{^{1}H\}$ NMR spectra of compounds **13**$^{cis/trans}$ (top)and **16**$^{cis/trans}$(bottom).

This ^{31}P NMR chemical shift is close to the previously reported *P*-borane complex **XCXXIV** ($\delta^{31}P$ = 33.3 ppm)[102], however, downfield-shifted compared to NHC-phosphinidene borane complexes **XCXXV**($\delta^{31}P$ = 4.0 ppm)[166]. The appearance of a broad resonance signal and the noticeable downfield shift could be attributed to the direct connectivity of *P*-atom to a quadrupolar boron center, thus confirming the occurrence of P-borylation. Pos ESI-MS spectrum showed a molecular ion peak at m/z 593.4 assigned to $[C_{30}H_{64}N_6P_2B_2H]^+$ (z = 1), which lends further support to the formation of the diborane adducts **16**$^{cis/trans}$.

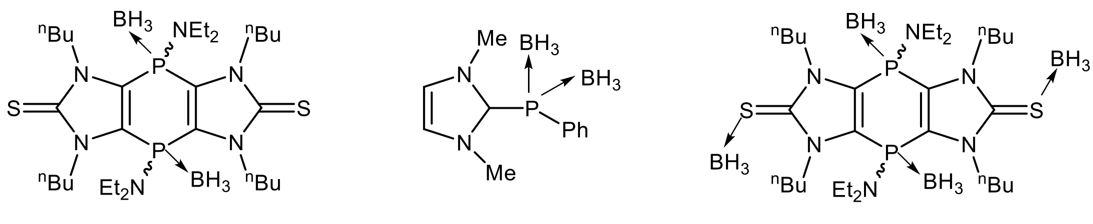

Figure. 5.11. Literature is known as borane phosphanido complexes **XCXXIV**[102],**XCXXV**[166], **XCXXVI**[103].

After having hands-on P-borane bis(NHC) complexes**16**$^{cis/trans}$, it was further explored towards the synthesis of hetero-tetratopic complexes. An initial study on the coordination abilities of $P^{V/V}$

systems having two phosphanoyl groups in the NHC backbone, was carried out by Majhi using titanium tetrachloride in methylene chloride (Scheme 5.10). The ^{31}P NMR spectroscopic data had revealed two sets of two resonances, which were attributed to two isomers of a mono-dentate phosphanoyl titanium(IV) adduct **XCXXVIII** with a single P-O-Ti interaction.[158] In another study, Koner had obtained some spectroscopic evidence for thebis(S-borane adduct) **XCXXVI,**[103],but due to reduced basicity of the *P*-centers, along with the formation of desired product **XCXXIV**. However, due to the partial S···B covalent bond, it could not be isolated.

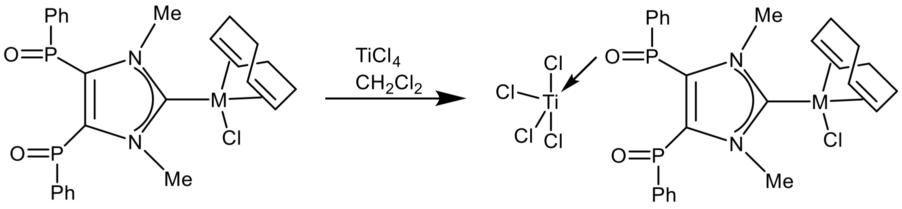

XCXXVII XCXXVIII[158]

Scheme 5.10. Literature known $P^{V/V}$ heterobimetallic (Ti(IV)/M(I)) complex **XCXXVIII**.[158]

These previous studies prompted us to further proceed using a deprotonation reaction of P-borane bis-NHC complexes**16**$^{cis/trans}$ followed by the addition of $[Rh(cod)Cl]_2$ (cod = 1,5-cyclooctadiene, 1 eq.), which afforded the desired tetratopic bis(NHC) complexes **17**$^{cis/trans}$ (Scheme 5.11).

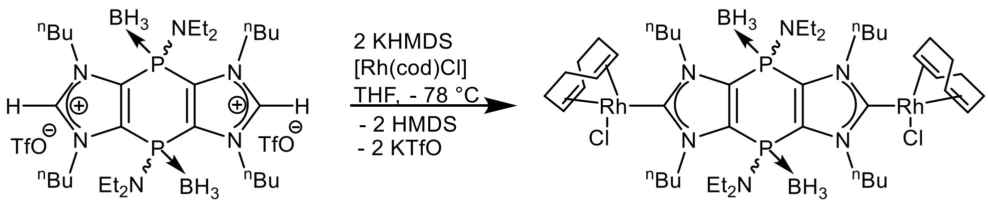

16$^{cis/trans}$ 17$^{cis/trans}$

Scheme 5.11. Synthesis of tricyclic heterobimetallic B/Rh(I) bis(NHC) complexes **17**$^{cis/trans}$.

Analysis of a THF solution of the product **17**$^{cis/trans}$ by ^{31}P{^{1}H} NMR spectroscopy showed a broad signal (δ = 36.9ppm). This signal was slightly downfield-shifted with respect to the starting material **16**$^{cis/trans}$ (35.2, 37. 3 ppm). The ^{13}C{^{1}H} NMR spectrum also supported the formation of compound **17**$^{cis/trans}$ with a downfield-shifted signal of theC^2nuclei at 187.4 (d, $^{1}J_{Rh,C}$= 52.4 Hz).

6. Synthesis and reactivity of first tricyclic anionic Janus bis(NHC)

6.1. Synthesis of a tricyclic 1,4 diphosphinine diselone

After getting access to $P^{V/V}$and $P^{III/III}$ bis(NHCs), our next objective was to synthesize low-coordinate *P*-functional bis(NHCs). Thus, we decided to target first a 1,4 diphosphinine diselone as a promising starting point. It should be noted that more than half-century of research has been devoted to the chemistry of phosphinine and related compounds.[47] However, the first example of a 1,4 diphosphinine, namely **LXX**, was reported by Kobayashi (Figure 6.1). Then after a long time in 2017 and 2018, imidazole-2-thione- and thiazole-2-thione-derived tricyclic 1,4-diphosphinines **LXXVI**[101], **XCXXIX**[104] were reported by Streubel's group, using scrambling and reduction of corresponding 1,4-dichloro-1,4-diphosphinines. Since then, several lines of research were followed, but the *C*-centered chemistry was less explored than that of the *P*-center. Especially development of the former could make them promising novel multidentate ligands in organometallic and supramolecular chemistry.

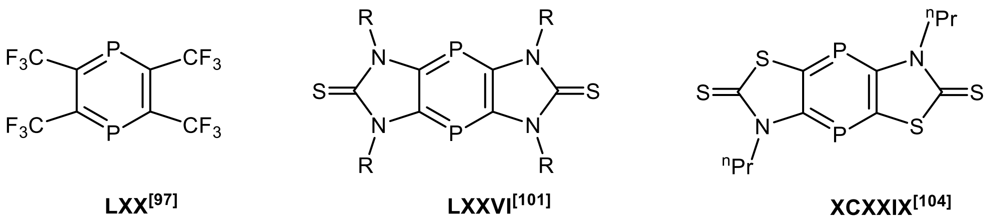

Figure. 6.1. Literature known examples of 1,4-diphosphinine **LXX**[97], **LXXVI**[101], **XCXXIX**[104].

Inorder to synthesize imidazole-derived 1,4-diphosphinine diselone, firstthe related scrambling reaction was performed with isomeric mixture of 1,4-dihydro-1,4-diphosphinine diselone **6**$^{cis/trans}$. Therefore, compounds **6**$^{cis/trans}$ were treated with PCl_3 (Scheme 6.1) in methylene chloride at - 40 °C. Reaction was monitored by $^{31}P\{^1H\}$ NMRspectrum revealing three prominent signals finally. The signal at 216 ppm and 162 ppm assigned to unreacted PCl_3 and $Et_2N\text{-}PCl_2$, respectively, however, the third signal at 4 ppm was assigned to compound **18**$^{cis/trans}$. Upon completion of the reaction, it was tried to isolate it by washing with *n*-pentane. Unfortunately, **18**$^{cis/trans}$could not be isolated by washing as it converted quite rapidlyintocompound **19**.

Later it was decided to add $^{n}Bu_3P$ to the above reaction mixture stirring for 5 minutes at room temperature. The colour of the reaction mixture turned to violet immediately. The $^{31}P\{^{1}H\}$ NMR spectrum of the reaction mixture showed a clean conversion to compound **19** with a resonance at 78.2 ppm and another signal at 104.6 ppm that was assigned to the known chloro-phosphonium chloride $[Bu_3PCl]Cl$[182]. The final product **19** was isolated in quite good yields (58 %) by filtration of the reaction mixture through a silica bed using a mixture of diethyl ether and toluene (1:1).The chlorophosphonium salt stayed on top of the silica column due to its high polarity and limited solubility.

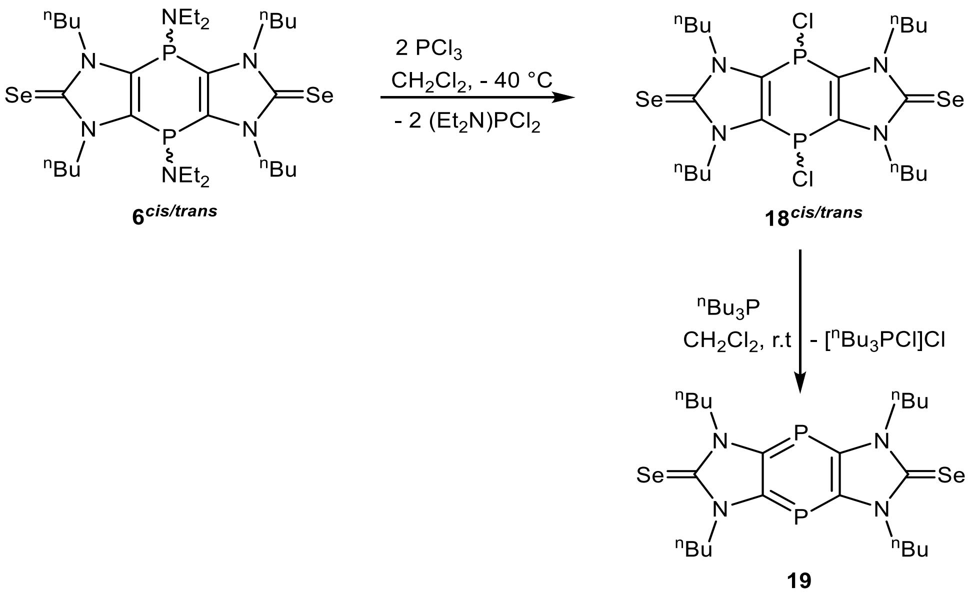

Scheme 6.1. Synthesis of tricyclic 1,4-diphosphinine diselone **19.**

Compound **19** was fully characterized using NMR, IR, MS and elemental analysis techniques. Finally, single-crystal X-ray diffraction analyses were performed using crystalsgrown from a methylene chloride solution at −20 °C. The solid-state structure shows the *trans*-oriented *n*-butyl groups at the plane of the tricyclic structure. The moleculecrystallizes centro-symmetrically in *P21/n* (Figure 6.2). The P–C bond length (P–C1 1.744(2) Å) of thecentral ring and N1-C1 1.366(3) of the imidazole ring are in good agreement with literature values for phosphinines (Figure 6.2).[167,168] and 1,4-diphosphinines.[101] The symmetry-equivalent C1–C3 bond lengths of 1.408(2) Å are comparable with those inbenzene (1.397 Å)[169] and other derivatives of 1,4-dihosphinine (imidazole C1-C3 1.409(7)[101], thiazole C1-C3 1.406(2)[116] in**19**. C2-Se bond length of 1.829(2) Å is comparable to C2-Se bond length of 1.828(2) Å in **6**$^{cis/trans}$. However, it is slightly smaller than C2-Se bond length of 1.857(13) Å in **7**$^{cis/trans,}$ which might be due to the electron-withdrawing effect of phenyl groups, resulting in comparatively longer bonds. Similarly, N1-C2-

N2 106.2(18)° bond angle is slightly shorter than N1-C2-N2 104.9(11)° in **6**$^{cis/trans}$ and relatively larger than N1-C2-N2 107.9(11)° in **6**$^{cis/trans}$.

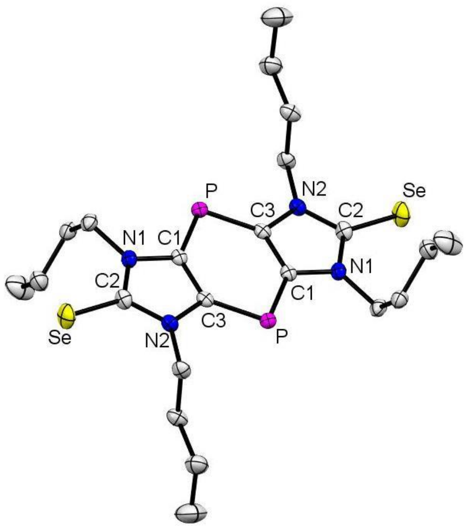

Figure 6.2. Molecular structure of **19**. Ellipsoids are set at 50 % probability and hydrogen atoms are omitted for clarity. Selected bond lengths [Å] and angles [°]: Se-C2 1.829(2), N1–C2 1.366(3), C1-C3 1.408(3), C1-P 1.744(2), C1-P-C3 96.92(10), N1-C2-N2 106.2(18).

6.1.1. UV/vis spectroscopy

The deep violet colour of tricyclic 1,4-diphosphinine **20** prompted us to investigate the type and strengths of transitions responsible for the colour of these compounds using UV/vis spectroscopic studies. The UV/vis spectrum (Figure 6.3) was measured in methylene chloride solutions at room temperature by taking dilute solutions (concentration ~ 10^{-5} molar) into sealed quartz and air-tight cells.The spectrum revealed a strong absorption at λ_{max} = 554 nm.[181]

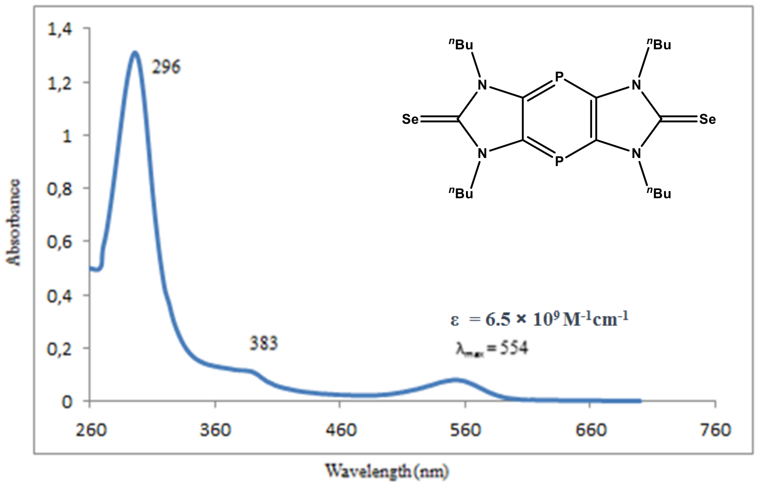

Figure 6.3. The UV/vis spectrum of **19** (2x10^{-7} mM) in CH_2Cl_2.

6.2. Reaction of tricyclic 1, 4-diphosphinine 19 with MeOTf

Reactions of an electrophile such as methyl iodide, etc. with imidazole-2-thiones,[170] thiazole-2-thione[171] and dithiole-2-thiones[172] result in the formation of corresponding S-methylated salts are well known for more than 50 years. Theoretical studies performed by Frontera on imidazole-2-thione-derived 1,4-diphosphinines[101] showed clearly the nucleophilic character for the C=S unit, thus suggestingto examine a reaction with an electrophile. When compound **19** was treated with two equivalents of MeOTf in methylene chloride (Scheme 6.2), the reaction mixture turned to light yellow after one-hour stirring, indicating the completion. A ^{31}P NMR spectrum showed a signal at 119.4 ppm, downfield-shiftedand without any proton coupling.

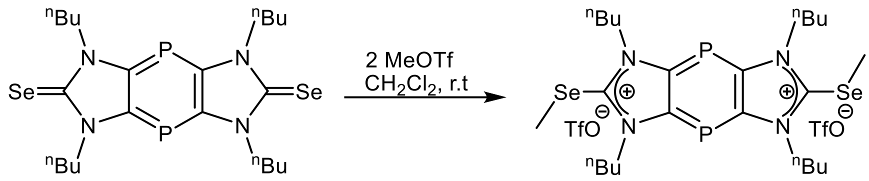

19 **20**

Scheme 6.2. Synthesis of doubly*Se*-methylated salt **20**.

After workup, a light yellow coloured powder was obtained in excellent yield (91 %). ^{1}H NMR spectroscopic measurement showed that Se-Me protons appeared as a singlet at 2.8 ppm. Moreover, in the ^{13}C{^{1}H} NMR spectrum, a resonance corresponding to the Se-Me carbon was observed at 11.7 ppm. HRMS (pos. ESI) m/z) 757.0750(calc.m/z757.0728) also supported the proposed chemical composition of the product. Firm evidence for the formation of compound **20**was obtained from the X-ray crystallographic measurement, for which thesingle crystals were grown from a saturated methylene chloride solution at -20 °C. The X-ray analysis revealed that compound **20**crystallizes in the orthorhombic crystal system with the $Pca2_1$space group (Figure 6.4).The molecular structure of **20** is given in Figure 6.4, and selected bond lengths and angles are given in the figure caption. Molecular structure shows *trans* orientation of ^{n}Bu and -SeMe groups relative to eachother. The Se1-C2 bond length of **20** is elongated compared to Se-C2 bond length of compound **19**. The change in N1-C2-N2 108.8(3) bond angle of compound **20** relative toN1-C2-N2 106.2(18) bond angle of compound **19** indicates the formation of a double Se-methylated product.

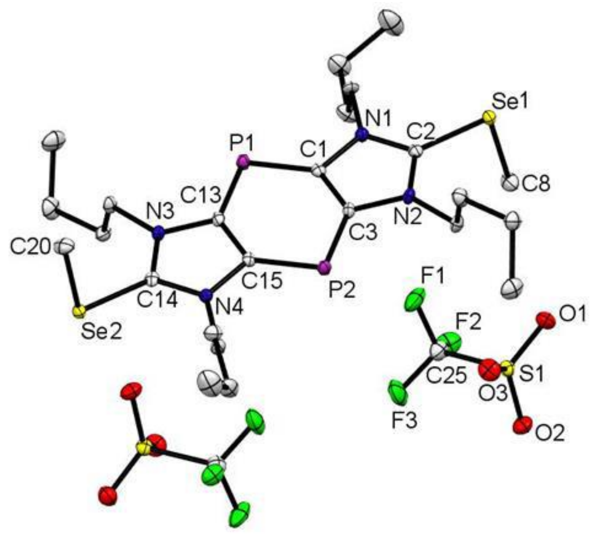

Figure 6.4. Molecular structure of **20** (two TfO anions). Ellipsoids are set at 50 % probability, and hydrogen atoms are omitted for clarity. Selected bond lengths [Å] and angles [°]:C2–Se1 1.896(4), Se1–C8 1.952(4), C2–N2 1.339(5), N2–C3 1.397(5), C3–P2 1.736(4), C1–C3 1.412(6); N1–C2-N2 108.8(3), C3–P2–C15 96.3(2).

6.3. Reductive deselenization of compound 20

Having compound **20** the reductive deselenization was explored under identical conditions as described before in chapter 4 for compound **11**$^{cis/trans}$. A methanolic solution of compound **20** was treated with small portions of $NaBH_4$ (excess) in either absence of [222]-cryptand or in the presence of [222]-cryptand at 0 °C (Scheme 6.3). The reaction mixture turned to light yellow (for **21a**) and dark orange-red (for **21b**) with the liberation of gaseous HSeMe. The progress of the reaction was monitored by ^{31}P NMR spectroscopy, showing complete consumption of starting material.

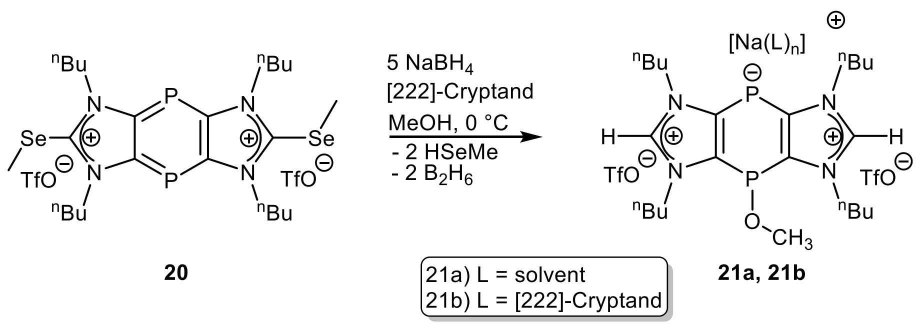

Scheme 6.3. Synthesis of anionic bis(imidazolium) salts**21a, 21b**.

However, surprisingly, two new singlets at δ = 20.1, - 67.3ppm (for **21a**) and δ = 19.9, - 67.4 ppm (for **21b**) were observed in 1:1 ratio, with a $^{3}J_{P,P}$ coupling constant magnitude of 1.7 Hz and 2.0 Hz, respectively, as shown in Figure 6.5.This AB-type spin system in the^{31}P NMR spectrum undoubtedly indicated the formation of the ionic adducts**21a**and **21b,**having two different *P*-centers. It might be formed via a nucleophilic attack of the methoxy anion on the *P*-center of **20**. Upon comparison with literature is known examples **XCXXX**[103] and **XLXXIII**[116], it is also evident that the resulting product containsa neutral and anionic phosphorus center (Figure 6.5).

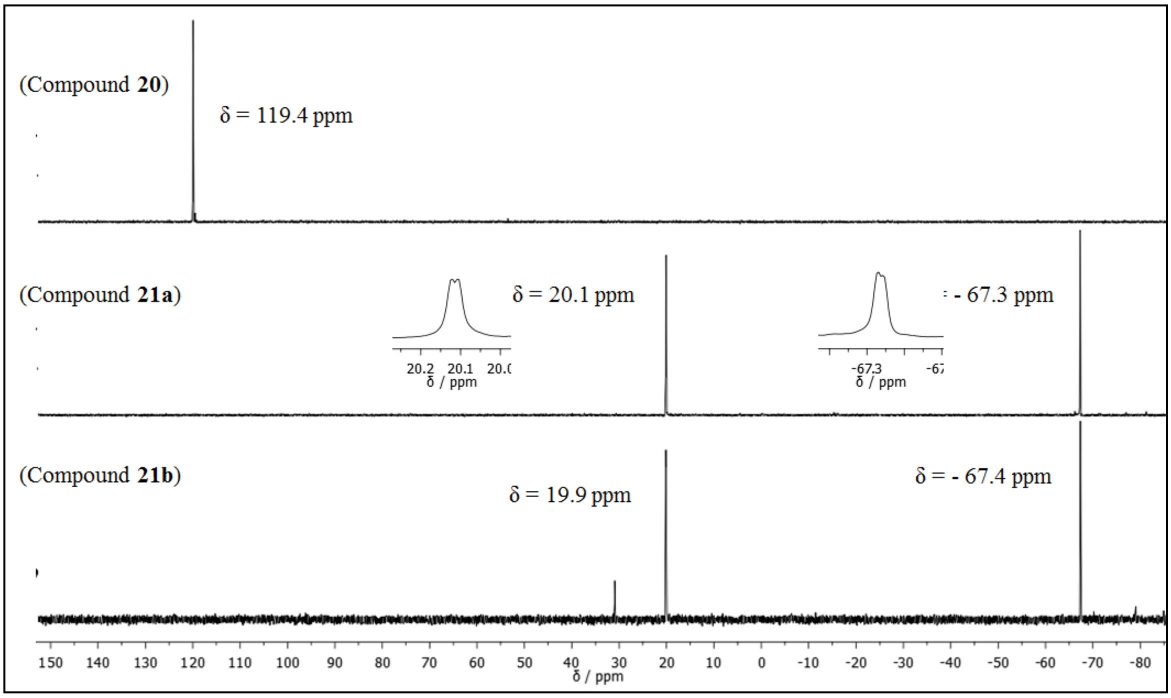

Figure 6.5.^{31}P{^{1}H} NMR spectrum of compounds**20** (top)and **21a**(middle) and **21b** (bottom)

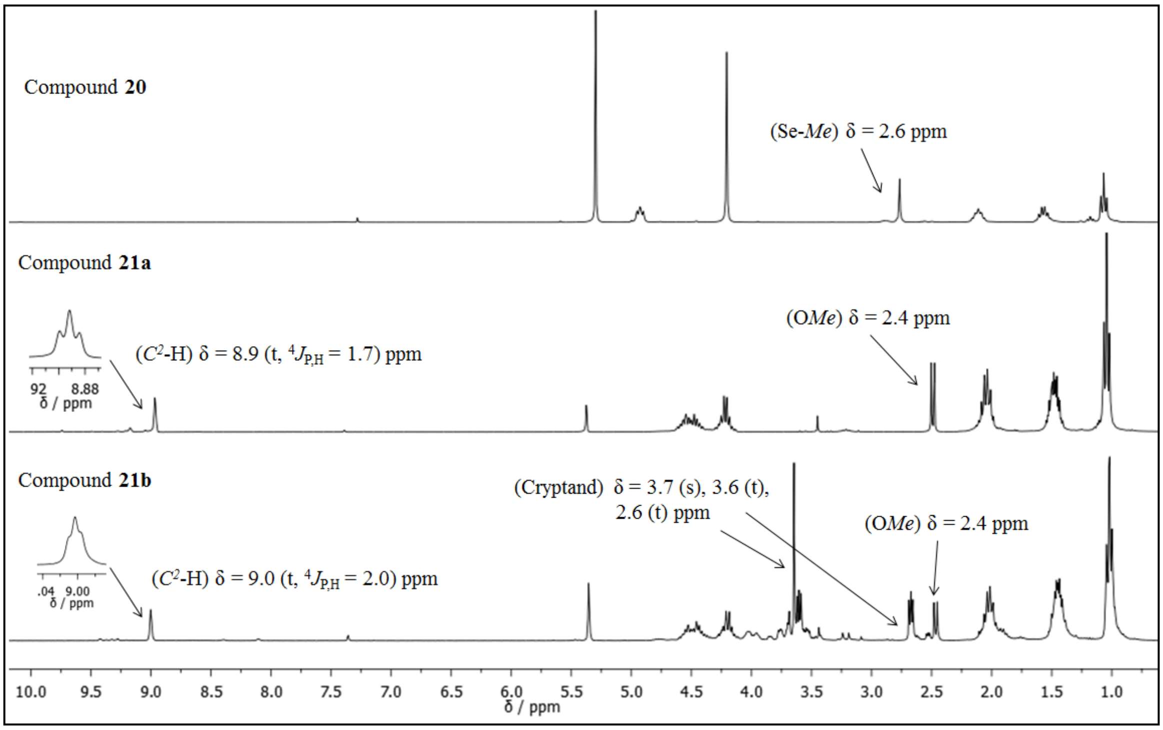

Figure 6.6. ^{1}H NMR spectrum of compounds **20** (top) and **21a** (middle), **21b** (bottom).

To get further insight into the reaction, the ^{1}H NMR spectrum after the isolated productsand by comparing the NMR spectrum of compound **21a** (middle) and **21b** (bottom) with **20** (top) as shown in Figure 6.6, we could observe a doublet at δ = 2.4 ($^{3}J_{P,H}$ = 7.3 Hz; **21a**) and δ = 2.4 ($^{3}J_{P,H}$ = 7.9Hz; **21b**)that belong to P-*OMe* protons. Besides, a new characteristic triplet appeared at (δ =8.9; **2a**) and (δ =9.0; **2b**) corresponding to imidazolium protons (Figure 6.6). A slight increase was observed in the coupling constant of magnitude $^{4}J_{P,H}$ = 1.7 Hz (**21a**) vs. $^{4}J_{P,H}$ = 2.0 Hz in (**21b**). A chemical shift difference of Δ^{31}P = 0.1 ppm was observed between **21a** and **21b**.Spectroscopic data of **21a**and **21b** is also comparable with literature known zwitterion **XLIV**(δ^{31}P{^{1}H} / ppm = -73.6 and *C*^{2}-H proton resonated at δ^{1}H / ppm = 7.0), **XCXXX** (δ^{31}P{^{1}H} / ppm = 12.1 (d), -76.1 (d) $^{3}J_{P,P}$ = 5.7 Hz) and **XLXXIII** (δ^{31}P{^{1}H} / ppm = 6.7 (br) -28.6 (br)) (Figure 6.7).[158, 103, 116] The formation of both compounds**21a**and **21b** was confirmed via pos. ESI-MS experiment, which showed the m/z value of 451.3 (100) $[M]^{\cdot+}$ with HRMS $[C_{23}H_{41}N_4OP_2]^+$ calcd (found) 451.2750 (451.2754).

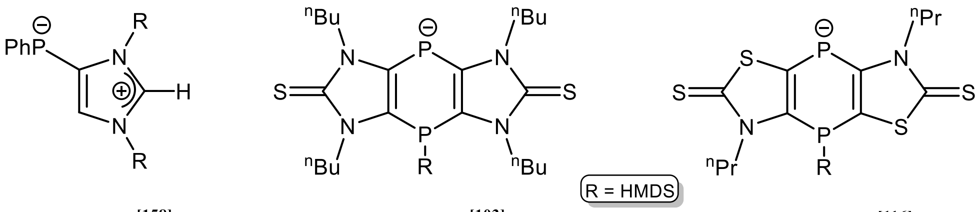

XLIV[158] **XCXXX**[103] **XLXXIII**[116]

Figure 6.7. Literature known phosphanido-type functional derivatives **XLIV**[158]**, XCXXX**[103] and **XLXXIII**.[116]

6.4. Deprotonation of bis(imidazolium) salt 21

The convenient availability of mono-phosphanido linked bis(imidazolium) salts **21a** and **21b,**and the ease of handling recommended that direct conversion of this salt into corresponding tricyclicbis(NHCs) **22a**, **22b** should be explored.Therefore, the deprotonation of both compounds (**21a**, **21b**) was carried out using potassium hexamethyldisilazide (KHMDS) at room temperature (Scheme 6.4).

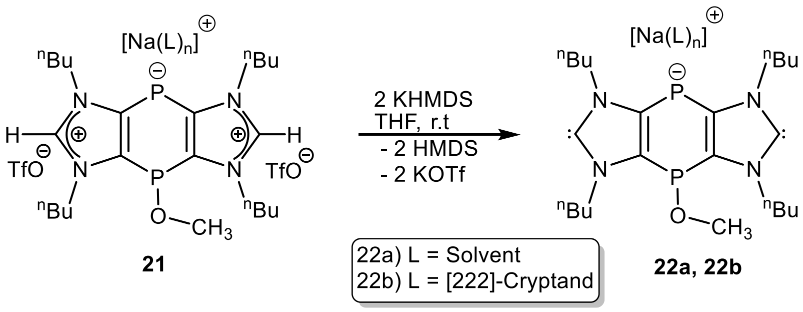

Scheme 6.4. Synthesis of tricyclic mono-phosphanido substituted bis(NHC)s**22a, 22b**.

Upon deprotonation of **21a** and **21b** in THF, ^{31}P NMR resonances appeared at δ = 25.1 ppm, -74.5(s) ppm (**22a**) and δ = -23.9 ppm, -75.8 (**21b**) corresponding to neutral and anionic phosphorus centers respectively, in the ^{31}P{^{1}H}NMR spectrum (Figure6.8). In addition, the disappearance of imidazolium protons in the ^{1}H NMR spectrum also supported the formation of a new type of bis(NHCs) **22a**and **22b** having a neutral and a phosphanido-type bridging phosphorus center.

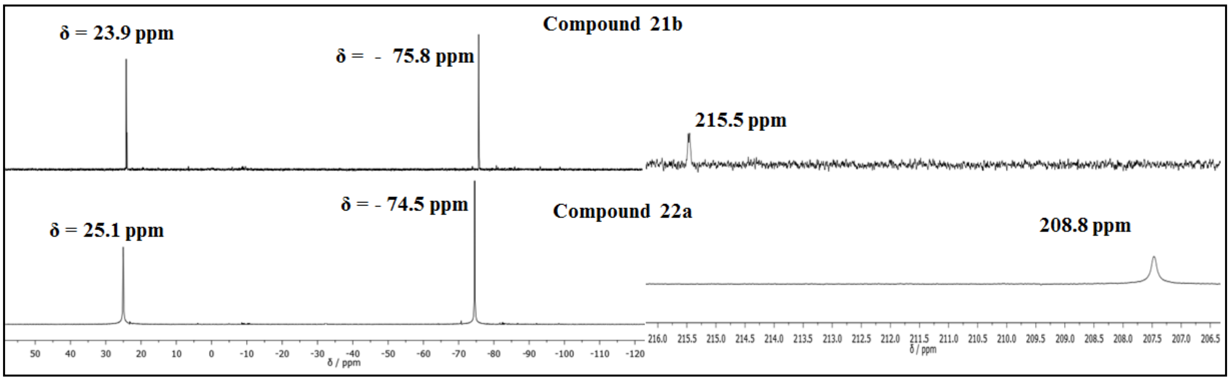

Figure 6.8. $^{31}P\{^{1}H\}$ NMR spectrum of compounds; **22b**(top)and **22a**(bottom).

Upon comparisonof spectroscopic data ($^{31}P\{^{1}H\}$ and $^{13}C\{^{1}H\}$) NMR spectra (Table 6.1) of **22a**and **22b,** it is obvious that values are very well in agreementwith literature known example **XLV**[158] and downfield-shifted comparison to **XLVII**[109](Table 6.1).

Table 6.1. Comparison of $^{31}P\{^{1}H\}$ and $^{13}C\{^{1}H\}$ NMR chemical shifts (ppm) between **XLV**,[158] **XLVII**[109], **22a**and **22b.**

	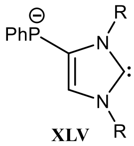 **XLV**	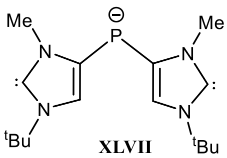 **XLVII**	**22a**	**22b**
δ ^{31}P/ppm	- 73.4	-116.0 (s)	25.2 (s), - 74.5(s)	23.9 (s), - 75.8 (s)
δ^{13}C{^{1}H}/ppm	210.4(br)	Not observed	208.8(br)	215.5 (d)

Furthermore, close analysis of the $^{13}C\{^{1}H\}$ NMR spectrum of both phosphanide derivatives **22a** and **22b** revealed that a signal for the C^{2}-H units was missing. The identification of signals at δ = 208.8 ppm (br; **22a**) and δ = 215.5 ppm (d, $J_{P,C}$ = 2.9 Hz; **22b**) in the $^{13}C\{^{1}H\}$ NMR spectrum is consistent with the presence of the C^{2} nuclei of the anionic bis(NHC) derivatives **22a**, **22b**; signals at 120.5 (d, $^{2}J_{P,\,C}$ = 7.5 Hz; **22a**) and 120.2 (d, $^{2}J_{P,\,C}$ = 7.4 Hz; **22b**) were assigned to the O-CH_3 center.It is evident from the solution ($^{31}P\{^{1}H\}$ and $^{13}C\{^{1}H\}$) NMR of **22a** and **22b**that the nature of the counter cation does not influence the chemical shift of the carbene carbon resonance significantly as well as that of the phosphanido and neutral phosphorus group, thus indicating that **22a** and **22b** exist as well separated ion pairs in solution.The neg-ESI-MS data gave further support for the elementary composition of **22a**, the m/z value 449.26 was obtained, thus showing a reasonably good agreement with the anion$[C_{23}H_{39}N_4OP_2]^{-}$ (theor. 449.2605).

6.4.1 Theoretical investigations

All calculations were carried out with the Gaussian 09 program package by Nyulaszi and co-workers.[130] Full geometry optimization calculations were performed, followed by the calculation of the second derivatives at the optimized structures to establish the nature of the stationary points obtained. The Gibbs free energies were calculated based on the harmonic vibrational frequencies (atmospheric pressure, 298.15 K). All of the tricyclic compounds were calculated with methyl substituents at the nitrogen atoms (instead of n-butyl) to reduce the computational time and they were labelled by the special character ‘. Kohn-Sahm orbitals were calculated at B3LYP/6-31+G*//M06-2X/6-31+G* for better comparisons with the former works.

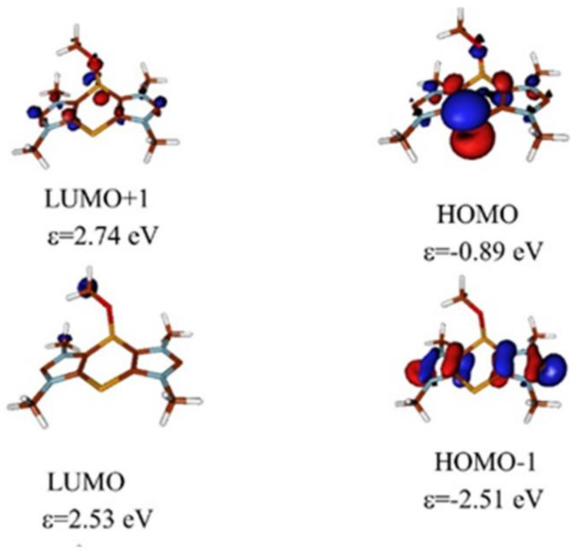

Figure 6.9. FMO topologies and energies for the model (R = CH_3) calculated structures of **22′**at the B3LYP/6-31+G*//M06-2X/6-31+G*level of theory (PCM solvent model).

To establish the stability of the carbene **22`**, an isodesmic reaction was applied,[133] which revealed that the stability is 113.3 kcal/mol for **22`**, which is very similar to **9*^cis/trans^*/14*^cis/trans^*** (113.3-111.7 kcal/mol). Compared to **21**, the aromaticity of the middle ring is slightly increased (NICS(0)=-5.5, while the outer rings decreased (NICS(0)=9.0), which indicate somewhat higher conjugation within the ring system.

6.4.2 Cyclic voltammetric studies

The electrochemical behaviour in a solution of the dicarbene **22** was investigated by cyclic voltammetry (CV) in THF (0.2 M [$^nBu_4N$][PF_6]) at gold ceramic screen printed electrodes (Au CSPE®) Voltammetric data was measured in an Ar-filled glove box using the Pine WaveNow potentiostat. The voltammetry of the novel anionic dicarbene **22** was also undertaken using $[CoCp_2][PF_6]$ as an internal reference. The key features of the voltammetry of **22** as depicted in Figure6.10 are the very facile first oxidation with E_p^{a1}= -1.16 V, and a large number of cascading waves for subsequent oxidation processes, all of which are chemically irreversible. Thus, E_p^{a2}= -0.99 V, E_p^{a3}= -0.74 V, E_p^{a4}= -0.36 V and E_p^{a5}= -0.19 V. There are, therefore (at least) four oxidation processes that are more facile for **22**, a remarkable achievement. The purpose of Figure6.11 is to show the relation of the observed peaks to that of the added $[CoCp_2][PF_6]$, which is a well-behaved redox process with ΔEp ~ 90 mV. The feature identified asE_p^{a6}at about -2.5 to -2.7 V, however, was present in traces that precede the cobaltocenium salt addition if they are run sufficiently negative. We are inclined to think that this is a surface reduction of some by-product of the (chemically) irreversible oxidations, rather than the actual reduction of **22**, which is probably not reached till ca. -3 V with severe sample degradation.

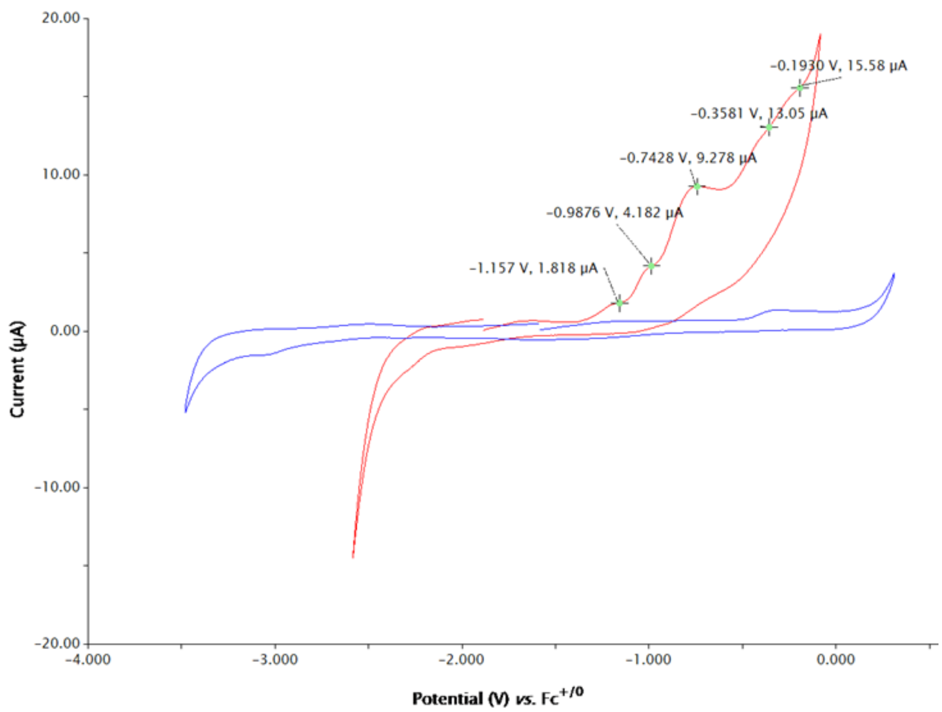

Figure 6.10. CV (red) of a 1.0 mM solution of **22** (0.2 M) $[^nBu_4N][PF_6]$ in THF) at 200 mVs^{-1}, and (blue) of the solvent/electrolyte background for the experiment.

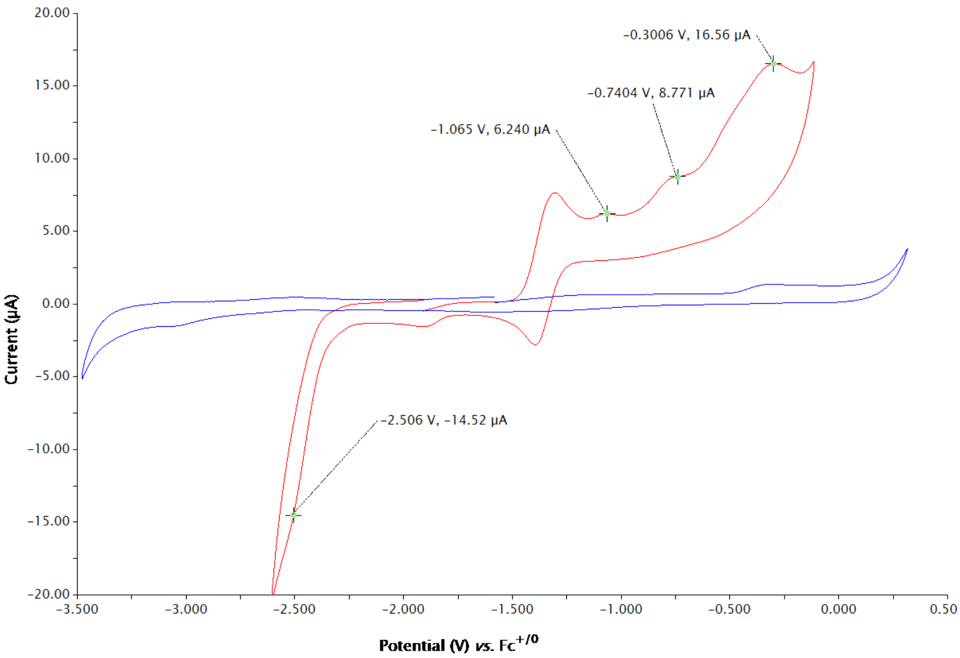

Figure 6.11. CV (red) of a 1.0 mM solution of **22** (0.2 M [^{n}Bu$_4$N][PF$_6$] in THF) at 100 mVs^{-1} also containing 1.0 mM Cc^{+}/Cc as internal reference, and (blue) background scan for solvent/electrolyte.

This is also obvious from the calculated LUMO energy of **22′,** which is some 4 eV higher than for the neutral species, whilst the solution reduction appears to have a more facile onset (compare Figures. 6.10 and 6.14). We also considered alternatives, including fortuitous protonation of reactive **22** under the CV conditions, which would stabilize the HOMO in favour of HOMO^{-1}, with standard dicarbene character. This could be disproven by experimental protonation studies, which indicate that the sites of protonation are C**:** Ion pairing of the Na^{+} with P^{-} in the THF solution is also a likely source of energy damping. However, the combination of facile oxidations and the multiple closely spaced processes reflect well the FMOs calculated for **22**. Moreover, the high reactivity of the HOMO attested to by the voltammetry is consistent with the coordination of this FMO to multiple Rh ions in complexes **26** and **27**, **27′**.

6.5. Reaction of compound 21b with an electrophile (MeI)

The unique feature of a low-lying LUMO, located largely onthe phosphorus atoms,thus leading to high electrophilic reactivity of 1,4-diphosphinines, was first studied byStreubel and co-workers in 2018. They proposed a nucleophilic addition of KHMDS or ^{n}BuLito the imidazole-based 1,4-diphosphinine(**XLXVI**) to generate the corresponding mono anions (**L a,b**).[115b] However, the above-mentioned mono anions were not isolated and only reacted *in situ* with the electrophile MeI to afford 1,4-disubstituted compounds (**LI a,b**) (Scheme 6.5).

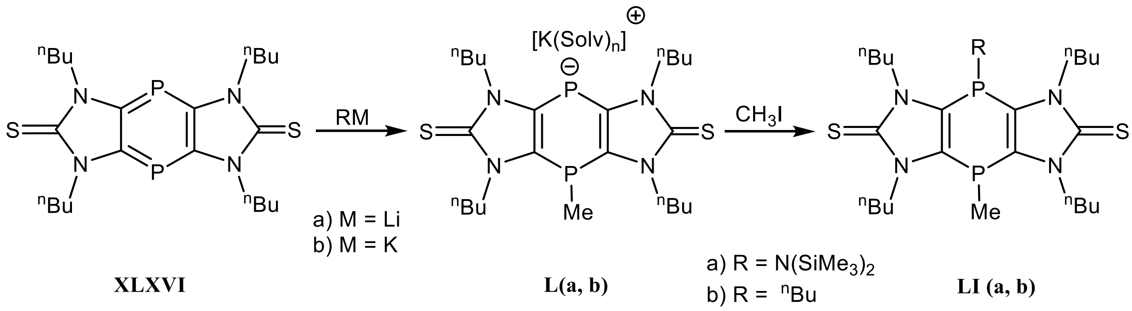

Scheme 6.5. Sequential nucleophilic and electrophilic reactions of tricyclic 1, 4-diphosphinine **XLXVI**.[115b]

To examine the reactivity of **21b** towards electrophiles, it was reacted with stoichiometric amounts of a mild electrophilic agent, methyl iodide, in Et_2O at -78°C and then slowly warmed to ambient temperature (Scheme 6.6). A colour change was observed from orange-red to light yellow after overnight stirring. After purification, a light yellow oil was obtained, which showed two sets of resonances at δ = -71.58 (d, $^3J_{P,P}$= 5.2 Hz), - 66.23 (d, $^3J_{P,P}$ = 4.9 Hz) and 39.57 (br), 43.7 (br) in the ^{31}P NMR spectrum, which were assigned to the *cis* and *trans* isomers (1: 0.3) of **23,23′**.

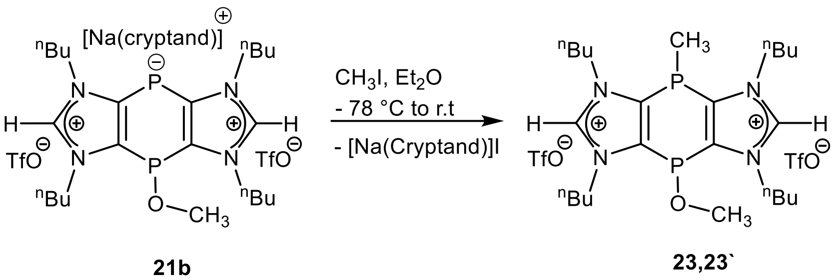

Scheme 6.6. Synthesis of mixed substituted P$^{III/III}$-functional bis(imidazolium) salts **23, 23′**.

In the^{1}H NMR spectrum, C^2-protons at δ = 9.5 and 9.6 belonging to two isomers showing triplet multiplicity with $J_{P,H}$ coupling constant magnitudes of 3.0 Hz. The NMR chemical shifts of selected examples [115b] of literature known related nucleophilic addition products are given in Table 6.2. Besides NMR measurements, the proposed constitution of **23, 23'** was also supported by HRMS(pos-ESI) in which the experimental and calculated values are in good agreement (615.2511/615.2505) and even by elemental analysis.

Table 6.2. Comparison of $^{31}P\{^1H\}$ NMR chemical shifts (ppm) between **La**,[115b] **Lb**[115b] and **23,23′.**

	La[115b]	**Lb[115b]**	**23,23'**
δ ^{31}P/ppm	-72.4 (dq, $^3J_{P,P}$ = 15.7 Hz, $^3J_{P,H}$ = 5.2 Hz, *P-Me*), -5.1 (br. d, $^3J_{P,P}$ = 15.7 Hz, *P-N(SiMe$_3$)$_2$*).	-75.8 (dq, $^3J_{P,P}$ = 9.6 Hz, $^3J_{P,H}$ = 4.9 Hz, *P-Me*), -69.4 (qd, $^3J_{P,H}$ = 5.2 Hz, $^3J_{P,H}$ = 4.8 Hz, *P-Me*); -65.4 (br, *P*-^{n}Bu), - 60.1 (br, *P*-^{n}Bu).	-71.58 (d, $^3J_{P,P}$ = 5.2 Hz), - 66.23 (d, $^3J_{P,P}$ = 4.9 Hz), 39.57 (br), 43.7 (br)

6.6. Synthesis of mixed-substituted $P^{III/III}$–functional bis NHCs 24,24′

After the successful synthesis of $P^{III/III}$-functional bis(imidazolium) salts **23, 23′**, deprotonation with KHMDS under the aforementioned reaction conditions (see Chapter 5) was met with great success (Scheme 6.7). Analysis of the reaction mixture by ^{31}P NMR spectroscopy suggested that a shift in the resonance signals of products **24, 24′** with isomer ratio (1: 0.2) was minimal compared to precursors **23, 23′**.

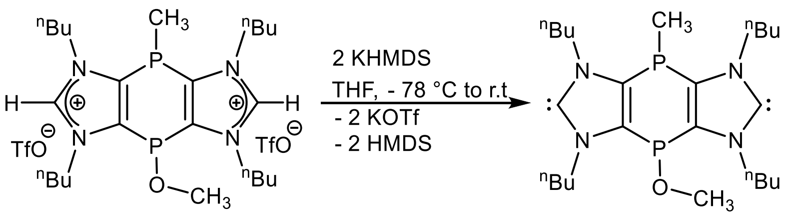

Scheme 6.7. Synthesis of mixed substituted $P^{III/III}$-functional bis(NHCs) **24, 24′.**

An isomeric mixture of compounds**24, 24′** (1: 0.3) was isolated in excellent yield (76 %) as a light yellow oil. Further characterization was done by $^{13}C\{^1H\}$ NMR spectroscopy, revealing resonances at δ = 223.4 ppm and 224.2ppm assigned to the carbenes carbon C^2 atom with a $^3J_{P,C}$ coupling constant magnitude of 2.7 Hz. These C^2 resonance signals are very close to previously reported bis(phosphanyl) substituted bis(NHCs) **14*cis/trans***[118] values but downfield shifted than **22** (Δδ = 14, δ = 208.8 ppm (br)).

In the ^{1}H NMR spectrum, C^2-H protons vanished in the downfield region, which also supported the formation of mixed substituted $P^{III/III}$–functional bis(NHC)s **24, 24′**. The constitution of compound

24, 24′ was further supported by mass spectrometry and EA data, e.g., the HRMS spectrum showed the exact mass value of **24, 24′**(calcd (found) 615.2505 (615.2511)).

6.6.1. Cyclic voltammetric studies supported by theoretical investigations

Two CV experiments for compounds **24, 24′** have been undertaken in THF/$^{n}Bu_4PF_6$ medium; the compounds are most stable in this solvent and specifically are not stable to CH_2Cl_2. In the first instance, a reference compound was not added because of concerns about interference with observed processes and an attempt was made to refer to an immediately proceeding external ferrocene (Fc) experiment for referencing to the $Fc^{0/+}$ = 0 V scale (IUPAC recommendation). This attempt was of questionably precision due to a very large ΔEp > 300 mV for the Fc signal and the inherent uncertainty of external referencing. In a second, shorter, experiment the major scans were repeated, and a cobaltocenium salt, [Cc][PF_6], was added as an internal reference, which indeed was found to induce about a 200 mV shift in the process peaks.

The major features of the voltammograms are a series of closely spaced and (chemically) irreversible oxidation steps at very facile potentials. These processes are shown in Figures. 6.12a, b, which show almost identical traces when scanned first in the anodic (to +0.25 V) and cathodic (to -2.0 V) directions.

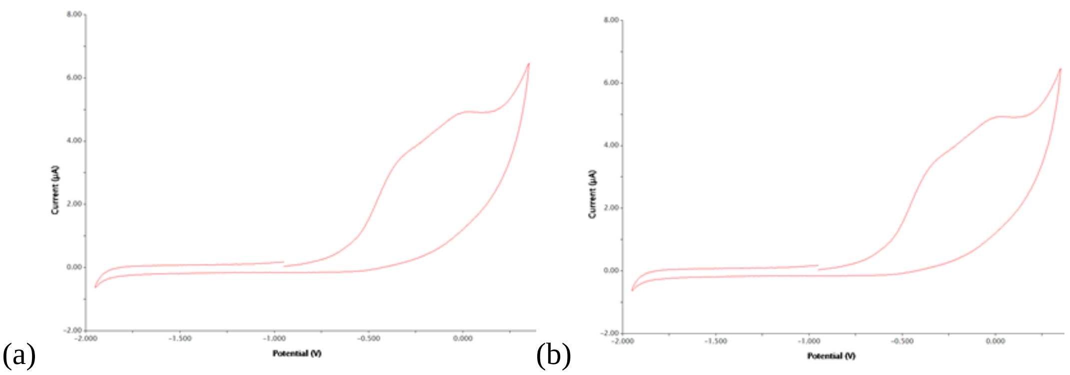

Figure 6.12. CVs depicting the primary oxidations of **24, 24′**in in THF/$^{n}Bu_4PF_6$ medium starting at the OCP scanning (a) first in the anodic and (b) first in the cathodic direction.

Thus, although these are chemically irreversible processes (no return peaks on fast scanning), they appear quite stable within the limited potential range. Moreover, they are facile oxidations occurring at negative potentials vs. $Fc^{+/0}$ in keeping with previous results from Streubel's group and consistent with the electron-rich dicarbene nature of **24,24′**. The multiple oxidations (see below) are attributed to subsequent oxidations of the analyte mixture and not to separate processes for **24** and **24′**. Figure. 6.13 depicts overlayed scans of the central processes described above with the background and

[Cc][PF_6]-containing scans, all from the second experiment undertaken to improve the referencing accuracy. The results with E_p^{a1}= -0.29 V and E_p^{a2}= +0.05 V are in broad agreement with the results of the first experiment where with E_p^{a1}= -0.14 V vs external $Fc^{+/0}$. We consider the internal [Cc][PF_6] results with $Cc^{+/0}$ = -1.35 V be the more accurate data.

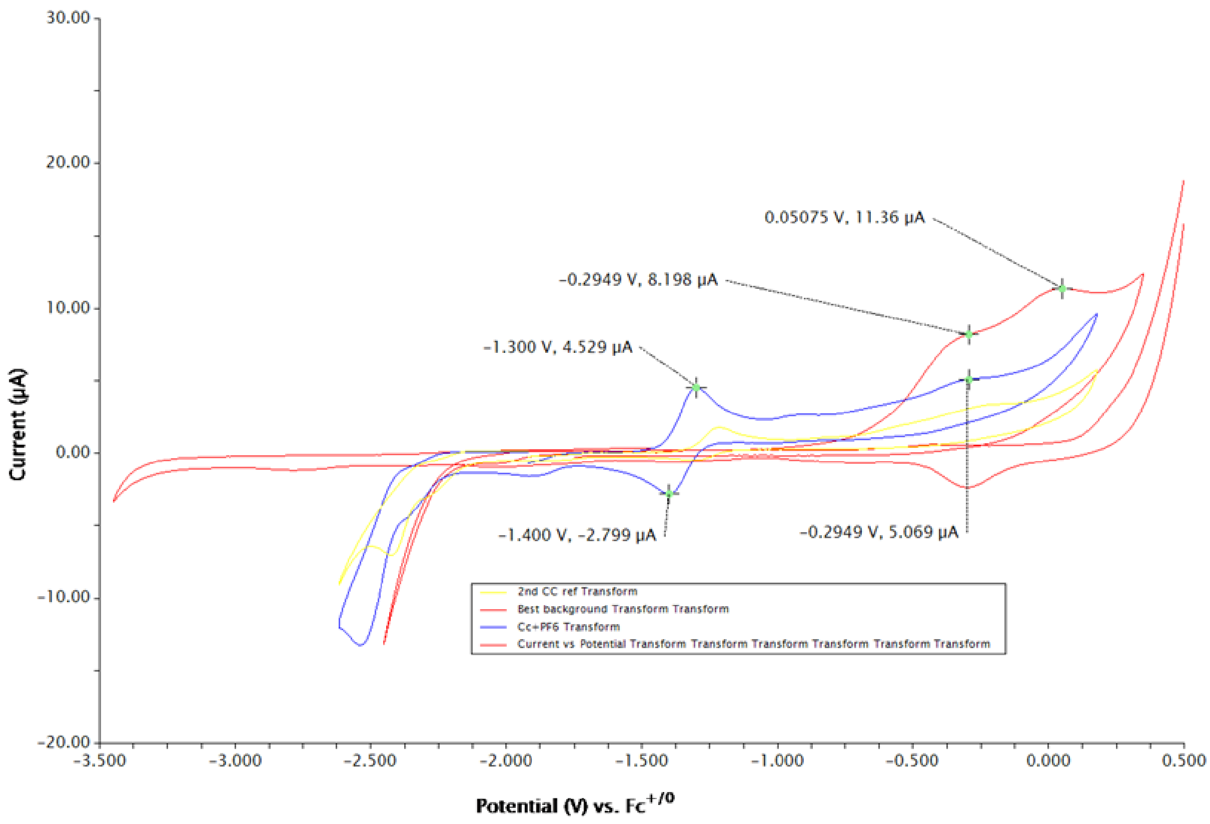

Figure 6.13. CVs depicting the central processes of **24, 24′** in in THF/$^nBu_4PF_6$ medium showing overlayed traces as explained in the figure legend.

When carefully conducted to avoid contaminating the ceramic screen-printed metal electrode surfaces, the CV experiments could be extended towards the solvent limits. The accessible window for the initial experiment was wider than the second attempt, and further discussion concerns this experiment, albeit with the voltage range scaled to $Fc^{0/+}$ using the outcome of the [Cc][PF_6] experiment (Figure 6.14). Scans taken more positive than +1.0 V result in major contamination of the working electrode and cannot be analysed, but at least one additional, also irreversible, oxidation could be measured with E_p^{a3}= +0.65. The reductive feature E_p^{a4}= -3.00 V is attributed to some surface-electrode process, likely from products resulting from the chemically irreversible oxidation processes. The strength of the peak increased strongly with multiple scans and also grow in intensity the longer that experiments are conducted on the sample. Hence, we doubt that under these conditions the true reduction of **24**$^{cis\prime}$; **24**$^{trans\prime}$can be measured but it likely exceeds -3.5 V as indicted by the limiting curve visible in Figure 6.14.

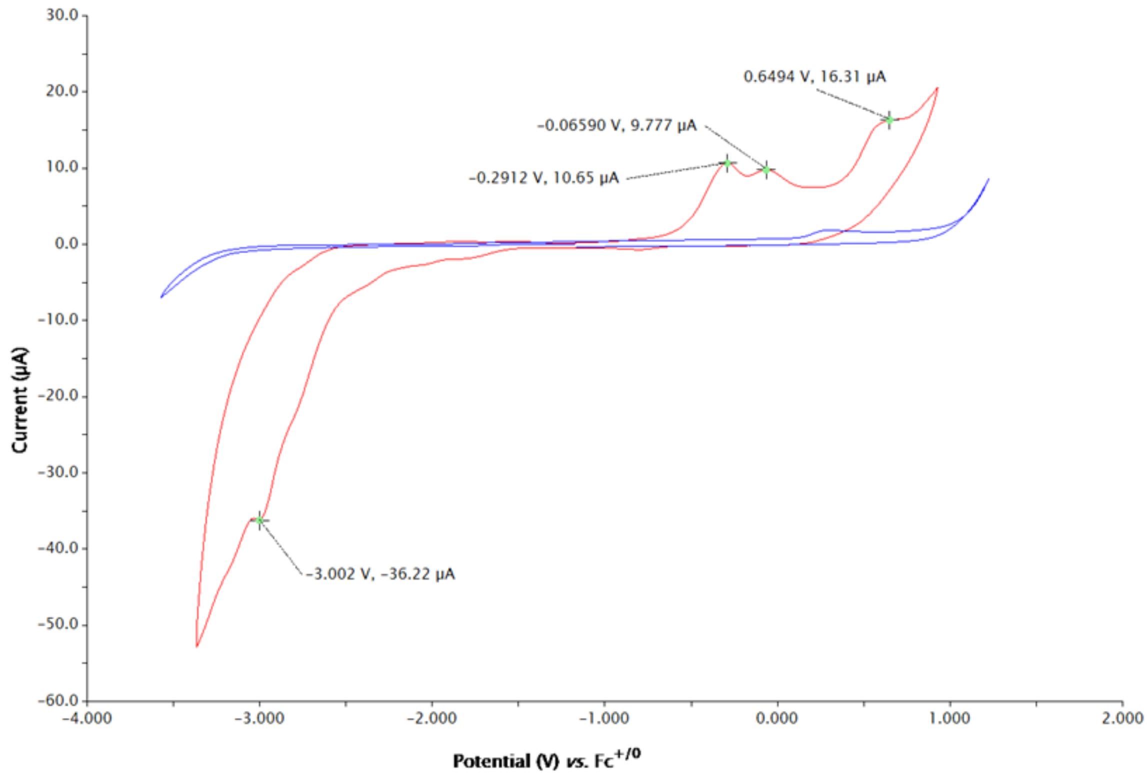

Figure 6.14. CVs depicting (in blue) the THF/$^nBu_4PF_6$ background scan and (in red) the full range of processes for **24, 24′** accessible in this medium. Beyond E_p^{a1} and E_p^{a2}, at least one further irreversible oxidation can be measured (E_p^{a3}= +0.65).

These voltammetry results can be interpreted by B3LYP/6-31+G*//M06-2X/6-31+G* undertaken a PCM solvent model with respect to the topologies and energies of the frontier molecular orbitals (FMOs) depicted in Figure 6.15. The two highest occupied molecular orbitals (HOMOs) are dominated by carbene σ(p) character, and thus resemble those of our first report on Janus dicarbenes bridged by phosphinidines, with either $P(NEt_2)^{III/III}$ or $\{P(O)NEt_2\}^{V/V}$ bridging atoms. The $P^{III/III}$ analogue to **24**$^{cis'}$ and **24**$^{trans'}$ have HOMO energies at an identical level of a theory of –5.78 and -5.77 eV, so just like **24**$^{cis'}$/**24**$^{trans'}$ virtually identical and likely to be experimentally indistinguishable. The CV experiments at similar ceramic Au-screen printed electrodes in THF/$^nBu_4PF_6$ for these analogue compounds showed E_p^{a1}= -0.61 V vs $Fc^{+/0}$; thus the slightly more difficult E_p^{a1}= -0.29 V for **24**$^{cis'}$/**24**$^{trans'}$ is fully consistent with the higher energy FMOs in the dicarbenes substituted by CH_3O/CH_3 compared to the two Et_2N substituents.

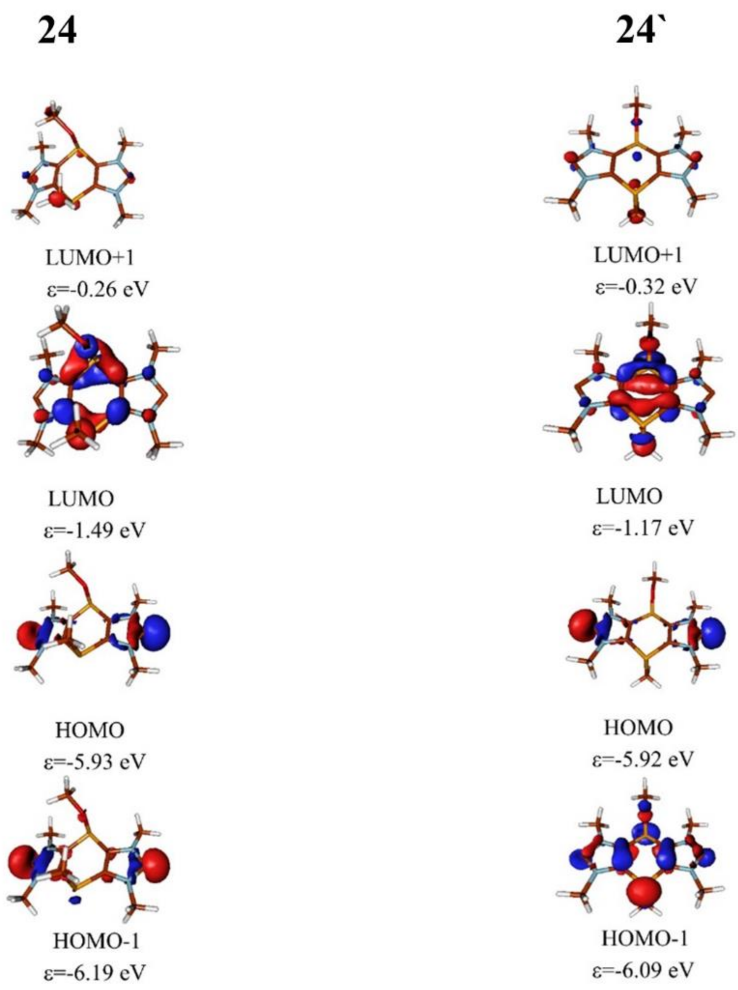

Figure 6.15. FMO topologies and energies for the model (R = CH_3) calculated structures of **24**$^{cis'}$and **24** $^{trans'}$ at the B3LYP/6-31+G*//M06-2X/6-31+G*level of theory (PCM solvent model).

6.7. Oxidation of anionic bis(NHC) 22a

In order to explore the oxidation of compound **22a**, we decided to react with an excess of selenium gray in THF for two hours (Scheme 6.8), which should also render the selone moiety (back). The reaction mixture changed to a yellow solution, and the $^{31}P\{^1H\}$ NMR spectrum of this solution showed two major signals at - 43.15 ($^1J_{Se,P}$ = 681 Hz) and 30.46($^1J_{Se,P}$ = 851 Hz),which were tentatively assigned to the two different phosphorus centers of compound **25 (**Figure 6.16). These two resonances are observed downfield-shifted compared to the starting material **22a**.

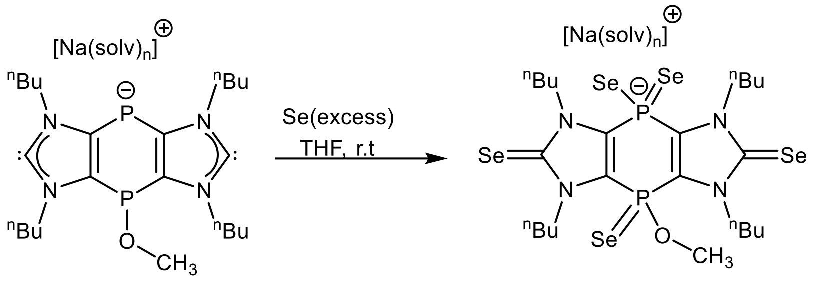

Scheme 6.8. Oxidation of monoanionic P-functional bis(NHC) **22a.**

In the $^{13}C\{^{1}H\}$ NMR spectrum disappearance of the C^2 signal and appearance of a new signal at 164.3 ppm assigned to a selone (C=Se) moiety was observed. Interestingly, the ^{77}Se NMR spectrum of compound **25** in THF showed four signals for four different selenium centers. The formation of **25** was also independently confirmed by negative ESI mass spectrometry with HRMS: theor. (exp.) 844.8464 (844.8461).

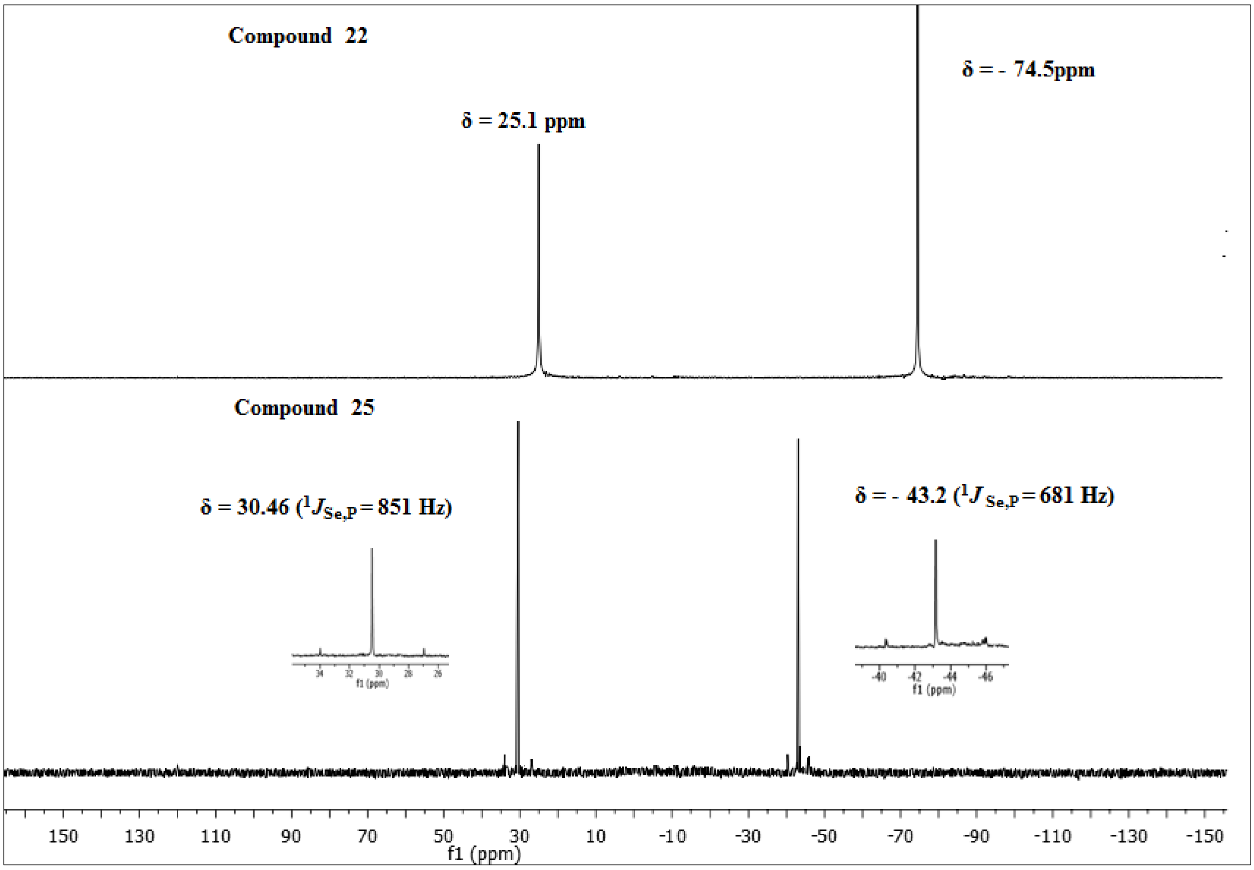

Figure 6.16. $^{31}P\{^{1}H\}$ NMR spectrum of compounds; **22a**(top)and **25**(bottom).

6.8. Complexation of phosphanido-bridged bis(imidazolium) salt 21b

Having anionic as well as neutral phosphorus centers in tricyclic bis(imidazolium) salts, it was interesting to study the preferred coordination site(s) of compound **21b** towards metal reagents. So, rhodium(I) complex [Rh(cod)$_2$Cl] was selected as a metal complex for two reasons: firstly,the Rh being an NMR active spin ½ nucleus, and secondly,the P-Rh bond is more robust compared to P-M$^{coinage\ metals}$. At first, only a half equivalent of the [Rh(cod)Cl] dimerwas treated with a THF solution of compound **21b** at room temperature (Scheme 6.9). The ^{31}P{^{1}H} NMR spectrum of the reaction mixture showed complete consumption of the starting material, and two new resonances were observed as a singlet at - 70.6 ppm and a doublet at 47.5 ppm with a $^{1}J_{Rh,P}$ coupling constant magnitude of 188.2 Hz.

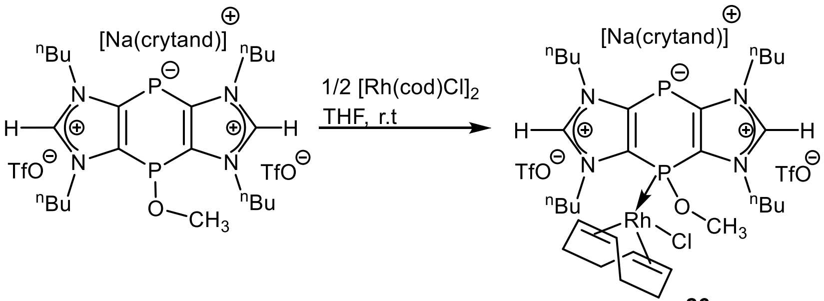

Scheme 6.9. Synthesis of anionic mono-rhodium complex **26**.

The singlet resonance signal was assigned to the anionic phosphorus center and the doublet due to coordination with the rhodium nucleus to the neutral phosphorus center. The outcome of the ^{31}P NMR measurement indicated the formation of anionic complex **26** (Figure 6.18). The ^{31}P NMR spectral resonances of compound **26** are comparable with literature known (somehow) related compound **LII** [173] {δ^{31}P = - 82.1 ppm,)} and **LIII**[174] {δ = 38.1 (dd, $J_{Rh,P}$ = 63 Hz, PPh$_2$), 5.06 (dd, $J_{Rh,P}$ = 136 Hz, PMe$_3$)} (Figure 6.17). Besides NMR measurements, the proposed composition of **26** was further confirmed by neg. ESI-MSspectrometry having m/z 995.151 that corresponds to [$C_{33}H_{53}ClF_3N_4O_7P_2RhS_2F_6$]$^-$.

Further investigation was done to study the reactivity of compound **21b** by changing the stoichiometric ratio relative to the metal reagent. Interestingly, the reaction of [Rh(cod)Cl]$_2$ with **21b**gave a somewhat different result, when **21b** and rhodium(I) dimer [Rh(cod)Cl]$_2$ were combined in a 1:1 ratio in THF (Scheme 6.10), and it turned to dark orange after three hours stirring.

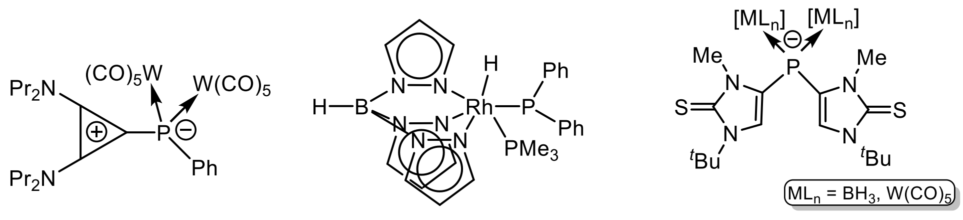

LII[174] **LIII**[109] **LIV**[173]

Figure 6.17. Literature known examples of metal phosphanido complexes **LII**[174], **LIII**[109] and **LIV** [173].

Reaction progress was monitored by ^{31}P NMR spectroscopy that revealed two sets of signals; one singlet{δ = -70.6 (s)} and a doublet {47. 5 (d, $^{1}J_{Rh,P}$ = 188.2 Hz)} corresponding to compound **26** and two triplets {δ = -123.4 (t), -120.3 (t) ($^{1}J_{Rh,P}$ = 123.2 Hz)}and two doublets {65.0 (d), 64.0 (d) ($^{1}J_{Rh,P}$ = 196.4 Hz)} corresponding to two isomers (1: 0.4) of compounds **27, 27′** (Figure 6.18). However, these two products could not be separated because of the rather small solubility differences.

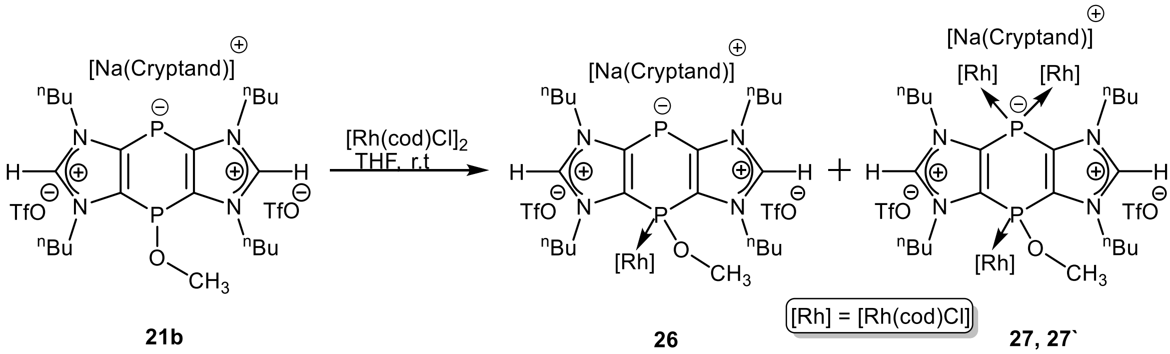

Scheme 6.10. Competing formation of mono-rhodium(I) and tri-rhodium(I) complexes **26** and **27**,**27′** respectively.

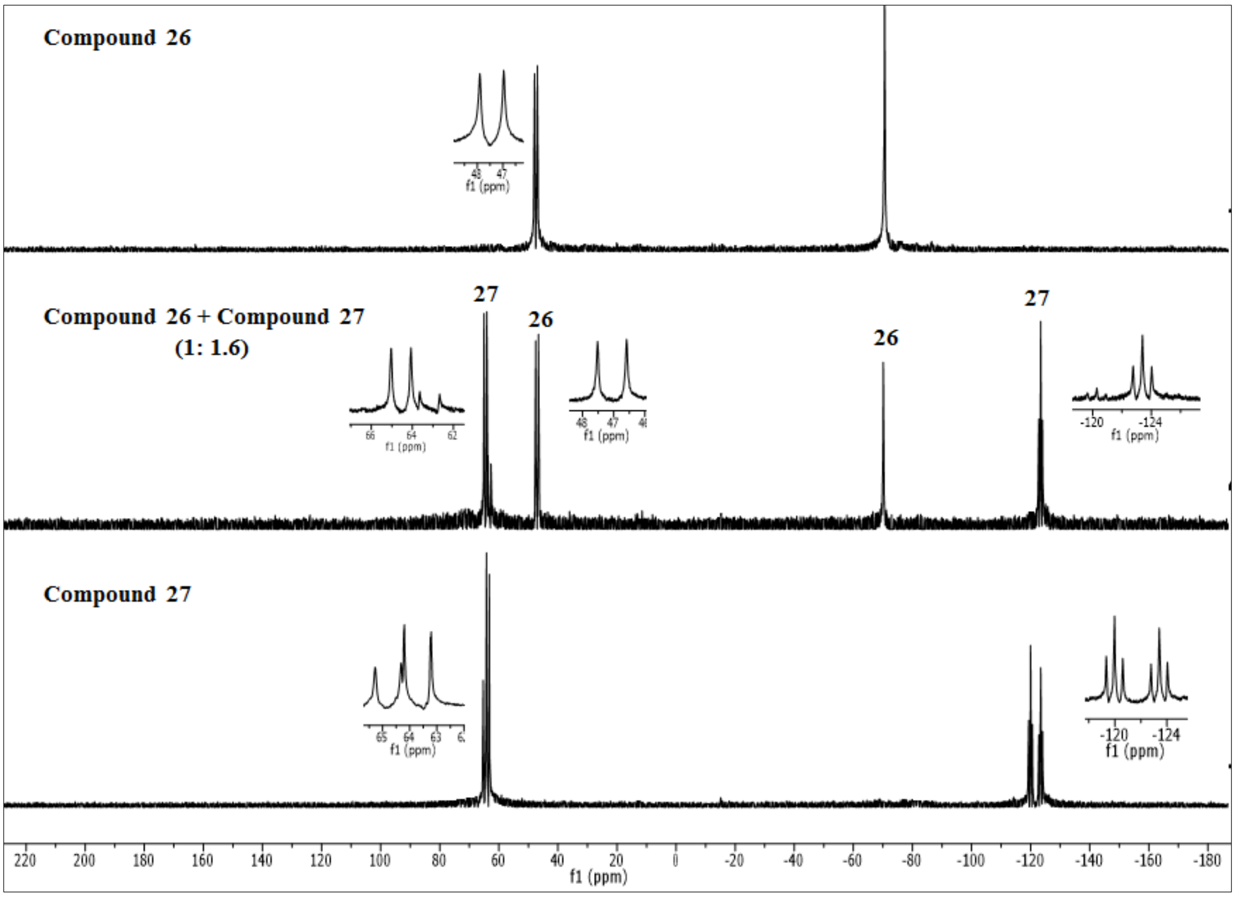

Figure 6.18. $^{31}P\{^{1}H\}$ NMR spectrum of reaction outcomes using different stoichiometric ratios of compound **21b**and $[Rh(cod)Cl]_2$; **1: 0.5**(top), **1: 1**(middle) and **1: 1.5**(bottom).

To check completion of the reaction, 1.5 equivalent of rhodium (I) dimer was treated with compound **21b** (Scheme 6.11). The reaction mixture turned cloudy, indicating lower solubility of the resulting product in THF. In the $^{31}P\{^{1}H\}$ NMR spectrum, complete consumption of the starting material **21b** and no signal for compound **26** was observed afterwards.

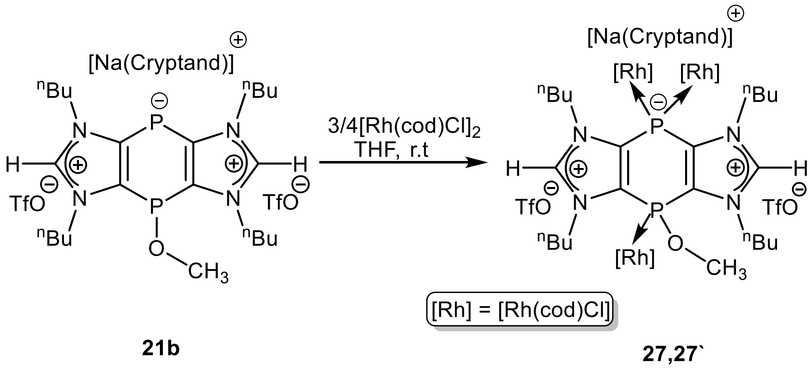

Scheme 6.11. Selective formation of trinuclear Rh(I) complexes **27,27′.**

Instead, clean transformation to compounds **27, 27′** was observed as indicated by two triplets {δ = -123.4 (t), -120.3 (t) ($^{1}J_{Rh,P}$ = 123.2 Hz)}and two doublets {65.0 (d), 64.0 (d) ($^{1}J_{Rh,P}$ = 192.4 Hz)} in the ^{31}P NMR spectrum assigned to two isomers (1:0.4); the latter were isolated in good yields (69 %) (Figure 6.18). Upon complexation, the phosphanido center of **27, 27′** appears significantly upfield-shifted compared to uncomplexed **21b** (δ = - 67.3 ppm) and showed similar trend as reported examples **LIV**[109](Figure. 6.17). Finally, the ESI-MS spectrum showed a molecular ion peak at m/z 1153.205 assigned to $[C_{47}H_{76}Cl_2N_4OP_2Rh_3]^+$ whichprovides further support to the formation of the anionic trinuclear Rh(I) complexes**27, 27′**.

7. “Methoxide”-induced P-C bond cleavagein 1,4-diphosphabarrelenes

After successful synthesis of $P^{V/V}$, $P^{III/III}$ and anionic Janus-type bis(NHCs), it was decided to extend the studies towards the synthesis of phosphabarrelene-derived bis(NHCs) and related compounds. The first exampleof a1,4-diphosphabarrelenewas reported by *Kobayashi* and co-workers in the 1980s. They proposed cycloaddition reactions of **XLX** with alkynes and sulphur to get access to **XLXIII** and **XLXIV**.[98, 100] Recently, different dienophiles were treated with tricyclic 1,4-diphosphinines to form **LV**and **LVI** (Figure 7.1) by *Streubel* and co-workers.[102, 105] As discussed beforehand (and earlier) reactivity studies of 1,4 diphosphinine, especially of the nucleophilic nature of C=E(E = S, Se), moieties has been intensively investigated. Keeping this in mind, we decided to explore the nucleophilic behaviour of the C=Se units of cycloaddition products to afford corresponding imidazolium salts, which can then act as precursors for hitherto unknown rigid, bent bis(NHCs).

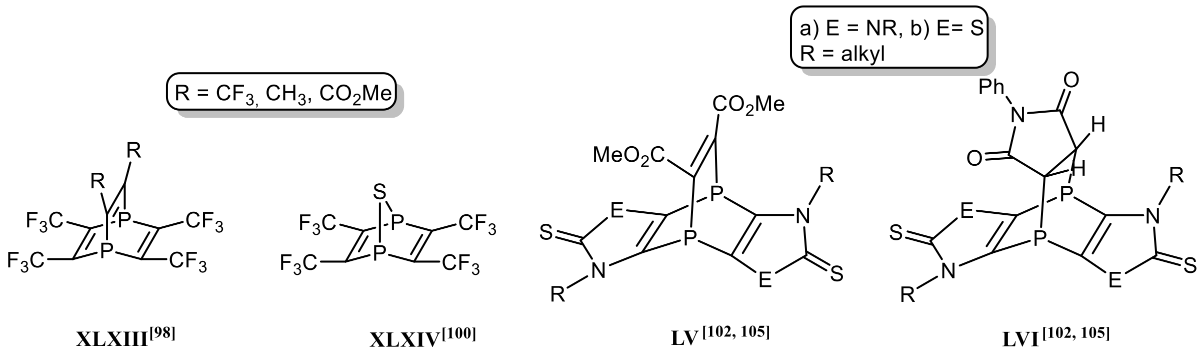

Figure 7.1*:* Literature known examples of cycloaddition products of 1,4-diphosphinines.[98, 100, 102, 105]

7.1 [4+2] cycloaddition reaction of compound 19

As a starting point, we performed a cycloaddition reaction of compound **19** with dimethyl acetylene-dicarboxylate (DMAD) at elevated temperature (60 °C) in THF (Scheme 7.1), following the well-established protocol by Koner.[102]

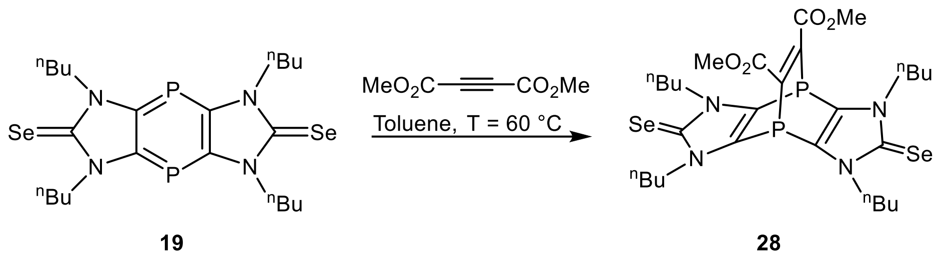

Scheme 7.1. Synthesis of 1,4-diphosphabarrelene diselone **28**.

Completion of the reaction was monitored by $^{31}P\{^1H\}$ NMR spectroscopy, revealing a chemical shift value of -86.6 ppm, very close to compound **LVa** (-87.3ppm)[102] indicating the formation of compound **28**. In the $^{13}C\{^1H\}$ NMR spectrum, a doublet at 128.7 ppm ($^1J_{P,C}$ = 59 Hz) corresponding to the sp^2-hybridized carbon atoms of the C_2-bridging unit, carrying the CO_2Me groups {166.1 ppm (dd, $^2J_{P,C}$ = 16.4 Hz)}, showed the presence of the 1,4 diphosphabarrelene unit. Further confirmation for the composition of **28** was obtained from an HRMS spectrum (*m/z* 720.1010), which was in agreement with the calculated m/z 720.1012.

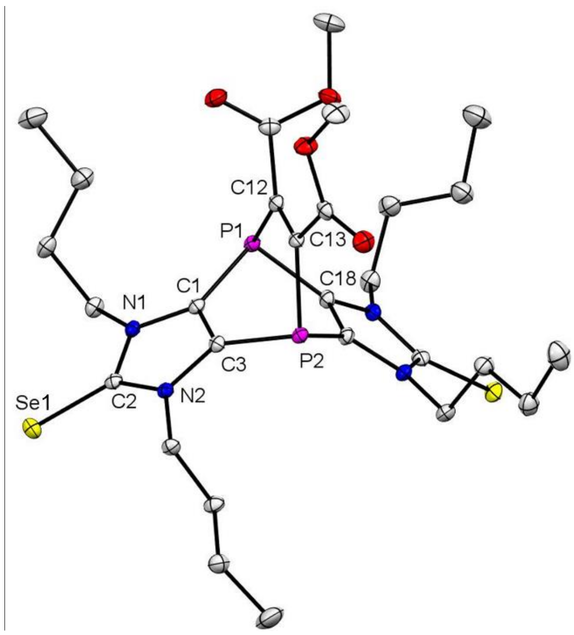

Figure 7.2. Displacement ellipsoids plot (50% probability) of the molecular structure of **28** in the crystal. Hydrogen atoms have been omitted for clarity. Selected bond lengths (Å) and angles (°) P1-C1 1.8181(18), P1-C12 1.8903(18), C1-C3 1.351(2), P1-C18 1.8225(18), C12-C13 1.335(2), C2-Se1 1.8453(18), C1-P1-C18 94.69(8), N1-C2-N2 106.43(15).

Compound **28** was finally confirmed by the results of an X-ray crystallographic measurement using single crystals grown from a saturated methylene chloride solution at -20 °C. Compound **28** crystallized in the triclinic crystal system with the P-1 space group (Figure 7.2). The C13-C14 bond distance 1.335(4) Åis in the normal range when compared to literature values of **LVa**(1.329(9) Å),[102] while the distance P1-C1 (1.846(3) Å) is within the range of phosphabarrelenes (1.864(2) Å)[175] or 1,4-diphosphabarrelenes **LVa** (1.820(6) Å).[102] Similarly, P1-C12 1.8903(18) Å is also fell well in the range of P1-C23 1.897(4) Å, showing values of "normal" sp^2-hybridized carbon centers.

7.2. Reaction of compound 28 with MeOTf

On route towards the synthesis of 1,4-diphosphabarrelene-containing bis(NHCs), the double Se-methylation of compound **28** was carried out using two equivalents of MeOTf in methylene chloride (Scheme 7.2). After 1 hour of stirring, the colour change was observed from orange-red to orange. The $^{31}P\{^1H\}$ NMR spectrum showed a slightly highfield-shifted signal compared to **28** at -90.0 ppm, which was also comparable to literature known compounds (−77.1 ppm)[176], so it was tentatively assigned to the double Se-methylated salt **29**.

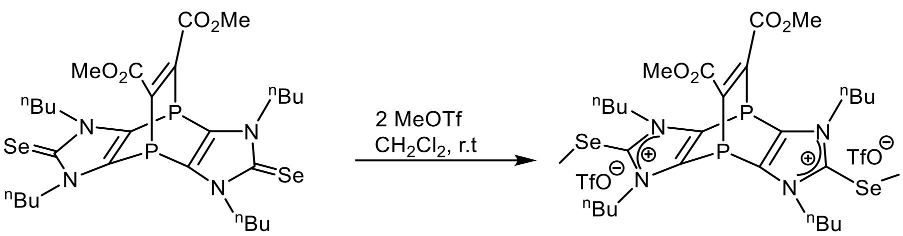

Scheme 7.2. Synthesis of double Se-methylated salt **29** containing a 1,4-diphosphabarrelene unit.

In the $^{13}C\{^1H\}$ NMR spectrum, apart from the signals of other unchanged substituents of compound **28**, a new signalwas observed at 11.4 ppm corresponding to the S-Me unit. This was supported by the presence of a signal at 2.5 ppm (Se-Me) in the ^1H NMRspectrum, which also paralleled previous cases. The proposed chemical composition of the product was further supported by HRMS (pos. ESI) m/z (calc./*exp.* 720.1012(720.1010))and elemental analysis.

7.3 Reductive deselenization and more

As mentioned above in chapters 5 and 6, $NaBH_4$ was successfully used as a reducing agent for reductive deselenization of compound **13***cis/trans*, **21a** and **21b** to synthesize, finally, bis(NHCs). So, we decided to follow the same strategy to reduce compound **29** using $NaBH_4$ in methanol. The reaction was carried out under identical conditions, as also shown in Scheme 7.3. The reaction mixture was primarily analyzed by $^{31}P\{^1H\}$ NMR spectroscopy, and the outcome was really surprising.

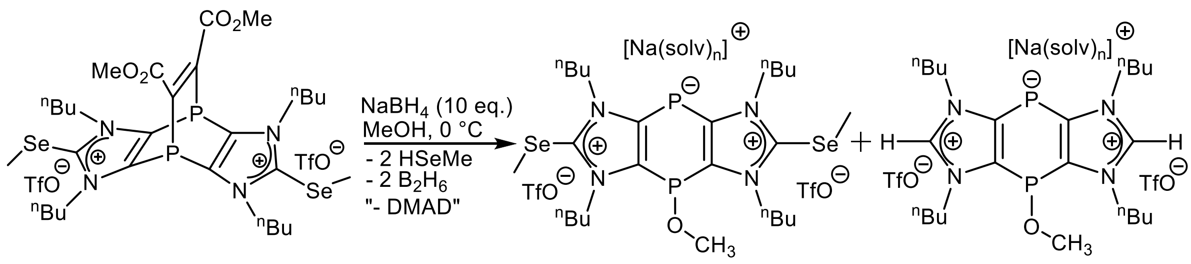

Scheme 7.3: Reaction of double Se-methylated salt **29** with $NaBH_4$.

At first glance, we observed clean conversion of starting material into two new products showing signals at δ = -67.4 (t) and 19.9(s) ppm with a coupling constant magnitude of 2.1 Hz (Figure 7.3).

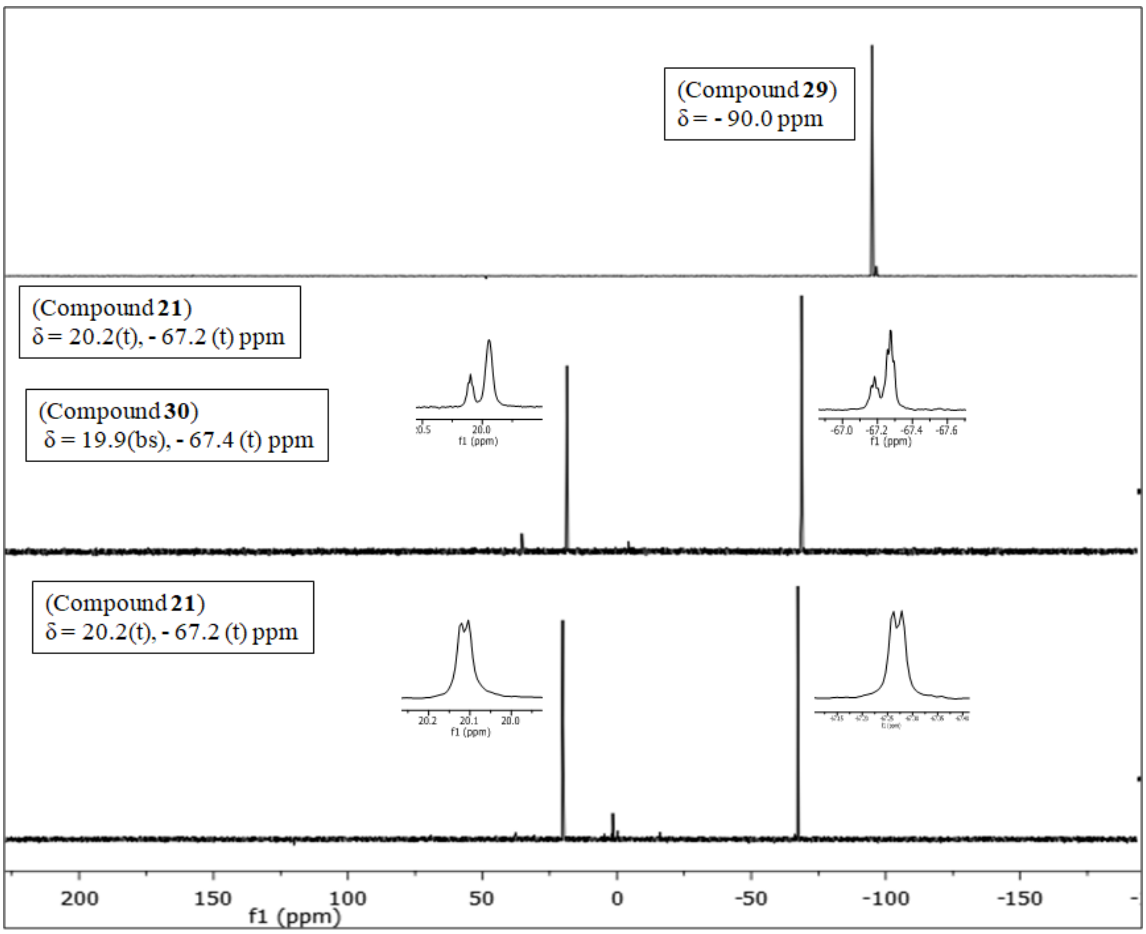

Figure 7.3. $^{31}P\{^1H\}$ NMR spectrum of compound **29** (top), reaction mixture having compound **30** and **21a** (1:0.35) (middle) and compound **21a**(bottom).

Change in chemical shift values compared to precursor **29** clearly indicated the formation of a new compound with different *P*-centers. Such chemical shift values were already detected for monoanionic compounds **La, b**.[115b] However, a closer look revealed that two new triplets at δ = -67.2, 20.2, assignable to the formation of another new compound with the same constitution of the *P*-centers, were observed. Unfortunately, this product mixture could not be separated.

To get further insight into this reaction, ^{1}H NMR spectrum was measured, as shown in figure 7.3(middle). Upon comparison with the^{1}H NMR data of compound **29** (Figure 7.4 top), two more new signals were observed at δ = 2.5(d, 7.9 Hz) and δ = 8.8(d, 7.9 Hz) corresponding to *Me*O and C^{2}-H protons, respectively. These observations highly suggested the assignments to compounds **30** and **21a**.

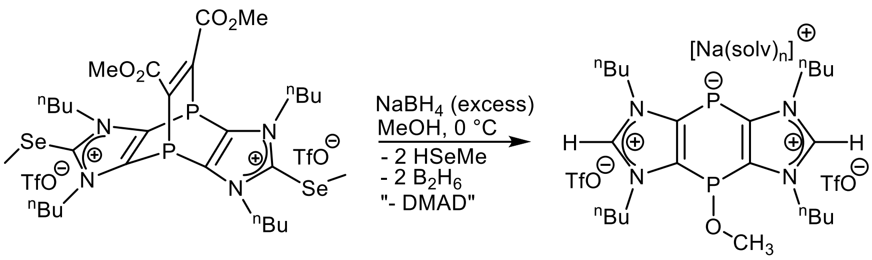

29 **21a**

Scheme 7.4. $NaBH_4$ induced P-C bond cleavage in compound **29**.

To achieve the completeness of the reaction, excess of $NaBH_4$was added under the similar condition as described in scheme 7.4, which led to full conversion of the starting material **29** and two signals at δ = -67.2 and 20.2 showing AB spin pattern with $^{3}J_{P,P}$ coupling of magnitude 2.1 Hz appeared. After isolation, ^{1}H NMR and ^{13}C NMR spectroscopic measurement confirmed the formation of compound **21a** (Figure 7.4), which was also proven by mass spectrometric analysis.

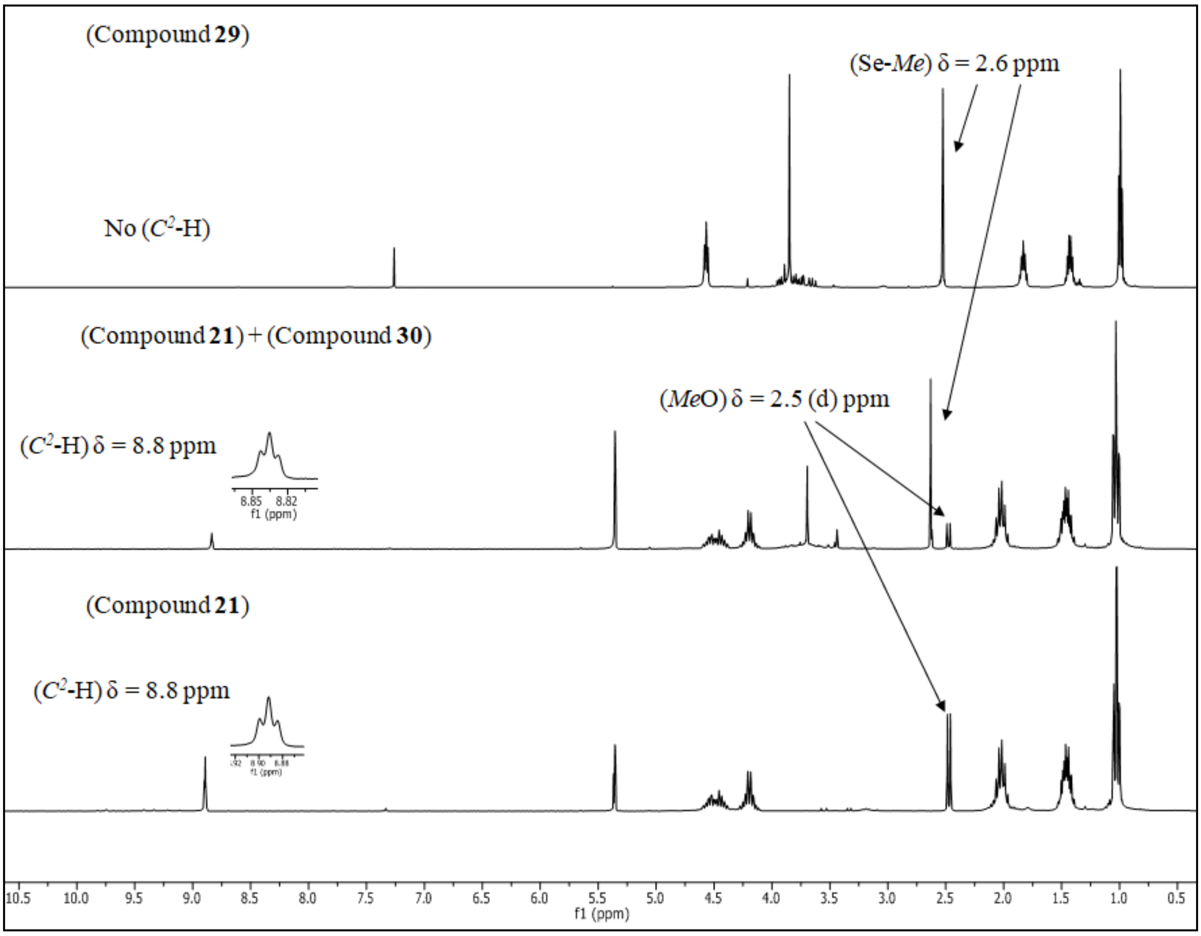

Figure 7.4. ^{1}H NMR spectrum of compound **29** (top), reaction mixture having compound **30** and **21a** (middle) and compound **21a** (bottom).

8. Reductive studies of a tricyclic imidazole-based 1,4-diphosphinine

There are several examples of λ^3-phosphinines being reduced by alkali metals to produce paramagnetic anion radicals and diamagnetic dianions.[177] Dimroth and co-workers reported the formation of para-magnetic trianion radicals via a reduction of 2,4,6-triphenylphosphinine with potassium metal in THF; nevertheless, ESR spectrum was not resolved.[177a] Later on, Märkl extended the investigations on the stepwise reduction of **LVII** using CV and ESR studies(Scheme 8.1).[178]

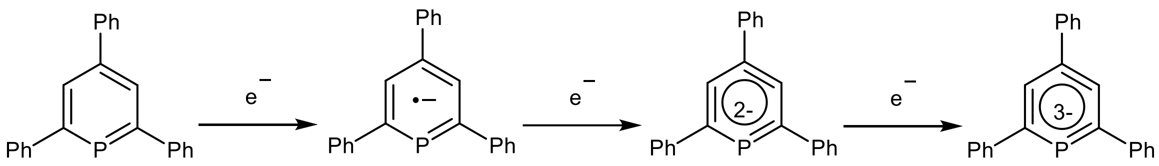

LVII **LVIII** **LIX** **LX**

Scheme 8.1 Reduction of phosphinine**LVII,** according to Märkl.[178]

Early attempts by Streubel and co-workerswere performed to achieve anantiaromatic dianion via two-fold reductive cleavage of exo-P-C bonds in 1,4-dihydro-1,4-diphosphinine **LXI** to form tricyclicbis(phosphanido)-bridged compound**LXII**. However, due to unsuccessful isolation, it was reacted *in situ* with 2 eq. of an electrophile (^{n}BuI) to get the final product **LXIII** (Scheme8.2).[115b]

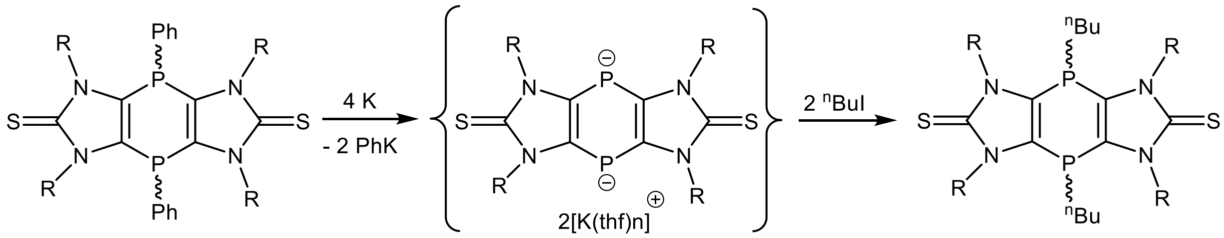

LXI **LXII** **LXIII**

Scheme 8.2. Generation of tricyclic bis(phosphanido)-bridged **LXII** and the *in situ* trapping reaction.[115b]

More recently, a two-fold reduction of thiazole-based 1,4-diphosphinine dithione**XCXIX** was successfully achieved by Begum using two equivalents of KC_8 or Li in Et_2O (Scheme 8.3). The resulting dianionic product **XLXIX** was stable enough to be isolated and structurally confirmed.[105]

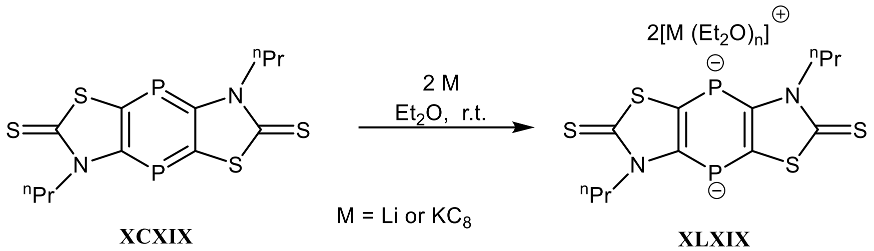

XCXIX **XLXIX**

Scheme 8.3. Two-fold reduction of thiazole-derived 1,4-diphosphinine**XLXIX**.[105]

The successful reduction of these 1,4-diphosphinine systems prompted us to investigate two- or even six-fold reduction processes to access dianionicand/or dianionic bis(NHCs), respectively. The formation of such antiaromatic ligands can be a promising starting point for a new field of research.

8.1. Studies on the reduction of imidazole-based 1,4-diphosphinine dithione

Initially, we tried to reduce 1,4 diphosphinine diselone **19** using the well-established protocol, as mentioned above.[105] However, we could not get a selective reaction (due to unknown reasons), which did not change when the reduction was performed at low(er) temperature (-80 °C) using two equivalents of potassium metal. Therefore, we decided to use the dithione derivative of imidazole-based 1,4-diphosphinine **XLXIV** and reacted it with potassium graphite at room temperature in E_2O (Scheme 8.4). The product **30**, a dark brown solid, precipitated out from the reaction mixture after one day of stirring which was then separated by filtration.

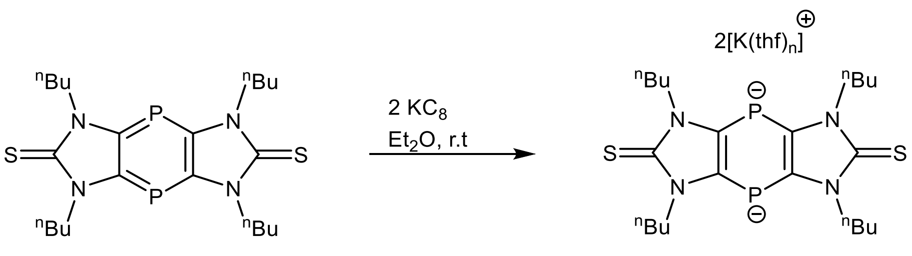

XLXIV **30**

Scheme 8.4. Two-fold reduction of 1,4-diphosphinine dithione **XLXIV**.

The $^{31}P\{^1H\}$ NMR spectrum of compound **30** solution showed a sharp signal at –114.9 ppm, thus showing a $\Delta\delta = -41$. The latter is huge compared to the previously *in situ* prepared imidazole-derived bis(phosphanido)-bridged tricycle **LXII** ($\delta^{31}P$ = –73.6)[115b] (Scheme 8.2). This might be explained with a different coordination mode ofthe dianion and additional interactions of the counter cation with the solvent molecules.The MS spectrum (neg. ESI) of **30**showed a peak at m/z483.1937 being in agreement with the calculated m/z value of the mono anion $[C_{22}H_{36}N_4P_2S_2]H^-$, formed due to protonation under the conditions of the ESI-MS experiment.

Compound **30** crystallized by slow evaporation of concentrated THF and Et_2O (1:0.2) solution at room temperature. The single crystal X-ray diffraction analysis confirmed the proposed constitution of compound **30a** being part of a coordination polymer possessing a monoclinic crystal system and $P2_1/c$ space group. The coordination network has the following interesting structural features: Each potassium cationis coordinated by two thione sulfur atoms of two molecules, one THF molecule and to the middle P_2C_4-ring via η^6 co-ordination.In case of **XLXIX**, K1 coordinated to the thione sulfur atoms of four molecules and one THF molecule. While the other potassium cation K2 is coordinated with the thione sulfur atoms of two molecules, together with three THF molecules.Furthermore, the two potassium cations have a K1-K2 distance of 4.4004(4) Å. A comparison of the bond lengths and bond angles of **30a** with the compound **XLXIV** showed that the P-C3 and P#1-C1 bond lengths are slightly longer than in **XLXIV** (P-C1 1.741(3), P–C3 1.741(3)). However, the C1-C3 bond length slightly shorter compared to **XLXIX** (C1-C3 1.400(4)), and the C1-P-C3 bond angle reduced to 93.03(3) when compared to its precursor **XLXIV** (C1-P-C3 97.14(15)). Likewise, the [K-S 3.190(2) and K-S#2 3.242(3)] distances in **30**are also slightly longer than those in **XLXIX**[K1-S4 3.191(3), K1-S6 3.194(4), K1-S10 3.164(4), K1-S14 3.113(3)].

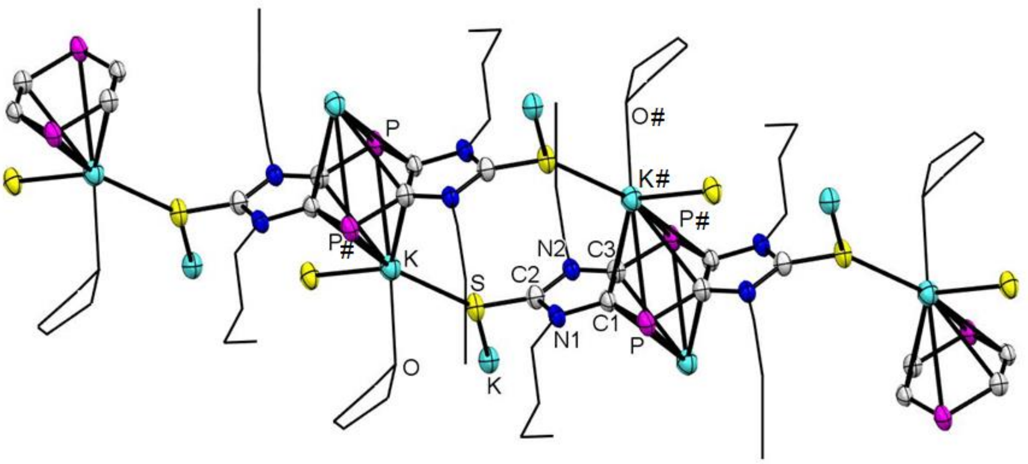

Figure 8.1.Cut-out of the coordination polymer of **30**in the crystal. Displacement ellipsoids plot (50% probability) andhydrogen atoms have been omitted for clarity. Selected bond lengths (Å) and angles (°) P#1-C1 1.815(8), P-C3 1.836(7), C1-C3 1.376(10), N1-C2 1.345(9), N2-C2 1.358(8), C2-S 1.715(7), C1-P1-C18 93.0(3), N1-C2-N2 106.2(5).

In order to test the coordination properties of the dianionic compound **30**, complexation was performed using the same Rhodium(I) dimer as before, and the reaction with two equivalents of $[Rh(cod)Cl]_2$ afforded the tetranuclear diphosphanido-type complex **31**(Scheme 8.5).

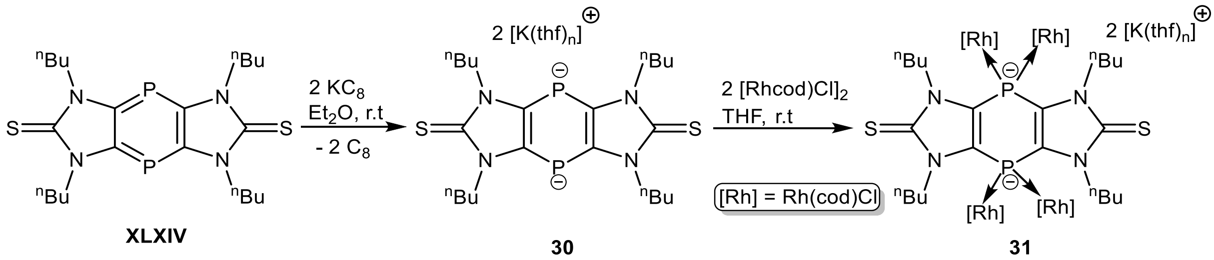

Scheme 8.5. Reaction of dianionic compound **30** with $[Rh(cod)Cl]_2$.

The $^{31}P\{^1H\}$ NMR spectrum of the reaction mixture showed only one resonance signal at −113.6(t) ppm with a $^1J_{Rh,P}$ coupling constant magnitude of 125.4 Hz (Figure 8.2). After purificationvia washing, **31** was completely characterized via various means (NMR, MS and IR).The proposed chemical composition of the product was further supported by HRMS (pos. ESI)m/z 203.0000 (calc.*m/z*202.9999).

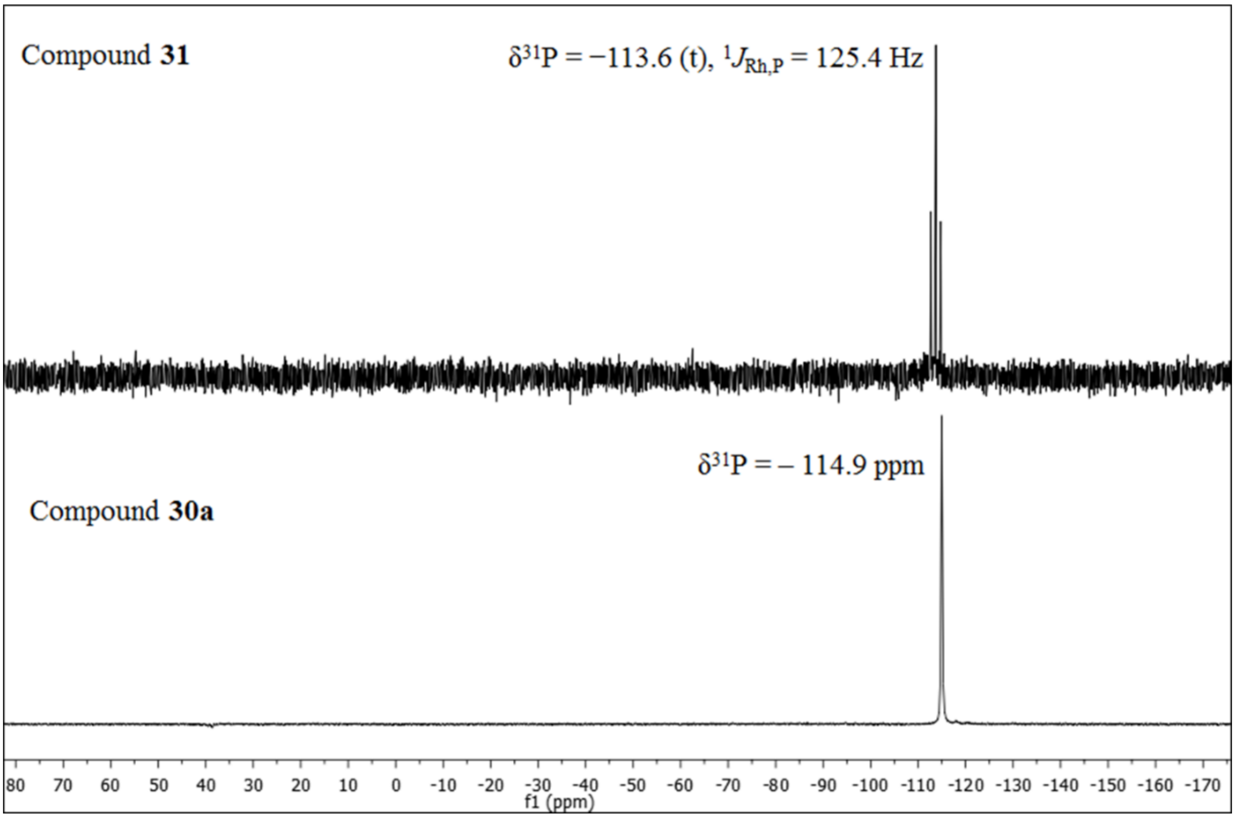

Figure 8.2. $^{31}P\{^1H\}$ NMR spectrum of compound **30**(bottom) and **31** (top).

8.2. Reductive desulfurization of compound 30

Reductive desulfurization of N-heterocyclic thiones with potassium metal to produce NHCs (**LIV**) has been shown first by Kuhn and co-workers for imidazole-2-thiones (Scheme 8.6).[179]

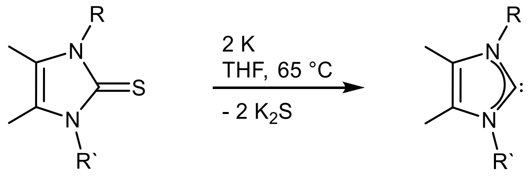

LIV

Scheme 8.6. Reduction of thiones to generate mono(NHCs) (R,R’ = alkyl groups).[179]

In a related reaction, Majhi has used **XLVI** and a six-fold excess of potassium metal in THF(Scheme 8.7).[49] The outcome was the formation of bis(NHC) **XLVII** having achemical shift at -116.2 ppm in the ^{31}P{^{1}H} NMR spectrum as well as a missing signal in the^{13}C{^{1}H} NMR spectrumfor the C=S carbon, thus suggesting that a C=S bond cleavage process must have been taken place.[49] Nevertheless, **XLVII** could neither be isolated nor structurally confirmed.

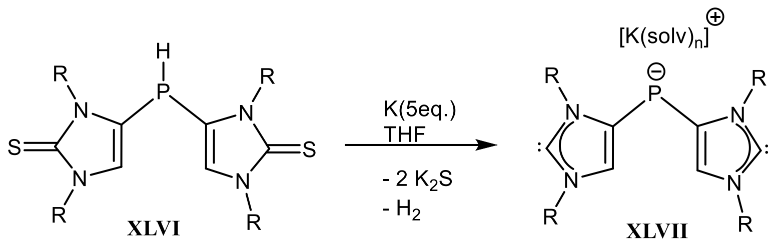

XLVI **XLVII**

Scheme 8.7. Synthesis of anionic bis(NHC),according to Majhi.[49]

Following these observations, we became curious to further reduce compound **30**. When compound **30** was treated with an excess of KC_8 at 65 °C the dianionic bis(NHC) **32** was formed (Scheme 8.8). The reaction mixture was filtered to remove potassium sulfide, and compound **32** was isolated as a dark red-brown solid.Product**32**displayed two major signals at δ = -117.7and -120.4 ppm in the ^{31}P{^{1}H} NMR spectrum (Figure 8.3).The ^{13}C{^{1}H} NMR spectrum allowed for the identification as a signal at δ = 207.4 ppm (br) was observed (Figure. 8.3), which is consistent with the presence of the C^2 nuclei of the dianionic bis(NHC) **32**.

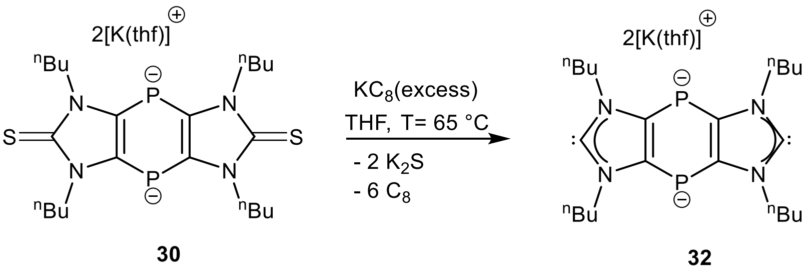

Scheme 8.8. Six-fold reduction of compound **30** with KC_8 leading to **32**.

Further confirmation for **32** came from the LIFDI-MS spectrum showing m/z 422.2 ($[M+3H]^{\cdot+}$).

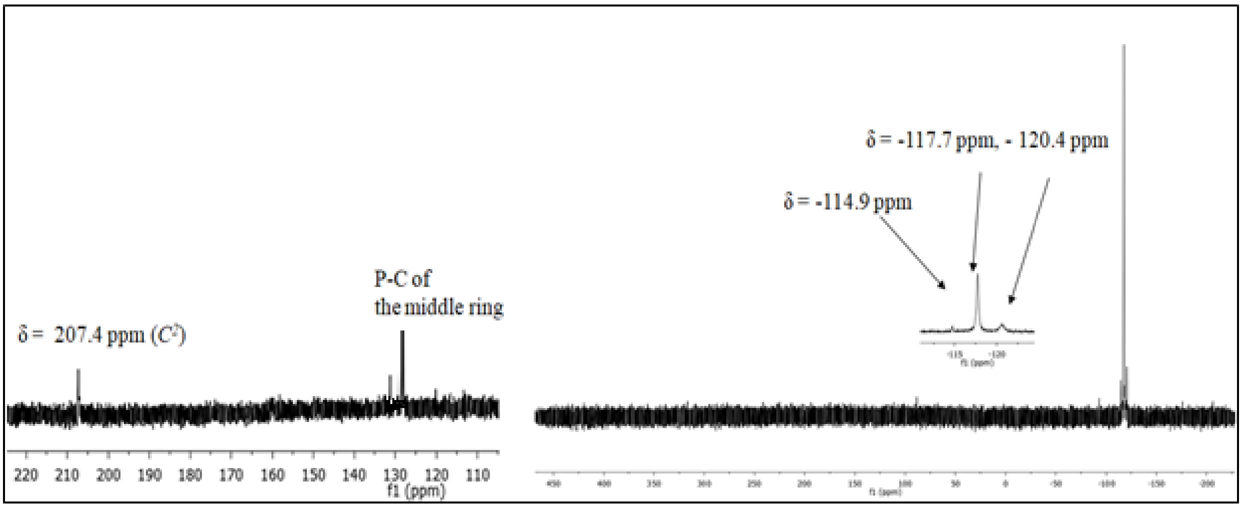

Figure 8.3. $^{31}P\{^1H\}$ NMR (right) and $^{13}C\{^1H\}$ NMR (left) spectrum of compound **32**.

8.3. Synthesis of the bis(imidazolium) diphosphanide zwitterion 33

To achieve the synthesis of neutral 1,4-diphosphinine bis(NHC), a different strategy was tested. Having handson compound **13^cis/trans^**, we performed a substitution reaction using PCl_3 in methylene chloride (Scheme 8.9). But the $^{31}P\{^1H\}$NMR resonance of product **33** showed a downfield shift signal thatappeared at δ = - 50.2 ppm together with the resonance of the by-product Et_2NPCl_2 at 162.2 ppm. Concentrating the reaction mixture *in vacuo* led to the decomposition of product **33,** leading to unknown products as observed in the $^{31}P\{^1H\}$ NMR spectrum (Figure 8.3). Therefore, isolation of the compound, even under inert and low temperature conditions, failed for unknown reasons.

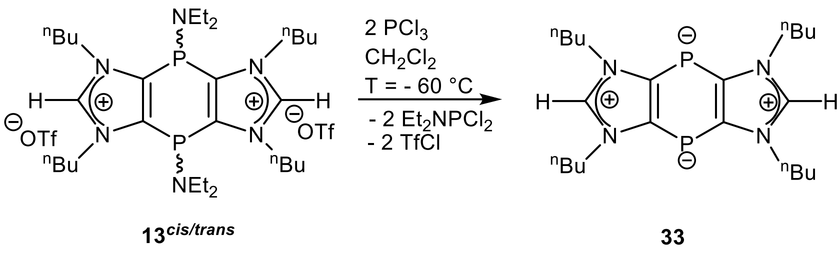

Scheme 8.9. Synthesis of double zwitterion **33**.

Nevertheless, the raw product could be characterized via its ^{1}H NMR spectrum as the C^{2}-H resonance signal appeared at δ = 9.1 ppm.Interestingly, the ease of protonation of compound **33** was confirmed by pos-ESI-MS showing m/z theor./exp. 210.128/210.128.

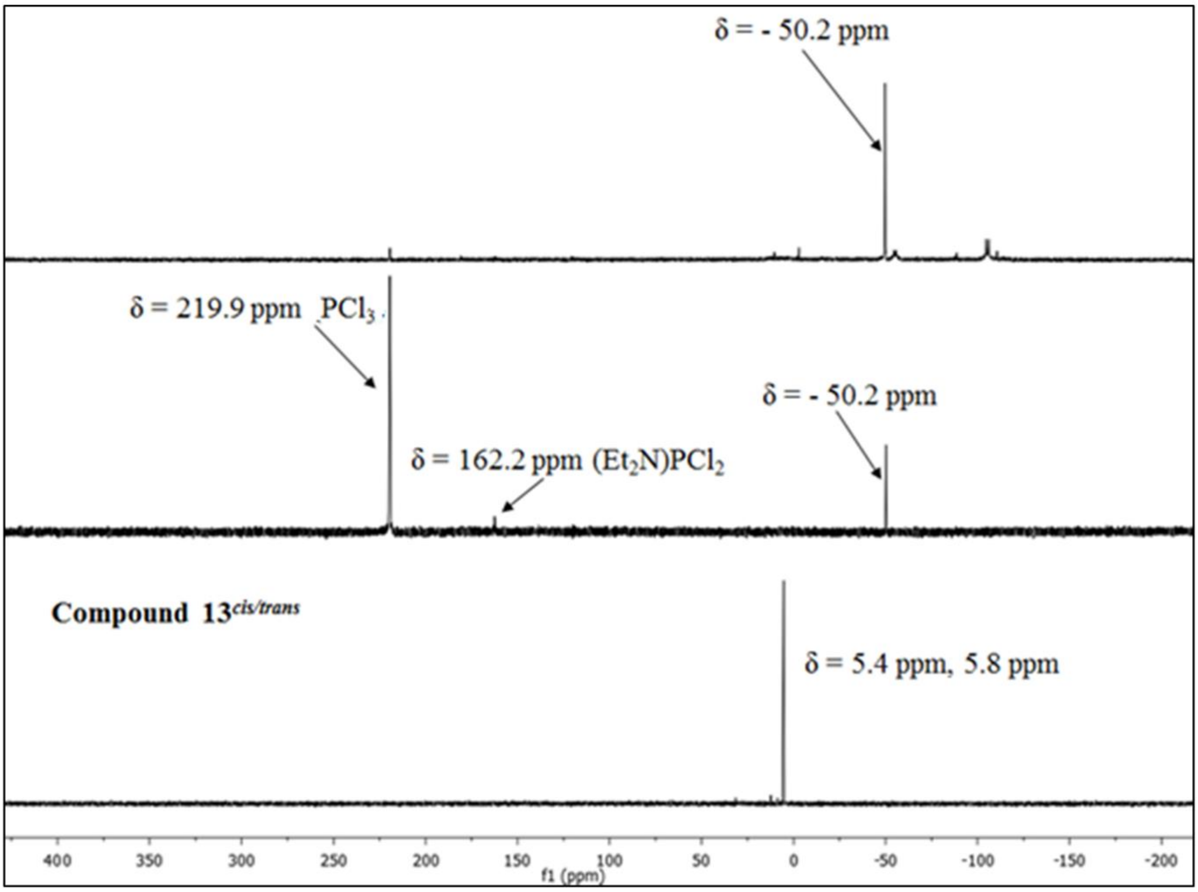

Figure 8.3. $^{31}P\{^{1}H\}$ NMR spectrum of compound **13*cis/trans***(bottom), the reaction mixture of compound **33** (middle) and reaction mixture after concentrating under reduced pressure(top).

9. Synthesis and reactions of {P(O)OH}-functional bis(NHCs)

As mentioned in the introductory section, oxidative desulfurization is a well-established pathway to get access to NHCs. On the other hand, oxidative hydrolysis of phosphinines using ambient conditions was proposed to proceed via the transientphosphinine oxide **LVI**, formed via reaction with O_2, that reacts readily due to its electrophilic naturewith 1 eq. of H_2O to form the phosphinic acid **LVII** (Scheme 9.1).[180] A similar pathway was also assumed for the tricyclic diphosphinine **XLXVI** thus forming bis(phosphinic) acid **XLXVII**.[103] However, the reaction mechanism remained to be established.

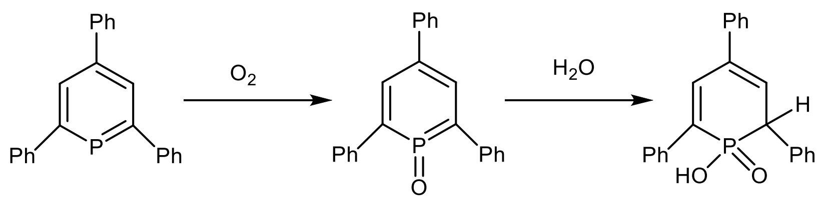

Scheme 9.1. Oxidative hydrolysis of a phosphinine.[180]

In the course of our aforementioned study, oxidative deselenization was quite promising to get access to $P^{V/V}$ bis(NHCs) by using H_2O_2. Following this, a reaction between compound **19** and hydrogen peroxide was performed in methylene chlorideat 0 °C. The reaction mixture turned to colourless after half an hour, and the $^{31}P\{^1H\}$ NMR spectrum showed complete consumption of the starting material **19** along with a new signal at -14.3 ppm.

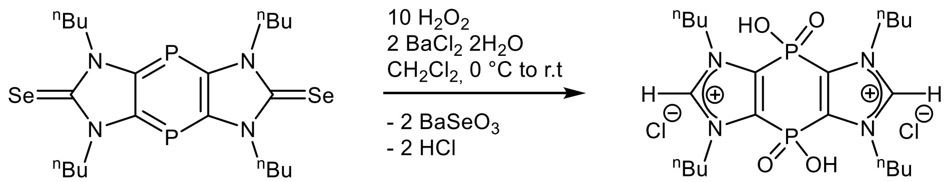

Scheme 9.2. Oxidative deselenization of compound **19.**

For compound **34, 34′**, we could not observe two signals as expected for the*cis* and *trans* isomers due to rapid intermolecular exchange of the POH proton with deuterium of solvent (CD_3CD) at room temperature. Furthermore, successful formation of **34, 34′** had to be confirmed by the ^{1}H and ^{13}C{^{1}H} NMR spectra of the isolated product. Importantly, the ^{1}H NMR spectrum showed a new resonance at 9.3 ppm (br) assigned to the C^{2}-H of imidazolium derivative **34, 34′**. Further evidence for the formation of **33** was collected from the ^{13}C{^{1}H} NMR spectrum as the resonance signal for the *C*=Se carbon nucleus was not present (162.4 ppm) and was replaced by a triplet at 139.3 ppm (t, $^{4}J_{P,H}$ = 6.1 Hz).

Conclusive confirmation for the assignment of the product as to be the imidazolium derivative **34, 34′** came from the (pos)ESI-MS spectrum, which showed an ion peak at m/z 487.2 correspondings to the cation of $C_{22}H_{42}N_4O_4P_2$.

Derivative **34, 34′** was then deprotonated to get access to the corresponding $P^{V/V}$ bis(NHC)s **35, 35′** following the conditions as described in scheme 9.3. A slight colour change was observed from colourless to light yellow. The ^{31}P NMR spectrum of the reaction mixture revealed only a minor change in the chemical shift of **35, 35′** (-14.3 ppm) compared to **34,34′** (-15.3 ppm). In addition, the C^{2}-H proton signal at 9.3 ppm was missingin the ^{1}H NMR spectrum, and the C^{2} signal of the carbene nuclei could not be observed in the^{13}C{^{1}H} NMR spectrum.

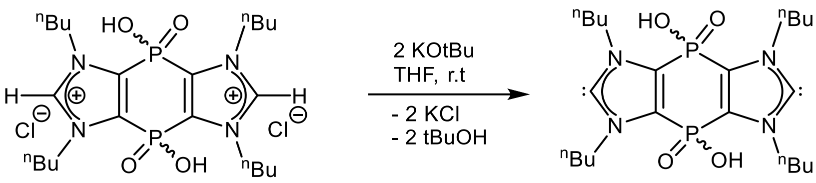

34, 34\`** **35, 35\`

Scheme 9.3. Synthesis of {P(O)OH}bis(NHC)s **35, 35′.**

In order to test a possible complexation of compound **35, 35′** it was decided to use the reaction using a methanolic solution of **34, 34′** and 2 equivalents of Ag_2O (Scheme 9.4). The reaction mixture was stirred for 3 hours and then subjected to filtration to remove the potassium chloride, thus finallygetting **36, 36′** as isomeric mixture (1: 0.35) in good yields (68 %).

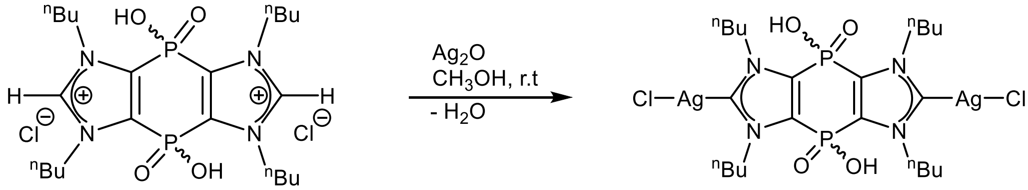

34, 34\`** **36, 36\`

Scheme 9.4. Synthesis of {P(O)OH}bis(NHC) Ag(I) complexes **36,36′.**

Multinuclear NMR experiments were performed to characterize the resulting bis(NHC) complexes **36, 36`**.The $^{31}P\{^{1}H\}$ NMR spectrum of **36, 36`** in CD_3OD showed two resonances at –12.6 and -10.2 ppm, which are shifted upfield compared to **34,34′**(δP = –14.3 ppm) (Figure 9.1). Nevertheless, the value is in good agreement with the related complex **10b***cis/trans*(-3.62 (*cis*), -4.10 (*trans*))[118] (Figure 9.1), reported recently.

Table 9.1. Comparison of $^{31}P\{^{1}H\}$ and $^{13}C\{^{1}H\}$ NMR chemical shifts (ppm) of (*C*²-*Ag*) between **LVIII**,[49] **10b***cis/trans*and **36, 36′.**

	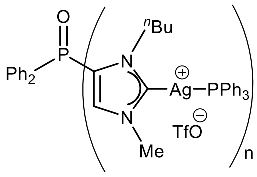 **LVIII**	**10b***cis/trans*	**36, 36′**
$\delta^{1}H$	8.5 (s)	- 4.10 (cis), - 3.62 (trans)	- 12.6 (s), - 10.2(s)
$\delta^{13}C\{^{1}H\}$	178.2 (d, $^{3}J_{P,C}$ = 3.6 Hz)	188.9 (br), 191.3 (br)	183.7 (br),185.3(br)

Furthermore, the appearance of two broad signals at 183.7 and 185.3 ppm, assigned to two isomers, in the $^{13}C\{^{1}H\}$ NMR spectrum provides evidence for the formation of the *C*²-Ag bond in **36, 36`**(Figure 9.1).The observed chemical shifts were in the typical range for the NHC silver(I) complexes, reported earlier. The selected $^{13}C\{^{1}H\}$ NMR chemical shifts of **36, 36′,** are listed in Table 9.1 and are compared with the previously discussedmonophosphanoyl substituted derivative **LVIII**[49] and **10b***cis/trans*. The introduction of diphenylphosphanoyl groups causes highfield shifts ofabout Δδ = 7 relative to the **36, 36′** with two P(O)OH groups. However, a downfield chemical shift of about Δδ = 6 was also observed for **10b***cis/trans* having the bis(diethylamino)phosphanoxyl group (Table 9.1).

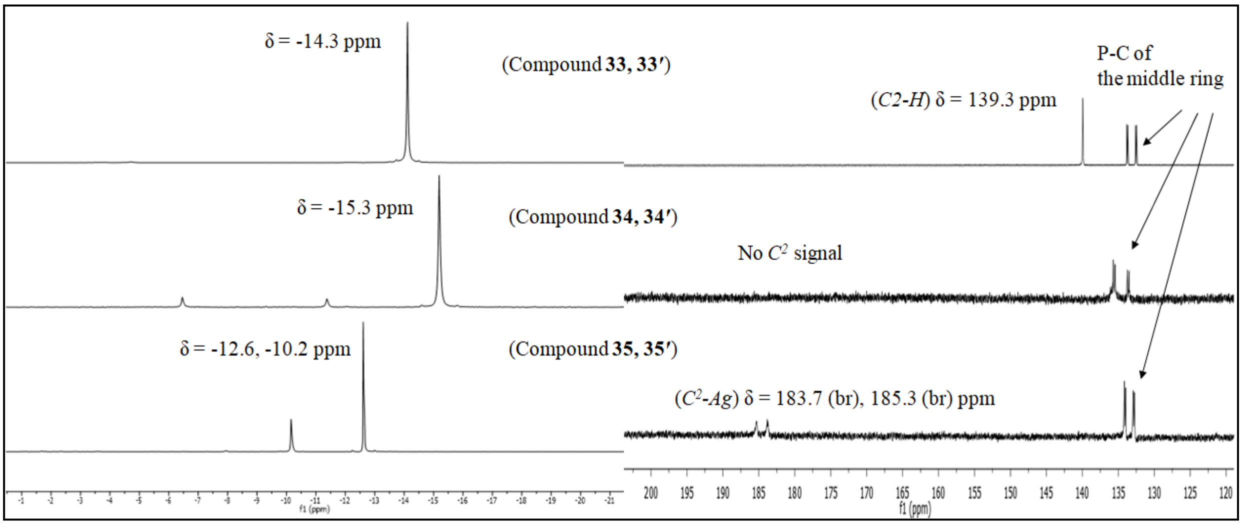

Figure 9.1. ^{31}P{^{1}H} NMR spectrum (left) and ^{13}C{^{1}H} NMR spectrum (right, C^2 nuclei) of **(34, 34′), (35, 35′)** and **(36, 36′)**

10. Summary

This thesis describesthe synthesis of a new series of *P*-bridged, rigid Janus-type tricyclic bis(NHCs) using imidazole-2-selone-derived new tricyclic 1, 4-dihydro-1,4-diphosphinines and transition metal complexes thereof. It further detailsthe problem of reduction of a 1,4-diphosphinine, leading finally to a novel, isolable tricyclic 1,4-dianionic bis(NHC) containing an8π-antiaromatic middle ring. Most of the new compounds were fully characterized by spectroscopic means, including X-ray diffraction and cyclic voltammetric studies.

Chapter 3 contains the synthesis and characterization of *C*-phosphanylated imidazole-2-selone derivatives (Scheme 10.1) using the reaction of *in-situ* generated lithiated imidazole-2-selones with chloro(organo)phosphane derivatives to synthesize phosphanylated imidazole-2-selones**2** and **3**. Reaction with phosphorus trichloride provided chlorophosphanyl substituted imidazole-2-selones**4**, **5**. Using an in-house synthetic protocol, 1,4 dihydro-1,4-diphosphinine diselones **6**$^{cis/trans}$, **7**$^{cis/trans}$were synthesized by deprotonation of 4-chloro(organo)phosphanyl imidazole-2-selones followed by an intermolecular nucleophilic substitution reaction with **4** and **5**. The separation of *cis* and *trans* isomers was successfully achieved in the case of **6**$^{cis/trans}$using low-temperature column chromatography.

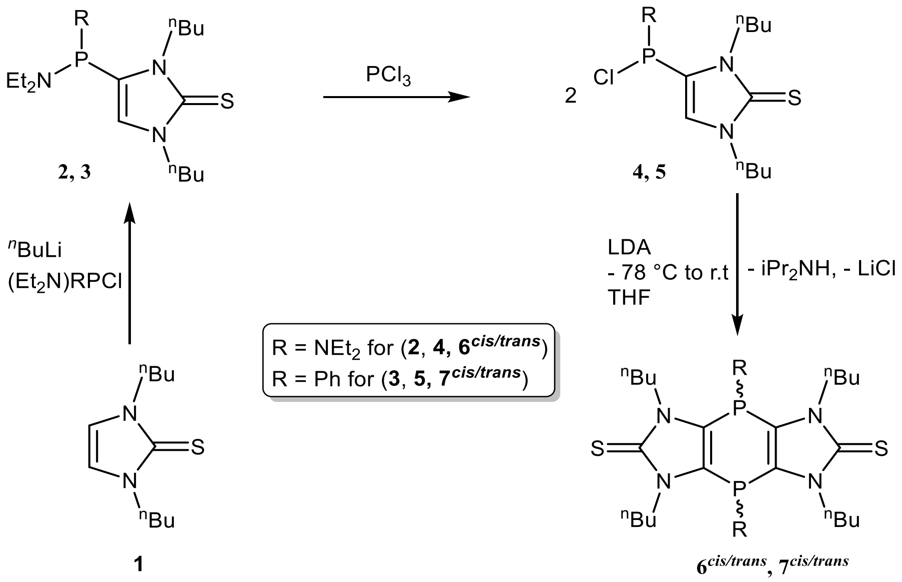

Scheme 10.1. Synthesis of tricyclic 1,4-dihydro-1,4-diphosphinines diselones.

In chapter 4, the synthesis of $P^{V/V}$-functionalized Janus bis(NHCs) and later, the formation of their metal complexes is discussed. Oxidative deselenization of **6**$^{cis/trans}$was successfully carried out by the treatment with ten equivalents of H_2O_2 in methylene chloride solution (Scheme 10.2). The imidazolium salts **8**$^{cis/trans}$, were isolated as solids being hygroscopic and having high melting points. These salts were deprotonated using KHMDS to get access to the first examples of stable and rigid $P^{V/V}$-bridged Janus-type bis(NHCs) **9**$^{cis/trans}$. Primary studies on their electrochemical behaviour were performed using cyclic voltammetry, which revealed that com-pounds **9**$^{cis/trans}$ canundergo multiple oxidation processes due to the existence of numerous filled MOs close in energy to the HOMO that has either carbene α (C) or ring π character.^{77}Se chemical shift of **9**$^{cis/trans}$(89.9/94.1 ppm) showing that the P^{V} substitution increases somewhat the electron acceptor ability of the carbene; however, still within the known range of imidazole-2-ylidenes.Moreover, the coordination properties of newly synthesized bis(NHCs) **9**$^{cis/trans}$ were explored by treating them with coinage metals(I) (M = Cu, Ag, Au) and group 9 metals Rh(I) and Ir(I). All the complexes were isolated in good yields and characterized by various analytical methods including NMR, MS, IR and single-crystal XRD in the case of Au(I) complex **10c**^{trans}.

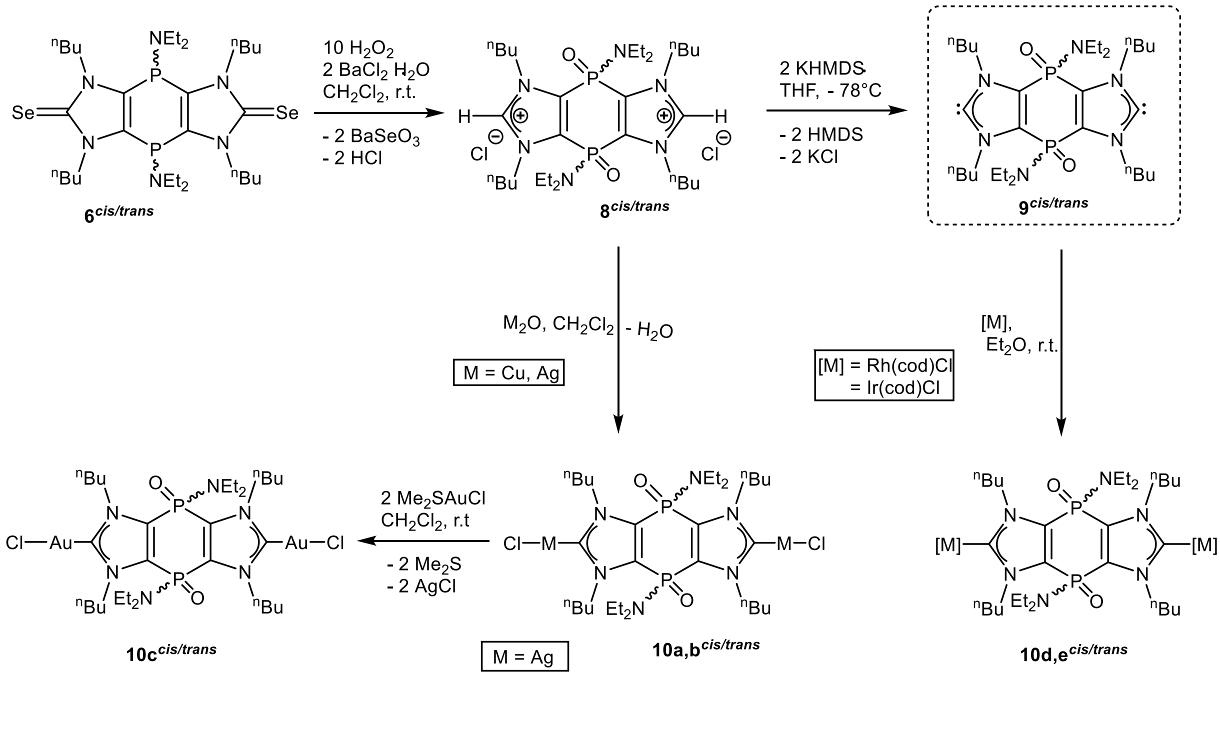

Scheme10.2. Synthesis of $P^{V/V}$ bridged bis (imidazolium) salt **8**$^{cis/trans}$, bis (NHC) **9**$^{cis/trans}$ and their coinage metal(I) complexes **10a-e**$^{cis/trans}$**.**

An important part of this thesis was devoted to the reductive deselenization of 1,4 dihydro-1,4-diphosphinine, results of which are presented in chapter 5. To obtain $P^{III/III}$-functional bis(NHCs), firstly **6**$^{cis/trans}$ and **7**$^{cis/trans}$, based on the background knowledge of DFT calculations (performed on the heterocyclic dithione-derived 1,4 dihydro-1,4-diphosphinine), the nucleophilicity of the Se centers was used by reaction with the hard electrophile MeOTf. This led selectivelyto the corresponding double Se-methylated bis(imidazolium) salts**11**$^{cis/trans}$ and **12**$^{cis/trans}$ possessing neutral tricyclic 1,4-dihydro-1,4-diphosphinine unit (Scheme 10.3). **11**$^{cis/trans}$ were further treated with sodium borohydride ($NaBH_4$) in methanol. An abrupt reaction was observed with the liberation of the strong odour of HMeSe formation resulting in the reductive deselenized product **13**$^{cis/trans}$ (Scheme 9.3). Later, deprotonation of bis(imidazolium) salts **13**$^{cis/trans}$ led to the synthesis of first neutral $P^{III/III}$-bridged bis(NHCs) **14**$^{cis/trans}$. *Trans* isomer was characterized by single crystal X-ray diffract-tion analysis showing surprisingly two different coordination modes of KHMDS with C^2-centers; one was K-$C^{2,}$ and the other was η^5 via C_3N_2 ring. Due to the high inversion barrier (44.2 kcal/mol) of phosphorus centers, the *cis* isomer is more stable than *trans* isomer in the case of **14**$^{cis/trans}$. Cyclic voltammetric studies on **14**$^{cis/trans}$ showed the irreversible nature of the oxidation processes, which is evidenced by a scan-rate of 200 mV and strong solvent dependencies of the potentials. **14**$^{cis/trans}$ are more easily oxidized than **9**$^{cis/trans}$ in accordance with the higher energy of their HOMO orbitals.

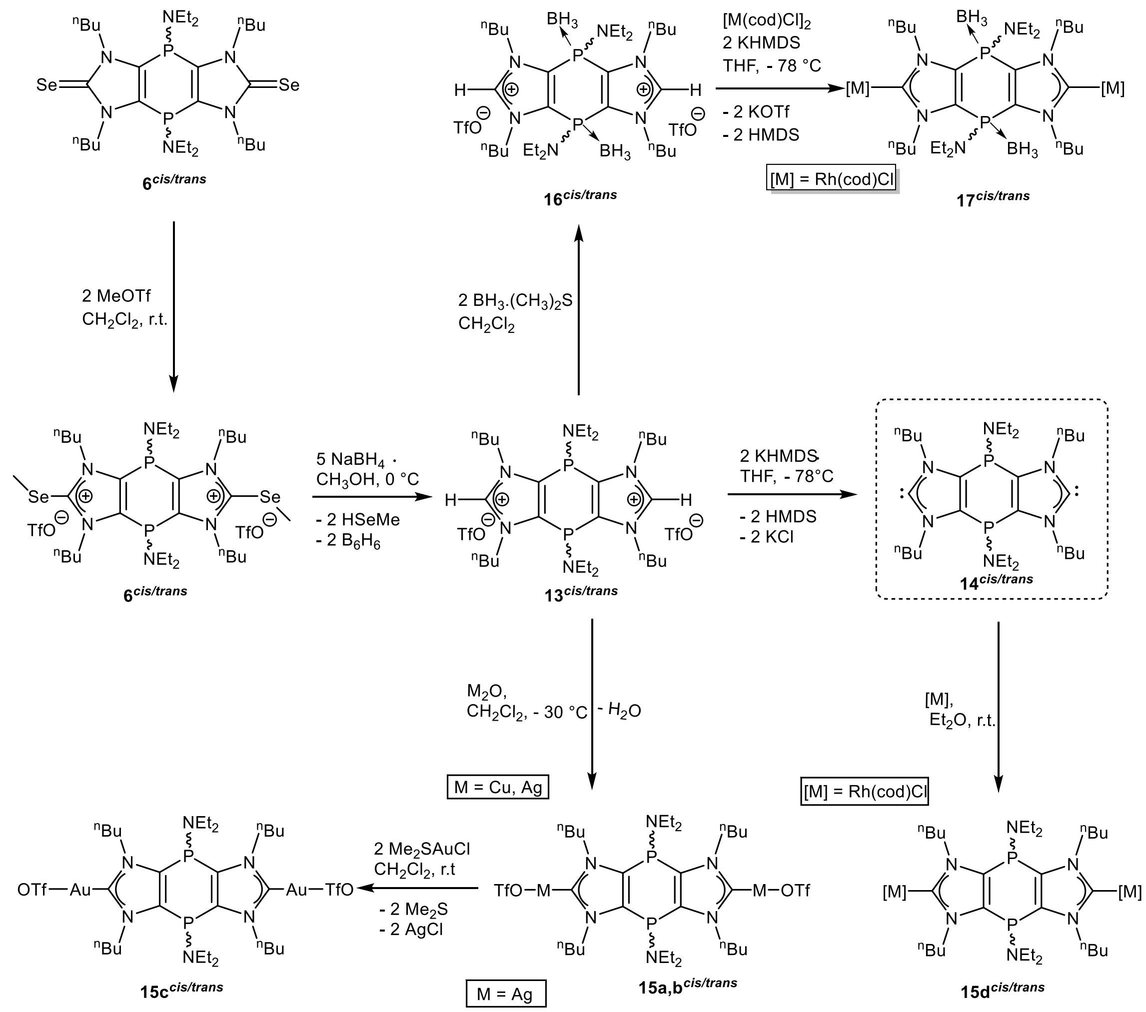

Scheme 10.3. Synthesis of $P^{III/III}$ bridged bis (imidazolium) salt **13**$^{cis/trans}$, bis (NHCs) **14**$^{cis/trans}$, their metal(I) complexes **15a-d**$^{cis/trans}$, **16**$^{cis/trans}$ and tetra-coordinated complexes **17**$^{cis/trans}$.

To study the donor properties of neutral bis(NHCs) **14***cis/trans*, coinage metals(I) (M =Cu, Ag) complexes (Scheme 10.3) were synthesized by treating imidazolium salts with metal oxides while Au(I) bis(NHC) complexes were obtained by the trans-metalation reaction. However, Rh(I) complexes were approached by the addition of $[Rh(cod)Cl]_2$ to neutral $P^{III/III}$ bridged bis(NHCs). In order to get *P* as well as C^2 centered complexes, firstly, *P*-centers of these tricyclic $P^{III/III}$ bridged bis(imidazolium) salts could be complexed to borane (**16***cis/trans*) upon treatment with borane-dimethyl sulfane complex, which was further reacted with KHMDS and rhodium(I) dimer to get access to tetra-nuclear complexes **17***cis/trans*(Scheme 10.3).

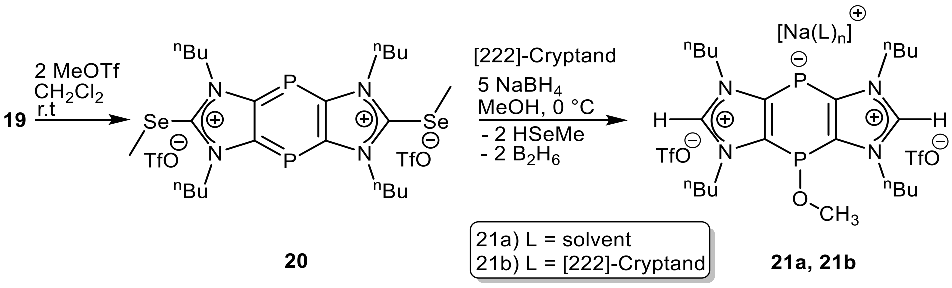

Scheme 10.4. Synthesis of doubly Se-methylated salt **20** and bis(imidazolium) salts **21a**, **21b**.

Chapter 6 describes the synthesis of low-coordinate 1, 4-diphosphinine diselone and its chemistry towards selective reductive deselenization resulting first monoanionic Janus-type bis(NHCs). The dark violet colour of the 1,4-diphosphinine changed to light yellow after treatment with the strong electrophile methyl triflate (Scheme 10.4).

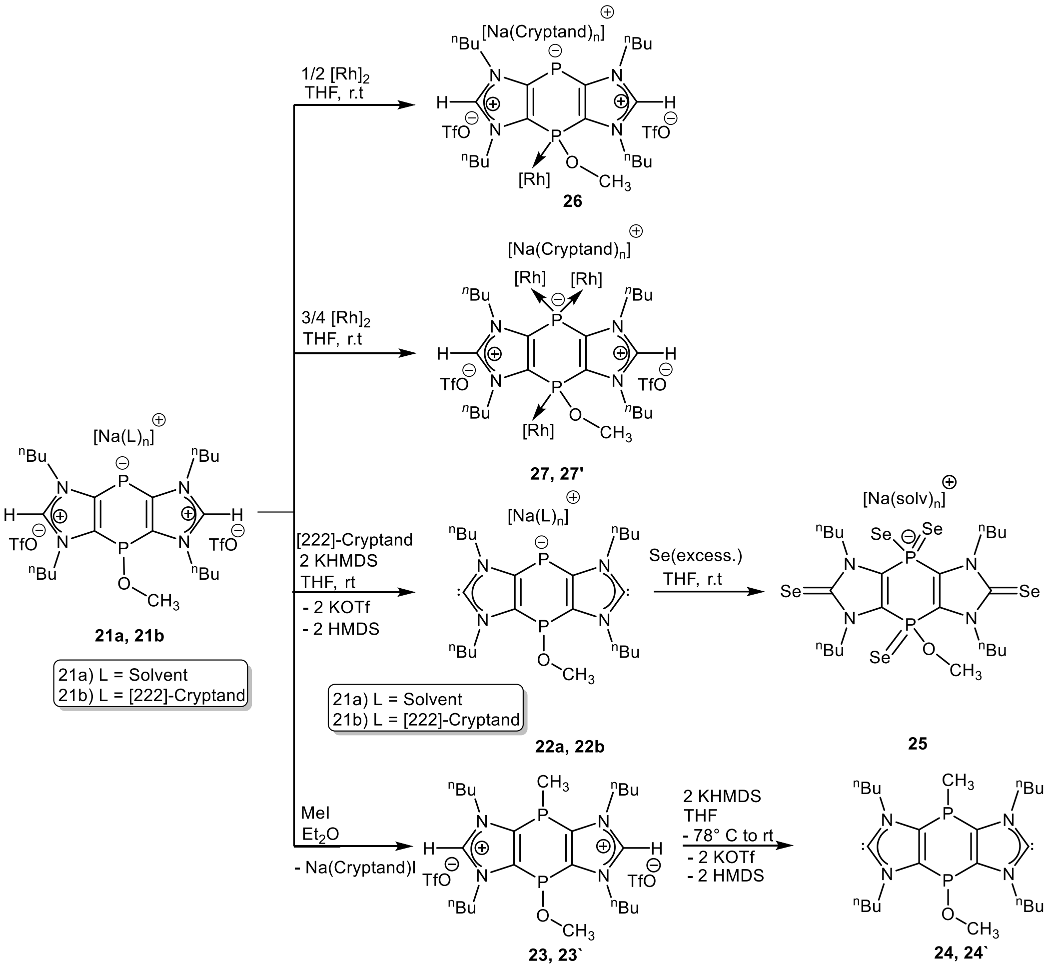

Scheme 10.5. Reactivity studies of compound **21a**, **21b**.

Compound **20** reacted selectively with $NaBH_4$ to give a surprising product that under went reductive deselenization as well as addition reaction at the phosphors centers **21a, b**. The deprotonation of this product resulted in novel tricyclic anionic bis(NHCs), which were isolated and characterized by various analytical means.The key features of the voltammetry of **22** are the very facile first oxidation with E_p^{a1}= -1.16 V, and a large number of cascading waves for subsequent oxidation processes, all of which are chemically irreversible. There are, therefore, (at least) four oxidation processes that are more facile for **22** than neutral bis(NHCs). Mixed substituted $P^{III/III}$-bridged bis(NHCs) were also targeted using compound **21a,b** under the same conditions described in scheme 10.5. In addition, the reactivity of phosphanido-type compounds **21a, b,** was also investigated towards complexation. So, these compounds **21a,b** were treated with $[Rh(cod)Cl]_2$ with different stoichiometric ratios to get access to mono rhodium(I) and tri rhodium(I) phosphanido-type complexes **26** and **27**, **27`**, respectively (Scheme 10.5). These reactions clearly showed the preferred coordinating site for Rh(I) metal.

Chapter 7 is focused on synthesis and reactions of 1,4-diphosphabarrelene diselone **28** towards electrophiles and, later on, reducing agents. The [4+2]-cycloaddition product **28** was obtained in a reaction of **19** with DMAD in excellent yield, and it was further reacted with MeOTf at room temperature to get the double Se-methylated salt **29** (Scheme 10.6). Targeting hitherto unknown bent rigid bis(NHCs), compound **28** was subjected to reductive deselenization using $NaBH_4$, which induced the cleavage of the P-C bond of the DMAD-derived bridge. This resulted in a clean conversion to give phosphanido-bridged bis(imidazolium) salt **21a,** which was fully characterized using different analytical methods.

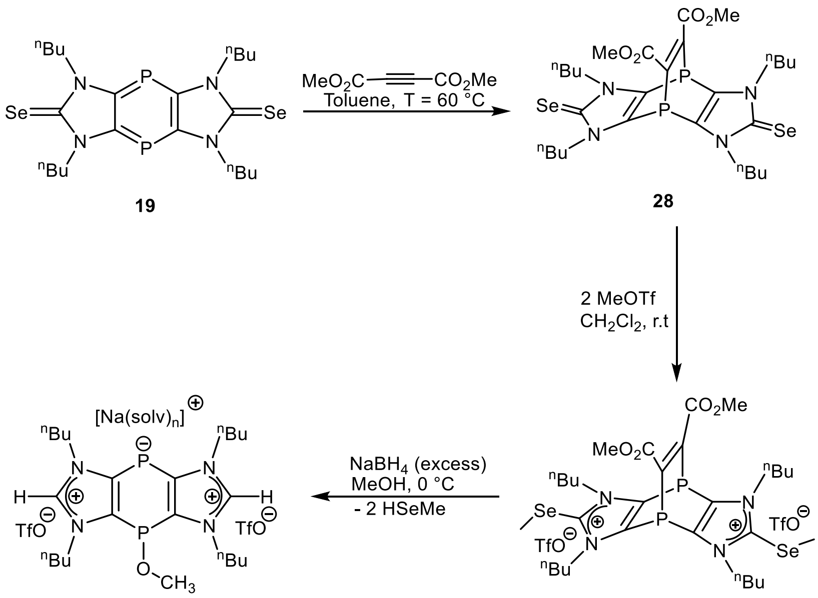

Scheme 10.6. Methoxide-induced P-C bond cleavage in 1,4-diphosphabarrelene.

The dianionic Janus-type bis(NHC), representing the first example of a bis(NHC) fused to an 8π-antiaromatic ring system was attempted via re-investigations of the reduction of 1,4-diphosphinine dithione **XCXIX**. The latter reacted with two equivalents of potassium graphite to give the corresponding dianionic compound **30** selectively, which was characterized via NMR spectroscopy and firmly established via single-crystal X-ray diffraction analysis. Further complexation of **30** using 2 eq. of $[Rh(cod)Cl]_2$ yielded **31** (Scheme 10.7).Using a4-fold reduction protocol for compound **30** employing KC_8 at 65 °C resulted in the very dark brownishdianionic bis(NHC) **32** (Scheme 10.7).

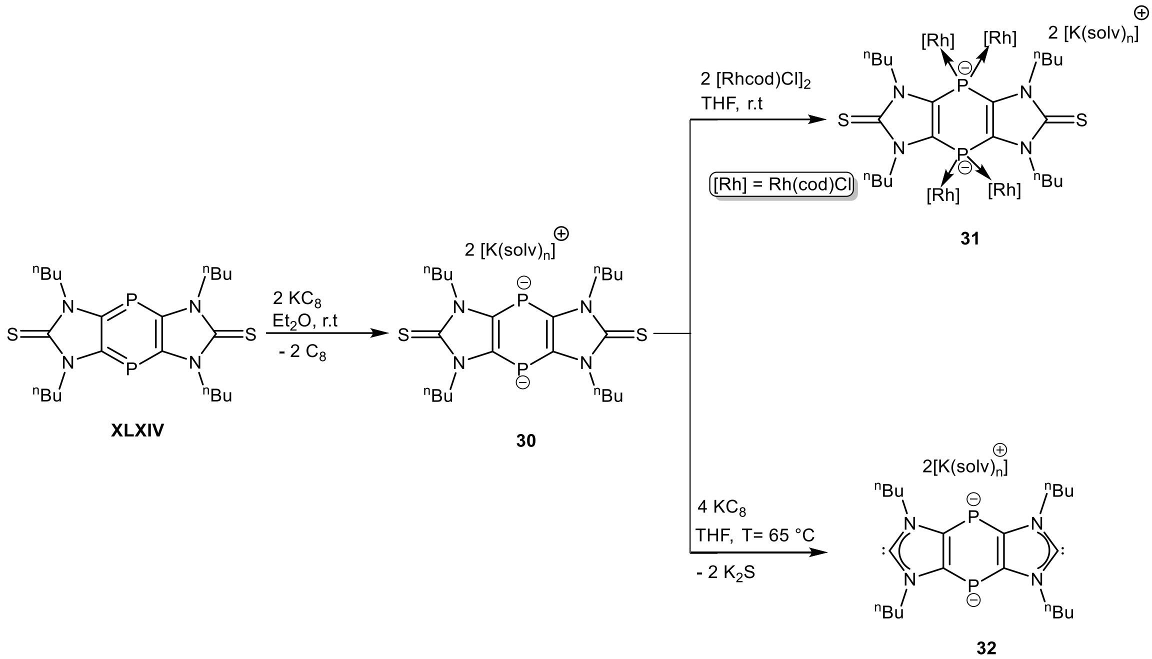

Scheme 10.7. 2-fold reduction of 1,4-diphosphinine to **30**and its subsequent complexation to give tetranuclear complex **31** and via further reduction to yield the 8π-antiaromatic bis(NHC) **32**.

Finally, chapter 9 describes the oxidative deselenization of 1, 4-diphosphinine diselone **19** to afford *P*$^{V/V}$-bridged bis(NHCs) and their complexes. Starting from a reaction of compound **19** with 10 equivalents of H_2O_2 to yield airstable bis(phosphinic acid)-bridged bis(imidazolium) salts **34**, **34`**. This isomeric mixture was deprotonated using KO^{t}Bu to access to the corresponding bis(NHCs), which was characterized by NMR spectra. Via a typical deprotonation/complexation reaction compounds **34**, **34′** reacted with silver(I) oxide to formthe corresponding Ag(I) bis(NHC) complexes **36,36′** (Scheme 10.8)**.**

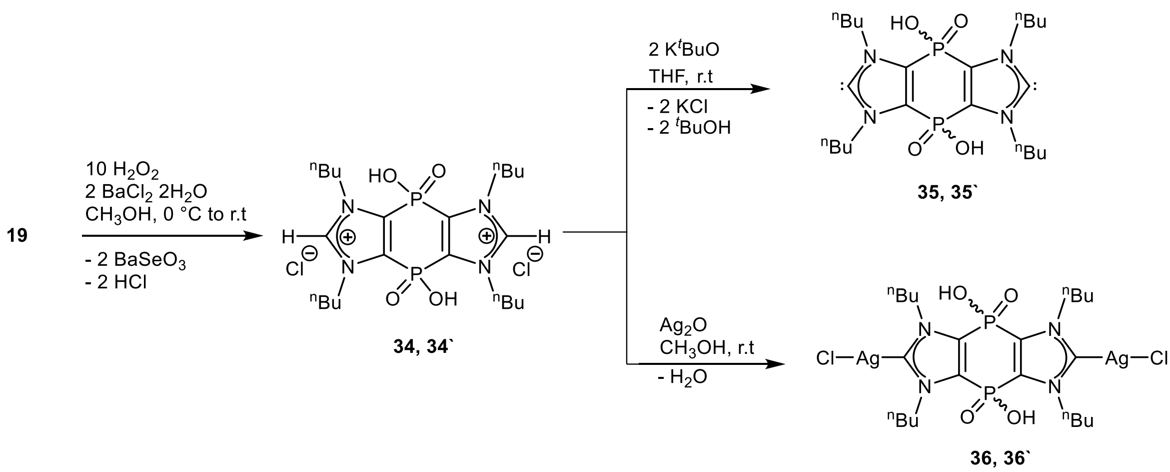

Scheme 10.8. Oxidative hydrolysis of **19** leading to bis(NHCs) **35,35’** and their Ag(I) complexes.

11. Experimental section

11.1. General Techniques

All reactions were performed under a stream of deoxygenated (using preheated BTS catalyst at 100-130 °C) and dried (using molecular sieve and phosphorus pentoxide) Argon gas, using standard Schlenk techniques. All sensitive chemicals were stored in either Schlenk flasks or handled in the glovebox. All the solvents used in reactions were dried and distilled over sodium wires or calcium hydride (for methylene dichloride) and stored in brown glass bottles having Schlenk connections. All glass wares used were pre-heated and dried in the oven prior to use. In case air sensitive reactive the Schlenk flasks or tubes were prepared by heating under high vacuo and subsequently refilling with Argon gas. All the glass joints were lubricated with OKS grease type 1112®. The high-temperature reactions were done with an oil bath whereas the low-temperature ones were performed using a liquid nitrogen/ethanol bath. For the purpose of removing salts formed in the reaction mixture, common G3 frits having two Schlenk joints were used, along with either silica gel (Merck 60-200) or Celite. For transferring solvents or filtering, stainless steel double needle or filter cannula were used, which were preheated and dried in the oven at 75 °C. Whatman filter papers or glass microfiber filter papers were used for filtration purposes. All the used glass wares were soaked overnight in a KOH-isopropanol bath having some NaOCl (for oxidizing the metal impurities) and then dipped into an HCl-water bath for the sake of neutralization prior to washing with soap water. Then the cleaned glasswares were rinsed with deionized water and acetone simultaneously before drying at 120 °C in the oven overnight.

11.1.1. Elemental analysis

All the elemental analyses were performed with an Elementar Vario Micro elemental analyzer by the microanalysis section of the Chemical Institute of the University of Bonn. The mean value of at least three measurements is given.

11.1.2. NMR spectroscopy

NMR spectra of all the compounds were recorded on Bruker Avance DMX-300, DPX-300, DPX-400 or DMX-500 spectrometers. Deuterated solvents ($CDCl_3$, THF-d_8 or C_6D_6) were dried using literature procedures and used for the multinuclear NMR characterizations and the chemical resonances are given relative to Tetramethylsilane (^{1}H, ^{13}C, ^{29}Si NMR), 1 M LiCl in D_2O (^{7}Li

NMR), 15 % $BF_3{\cdot}OEt_2$in $CDCl_3$ (^{11}B NMR), $CFCl_3$ (^{19}F NMR) or 85% H_3PO_4 (^{31}P NMR), respectively. The chemical shifts are expressed in parts per million, ppm. Coupling constants are abbreviated as $^{n}J_{X,Y}$, where X and Y denote the coupling nuclei (ordered by decreasing atomic number, n is the number of bonds that separate X and Y). The following abbreviations were used for expression of the multiplicities of the resonance signals: s = singlet, d = doublet, t = triplet, q = quartet, m = multiplet and br = broad signal. All the measurements were recorded at 298K unless some specific temperature is given.

11.1.3. UV/vis spectroscopy

UV/vis spectra were obtained from a Shimadzu UV-1650PC spectrometer (λ = 190-900 nm) using methylene chloride as the solvent and quartz glass cells (Hellma) of optical path 1cm at room temperature.

11.1.4. Mass spectrometry

Mass spectrometric data were acquired from a Bruker Daltonik micrOTOF-Q using ESI (+/-), a Thermo Finnigan MAT 90 sector instrument equipped with a LIFDI ion source (Linden CMS) or MAT 95 XL Finnigan using EI (70 eV). Only selected data are given for the detected ions (mass to charge ratio, relative intensity in percent).

11.1.5. Infrared spectroscopy

IR-spectra were recorded from the pure solids on a Thermo IR spectrometer with an attenuated total reflection (ATR) attachment or on a Bruker Alpha Diamond ATR FTIR spectrometer at room temperature. The following abbreviations were used for expression of the intensities of the absorption bands: vs = very strong, s = strong, m = medium, w = weak.

11.1.6. Cyclic voltammetry

The custom-tailored glassware for the electrochemical measurements, equipped with three Pt electrodes (working, reference and counter electrodes), has been prepared. Electrochemical experiments were carried out on an ALS 1140A potentiostat/galvanostat. Electrochemical samples were recorded with scan rates of 10–500 mVs^{-1}at r.t. under Ar atmosphere. Ferrocene was used as internal/external reference to determine the potentials. Sample solutions (THF) were 3 mM in analyte and 0.1 M in n-Bu_4NPF_6 as the supporting electrolyte.

11.1.7. Single crystal X-ray diffraction studies

Single crystal were grown by evaporation of saturated solutions of the compounds at -20°C or by diffusion technique. After crystal growing the single crystals were separated from the supernatant solution and were covered with Fomblin for the purpose of protection from further decomposition. A suitable single crystal was selected under the microscope and loaded onto the diffractometer. The crystallographic data was collected on Brucker D_8-Venture diffractometer, Bruker X_8-KappaApexII, Bruker APEX-II CCD, Nonius KappaCCD or STOE IPDS 2T diffractometer equipped with a lowtemperature device at 100.0 K using graphite monochromated Cu-Kα radiation (λ = 1.54178 Å) or Cu-*K*αradiation (λ = 1.54178). The absorption correction, structure solution and structure refinement was performed by Patterson methods or by full-matrix least squares on F_2 using the SHELXL-97 programs. All non-hydrogen atoms were refined anisotropically, the hydrogen atoms were included isotropically using the riding model on the bound carbon atoms. Data analyses and the picture preparation of the molecular structure for all the compounds were done using Diamond 3.0 program.

Commercially available chemicals

11.1.8. Chemicals used

All the commercially available chemicals used for experiments are listed below along with the supplier name in the brackets.

11.1.8.1. List of chemicals used (commercially available)

Chemicals Supplier Chemicals Supplier

- n-Butylamine (Acros)
- n-Butyllithium (Acros)
- Chloroform (Fisher Scientific)
- Chloroform-d (Eurisotop)
- Diethylether (VWR)
- Methylene chloride (Biesterfeld)
- Diisopropylamine (Acros)
- Dimethylaminodichlorophosphane (Sigma-Aldrich)
- Dimethylsulfoxide (Acros)
- Ethanol (Hofmann)
- Methanol (Aldrich)

- Potassium metal (Riedel de Haen)
- *n*-Pentane (Grüssing)
- Petrol ether 40/60 (Biesterfeld)
- Phosphorustrichloride (Acros)
- Sodium hydroxide(Sigma-Aldrich)
- Selenium (Acros)
- Sulfuricacid (Fluka)
- Tetrahydrofuran (Fisher Scientific)
- THF-d8 (Eurisotop)
- Tributylphosphane (Acros)
- Triethylamine (Sigma-Aldrich)
- Toluene (Fisher Scientific)
- Hydrogen peroxide (Acros)
- Isopropylamine(Sigma-Aldrich)
- Isopropanol (Biesterfeld)
- Water-d2 (Eurisotop)
- Sodium borohydride (Aldrich)
- Chloro(dimethylsulfide)gold(I) (Aldrich)
- Chloro(1,5-cyclooctadiene)rhodium(I) dimer (Aldrich)
- Formaldehyde (Grüssing: 37% bzw. 40% in water)
- Glyoxal (Acros: 40% in Water)
- Silver(I) oxide (Riedel-de Haën)
- Copper(I) oxide (Riedel-de Haën)
- Chloro(1,5-cyclooctadiene)iridium(I) dimer (Aldrich)
- Cryptand-222(Acros)
- Methyl triflate(Merck)
- Sodiumhydride (Aldrich: 97% and 80% in paraffin oil)
- Potassium bis(trimethylsilyl)amide (Aldrich)

The following compounds were synthesized according to published procedures:

- Bis(diethylamino)chlorophosphane[183]
- Lithium diisopropylamide[184]
- 1,3-Dibutylimidazole-2-thione[106, 107]
- 1,3-Dibutylimidazole-2-selone[16, 27]

11.2. Syntheses of 4-phosphanyl-imidazole-2-selones 2, 3

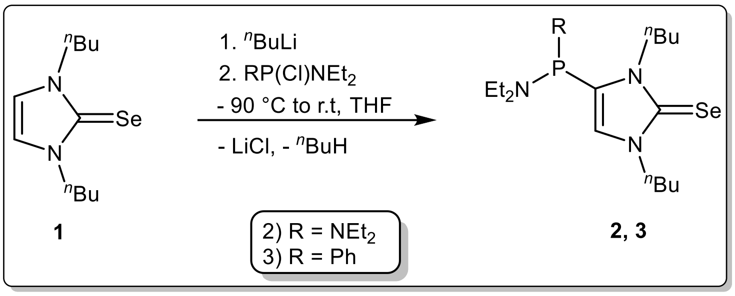

To a solution of the 1,3-di-*n*-butyl-imidazole-2-selone **1** in THF, *n*-butyllithium was added at - 90 °C and the reaction mixture was stirred for 3 h at the same temperature. Subsequently, the dropwise addition of $Et_2N(R)PCl$ was done at – 90 °C. The reaction mixture was stirred overnight by warming up to ambient temperature. The light yellow coloured solution was concentrated in *vacuo* ($2×10^{-2}$ mbar) to get the oily residue. Column chromatography was performed to purify the compounds using silica bed and *n*-pentane **2**/ 1:3(diethyl ether/*n*-pentane) **3** as eluent. The solvent was removed from the collected solutions and the resulted products were dried *in vacuo* ($2×10^{-2}$ mbar). Light yellow oily compounds (**2, 3**) were obtained.

11.2.1 1, 3-*n*-Butyl-4-bis(diethylamino)phosphanyl-imidazole-2-selone (2)

Chemicals	Amounts(g or mL)	mmol
1	30 g	116.0
^{n}BuLi(1.6 M in hexane)	80.32 mL	128.0
$(Et_2N)_2PCl$	26.86 mL	128.0
THF	750 mL	

Reaction code: NRN-122, NRN-313

Yield: 51.2g (106.0 mmol) 91.4 %; light yellow oil.

Elemental composition: $C_{19}H_{39}N_4PSe$

Molecular weight: 433.5 g/mol

MS (EI, 70 eV): *m/z*(%) 435.213 (100) $[M]^+$, 355 (75) $[M-C_4H_{10}N]^+$.

HR-MS: found: 435.2145 calc. 435.2151.

IR (ATR,ῡ{cm^{-1}}): ῡ= 2970 (s), 2929 (s), 2759 (m), 2705 (s), 2518 (s), 1656 (vs), 1558(vs), 1375 (vs), 1335 (vs), 1293 (vs), 1133 (vs), 1013 (s), 987 (vs), 917 (vs), 901 (s), 847 (s), 791 (s), 703(s), 662(s).

^{1}H NMR (300.1 MHz, CDCl$_3$): δ = 0.9 (t, $^3J_{H,H}$ = 7.5 Hz, 6H, $NCH_2CH_2CH_2$*Me*), 1.1 (t, $^3J_{H,H}$ = 7.2 Hz, 12H, NCH_2*Me*), 1.3-1.4 (m, 4H, NCH_2CH_2*CH_2*Me), 1.7-1.8 (m, 4H, NCH_2*CH_2*CH_2Me), 3.0-3.2 (t, $^3J_{H,H}$ = 7.2 Hz, 8H, N*CH_2*Me), 4.1-4.2 (m, 4H, N*CH_2*CH_2CH_2Me), 6.7 (t, $^3J_{P,H}$ = 2.6 Hz, 1H, *C^5H*)

^{13}C{^{1}H} NMR (75.5 MHz, CDCl$_3$): δ = 13.7 (s, 6H, $NCH_2CH_2CH_2$*Me*), 13.2 (s, 6H, NCH_2*Me*),19.8(s, 2H, NCH_2CH_2*CH_2*Me), 20.1 (s, 2H , NCH_2CH_2*CH_2*Me), 30.5(d,$^4J_{P,C}$=4.6Hz,NCH_2*CH_2*CH_2Me), 31.1(s,NCH_2*CH_2*CH_2Me), 43.0(d, 8H, $^2J_{P,C}$=18.4Hz, NCH_2Me), 47.6 (s,2H,N*CH_2*CH_2CH_2Me), 49.3(s, 2H, N*CH_2*CH_2CH_2Me), 126.7 (d,$^2J_{P,C}$=8.0Hz,*C^5*), 156.9(d,$^3J_{P,C}$=2.4Hz *C*=Se).

^{31}P{^{1}H}-NMR (121.5 MHz, CDCl$_3$): δ= 72.5(s).

^{77}SeNMR (57.28 MHz, CDCl$_3$): 36.6 (s)

11.2.2. 1, 3-*n*-Butyl-4-phenyl(diethylamino)phosphanyl-imidazole-2-selone (3)

Chemicals	Amounts(g or mL)	mmol
1	6.3g	24.0
^{n}BuLi(1.6 M in hexane)	16.80 mL	26.0
$(Et_2N)PhPCl$	5.6 mL	26.0
THF	150 mL	

Reaction code: NRN-153

Yield: 8.7g (19.84 mmol) 82.6 %; yellow oil.

<u>Elemental composition</u>: $C_{21}H_{34}N_3PSe$

<u>Molecular weight</u>: 438.5 g/mol

<u>MS (EI, 70 eV)</u>: *m/z*(%) 439.1652 (48) $[M]^+$, 367.0837(58) $[M\text{-}C_4H_{10}N]^+$, 360.2564 (100) $[M\text{-}Se+H]^+$

<u>HR-MS</u>: theor. 439.1652 exp. 439.1649.

<u>IR (ATR,ῦ{cm^{-1}})</u>: ῦ= 2760 (s), 2709 (s), 2559 (m), 2528 (s), 1556 (vs), 1512(vs), 1415 (m), 1305 (s), 1093 (vs), 967 (vs), 927 (vs), 889 (s), 831 (s), 764 (s), 701(s), 642(s).

<u>^{1}H NMR (300.1 MHz, C_6D_6)</u>: δ = 0.8 (t, $^3J_{H,H}$ = 7.2 Hz, 6H, $CH_2CH_2CH_2$<u>*Me*</u>), 1.0 (t, $^3J_{H,H}$ = 7.3 Hz, 6H, NCH_2<u>*Me*</u>), 1.3-1.5 (m, 4H, CH_2CH_2<u>*CH_2*</u>Me), 1.7-1.9 (m, 4H, CH_2<u>*CH_2*</u>CH_2Me), 3.1-3.2 (m, 4H, N<u>*CH_2*</u>Me), 3.9-4.4 (m, 4H, <u>*CH_2*</u>CH_2CH_2Me), 6.6 (s, 1H, <u>*C^5H*</u>), 7.3-7.5 (m, 5H, *Ph ring protons*)

<u>^{13}C{^{1}H} NMR (75.5 MHz, C_6D_6)</u>: 13.5 (s, $NCH_2CH_2CH_2$<u>*Me*</u>), 14.2 (s, NCH_2<u>*Me*</u>),19.5(s,NCH_2CH_2<u>*CH_2*</u>Me),20.1(s, NCH_2CH_2<u>*CH_2*</u>Me),31.1(s, NCH_2<u>*CH_2*</u>CH_2Me),31.4(d, $^2J_{P,C}$=3.5HzNCH_2<u>*CH_2*</u>CH_2Me),43.7(br, N<u>*CH_2*</u>Me),47.8 (d,$^2J_{P,C}$=9.5Hz, N<u>*CH_2*</u>CH_2CH_2Me),48.9(s, N<u>*CH_2*</u>$CH_2CH_2CH_2$Me),123.5 (br,<u>*C^5*</u>),130.3 (s, <u>*C_6*</u>H_5), 130.7 (d, $J_{P,C}$ = 18.3 Hz, *C_6*H_5), 138.6 (d, $^1J_{P,C}$ = 7.2 Hz, <u>*ipso*</u>-C_6H_5),160.3(s,<u>*C*</u>=Se).

<u>^{31}P{^{1}H}-NMR (121.5 MHz, $CDCl_3$)</u>: δ= 32.9 (s).

11.3. Synthesis of backbone substituted (chloro)phosphanyl imidazole-2-selone (4, 5)

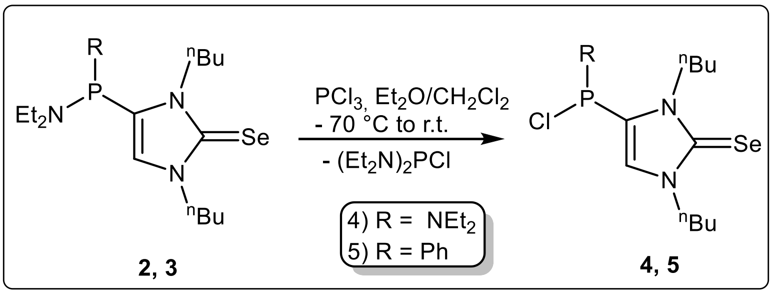

C^4-Phosphanyl-imidazole-2-selones**2, 3** solutions in dry diethyl ether (**4**) or methylene chloride (**5**) was treated with phosphorus trichloride at − 90 °C. The reaction mixture was stirred for 1 hour

while keeping the temperature constant. The solvent was removed *in vacuo* (2×10^{-2} mbar). The residue was extracted with *n*-pentane and bis(diethylamino)chloro phosphane was distilled out. Finally, the products **4, 5** were obtained as light yellow oils.

11.3.1. 1,3-Di-*n*-butyl-4-diethylamino(chloro)phosphanyl-imidazole-2-selone(4)

Chemicals	Amounts(g or mL)	mmol
2	1.0 g	2.3
PCl_3(ρ = 1.570 g/cm^3)	0.32 mL	2.3
Et_2O	25 mL	

Reaction code: NRN-126, NRN-442

Yield: 0.76g (1.9 mmol) 83.3 %; yellow oil.

Elemental composition: $C_{15}H_{29}ClN_3PSe$

Molecular weight: 396.80 g/mol

MS (EI, 70 eV): *m/z*(%) 397.1 (43) $[M]^{\cdot+}$, 362.1 (21) $[M\text{-}Cl]^{\cdot+}$, 175.1 (100) $[C_8H_{20}N_2P]^{\cdot+}$, 72.1 (61) $[C_4H_{10}N]^{\cdot+}$.

HR-MS: theor./exp. for $[C_{15}H_{29}ClN_3PSe]$: 397.0953 /397.0958.

IR (ATR,ῦ{cm^{-1}}): ῦ= 2920(s), 2901 (m), 2856 (m), 2691 (s), 2523 (s), 1514 (s), 1478(s), 1385 (s), 1325 (s), 1267 (s), 1195 (s), 1048 (m), 964 (s), 937 (s), 878 (s)

^{1}H NMR (300.1 MHz, C_6D_6): δ = 0.8 (t, $^3J_{H,H}$ = 7.1Hz, 6H, $NCH_2CH_2CH_2\underline{CH_3}$), 0.9 (t, $^3J_{H,H}$ = 7.4 Hz, 6H, $NCH_2\underline{CH_3}$), 1.1-1.2 (m, 4H, $NCH_2CH_2\underline{CH_2}CH_3$), 1.4-1.9 (m, 4H, $NCH_2\underline{CH_2}CH_2CH_3$), 2.7-3.2 (m, 4H, $N\underline{CH_2}CH_3$), 3.9 (t, $^3J_{H,H}$ = 7.1Hz, 2H, $N\underline{CH_2}CH_2CH_2CH_3$), 4.5(m, 2H, $N\underline{CH_2}CH_2CH_2CH_3$), 7.1 (d, $^3J_{P,H}$= 2.1 Hz, 1H, $\underline{C^5H}$).

^{13}C NMR (75.5 MHz, C_6D_6): δ = 13.4 (s, $NCH_2CH_2CH_2$*CH_3*), 13.6 (s, NCH_2*CH_3*),19.6(s,NCH_2CH_2*CH_2*CH_3),19.9 (s, 4H, NCH_2CH_2*CH_2*CH_3),30.6(d,$^4J_{P,C}$=4.2Hz, N CH_2*CH_2*CH_2CH_3),30.9(s,NCH_2*CH_2*CH_2CH_3),43.3(d,$^3J_{P,C}$=8.3Hz,N*CH_2*CH_3),47.6 (d,$^2J_{P,C}$=5.7Hz,N *CH_2*$CH_2CH_2CH_3$),49.1(s,N*CH_2*$CH_2CH_2CH_3$),125.9 (d,$^2J_{P,C}$=6.8Hz,*C^5*),162.1(s,*C^2*=Se).

^{31}P{^{1}H} NMR (121.5 MHz, C_6D_6): δ= 105.8(s).

^{77}SeNMR (57.28 MHz, C_6D_6): 49.8 (s)

11.3.2 1,3-Di-*n*-butyl-4-phenyl(chloro)phosphanyl-imidazole-2-selone(5)

Chemicals	Amount(g or mL)	mmol
3	4.74 g	1.1
PCl_3(ρ = 1.570 g/cm^3)	0.95 mL	1.1
CH_2Cl_2	125 mL	

Reaction code: NRN-156

Yield: 3.9 g (0.97 mmol) 88 %; yellow oil.

Elemental composition: $C_{17}H_{24}ClN_2PSe$

Molecular weight: 401.7 g/mol

MS (EI, 70 eV): *m/z*(%) 402.0 (32) $[M+H]^{\cdot+}$

IR (ATR,ṽ{cm^{-1}}): ṽ= 2720 (s), 2619 (s), 2547 (m), 2498 (s), 1606 (vs), 1542(vs), 1425 (m), 1315 (s), 1193 (vs), 897 (vs), 827 (vs), 819 (s), 797 (s), 754 (s), 721(s), 672(s).

^{1}H NMR (300.1 MHz, $CDCl_3$): δ = 0.9 (t, ^3JH,H = 7.3 Hz, 6H, $CH_2CH_2CH_2$*Me*), 1.2-1.4 (m, 4H, CH_2CH_2*CH_2*Me), 1.7-1.8 (m, 4H, CH_2*CH_2*CH_2Me), 3.02-3.15 (t, $^3J_{H,H}$ = 7.2 Hz, 8H, N*CH_2*Me), 4.1-4.2 (m, 4H, *CH_2*CH_2CH_2Me), 6.6 (br, 1H, *C^5H*), 7.5-7.8 (m, 5H, *Ph* ring protons)

^{13}C NMR (75.5 MHz, CDCl$_3$): δ = 13.6 (s, NCH$_2$CH$_2$CH$_2$*CH$_3$*), 19.7(s,NCH$_2$CH$_2$*CH$_2$*CH$_3$),20.0(s, NCH$_2$CH$_2$*CH$_2$*CH$_3$),30.7(d,$^4J_{P,C}$=1.9Hz, NCH$_2$*CH$_2$*CH$_2$CH$_3$),30.9(s,NCH$_2$*CH$_2$*CH$_2$CH$_3$),48.60 (d,$^2J_{P,C}$=6.3Hz,N*CH$_2$*CH$_2$CH$_2$CH$_3$),49.9(s,N*CH$_2$*CH$_2$CH$_2$CH$_3$),126.5 (d, $^1J_{P,C}$ = 16.1 Hz, *C*5), 129.1(d, $J_{P,C}$ = 8.1 Hz, P*C*$_6$H$_5$); 130.6 (d, $J_{P,C}$ = 25.1 Hz, P*C*$_6$H$_5$), 131.6 (s, P*C*$_6$H$_5$), 133.5 (d, $J_{P,C}$ = 25.7 Hz, *ipso*-C$_6$H$_5$), 160.2 (s, *C*^{2}=Se).

^{31}P{^{1}H}-NMR (121.5 MHz, CDCl$_3$): δ= 48.9 (s).

11.4. Synthesis of 1,4-dihydro-1,4-diphosphinines (6$^{cis/trans}$, 7$^{cis/trans}$)

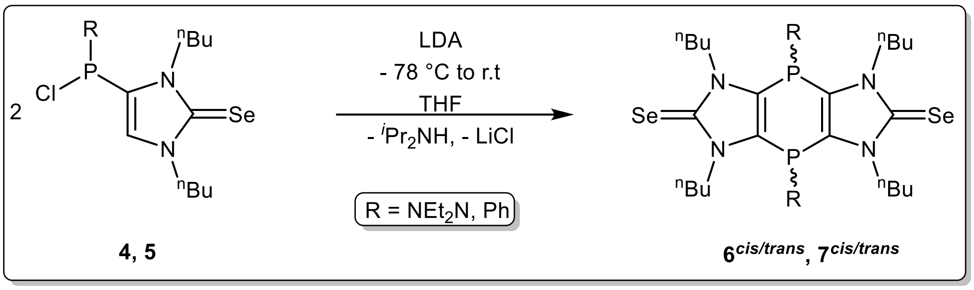

A solution of LDA in THF was added dropwise to a solution ofmono-chloro phosphanylated imidazole 2-selone **4, 5** in 30 mL THF with continuous stirring through a double-ended needle over 30 minutes at - 80 ˚C. The reaction mixture was stirred for one hour. The solvent was then removed to get a dark brown residue Column chromatography was performed using 150 ml of diethyl ether and *n*-pentane mixture (1: 0.6) (**4**) and diethyl ether(**5**)and filtered through a silica bed to remove LiCl,and other dark brown polymeric impurities form during the course of the reaction. The filtrate was concentrated under reduced pressure (2×10^{-2} mbar) to obtain a light brown solid, which was then washed again with *n*-pentane (twice) to get a light yellow powder and, finally, dried under reduced pressure (2×10^{-2} mbar) for 2 h to get the pure compounds as *cis/trans* mixtures.

11.4.1. 4,8-Bis(diethylamino)-1,3,5,7-tetra-*n*-butyl-4,8-dihydro[1,4]diphosphinine[2,3 d:5,6-d']bisimidazole-2,6-diselone (6$^{cis/trans}$)

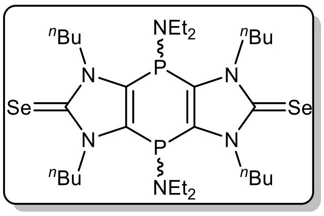

Chemicals	Amounts(g or mL)	mmol
4	0.88 g	2.2
LDA	0.36 g	3.3
THF	33 mL	

Reaction code: NRN-142

Yield: 0.42 g (0.6 mmol) 53 %; light yellow solid.

Melting point: 136 °C

Elemental composition: $C_{30}H_{56}N_6P_2Se_2$

Molecular weight: 720.70 g/mol

Elemental analysis: for $C_{30}H_{56}N_6P_2Se_2$:

Theor.	C	50.00	H	7.83		11.66
Exp.	C	49.60	H	7.81	N	11.02

MS (EI, 70 eV): *m/z* (%) = 722.2 (76) $[M]^{\cdot+}$, 577.1 (100) $[M\text{-}2NEt_2\text{+}H]^{\cdot+}$.

HR-MS: *m/z* = theor./exp. for $[C_{30}H_{56}N_6P_2Se_2]$: 722.2373/722.2385.

IR (ATR,ῦ{cm^{-1}}): ῦ= 2957 (m), 2917 (m), 2884 (w), 1532 (w), 1435 (m), 1393 (s), 1195 (m), 1164 (m), 1135 (m), 1016 (s), 927 (s).

^{1}H NMR (300.1 MHz, C_6D_6, 25 °C): δ = 0.8 (s, 12H, P-NCH_2*Me*), 0.9 (t, 12H, $^3J_{H,H}$ = 7.1 Hz, $NCH_2CH_2CH_2$*Me*), 1.3-1.5 (m, 8H,NCH_2CH_2*CH_2*Me), 1.9-2.2 (m, 8H, NCH_2*CH_2*CH_2Me), 2.7- 2.8 (m, 8H, P-N*CH_2*Me), 4.0-4.1 (m, 4H, N*CH_2*CH_2CH_2Me), 4.7- 4.6 (m, 4H, N*CH_2*CH_2CH_2Me; 2ndisomer).

^{13}C{^{1}H} NMR (75.5 MHz, C_6D_6, 25 °C): δ = 13.6 (s, $NCH_2CH_2CH_2$*Me*), 14.8 (br, P-NCH_2*CH_3*), 20.0 (s, NCH_2CH_2*CH_2*Me), 20.2 (s, NCH_2CH_2*CH_2*Me; 2nd isomer), 30.5 (br, NCH_2*CH_2*CH_2Me), 30.7 (br, NCH_2*CH_2*CH_2Me; 2nd isomer), 44.3 (d, $^2J_{P,C}$ = 18.9 Hz, P-N*CH_2*CH_3), 47.3 (br, N*CH_2*CH_2CH_2Me), 48.6 (t, $^2J_{P,C}$ = 3.1 Hz, N*CH_2*CH_2CH_2Me; 2nd isomer), 126.7 (t, $^1J_{P,C}$ = 2.0 Hz

P-*C* of the middle ring), 130.9 (t, $^{1}J_{P,C}$ = 2.3 Hz, *P*-*C* of the middle ring; 2nd isomer), 164.5 (t, $^{3}J_{P,C}$ = 1.7 Hz, C^2=*Se*).

$^{31}P\{^{1}H\}$ NMR (121.5 MHz, C_6D_6, 25 °C): δ = 0.9 (s), 3.7 (s)

Isomer ratio: 1: 0.75

^{77}SeNMR (57.28 MHz, C_6D_6): 35.9 (s), 37.9 (s)

UV-vis (CH_2Cl_2): λ_{max} [nm] (abs.): 230 (0.979), 293 (0.822).

11.4.2. 4,8-Bis(diphenyl)-1,3,5,7-tetra-*n*-butyl-4,8-dihydro[1,4]diphosphinine[2,3 d:5,6-d']bis(imidazole-2,6-diselone)(7$^{cis/trans}$)

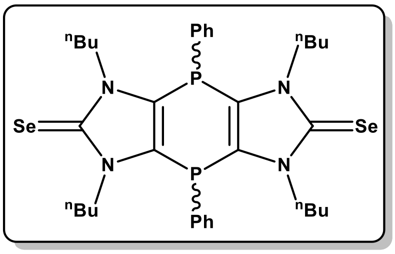

Chemicals	Amounts(g or mL)	mmol
5	3.2 g	7.9
LDA	0.93 g	8.7
THF	60 mL	

Reaction code: NRN-157

Yield: 1.4 g (1.9 mmol) 48 %; light yellow solid.

Melting point: 154 °C

Elemental composition: $C_{34}H_{46}N_4P_2Se_2$

Molecular weight: 730.64 g/mol

MS (EI, 70 eV): *m/z* (%) = 732.1 (100) $[M]^+$, 655.1 (20) $[M\text{-}Ph]^+$.

HR-MS: *m/z* = theor./exp.: 732.1537/732.1541.

IR (ATR,ῦ{cm⁻¹}): ῦ= 2968 (w), 2912 (w), 2898 (m), 1417 (s), 1370 (s), 1304 (m), 1198 (s), 1158 (m), 1094 (s), 921 (s).

^{1}H NMR (300.1 MHz, C_6D_6, 25 °C): δ = 0.8 (t, $^3J_{H,H}$ = 7.2 Hz, 12H, $CH_2CH_2CH_2$*Me*), 1.2-1.3 (m, 8H, CH_2CH_2*CH_2*Me), 1.8-1.9 (m, 8H, CH_2*CH_2*CH_2 Me), 4.1-4.2 (m, 8H, *CH_2*CH_2CH_2 Me), 7.3-7.6 (m, 10H, P-*Ph*)

^{13}C{^{1}H} NMR (75.5 MHz, C_6D_6, 25 °C): δ = 12.1 (s, $NCH_2CH_2CH_2$*Me*), 19.4 (s, NCH_2CH_2*CH_2*Me), 19.8 (s, NCH_2CH_2*CH_2*Me; 2nd isomer), 29.8 (br, NCH_2*CH_2*CH_2Me), 30.2(br, NCH_2*CH_2*CH_2Me; 2nd isomer), 46.1 (br, N*CH_2*CH_2CH_2Me), 47.6 (br, N*CH_2*CH_2CH_2Me; 2nd isomer), 127.3 (t, $^1J_{P,C}$ = 2.6 Hz*P-C* of the middle ring), 128.4 (t, $^1J_{P,C}$ = 2.4 Hz, *P-C* of the middle ring; 2nd isomer), 162.3 (t, $^3J_{P,C}$ = 2.1 Hz, *C^2=Se*).

^{31}P NMR (121.5 MHz, C_6D_6, 25 °C): δ = - 54.9 (s) and - 53.9 (s),

Isomer ratio: 1:1

^{77}SeNMR (57.28 MHz, C_6D_6): 0.0 (s)

11.5. Synthesis of tricyclic {P(O)NEt₂}-bridged bis(imidazolium) salts 8*cis/trans*

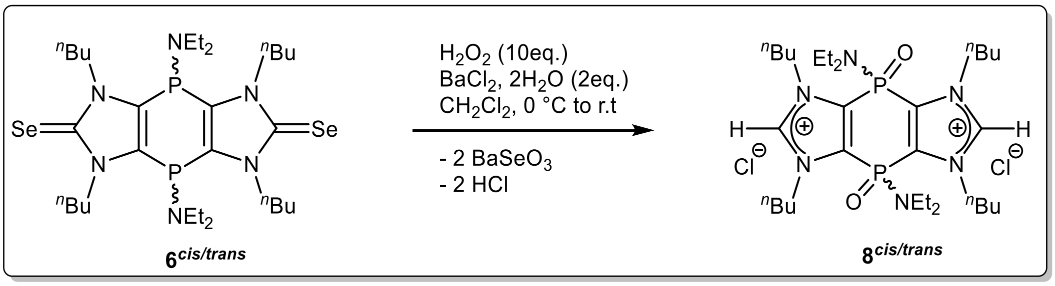

To a solution of **6***cis/trans* in 2 mL of methylene chloride, H_2O_2 (35 % in water) was added at 0 °C. The reaction mixture was stirred at 0 °C for 30 min, then at ambient temperature for 14 h. After the reaction was completed (^{31}P NMR control), $BaCl_2{\cdot}2H_2O$ in 2mL water was added into it and stirred for an additional two hours. The reaction mixture was then filtered over a frit equipped with a layer of celite® to remove barium selenite. The filtrate was collected and concentrated *in vacuo* (2×10^{-2} mbar). The resulting compound was crystallized from mixture of water and isopropanol at - 20 °C followed by washing with *n*-pentane (2 × 10mL) and then dried *in vacuo*.

11.5.1 {4,8-Bis(diethylamino)-4,8-dioxo-1,3,5,7-tetra-*n*-butyl-4,8-dihydro-1,4-diphosphinine[2,3d:5,6-d′]-bis(imidazole-2,6-ium}dichloride ($8^{cis/trans}$)

Chemicals	Amounts(g or mL)	mmol
$6^{cis/trans}$	0.04 g	0.055
H_2O_2	0.48 mL	0.55
$BaCl_2.2H_2O$	0.0134g	1.1
CH_2Cl_2	2 mL	

<u>Reaction code</u>: NRN-148, NRN-404

<u>Yield</u>: 0.022 g (0.033 mmol) 60 %; white solid.

<u>Melting point</u>: 226 °C

<u>Elemental composition</u>: $C_{30}H_{58}N_6Cl_2O_2P_2$

<u>Molecular weight</u>: 667.68 g/mol

<u>Elemental analysis</u>: for $C_{30}H_{58}N_6Cl_2O_2P_2$:

Theoretical	C	53.97	H	8.76	N	12.59
Experimental	C	51.04	H	8.96	N	11.63

<u>Pos. ESI-MS</u>: *m/z*(%) 595.4 (11) $[M-2H]^{\cdot+}$, 298.2 (100) $[M-2Cl]^{\cdot+2}$

<u>HR-MS</u>: *m/z* = theor./exp. for $[C_{30}H_{58}N_6P_2O_2Cl_2Na]^+$:689.3366. (689.3351)

<u>IR (ATR,ῦ{cm^{-1}})</u>: ῦ= 3375 (w), 2960 (m), 2921 (m), 1549 (w), 1462 (w), 1379 (w), 1245 (m), 1160 (m), 1146 (m), 1018 (s), 955 (m).

<u>^{1}H NMR (300.1 MHz, $CDCl_3$, 25 °C)</u>: δ = 0.9- 1.1 (br, 12H, NCH_2*<u>Me</u>*), 1.3 (t, 12H, $^{3}J_{H,H}$ = 7.4 Hz, $NCH_2CH_2CH_2$*<u>Me</u>*), 1.3- 1.4 (m, 8H, NCH_2CH_2*<u>CH_2</u>*Me), 2.1-2.3 (br, 8H, NCH_2*<u>CH_2</u>*CH_2Me), 3.2- 3.5 (m, 8H, N*<u>CH_2</u>*Me), 4.3 (br, 4H, N*<u>CH_2</u>*CH_2CH_2Me), 4.7 (br, 4H, N*<u>CH_2</u>*CH_2CH_2Me; 2ndisomer), 11.1 (br, 1H, *<u>C^2H</u>*), 11.8 (bs, 1H, *<u>C^2H</u>*; 2ndisomer).

<u>^{13}C{^{1}H} NMR (75.5 MHz, $CDCl_3$, 25 °C)</u>: δ = 11.1 (s, $NCH_2CH_2CH_2$*<u>Me</u>*), 13.5 (br, P-NCH_2*<u>CH_3</u>*), 19.7 (s, NCH_2CH_2*<u>CH_2</u>*Me), 19.7 (s, NCH_2CH_2*<u>CH_2</u>*Me; 2nd isomer), 31.9 (s, NCH_2*<u>CH_2</u>*CH_2Me), 32.4 (s, NCH_2*<u>CH_2</u>*CH_2Me; 2nd isomer), 38.9 (d, $^{2}J_{P,C}$ = 26.4 Hz, N*<u>CH_2</u>*CH_3), 41.3 (br, N*<u>CH_2</u>*CH_2CH_2Me), 51.2 (br, N*<u>CH_2</u>*CH_2CH_2Me; 2nd isomer), 130.3 (t, $^{1}J_{P,C}$ = 2.0 Hz *<u>P-C</u>* of the middle ring), 131.6 (t, $^{1}J_{P,C}$ = 2.3 Hz, *<u>P-C</u>* of the middle ring; 2nd isomer), 147.2 (br, *<u>C=Se</u>*).

<u>^{31}P NMR (121.5 MHz, $CDCl_3$, 25 °C)</u>: δ = - 5.9 (s), - 6.2 (s).

<u>Isomer ratio</u>: 1: 0.62

<u>UV-vis (CH_2Cl_2)</u>: λ_{max} [nm] (abs.): 234 (1.006).

11.6. Synthesis of tricyclic {P(O)NEt_2}-bridged bis(NHCs) 9$^{cis/trans}$

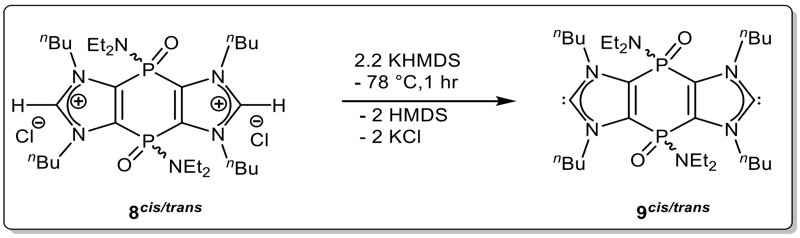

A solution of KHMDS inTHF was added dropwise to a solution of bis(imidazolium) salts **8**$^{cis/trans}$ in THF with continuous stirring through a double-ended needle over 10 minutes at - 78 ˚C. The reaction mixture was stirred for 0.5 h while warming up to - 60 °C. THF was removed *in vacuo* (2×10^{-2} mbar), and the residue was dissolved ina mixture of diethyl ether and *n*-pentane (1: 1.5) the solid potassium chloride was removed via filtering cannulation. The solvent was then dried then *in vacuo* (2×10^{-2} mbar).

11.6.1. {4,8-Bis(diethylamino)-4,8-dioxo-1,3,5,7-tetra-*n*-butyl-4,8-dihydro-1,4-diphosphinine[2,3 d:5,6-d']bis(imidazole-2,6-diylidene}($9^{cis/trans}$)

Chemicals	Amounts(g or mL)	mmol
$8^{cis/trans}$	0.1 g	0.15
KHMDS	0.07 g	0.33
THF	4 mL	

Reaction code: NRN-202

Yield: 0.07 g (0.12 mmol) 78 %; light yellow solid.

Melting point: 110 °C

Elemental composition: $C_{30}H_{56}N_6O_2P_2$

Molecular weight: 594.77 g/mol

Elemental analysis: for $C_{30}H_{56}N_6O_2P_2$:

Theor.	C	60.58	H	9.49	N	14.13
Exp.	C	58.88	H	9.40	N	13.19

MS (EI, 70 eV): *m/z* (%) = 594.4 (52) $[M]^{\cdot+}$.

HR-MS: *m/z* = theor. /exp. : 594.3933/594.3926.

IR (ATR,ῦ{cm^{-1}}): ῦ=2956.7 (m), 2930.4 (m), 2870.7 (w), 1464.3 (w), 1434.3 (w), 1398.3 (s), 1217.7 (m), 1176.8 (m), 1146.9 (m), 1016.5 (S), 926.5 (s).

^{1}H NMR (300.1 MHz, C_6D_6, 25 °C): δ = 0.6 (t, 12H, $^3J_{H,H}$ = 6.9 Hz, NCH_2*Me*), 0.9 (t, 12H, $^3J_{H,H}$ = 7.35 Hz, $NCH_2CH_2CH_2$*Me*), 1.0- 1.1 (m, 8H, NCH_2CH_2*CH_2*Me), 2.2- 2.3 (m, 8H, NCH_2*CH_2*CH_2Me), 2.8- 2.9(m, 8H, N*CH_2*Me), 4.3- 4.4 (m, 8H, N*CH_2*CH_2CH_2Me).

$^{13}C\{^1H\}$ NMR (75.5 MHz, C_6D_6, 25 °C): δ = 12.9 (s, $NCH_2CH_2CH_2$*Me*), 13.6 (br, NCH_2*CH_3*), 19.9 (s, NCH_2CH_2*CH_2*Me), 19.9 (s, NCH_2CH_2*CH_2*Me; 2nd isomer), 33.7 (s, NCH_2*CH_2*CH_2Me), 33.9 (s, NCH_2*CH_2*CH_2Me; 2nd isomer), 37.4 (t, $^2J_{P,C}$ = 3.18 Hz, N*CH_2*CH_3), 37.6 (t, $^2J_{P,C}$ = 2.7 Hz, P-N*CH_2*CH_3; 2nd isomer), 50.4 (br, N*CH_2*CH_2CH_2Me), 50.4 (br, N*CH_2*CH_2CH_2Me; 2nd isomer), 130.2 (d, $^1J_{P,C}$ = 27.1 Hz *P-C* of the middle ring), 132.1 (d, $^1J_{P,C}$ = 27.1 Hz, *P-C* of the middle ring; 2nd isomer), 225.1 (t, $^3J_{P,C}$ = 2.4 Hz, *C^2*), 225.3 (t, $^3J_{P,C}$ = 2.4 Hz, *C^2*; 2nd isomer).

^{31}P NMR (121.5 MHz, C_6D_6, 25 °C): δ = - 1.2 (s), -2.3 (s)

Isomer ratio: 1: 0.64

UV-vis (THF): λ_{max} [nm] (abs.): 230 (0.976).

11.7. Synthesis of tricyclic {P(O)NEt2}-bridged bis(NHC) coinage metal(I) complexes 10a-b$^{cis/trans}$

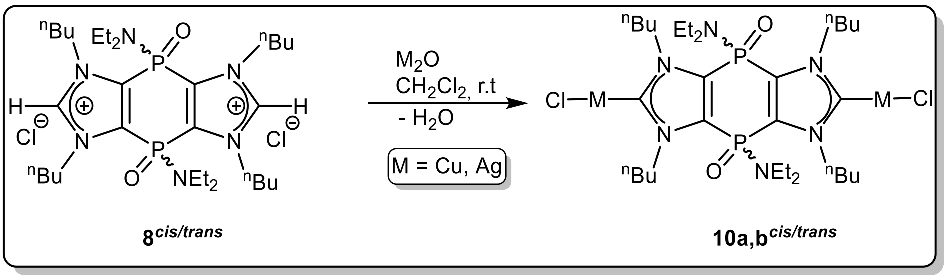

To a solution of bis(imidazolium) salts **8**$^{cis/trans}$ in methylene chloride, M(I) = Cu, Ag oxide was added as solid at room temperature. The reaction mixture was stirred under darkness containing molecular sieves (to adsorb H_2O) for 8 h. The solution was then concentrated *in vacuo* (2×10^{-2} mbar). It was filtered over silica with methylene chloride to get a clear solution. The solvent was evaporated *in vacuo* (2×10^{-2} mbar) followed by washing with *n*-pentane (2 × 5 mL) to get white solids.

11.7.1. {4,8-Bis(diethylamino)-4,8-dioxo-1,3,5,7-tetra-*n*-butyl-4,8-dihydro-1,4-diphosphinine[2,3d:5,6d']-bis(imidazol-2,6-diylidene)- *κ*C, *κ*C}di(copperchloride) (10a$^{cis/trans}$)

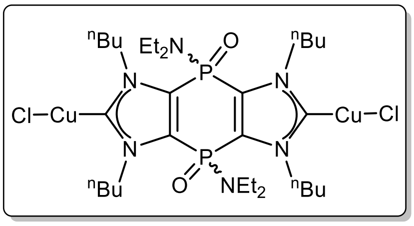

Chemicals	Amounts(g or mL)	mmol
8$^{cis/trans}$	0.1 g	0.15
Cu_2O	0.02 g	0.15
CH_2Cl_2	5 mL	

Reaction code: NRN-203

Yield: 0.082 g (0.1 mmol) 68 %; ivory colored solid.

Melting point: 132 °C

Elemental composition: $C_{30}H_{58}Cl_2Cu_2N_6O_2P_2$

Molecular weight: 794.77 g/mol

Elemental analysis: for $C_{30}H_{58}Cl_2Cu_2N_6O_2P_2$:

Theor.	C	45.34	H	7.36	N	10.56
Exp.	C	44.93	H	7.21	N	10.60

Pos. ESI-MS: *m/z* = theor.(exp.) for $[C_{32}H_{59}Cu_2ClN_7O_2P_2]^{\cdot+}$: 798.2472 (798.2464).

IR (ATR,ῦ{cm^{-1}}): ῦ = 2956 (m), 2930 (m), 2870 (w), 1464 (w), 1434 (w), 1398 (s), 1217 (m), 1176 (m), 1146 (m), 1016 (s), 926 (s).

<u>^{1}H NMR (300.1 MHz, CD_2Cl_2, 25 °C)</u>: δ = 0.9 (t, 12H, $^{3}J_{H,H}$ = 7.3 Hz, P-NCH_2<u>*Me*</u>), 1.0 (t, 12H, $^{3}J_{H,H}$ = 7.48 Hz, $NCH_2CH_2CH_2$<u>*Me*</u>), 1.4- 1.5 (m, 8H, NCH_2CH_2<u>*CH_2*</u>Me), 1.9- 2.2 (m, 8H, NCH_2<u>*CH_2*</u>CH_2Me), 3.1- 3.3 (m, 8H, P-N<u>*CH_2*</u>Me), 4.1-4.2 (m, 4H, N<u>*CH_2*</u>CH_2CH_2Me), 4.5- 4.6 (m, 4H, N<u>*CH_2*</u>CH_2CH_2Me; 2ndisomer).

<u>^{13}C{^{1}H} NMR (75.5 MHz, CD_2Cl_2, 25 °C)</u>: δ = 13.1 (s, $NCH_2CH_2CH_2$<u>*Me*</u>), 13.2 (s, $NCH_2CH_2CH_2$<u>*Me*</u>; 2nd isomer), 13.6 (s, P-NCH_2<u>*CH_3*</u>), 13.6 (s, P-NCH_2<u>*Me*</u>; 2nd isomer), 19.9 (s, NCH_2CH_2<u>*CH_2*</u>Me), 20.0 (s, NCH_2CH_2<u>*CH_2*</u>Me; 2nd isomer), 33.7 (s, NCH_2<u>*CH_2*</u>CH_2Me), 33.9 (s, NCH_2<u>*CH_2*</u>CH_2Me; 2nd isomer), 37.9 (t, $^{2}J_{P,C}$ = 2.51 Hz, P-N<u>*CH_2*</u>CH_3), 38.1 (t, $^{2}J_{P,C}$ = 2.51 Hz, P-N<u>*CH_2*</u>CH_3), 51.7 (br, N<u>*CH_2*</u>CH_2CH_2Me), 130.9 (br, <u>*P-C*</u>of the middle ring), 131.78 (br, <u>*P-C*</u> of the middle ring; 2ndisomer), 186.1 (br, <u>*C^2*</u>).

<u>^{31}P NMR (121.5 MHz, CD_2Cl_2, 25 °C)</u>: δ = - 3.3 (s), - 3.9 (s)

<u>Isomer ratio</u>: 1: 0. 4

<u>UV-vis (CH_2Cl_2)</u>: λ_{max} [nm] (abs.): 229(1.005).

11.7.2 {4,8-Bis(diethylamino)-4,8-dioxo-1,3,5,7-tetra-*n*-butyl-4,8-dihydro-1,4-diphosphinine[2,3d:5,6-d']-bis(imidazole-2,6-diylidene)-*κ*C,*κ*C}di(silverchloride) (10b$^{cis/trans}$)

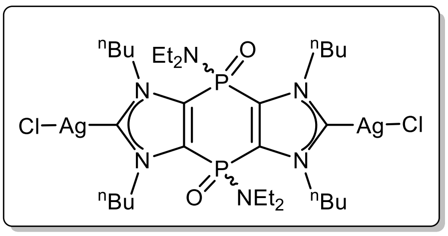

Chemicals	Amounts(g or mL)	M mol
8$^{cis/trans}$	0.07 g	0.1
Ag_2O	0.023 g	0.1
CH_2Cl_2	7 mL	

<u>Reaction code</u>: NRN-161

<u>Yield</u>: 0.055 g (0.062 mmol) 62 %; ivory colored solid.

Melting point: 151 °C

Elemental composition: $C_{30}H_{58}Ag_2Cl_2N_6O_2P_2$

Molecular weight: 883.41 g/mol

Elemental analysis: for $C_{30}H_{58}Ag_2Cl_2N_6O_2P_2$:

Theor.	C	40.79	H	6.62	N	9.55
Exp.	C	40.26	H	6.48	N	9.51

Pos. ESI-MS: $[C_{32}H_{59}Ag_2ClN_7O_2P_2]^{\cdot+}$ Theor.(Exp.) 886.1985 (886.1987).

IR (ATR,ῦ{cm^{-1}}): ῦ = 2987.5 (w), 2942.4 (m), 2892.7 (w), 1492.3 (w), 1412.3 (m), 1302.3 (m), 1256.1 (m), 1098.6 (m), 1023.7 (m), 986.7 (s), 963.0 (s).

^{1}H NMR (300.1 MHz, CD_2Cl_2, 25 °C): δ = 1.0 (t, 12H, $^{3}J_{H,H}$ = 4.1 Hz, P-NCH_2*Me*), 1.0 (t, 12H, $^{3}J_{H,H}$ = 4.8 Hz, $NCH_2CH_2CH_2$*Me*), 1.4- 1.5 (m, 8H, NCH_2CH_2*CH_2*Me), 1.9- 2.2 (m, 8H, NCH_2*CH_2*CH_2Me), 3.1- 3.3 (m, 8H, P-N*CH_2*Me), 4.2-4.3 (m, 4H, N*CH_2*CH_2CH_2Me), 4.5- 4.5 (m, 4H, N*CH_2*CH_2CH_2Me; 2nd isomer).

^{13}C{^{1}H} NMR (75.5 MHz, CD_2Cl_2, 25 °C): δ = 12.9 (s, $NCH_2CH_2CH_2$*Me*), 13.0 (s, $NCH_2CH_2CH_2$*Me*; 2nd isomer), 13.5 (s, P-NCH_2*CH_3*), 13.5 (s, P-NCH_2*CH_3*; 2nd isomer), 19.8 (s, NCH_2CH_2*CH_2*Me; 20.04 (s, NCH_2CH_2*CH_2*Me; 2nd isomer), 34.2 (s, NCH_2*CH_2*CH_2Me), 34.4 (s, NCH_2*CH_2*CH_2Me; 2nd isomer), 37.9 (t, $^{2}J_{P,C}$ = 2.35 Hz, P-N*CH_2*CH_3), 52.0 (br, N*CH_2*CH_2CH_2Me, 131.1 (br, *P-C* of the middle ring), 132.2 (br, *P-C* of the middle ring; 2nd isomer), 188.9 (br,*C^2*), 191.3 (br, *C^2*; 2nd isomer).

^{31}P NMR (121.5 MHz, CD_2Cl_2, 25 °C): δ = - 3.8 (s), - 4.3 (s)

Isomer ratio: 1: 0. 3

UV-vis (CH_2Cl_2): λ_{max} [nm] (abs.): 229(0.996), 288 (0.504).

11.8. Synthesis of tricyclic {P(O)NEt$_2$}-bridged bis(NHC) coinage Au(I) complexes 10c$^{cis/trans}$

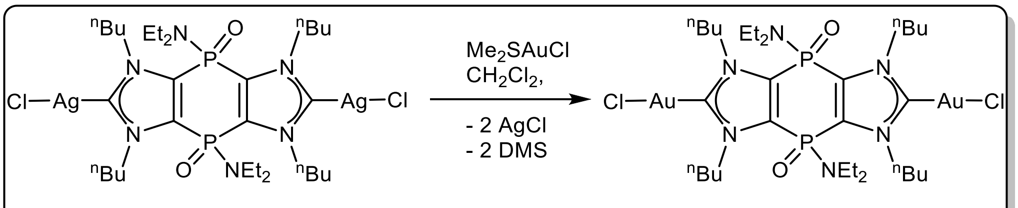

To a solution of **10b**$^{cis/trans}$, in methylene chloride, dimethyl sulfide gold (I) was added as solid at room temperature. The reaction mixture was stirred for 2 hours. The solvent was removed in *vacuo* (2×10^{-2} mbar), and the residue was dissolved in 20 mL of methylene chloride and the solid AgCl was removed via filtration over celite@. The solvent was then dried in *vacuo* (2×10^{-2} mbar).

11.8.1. {4,8-Bis(diethylamino)-4,8-dioxo-1,3,5,7-tetra-*n*-butyl-4,8-dihydro-1,4-diphos-phinine[2,3d:5,6-d']bis(imidazole-2,6-diylidene)-*κ*C,*κ*C}di(gold(I)chloride) (10c$^{cis/trans}$)

Chemicals	Amounts(g or mL)	mmol
10c$^{cis/trans}$	0.5 g	0.60
$(CH_3)_2SAuCl$	0.35 g	1.20
CH_2Cl_2	15 mL	

Reaction code: NRN-198

Yield: 0.38 g (0.36 mmol) 60 %; ivory colored solid.

Melting point: 184 °C

Elemental composition: $C_{30}H_{58}Cl_2Au_2N_6O_2P_2$

Molecular weight: 1061.61 g/mol

Elemental analysis: for $C_{30}H_{58}Cl_2Au_2N_6O_2P_2$:

Theor.	C	33.94	H	5.51	N	7.92
Exp.	C	34.17	H	5.80	N	7.46

Pos. ESI-MS: *m/z* =theor.(Exp.) for $[C_{32}H_{59}Au_2ClN_7O_2P_2]^+$: 1064.3220 (1064.3221).

IR (ATR,ṽ{cm^{-1}}): ṽ = 2956 (m), 2930 (m), 2870 (w), 1464 (w), 1434 (w), 1398 (s), 1217 (m), 1176 (m), 1146 (m), 1016 (s), 926 (s).

^{1}H NMR (300.1 MHz, CDCl$_3$, 25 °C): δ = 0.9 (t, 12H, $^3J_{H,H}$ = 7.3 Hz, P-NCH$_2$*Me*), 1.0 (t, 12H, $^3J_{H,H}$ = 7.5 Hz, NCH$_2$CH$_2$CH$_2$*Me*), 1.4- 1.52 (m, 8H, NCH$_2$CH$_2$*CH$_2$*Me), 1.9- 2.2 (m, 8H, NCH$_2$*CH$_2$*CH$_2$Me), 3.1- 3.3 (m, 8H, P-N*CH$_2$*Me), 4.1- 4.2 (m, 4H, N*CH$_2$*CH$_2$CH$_2$Me), 4.3- 4.5 (m, 4H, N*CH$_2$*CH$_2$CH$_2$Me; 2ndisomer).

^{13}C{^{1}H} NMR (75.5 MHz, CDCl$_3$, 25 °C): δ = 13.2 (s, NCH$_2$CH$_2$CH$_2$*Me*), 13.2 (s, NCH$_2$CH$_2$CH$_2$*Me*; 2nd isomer), 13.6 (s, P-NCH$_2$*CH$_3$*), 13.7 (s, P-NCH$_2$*CH$_3$*; 2nd isomer), 20.0 (s, NCH$_2$CH$_2$*CH$_2$*Me), 20.1 (s, NCH$_2$CH$_2$*CH$_2$*Me; 2nd isomer), 33.5 (s, NCH$_2$*CH$_2$*CH$_2$Me), 33.6 (s, NCH$_2$*CH$_2$*CH$_2$Me; 2nd isomer), 37.9 (t, $^2J_{P,C}$ = 2.55 Hz, P-N*CH$_2$*CH$_3$), 39.0 (t, $^2J_{P,C}$ = 2.53 Hz, P-N*CH$_2$*CH$_3$), 52.0 (br, N*CH$_2$*CH$_2$CH$_2$Me), 132.1 (br, *P-C* of the middle ring), 132.4 (br, *P-C* of the middle ring; 2nd isomer), 181.8 (t, $^2J_{P,C}$ = 2.3 Hz,*C^2*), 181.5 (t, $^2J_{P,C}$ = 2.3 Hz, *C^2*; 2nd isomer).

^{31}P NMR (121.5 MHz, CDCl$_3$, 25 °C): δ = - 3.8 (s), - 4.4 (s).

Isomer ratio: 1: 0.4

UV-vis (CH$_2$Cl$_2$): λ_{max} [nm] (abs.): 234(0.585), 288(0.229).

11.9. Synthesis of tricyclic {P(O)NEt$_2$}-bridged bis(NHC) [M(cod)Cl] complexes 10d,e$^{cis/trans}$

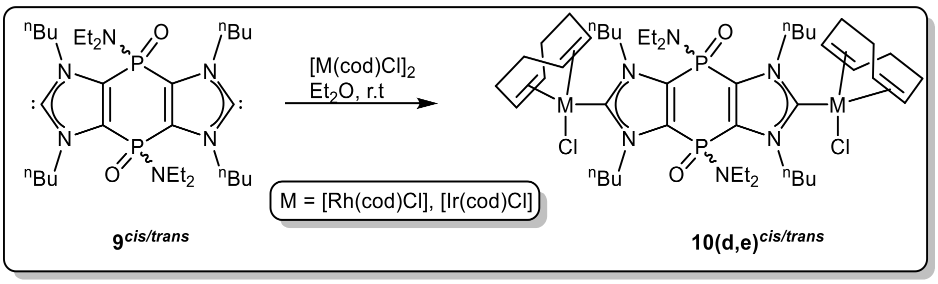

To a solution of **9**$^{cis/trans}$, in diethyl ether, [M(cod)Cl] dimer (M(I) = Rh, Ir) was added as solid at room temperature. The reaction mixture was stirred for 2 hours. Precipitates formed, which was filtered using a filtering cannula. Solid was dried in *vacuo* (2 × 10^{-2} mbar), and the residue was washed with *n*-pentane. Finally, the solvent was then dried in *vacuo* (2 × 10^{-2} mbar) to get pure yellow solid.

11.9.1. [{4,8-Bis(diethylamino)-4,8-dioxo-1,3,5,7-tetra-*n*-butyl-4,8-dihydro[1,4]diphosphinine[2,3-d:5,6-d']bis(imidazole-2,6-diylidene)-κC,κC}bis((1,2,5,6-η^4)-1,5-cyclooctadiene)chlororhodium(I)](10d$^{cis/trans}$)

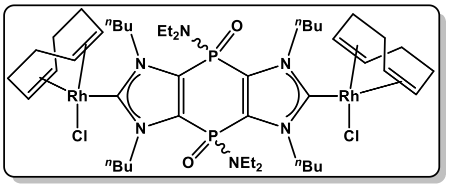

Chemicals	Amounts(g or mL)	mmol
9$^{cis/trans}$	0.5 g	0.84
Rh(cod)Cl	0.42 g	0.84
Et_2O	10 mL	

Reaction code: NRN-511

Yield: 0.62 g (0.57 mmol) 68 %; yellow colored solid.

Melting point: 196 °C

Elemental composition: $C_{46}H_{82}Cl_2Rh_2N_6O_2P_2$

Molecular weight: 1089.86 g/mol

Elemental analysis: for $C_{46}H_{82}Cl_2Rh_2N_6O_2P_2$:

Theor.	C	50.70	H	7.85	N	7.71
Exp.	C	49.94	H	7.25	N	6.68

Pos. ESI-MS: $C_{48}H_{83}Rh_2ClN_7O_2P_2^+$ Theor. (Exp.) 1092.3897 (1092.3894).

IR (ATR,ῦ{cm^{-1}}): ῦ = 2851 (m), 2790 (m), 2670 (w), 1502 (w), 1444 (w), 1320 (s), 1238 (m), 1108 (m), 1048 (m), 984 (s), 881 (s).

^{1}H NMR (300.1 MHz, CD_2Cl_2, 25 °C): δ = 0.9 (t, 12H, $^3J_{H,H}$ = 7.1 Hz, P-NCH$_2$*Me*), 1.0 (t, 12H, $^3J_{H,H}$ = 7.5 Hz, NCH$_2$CH$_2$CH$_2$*Me*), 1.4- 1.5 (m, 8H, NCH$_2$CH$_2$*CH$_2$*Me), 1.8 (m, 4H, cod), 1.8- 2.2 (m, 8H, NCH$_2$*CH$_2$*CH$_2$Me), 2.3 (m, 4H, cod), 3.1- 3.3 (m, 8H, P-N*CH$_2$*Me), 3.7 (m, 2H, cod), 4.1- 4.2 (m, 4H, N*CH$_2$*CH$_2$CH$_2$Me), 4.3- 4.5 (m, 4H, N*CH$_2$*CH$_2$CH$_2$Me; 2ndisomer), 5.1 (m, 2H, cod).

^{13}C{^{1}H} NMR (75.5 MHz, CD_2Cl_2, 25 °C): δ = 12.6 (s, NCH$_2$CH$_2$CH$_2$*Me*), 12.8 (s, NCH$_2$CH$_2$CH$_2$*Me*; 2nd isomer), 13.5 (s, P-NCH$_2$*CH$_3$*), 13.7 (s, P-NCH$_2$*CH$_3$*; 2nd isomer), 20.4 (s, NCH$_2$CH$_2$*CH$_2$*Me), 20.5 (s, NCH$_2$CH$_2$*CH$_2$*Me; 2nd isomer), 28.7 (s, cod), 32.5 (s, NCH$_2$*CH$_2$*CH$_2$Me),32.9 (s, cod), 33.5 (s, NCH$_2$*CH$_2$*CH$_2$Me; 2nd isomer), 37.9 (t, $^2J_{P,C}$ = 2.4 Hz, P-N*CH$_2$*CH$_3$), 39.1 (t, $^2J_{P,C}$ = 2.5 Hz, P-N*CH$_2$*CH$_3$), 52.7 (br, N*CH$_2$*CH$_2$CH$_2$Me),69.3 (d, $^1J_{Rh,C}$ = 14.1 Hz, cod), 99.4 (d, $^1J_{Rh,C}$ = 6.7 Hz, cod), 130.5 (br, *P-C* of the middle ring), 132.2 (br, *P-C* of the middle ring; 2nd isomer), 195.2 (ddd, $^1J_{C,Rh}$ = 52.1 Hz, $^3J_{P,C}$ = 1.8 Hz, *C*^{2}), 195.9 (ddd, $^1J_{C,Rh}$ = 52.1 Hz, $^3J_{P,C}$ = 1.7 Hz, *C*^{2}; 2nd isomer).

^{31}P NMR (121.5 MHz, CD_2Cl_2, 25 °C): δ = - 4.0(s), -4.6 (s).

Isomer ratio: 1: 0.3

11.9.2 [{4,8-Bis(diethylamino)-4,8-dioxo-1,3,5,7-tetra-*n*-butyl-4,8-dihydro[1,4]diphosphinine[2,3-d:5,6-d']bis(imidazole-2,6-diylidene)-κC,κC}bis((1,2,5,6-η^4)-1,5-cyclooctadiene)chloroiridium(I)](10e$^{cis/trans}$)

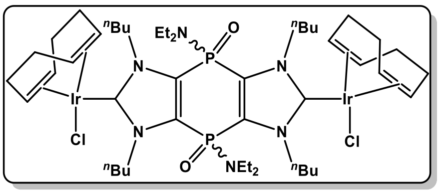

Chemicals	Amounts(g or mL)	mmol
9$^{cis/trans}$	0.5 g	0.84
Ir(cod)Cl	0.56 g	0.84
Et_2O	10 mL	

Reaction code: NRN-513

Yield: 0.69 g (0.54 mmol) 65 %; yellow colored solid.

Melting point: 174 °C

Elemental composition: $C_{46}H_{82}Cl_2Ir_2N_6O_2P_2$

Molecular weight: 1268.48 g/mol

Elemental analysis: for $C_{46}H_{82}Cl_2Ir_2N_6O_2P_2$:

Theor.	C	43.55	H	6.52	N	6.63
Exp.	C	43.81	H	6.36	N	6.69

Pos. ESI-MS: *m/z* = theor. (Exp.) for $[C_{46}H_{80}Cl_2Ir_2N_6O_2P_2]^+$: 1266.453 (1266.443).

IR (ATR,ῦ{cm^{-1}}): ῦ = 2821 (m), 2802 (m), 2665 (w), 1510 (w), 1450 (w), 1318 (s), 1208 (m), 1112 (m), 1030 (m), 968 (s), 901 (s).

^{1}H NMR (300.1 MHz, CD_2Cl_2, 25 °C): δ = 0.9 (t, 12H, $^3J_{H,H}$ = 7.1 Hz, P-NCH_2*Me*), 1.0 (t, 12H, $^3J_{H,H}$ = 7.5 Hz, $NCH_2CH_2CH_2$*Me*), 1.4- 1.5 (m, 8H, NCH_2CH_2*CH_2*Me), 1.6 (m, 4H, cod), 1.7- 2.1 (m, 8H, NCH_2*CH_2*CH_2Me), 2.1 (m, 4H, cod), 2.9- 3.2 (m, 8H, P-N*CH_2*Me), 3.4 (m, 2H, cod), 4.0- 4.2 (m, 4H, N*CH_2*CH_2CH_2Me), 4.3- 4.5 (m, 4H, N*CH_2*CH_2CH_2Me; 2nd isomer), 4.8 (m, 2H, cod).

^{13}C{^{1}H} NMR (75.5 MHz, CD_2Cl_2, 25 °C): δ = 12.8 (s, $NCH_2CH_2CH_2$*Me*), 12.8 (s, $NCH_2CH_2CH_2$*Me*; 2nd isomer), 13.5 (s, P-NCH_2*CH_3*), 13.7 (s, P-NCH_2*CH_3*; 2nd isomer), 20.0 (s, NCH_2CH_2*CH_2*Me), 20.4 (s, NCH_2CH_2*CH_2*Me; 2nd isomer), 29.2 (s, cod), 31.8 (s, NCH_2*CH_2*CH_2Me),33.1 (s, cod), 33.5 (s, NCH_2*CH_2*CH_2Me; 2nd isomer), 37.5 (t, $^2J_{P,C}$ = 2.2 Hz, P-N*CH_2*CH_3), 38.5 (t, $^2J_{P,C}$ = 2.3 Hz, P-N*CH_2*CH_3), 52.4 (br, N*CH_2*CH_2CH_2Me),86.8 (d, $^1J_{Rh,C}$ = 6.5 Hz, cod), 130.4 (br, *P-C* of the middle ring), 131.7 (br, *P-C* of the middle ring; 2nd isomer), 191.1 (t, $^3J_{P,C}$ = 2.1 Hz, C^2), 191.8 (t, $^3J_{P,C}$ = 1.7 Hz, C^2; 2nd isomer).

^{31}P NMR (121.5 MHz, CD_2Cl_2, 25 °C): δ = - 3.1(s), - 4.2 (s)

Isomer ratio: 1: 0.6

11.10. Synthesis of double Se-methylated salts of 1,4-dihydro-1,4-diphosphinine diselone

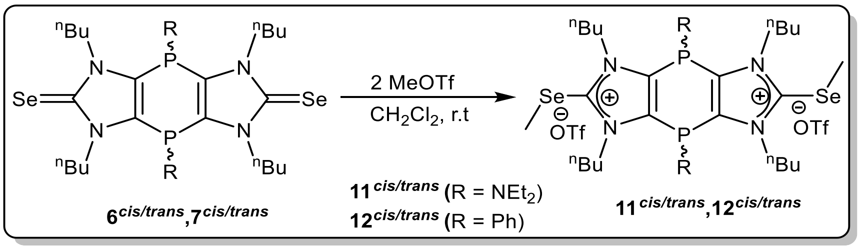

To a solution of **6**$^{cis/trans}$/**7**$^{cis/trans}$in 10 mL methylene chloride, 2 equivalent of trifluoromethanesulfonate was added slowly at room temperature. It was left on stirring for 12 hours. The reaction mixture was concentrated under reduced pressure (2 × 10^{-2} mbar). The products were washed with diethyl *ether* and dried under reduced pressure to get rid of traces of CH_2Cl_2.

11.10.1. {4,8-Bis(diethylamino)-1,3,5,7-tetra-*n*-butyl-4,8-dihydro[1,4]diphosphinine[2,3-d:5,6-d']bis(imidazole-2,6-methylselanylium)}bis(trifluoromethanesulfonate) (11$^{cis/trans}$)

Chemicals	Amounts(g or mL)	mmol
6$^{cis/trans}$	0.20 g	0.27
MeOTf	0.06mL	0.55
CH_2Cl_2	4 mL	

Reaction code: NRN-155, NRN-423, NRN-452

Yield: 0.24 g (0.23 mmol) 85 %; yellow sticky compound

Elemental composition: $C_{34}H_{64}F_6S_2N_6O_6P_2Se_2$

Molecular weight: 1050.90 g/mol

Elemental analysis: for $C_{34}H_{64}F_6N_6O_6P_2S_2Se_2$:

Theor.	C	38.93	H	5.95	N	8.01
Exp.	C	38.69	H	6.46	N	8.15

Pos. ESI-MS: *m/z* = theor. (exp.) for $[C_{32}H_{62}N_6P_2Se_2]^{+2}$: 376.1419 (376.1418).

IR (ATR,ῡ{cm^{-1}}): ῡ = 2955 (m), 2812.5 (m), 2812.2 (w), 1698.2 (w), 1612.4 (m), 1475.8 (m), 1347.4 (s), 1096.6 (s), 1095.4 (s), 1009.5 (s).

^{1}H NMR (300.1 MHz, $CDCl_3$, 25 °C): δ =0.9 (br, 12H, P-NCH_2*Me*), 1.0 (t, 12H, $^3J_{H,H}$ = 7.2 Hz, $NCH_2CH_2CH_2$*Me*), 1.4-1.5 (m, 8H, NCH_2CH_2*CH_2*Me), 1.7-1.9 (m, 4H, NCH_2*CH_2*CH_2Me), 1.9 - 2.1 (m, 4H, NCH_2*CH_2*CH_2Me; 2nd isomer), 2.52 (br, Se-*Me*), 2.5 (br, Se-*Me*; 2nd isomer), 2.8-3.1 (m, 8H, P-N*CH_2*Me), 4.3- 4.4 (m, 4H, N*CH_2*CH_2CH_2Me), 4.5-4.7 (m, 4H, N*CH_2*CH_2CH_2Me; 2nd isomer).

^{13}C{^{1}H} NMR (75.5 MHz, $CDCl_3$, 25 °C): δ = 11.8 (br, $NCH_2CH_2CH_2$*Me*), 13.5 (br, P-NCH_2*Me*), 19.9 (Se-*Me*), 20.0 (Se-*Me*), 19.9 (s, NCH_2CH_2*CH_2*Me), 20.0 (s, NCH_2CH_2*CH_2*Me; 2nd isomer), 32.2 (br, NCH_2*CH_2*CH_2Me), 32.4 (br, NCH_2*CH_2*CH_2Me; 2nd isomer), 43.5 (br, PN*CH_2*Me), 45.8 (d, $^2J_{P,C}$ = 1913 Hz, P-N*CH_2*Me; 2nd isomer), 49.6 (br, N*CH2*CH2CH2Me), 50.8 (br, N*CH2*CH2CH2Me; 2nd isomer), 120.8 (q, $^1J_{P,F}$ = 321.7 Hz, $CF_3SO_3^-$), 136.8 (br , 6.8 Hz, *P-C* of the middle ring), 142.6 (br,*C^2*), 143.1 (br, *C^2*; 2nd isomer).

^{31}P NMR (121.5 MHz, $CDCl_3$, 25 °C): δ = 2.8, 3.7

Isomer ratio: 1: 0.3

^{77}SeNMR (57.28 MHz, C_6D_6): 115.1, 119.1

UV-vis (CH_2Cl_2): λ_{max} [nm] (abs.): 231(0.866).

11.10.2 {4,8-Bis(phenyl)-1,3,5,7-tetra-*n*-butyl-4,8-dihydro[1,4]diphosphinine[2,3-d:5,6-d']bis(imidazole-2,6-methylselanylium)}bis(trifluoromethane sulfonate) ($12^{cis/trans}$)

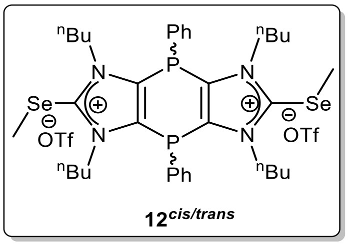

Chemicals	Amounts(g or mL)	mmol
$\mathbf{6}^{cis/trans}$	0.05 g	0.068
MeOTf	0.02 mL	0.136
CH_2Cl_2	2 mL	

Reaction code: NRN-166

Yield: 0.062 g (0.058 mmol) 86%; very light yellow compound

Elemental composition: $C_{38}H_{52}F_6S_2N_4O_6P_2Se_2$

Molecular weight: 1059.89 g/mol

Elemental analysis: for $C_{34}H_{64}F_6S_2N_6O_6P_2Se_2$:

Theor.	C	43.11	H	4.95	N	5.29
Exp.	C	40.40	H	4.72	N	4.83

Pos. ESI-MS: *m/z* = theor.(exp.) for$[C_{37}H_{52}N_4P_2Se_2]^+$:911.1518 (911.1492).

IR (ATR,ῦ{cm^{-1}}): ῦ = 3025 (m), 2982 (m), 2712.2 (m), 1495 (m), 1484 (s), 1246 (m), 1215 (s), 1069 (m), 742 (m).

^{1}H NMR (300.1 MHz, $CDCl_3$, 25 °C): 0.8 (t, 12H, $^3J_{H,H}$ = 7.2 Hz, $NCH_2CH_2CH_2$*Me*), 0.9 (t, 12H, $^3J_{H,H}$ = 7.2 Hz, $NCH_2CH_2CH_2$*Me*; 2nd isomer), 1.3-1.4 (m, 8H, NCH_2CH_2*CH_2*Me), 1.6-1.7 (m, 4H,

NCH_2<u>CH_2</u>CH_2Me), 1.7 -1.9 (m, 4H, NCH_2<u>CH_2</u>CH_2Me; 2nd isomer), 2.4 (s, Se-*Me*), 2.5 (s, Se-*Me*; 2nd isomer), 4.2- 4.6 (m, 8H, N<u>CH_2</u>CH_2CH_2Me), 7.4-4.8 (br, 10H, P-<u>*Ph*</u>).

<u>$^{13}C\{^1H\}$ NMR (75.5 MHz, $CDCl_3$, 25 °C)</u>: δ = 12.9 (br, $NCH_2CH_2CH_2$<u>*Me*</u>), 20.1 (s, NCH_2CH_2<u>CH_2</u>Me),22.3 (Se-*Me*), 33.4 (br, NCH_2<u>CH_2</u>CH_2Me),52.8 (br, N<u>CH_2</u>CH_2CH_2Me), 121.8 (q, $^1J_{P,F}$ = 321.7 Hz, $CF_3SO_3^-$), 132.1 (br, Ph-C),136.8 (br , 6.8 Hz,<u>*P-C*</u> of the middle ring), 142.2 (br, <u>C^2</u>).

<u>^{31}P NMR (121.5 MHz, $CDCl_3$, 25 °C)</u>: δ = - 52.8 (s), - 49.8 (s)

<u>Isomer ratio</u>: 1: 1

<u>^{77}SeNMR (57.28 MHz, C_6D_6)</u>: 118.2, 121.4

11.11. Synthesis of tricyclic (P-NEt_2)-bridged bis(imidazolium) salts 13*cis/trans*

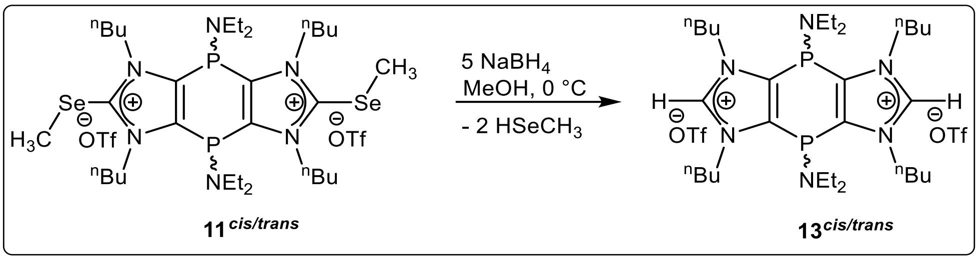

To a solution of **11***cis/trans*in methanol, 5equivalent of sodium tetraborohydridewas added as solid at 0 °C. The reaction mixture was stirred for 0.5 h. The solution was then concentrated *in vacuo* (2×10^{-2} mbar). Column chromatography was performed to isolate it using silica bed with mixture of ether and THF as second fraction. Solvent was evaporated *in vacuo* (2×10^{-2} mbar) followed by washing with *n*-pentane (2 × 5 mL) to get orange liquid.

11.11.1. {4,8-Bis(diethylamino)-1,3,5,7-tetra-*n*-butyl-4,8-dihydro[1,4]diphosphinine[2,3-d:5,6-d']bis(imidazole-2,6-ium)}bis(trifluoromethanesulfonate) (13*cis/trans*)

Chemicals	Amounts(g or mL)	mmol
11*cis/trans*	1.0 g	0.95
$NaBH_4$	0.18 g	4.6
MeOH	30 mL	

Reaction code: NRN-163, NRN-289, NRN-411

Yield: 0.498g (0.57 mmol) 61 %; orange oil

Elemental composition: $C_{32}H_{58}F_6S_2N_6O_6P_2$

Molecular weight: 862.910 g/mol

Elemental analysis: for $C_{32}H_{58}F_6N_6O_6P_2S_2$:

Theor.	C	44.54	H	6.78	N	9.74
Exp.	C	44.87	H	6.56	N	9.27

Pos. ESI-MS: $[C_{30}H_{58}N_6P_2]^{\cdot+2}$ theor.(exp.)565.428 (565.429)

Neg. ESI-MS: OTf^- theor.(exp.)148.95(149.0).

IR (ATR,ῡ{cm^{-1}}): ῡ = 2955 (m), 2941 (m), 2860 (w), 1421 (w), 1420 (m), 1388 (m), 1237 (s), 1196 (m), 1136 (m), 1023 (s), 910 (s).

^{1}H NMR (300.1 MHz, CD_2Cl_2, 25 °C): δ = 0.9-1.0 (t, 12H, $^3J_{H,H}$ = 7.4 Hz, P-NCH$_2$*Me*), 1.0-1.1 (t, 12H, $^3J_{H,H}$ = 7.14 Hz, NCH$_2$CH$_2$CH$_2$*Me*), 1.3- 1.4 (m, 8H, NCH$_2$CH$_2$*CH$_2$*Me), 1.5- 1.8 (m, 8H, NCH$_2$*CH$_2$*CH$_2$Me), 3.0- 3.3 (m, 8H, P-N*CH$_2$*Me), 4.2- 4.4 (m, 8H, N*CH$_2$*CH$_2$CH$_2$Me), 9.5 (t, $^4J_{H,H}$ = 1.82 Hz, 1H, *C^{2}H*), 9.5 (t, $^4J_{H,H}$ = 1.67 Hz, 1H, *C^{2}H*; 2ndisomer).

^{13}C{^{1}H} NMR (75.5 MHz, CD_2Cl_2, 25 °C): δ = 13.2 (s, NCH$_2$CH$_2$CH$_2$*Me*), 13.7 (s, P-NCH$_2$*CH$_3$*), 19.5 (s, NCH$_2$CH$_2$*CH$_2$*Me), 20.2 (s, NCH$_2$CH$_2$*CH$_2$*Me; 2nd isomer), 30.8 (br, NCH$_2$*CH$_2$*CH$_2$Me), 31.6 (t, $^4J_{P,C}$ = 1.7 Hz, NCH$_2$*CH$_2$*CH$_2$Me; 2nd isomer), 44.1 (br, P-N*CH$_2$*CH$_3$), 47.8(t, $^2J_{P,C}$ = 3.05 Hz, P-N*CH$_2$*CH$_3$; 2ndisomer). 52.7 (br, N*CH$_2$*CH$_2$CH$_2$Me), 121.1 (q, $^1J_{P,F}$ = 322.4 Hz, $CF_3SO_3^-$),131.8 (br, *P-C* of the middle ring), 133.3 (br, *P-C* of the middle ring; 2nd isomer), 140.9 (br,*C^2*).

^{31}P NMR (121.5 MHz, CD_2Cl_2, 25 °C): δ = 5.4 (s), 5.8 (s)

Isomer ratio: 1: 0.35

UV-vis (CH_2Cl_2): λ_{max} [nm] (abs.): 255(0.471), 314(0.259).

11.12. Synthesis of tricyclic (P-NEt$_2$)-bridged bis(NHCs) $14^{cis/trans}$

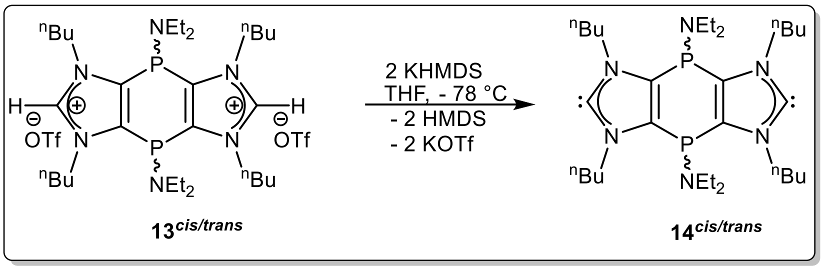

A solution of KHMDS in 5ml THF was added dropwise through a double-ended needle over 5 minutes to a solution of bis(imidazolium) salts **13**$^{cis/trans}$ in 10mL THF with continuous stirring at -78 ˚C. The reaction mixture was stirred for 1 h while warming up to -40 °C. The tetrahydrofuran was removed *in vacuo* (2×10^{-2} mbar), and the residue was dissolved with 20 mL of diethyl ether and *n*-pentane mixture (1:1.5) and the solid potassium triflate was removed via cannulation. The solvent was then dried *in vacuo* (2×10^{-2} mbar).

11.12.1. 4,8-Bis(diethylamino)-1,3,5,7-tetra-*n*-butyl-4,8-dihydro[1,4]diphosphinine[2,3-d:5,6-d']bis(imidazole-2,6-ylidene) ($14^{cis/trans}$)

Chemicals	Amounts(g or mL)	mmol
13$^{cis/trans}$	0.2 g	0.23
KHMDS	0.1 g	0.51
THF	5 mL	

Reaction code: NRN-176, NRN-281, NRN-516

Yield: 0.124 g (0.22mmol) 62 %; orange oily compound

Elemental composition: $C_{30}H_{56}N_6P_2$

Molecular weight: 562.77 g/mol

Elemental analysis: for $C_{30}H_{56}N_6P_2$:

Theor.	C	64.03	H	10.03	N	14.93
Exp.	C	63.24	H	9.30	N	13.83

MS (EI, 70 eV): *m/z* (%) = 563.4 (28) $[M+H]^{\cdot +}$, 483.1 (100) $[M\text{-}2NEt_2+H]^{\cdot +}$.

HR-MS: *m/z* = theor./exp. for $[C_{30}H_{56}N_6P_2]$: 563.4118/563.4116.

IR (ATR,ῦ{cm^{-1}}): ῦ = 2945 (m), 2889 (m), 2895 (m), 1320 (w), 1312 (w), 1298 (s), 1163 (m), 1123 (m), 1064 (m), 993 (s), 909 (s).

^{1}H NMR (300.1 MHz, THF,d$_8$, 25 °C): δ = 0.8 (br, 12H, P-NCH_2*Me*), 0.9 (br, 12H, $NCH_2CH_2CH_2$*Me*), 1.4- 1.5 (m, 8H, NCH_2CH_2*CH_2*Me), 1.8- 2.0 (m, 8H, NCH_2*CH_2*CH_2Me), 2.8- 3.3 (m, 8H, P-N*CH_2*Me), 4.0- 4.3 (m, 8H, N*CH_2*CH_2CH_2Me).

^{13}C{^{1}H} NMR (75.5 MHz, THF-d$_8$, 25 °C): δ = 13.2 (s, $NCH_2CH_2CH_2$*Me*), 13.4 (br, P-NCH_2*CH_3*), 19.7 (s, NCH_2CH_2*CH_2*Me), 20.2 (s, NCH_2CH_2*CH_2*Me; 2nd isomer), 29.6 (s, NCH_2*CH_2*CH_2Me), 31.1(s, NCH_2*CH_2*CH_2Me; 2nd isomer), 33.4 (t, $^2J_{P,C}$ = 2.11 Hz, P-N*CH_2*CH_3), 33.5 (t, $^2J_{P,C}$ = 2.11 Hz, P-N*CH_2*CH_3; 2nd isomer), 49.17 (t, $^3J_{P,C}$ = 2.69 Hz N*CH_2*CH_2CH_2Me), 50.0 (br, N*CH_2*CH_2CH_2Me) (2nd isomer), 131.5 (br, *P-C* of the middle ring), 132.1 (t, $^1J_{P,C}$ = 2.4 Hz, *P-C* of the middle ring; 2nd isomer), 220.2 (t, $^3J_{P,C}$ = 3.5 Hz, *C^2*).

^{31}P NMR (121.5 MHz, THF-d$_8$, 25 °C): δ = 6.6 (s) and 6.9 (s)

Isomer ratio: 1: 0.2

UV-vis (CH_2Cl_2): λ_{max} [nm] (abs.): 272(0.911), 348(0.671), 400(0.512).

11.13. Synthesis of tricyclic (P-NEt$_2$)-bridged bis(NHC) coinage metal complexes 15a-b$^{cis/trans}$

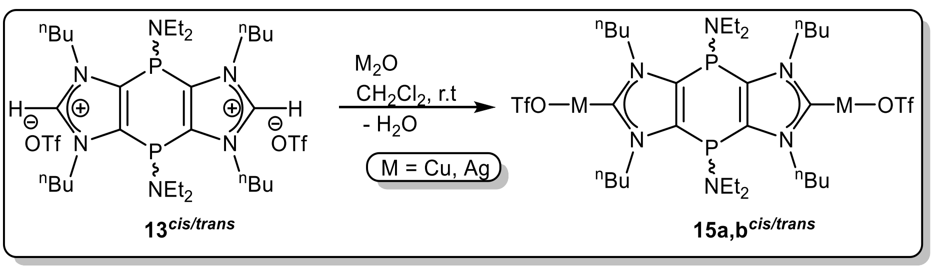

To a solution of bis(imidazolium) salts **13**$^{cis/trans}$ in 15 mL CH_2Cl_2, M_2O(M = Cu, Ag) (0.58 mmol)) was added as solid at – 30 °C temperature. The reaction mixture was stirred under darkness containing molecular sieves (to adsorb H_2O) for 8 h. The solution was then concentrated *in vacuo* (2 × 10^{-2} mbar). It was filtered over silica with methylene chloride to get light yellow solution. Solvent was evaporated *in vacuo* (2 × 10^{-2} mbar) followed by washing with *n*-pentane (2 × 5 mL) to get yellow solid.

10.13.1. [{4,8-Bis(diethylamino)-1,3,5,7-tetra-*n*-butyl-4,8-dihydro[1,4]diphosphinine[2,3-d:5,6-d']bis(imidazole-2,6-diylidene)-*κ*C,*κ*C}bis(copper(I)trifluoromethanesulfonate](15a $^{cis/trans}$)

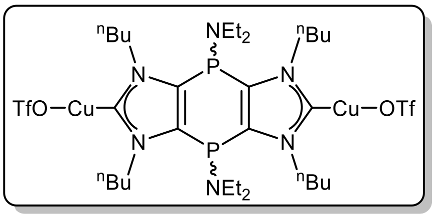

Chemicals	Amounts(g or mL)	mmol
13$^{cis/trans}$	0.5 g	0.58
Cu_2O	0.08 g	0.58
THF	15 mL	

<u>Reaction code</u>: NRN-215

<u>Yield</u>: 0.42 g (0.46 mmol) 71 %; yellow brown solid

<u>Melting point</u>: 84 °C

<u>Elemental composition</u>: $C_{32}H_{58}Cu_2F_6O_6N_6P_2S_2$

<u>Molecular weight</u>: 990.00 g/mol

<u>Elemental analysis</u>: for $C_{32}H_{58}Cu_2F_6O_6N_6P_2S_2$:

Theor.	C	38.82	H	5.91	N	8.49
Exp.	C	38.21	H	6.28	N	9.47

Pos. ESI-MS: *m/z* =theor. (exp.) for $[C_{33}H_{59}Cu_2F_3N_7O_3P_2S]^{\cdot+}$: 880.257 (880.257).

IR (ATR,ῦ{cm⁻¹}): ῦ = 2845 (m), 2812 (m), 2786.0 (m), 1504 (m), 1469 (s), 1268 (s), 1095 (s), 940 (m).

^{1}H NMR (300.1 MHz, CD_2Cl_2, 25 °C): δ = 1.0 (t, 12H, $^{3}J_{H,H}$ = 7.6 Hz, P-NCH_2*Me*), 1.1 (t, 12H, $^{3}J_{H,H}$ = 7.48 Hz, $NCH_2CH_2CH_2$*Me*), 1.4- 1.5 (m, 8H, NCH_2CH_2*CH_2*Me), 1.9- 2.1 (m, 8H, NCH_2*CH_2*CH_2Me), 3.1- 3.2 (m, 8H, P-N*CH_2*Me), 4.2-4.3 (m, 4H, N*CH_2*CH_2CH_2Me), 4.4- 4.5 (m, 4H, N*CH_2*CH_2CH_2Me; 2ndisomer)

^{13}C{^{1}H} NMR (75.5 MHz, CD_2Cl_2, 25 °C): δ = 12.9 (s, $NCH_2CH_2CH_2$*Me*), 13.0 (s, $NCH_2CH_2CH_2$*Me*; 2nd isomer), 13.5 (s, P-NCH_2*CH_3*), 13.8 (s, P-NCH_2*CH_3*; 2nd isomer), 19.9 (s, NCH_2CH_2*CH_2*Me), 20.0 (s, NCH_2CH_2*CH_2*Me; 2nd isomer), 29.6 (s, NCH_2*CH_2*CH_2Me), 29.6 (s, NCH_2*CH_2*CH_2Me; 2nd isomer), 34.9 (t, $^{2}J_{P,C}$ = 2.4 Hz, P-N*CH_2*CH_3), 37.9 (t, $^{2}J_{P,C}$ = 2.5 Hz, P-N*CH_2*CH_3), 51.9 (br, N*CH_2*CH_2CH_2Me), 119.4 (q,$^{1}J_{P,F}$ = 322.2 Hz, CF_3SO^{3-}), 132.0 (dt, $^{1}J_{P,C}$ = 15.5 Hz, $^{2}J_{P,C}$ = 7.2 Hz, *P-C* of the middle ring; 2nd isomer), 170.5 (t, $^{3}J_{P,C}$ = 2.8 Hz, *C^2*), 170.5 (t, $^{3}J_{P,C}$ = 2.8 Hz, *C^2*; 2nd isomer).

^{31}P NMR (121.5 MHz, CD_2Cl_2, 25 °C): δ = 5.1 (s) and 4.2 (s)

Isomer ratio: 1: 0.3

11.13.2 {4,8-Bis(diethylamino)-1,3,5,7-tetra-*n*-butyl-4,8-dihydro[1,4]diphosphinine[2,3-d:5,6-d']bis(imidazole-2,6-diylidene) κC,κC}bis(silver(I)trifluoromethanesulfonate)(15b$^{cis/trans}$)

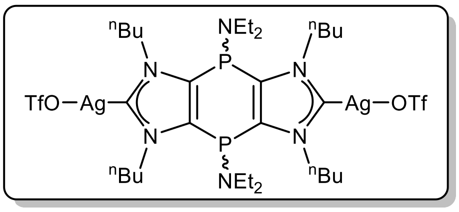

Chemicals	Amounts(g or mL)	mmol
13$^{cis/trans}$	0.5 g	0.58
Ag_2O	0.13 g	0.58
CH_2Cl_2	15 mL	

Reaction code: NRN-210

Yield: 0.39 g (0.36 mmol) 62 %; yellow brown solid

Melting point: 98 °C

Elemental composition: $C_{32}H_{58}Ag_2F_6O_6N_6P_2S_2$

Molecular weight: 1078.64 g/mol

Elemental analysis: for $C_{32}H_{58}Cu_2F_6O_6N_6P_2S_2$:

Theor.	C	35.63	H	5.42	N	7.79
Exp.	C	33.96	H	6.29	N	8.13

Pos. ESI-MS: *m/z* (%) =$C_{33}H_{59}Ag_2F_3N_7O_3P_2S^+$theor.(exp.) 968.208 (968.208).

IR (ATR,ῦ{cm^{-1}}): ῦ = 2991 (v), 2982.4 (m), 2876.0 (w), 1584.1 (w), 1532.9 (w), 1422.9 (s), 1384.7 (m), 1305.4 (m), 1299.9 (m), 1187.5 (s), 954.5 (s).

^{1}H NMR (300.1 MHz, $CDCl_3$, 25 °C): δ = 0.8 (t, 12H, $^3J_{H,H}$ = 7.7 Hz, P-NCH_2*Me*), 1.0 (t, 12H, $^3J_{H,H}$ = 7.6 Hz, $NCH_2CH_2CH_2$*Me*), 1.3- 1.4 (m, 8H, NCH_2CH_2*CH_2*Me), 1.9- 2.1 (m, 8H, NCH_2*CH_2*CH_2Me), 2.9- 3.1 (m, 8H, P-N*CH_2*Me), 4.1-4.2 (m, 4H, N*CH_2*CH_2CH_2Me), 4.2- 4.2 (m, 4H, N*CH_2*CH_2CH_2Me; 2ndisomer)

^{13}C{^{1}H} NMR (75.5 MHz, $CDCl_3$, 25 °C): δ = 13.4 (s, $NCH_2CH_2CH_2$*Me*), 13.4 (s, $NCH_2CH_2CH_2$*Me*; 2nd isomer), 13.9 (s, P-NCH_2*CH_3*), 14.0 (s, P-NCH_2*CH_3*; 2nd isomer), 20.3 (s, NCH_2CH_2*CH_2*Me), 20.3 (s, NCH_2CH_2*CH_2*Me; 2nd isomer), 29.7 (s, NCH_2*CH_2*CH_2Me), 31.9 (s, NCH_2*CH_2*CH_2Me; 2nd isomer), 47.8 (d, $^2J_{P,C}$ = 11.4 Hz, P-N*CH_2*CH_3), 48.8 (d, $^2J_{P,C}$ = 13.1 Hz, P-

N*CH*$_2$CH$_3$), 51.5 (br, N*CH*$_2$CH$_2$CH$_2$Me), 122.4 (q, $^{1}J_{P,F}$ = 324.2 Hz, CF$_3$SO^{3-}) 135.0 (dt, $^{1}J_{P,C}$ = 14.5 Hz, $^{2}J_{P,C}$ = 6.8 Hz, *P-C* of the middle ring), 179.1 (br, *C*^{2}).

^{31}P NMR (121.5 MHz, CDCl$_3$, 25 °C): δ = 3.7 (s), 3.3 (s)

Isomer ratio: 1: 0. 15

11.14. Synthesis of tricyclic (P-NEt2)-bridged bis(NHC) Au(I) complexes 15c$^{cis/trans}$

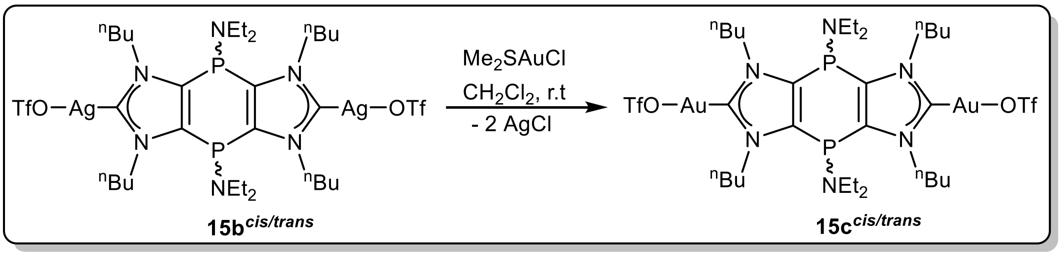

To a solution of **15b**$^{cis/trans}$in methylene chloride (2 mL), dimethyl sulfide gold (I) was added as solid at room temperature.The reaction mixture was stirred for 3 hours. Solvent was removed *in vacuo* (2 × 10^{-2} mbar), and the residue was dissolved in 5mL of diethyl ether and the solid AgCl was removed via filtering cannulation. The solvent was then dried *in vacuo*to get pure compound compound.

11.14.1. {4,8-Bis(diethylamino)-1,3,5,7-tetra-*n*-butyl-4,8-dihydro[1,4]diphosphinine[2,3-d:5,6-d']bis(imidazole-2,6-diylidene)-κC,κC}bis(gold(I)trifluoromethanesulfonate)(15c$^{cis/trans}$)

Chemicals	Amounts(g or mL)	mmol
15b$^{cis/trans}$	0.08 g	0.07
Me$_2$SAuCl	0.043 g	0.14
CH$_2$Cl$_2$	2 mL	

Reaction code: NRN-207

Yield: 0.061 g (0.05 mmol) 64 %; yellow brown solid

Melting point: 101 °C

Elemental composition: $C_{32}H_{58}Au_2F_6O_6N_6P_2S_2$

Molecular weight: 1256.64 g/mol

Elemental analysis: for $C_{32}H_{58}Au_2F_6O_6N_6P_2S_2$:

Theor.	C	30.58	H	4.65	N	6.69
Exp.	C	31.97	H	5.99	N	7.47

Pos. ESI-MS: *m/z* (%) =$[C_{33}H_{59}Au_2F_3N_7O_3P_2S]^+$ theor. (exp.) 1148.331 (1148.331).

IR (ATR,ῦ{cm⁻¹}): ῦ = 2992 (m), 2954 (m), 1623.0 (w), 1529.1 (m), 1461.5 (m), 1236.2 (s), 1201.3 (s), 1075.4 (m), 1032.2 (s), 974.0 (s).

^{1}H NMR (300.1 MHz, CD_2Cl_2, 25 °C): δ = 0.9 (t, 12H, $^3J_{H,H}$ = 7.7 Hz, P-NCH_2*Me*), 1.0 (t, 12H, $^3J_{H,H}$ = 7.6 Hz, $NCH_2CH_2CH_2$*Me*), 1.3- 1.5 (m, 8H, NCH_2CH_2*CH_2*Me), 1.9- 2.0 (m, 8H, NCH_2*CH_2*CH_2Me), 2.9- 3.1 (m, 8H, P-N*CH_2*Me), 4.2 (m, 4H, N*CH_2*CH_2CH_2Me), 4.3 (m, 4H, N*CH_2*CH_2CH_2Me; 2ndisomer).

$^{13}C\{^1H\}$ NMR (75.5 MHz, CD_2Cl_2, 25 °C): δ = 13.8 (s, $NCH_2CH_2CH_2$*Me*), 13.9 (s, $NCH_2CH_2CH_2$*Me*; 2nd isomer), 13.9 (s, P-NCH_2*CH_3*), 14.1 (s, P-NCH_2*CH_3*; 2nd isomer), 20.6 (s, NCH_2CH_2*CH_2*Me), 20.9 (s, NCH_2CH_2*CH_2*Me; 2nd isomer), 29.8 (s, NCH_2*CH_2*CH_2Me), 30.9 (s, NCH_2*CH_2*CH_2Me; 2nd isomer), 49.8 (d, $^2J_{P,C}$ = 12 Hz, P-N*CH_2*CH_3), 51.2 (d, $^2J_{P,C}$ = 14 Hz, P-N*CH_2*CH_3), 52.3 (br, N*CH_2*CH_2CH_2Me), 125.4 (q,$^1J_{P,F}$ = 323.1 Hz, CF3SO^{3-}) 133.1 (dt, $^1J_{P,C}$ = 14.0 Hz, $^2J_{P,C}$ = 6.9 Hz, *P-C* of the middle ring), 172.1 (t, $^3J_{P,C}$ = 2.6 Hz, *C^2*), 172.3 (t, $^3J_{P,C}$ = 2.6 Hz, *C^2*; 2nd isomer).

^{31}P NMR (121.5 MHz, CD_2Cl_2, 25 °C): δ = 3.1 (s) and 2.4 (s)

Isomer ratio: 1: 0.35

10.15. Synthesis of tricyclic {P-NEt2}-bridged bis(NHC) Rh(I) complexes 15d*cis/trans*

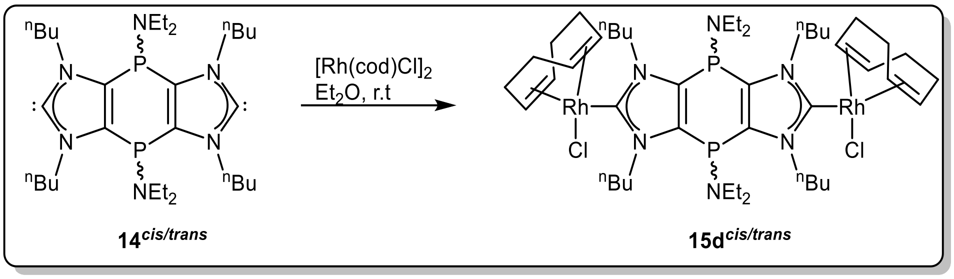

To a solution of **14***cis/trans*, in diethyl ether, [Rh(cod)Cl] dimer was added as solid at room temperature. The reaction mixture was stirred overnight. Precipitates formed which were filtered using filtering cannula. Solid was dried in *vacuo* (2×10^{-2} mbar), and the residue was washed with *n*-pentane thrice (3 ×5mL). Finaly, solvent was then dried in *vacuo* (2×10^{-2} mbar) to ge pure solid

10.15.1. {4,8-Bis(diethylamino)-4,8-dioxo-1,3,5,7-tetra-*n*-butyl-4,8-dihydro[1,4]diphosphinine[2,3-d:5,6-d']-bis(imidazole-2,6-diylidene)-κC,κC}bis((1,2,5,6-η^4)-1,5-cyclooctadiene)trifluoromethanesulfonaterhodium(I)(15d*cis/trans*)

Chemicals	Amounts(g or mL)	mmol
14*cis/trans*	1.0 g	1.8
$[Rh(cod)Cl]_2$	0.9 g	1.8
Et_2O	10 mL	

<u>Reaction code</u>: NRN-517

<u>Yield</u>: 1.2 g (1.1 mmol) 63 %; yellow brown colored solid.

<u>Melting point</u>: 134 °C

<u>Elemental composition</u>: $C_{46}H_{82}Cl_2Rh_2N_6P_2$

<u>Molecular weight</u>: 1057.86 g/mol

Pos. ESI-MS: *m/z* (%) = $[C_{48}H_{83}Rh_2ClN_7P_2]^{+\cdot}$ theor. (exp.) 1060.3989 (1060.3975).

IR (ATR,ῦ{cm⁻¹}): ῦ = 2816 (m), 2790 (m), 2754 (w), 1504 (w), 1464 (w), 1388 (s), 1226 (m), 1066 (m), 1028 (m), 976 (s).

^{1}H NMR (300.1 MHz, CD_2Cl_2, 25 °C): δ = 0.9 (t, 12H, $^{3}J_{H,H}$ = 7.4Hz, P-NCH_2*Me*), 1.1 (t, 12H, $^{3}J_{H,H}$ = 7.5 Hz, $NCH_2CH_2CH_2$*Me*), 1.3- 1.4 (m, 8H, NCH_2CH_2*CH_2*Me), 1.7 (br, 4H, cod), 2.1 (br, 8H, NCH_2*CH_2*CH_2Me), 2.4 (br, 4H, cod), 3.4 (m, 8H, P-N*CH_2*Me), 3.5 (m, 2H, cod), 4.4 (m, 8H, N*CH_2*CH_2CH_2Me), 5.3 (m, 2H, cod).

^{13}C{^{1}H} NMR (75.5 MHz, CD_2Cl_2, 25 °C): δ = 13.1 (s, $NCH_2CH_2CH_2$*Me*), 13.3 (s, $NCH_2CH_2CH_2$*Me*; 2nd isomer), 14.8 (s, P-NCH_2*CH_3*), 20.1 (s, NCH_2CH_2*CH_2*Me), 20.6 (s, NCH_2CH_2*CH_2*Me; 2nd isomer), 25.7 (s, cod), 31.5 (s, NCH_2*CH_2*CH_2Me),32.4 (s, cod), 33.1 (s, NCH_2*CH_2*CH_2Me; 2nd isomer), 36.5 (s, P-N*CH_2*CH_3), 38.2 (s, P-N*CH_2*CH_3), 51.9 (br, N*CH_2*CH_2CH_2Me),72.3 (d, $^{1}J_{Rh,C}$ = 14.6 Hz, cod), 98.4 (d, $^{1}J_{Rh,C}$ = 6.7 Hz, cod), 129.9 (br, *P-C* of the middle ring), 130.9 (br, *P-C* of the middle ring; 2nd isomer), 190.3 (ddd, $^{1}J_{C,Rh}$ = 50.7 Hz, $^{3}J_{P,C}$ = 3.6 Hz, C^2), 190.5 (ddd, $^{1}J_{C,Rh}$ = 50.7 Hz, $^{3}J_{P,C}$ = 3.6 Hz, C^2; 2nd isomer).

^{31}P NMR (121.5 MHz, CD_2Cl_2, 25 °C): δ = 3.7 (s), 4.6 (s)

Isomer ratio: 1: 0.65

11.16. Synthesis of tricyclic (P-NEt_2)-bridged bis(NHC) borane complexes 16$^{cis/trans}$

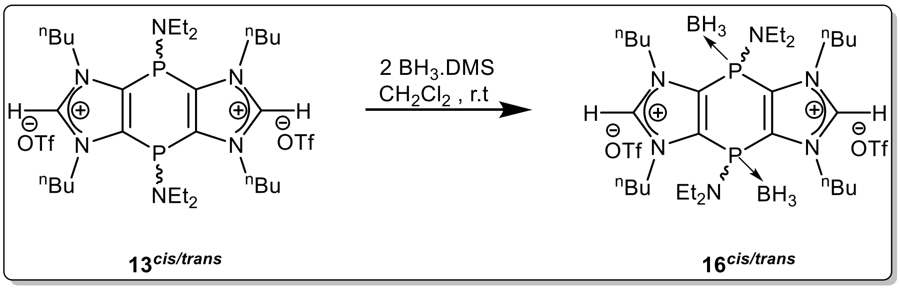

To a solution of **13**$^{cis/trans}$ in methylene chloride (10 mL), the dimethylsulfane boron-adduct was added at room temperature. The reaction mixture was stirred for 3 hours at the same temperature. Solvent was removed *in vacuo* (2×10^{-2} mbar), and the residue was washed with *n*-pentane (3 × 5 mL). Finally, an orange-yellow solid was obtained as pure compound.

11.16.1. {4,8-Bis(diethylamino)-1,3,5,7-tetra-*n*-butyl-4,8-dihydro[1,4]diphosphinine[2,3-d:5,6-d']bis(imidazole-2,6-ium-4,6-diborane}-bis(trifluoromethanesulfonate) ($16^{cis/trans}$)

Chemicals	Amounts(g or mL)	mmol
13$^{cis/trans}$	1.0 g	1.15
$BH_3{\cdot}(CH_3)_2S$	0.2 mL	2.3
CH_2Cl_2	20 mL	

Reaction code: NRN-539

Yield: 0.91 g (1.0 mmol) 88 %; orange solid

Melting point: 78 °C

Elemental composition: $C_{32}H_{64}B_2F_6O_6N_6P_2S_2$

Molecular weight: 890.6 g/mol

Pos. ESI-MS: *m/z* (%) = 593.494 (100) $[M]^+$
Neg. ESI-MS: *m/z* (%) = 149.3 (100) $[OTf]^+$

HR-MS: $[C_{30}H_{65}N_6P_2B_2]^+$ calcd (found) 593.4929 (593.4935).

IR (ATR,ῦ{cm^{-1}}): ῦ = 2964 (v), 2930 (m), 2894 (m), 1598 (w), 1509 (w), 1423 (m), 1184 (m), 1101 (w), 1051 (m), 1001 (v), 945 (s).

^{1}H NMR (300.1 MHz, CD_2Cl_2, 25 °C): δ = 0.9 (t, 12H, $^3J_{H,H}$ = 7.7 Hz, P-NCH_2*Me*), 1.0 (t, 12H, $^3J_{H,H}$ = 7.6 Hz, $NCH_2CH_2CH_2$*Me*), 1.3- 1.4 (m, 8H, NCH_2CH_2*CH_2*Me), 1.9- 2.0 (m, 8H, NCH_2*CH_2*CH_2Me), 2.9- 3.1 (m, 8H, P-N*CH_2*Me), 4.2-4.3 (m, 4H, N*CH_2*CH_2CH_2Me), 4.3 (m, 4H, N*CH_2*CH_2CH_2Me; 2ndisomer).

^{13}C{^{1}H} NMR (75.5 MHz, CD_2Cl_2, 25 °C): δ = 13.8 (s, $NCH_2CH_2CH_2$*Me*), 13.9 (s, $NCH_2CH_2CH_2$*Me*; 2nd isomer), 13.9 (s, P-NCH_2*CH_3*), 14.1 (s, P-NCH_2*CH_3*; 2nd isomer), 20.6 (s, NCH_2CH_2*CH_2*Me), 20.9 (s, NCH_2CH_2*CH_2*Me; 2nd isomer), 29.8 (s, NCH_2*CH_2*CH_2Me), 30.9 (s, NCH$_2$<u>*CH$_2$*</u>CH$_2$Me; 2nd isomer), 49.8 (d, $^2J_{P,C}$ = 12 Hz, P-N<u>*CH$_2$*</u>CH$_3$), 51.1 (d, $^2J_{P,C}$ = 14 Hz, P-N<u>*CH$_2$*</u>CH$_3$), 52.3 (br, N<u>*CH$_2$*</u>CH$_2$CH$_2$Me), 125.4 (q,$^1J_{P,F}$ = 323.1 Hz, CF3SO^{3-}) 133.1 (dt, $^1J_{P,C}$ = 14.0 Hz, $^2J_{P,C}$ = 6.9 Hz, <u>*P-C*</u> of the middle ring), 172.1 (t, $^3J_{P,C}$ = 2.6 Hz, <u>*C^2*</u>), 172.3 (t, $^3J_{P,C}$ = 2.6 Hz, <u>*C^2*</u>; 2nd isomer).

<u>^{31}P NMR (121.5 MHz, CD$_2$Cl$_2$, 25 °C)</u>: δ = 3.1 (s), 2.7 (s)

<u>Isomer ratio</u>: 1: 0.1

<u>^{11}B NMR (96.29 MHz, CDCl$_3$, 25 °C)</u>: - 37.0 (br) ppm

11.17. Synthesis of tricyclic 1,4-diphosphinine-diselone 19

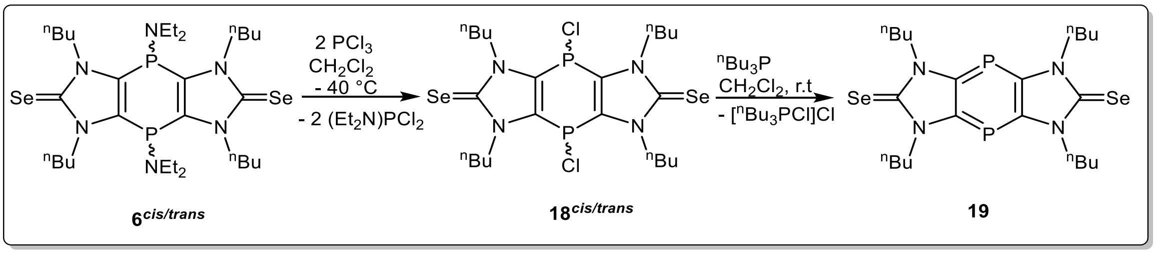

Toa clear solution of**6**$^{cis/trans}$inmethylene chloride, PCl$_3$ was added and stirred for 4 hours at – 40 °C. Reaction mixture was warmed to room temperature and tris(*n*-butyl)phosphane was added dropwise to it.After 10 minutes stirring, a changeof the solution from orangetoviolet was observed.After concentrating the reaction mixture under reduced pressure, residue was filtered via a silica® bed with diethyl ether and toluene mixture (1:1). It was dried under reduced pressure (2 × 10^{-2} mbar and washed with *n*-pentane (3 ×10 mL) to get rid of the aminophosphine Et$_2$NPCl$_2$. Finally, the solution was concentrated *in vacuo* (2 × 10^{-2} mbar) to get the pure compound.

11.17.1. {1,3,5,7-Tetra-*n*-butyl-[2,3-d:5,6-d']bis(imidazole-2,6-diselone)-4,8-[1,4]diphosphinine (19)

Chemicals	Amounts(g or mL)	mmol
6$^{cis/trans}$	2.5 g	3.4
PCl$_3$	0.61 mL	6.9
^{n}Bu$_3$P	0.34 mL	1.4
CH$_2$Cl$_2$	30 mL	

Reaction code: NRN-174, NRN-443

Yield: 1.2 g (2.1 mmol) 61 %; violet solid

Melting point: 223 °C

Elemental composition: $C_{22}H_{36}N_4P_2Se_2$

Molecular weight: 576.47 g/mol

Elemental analysis: for $C_{22}H_{36}N_4P_2Se_2$:

Theor.	C	45.84	H	6.30	N	9.72
Exp.	C	45.05	H	6.55	N	9.61

MS (EI, 70 eV): *m/z* (%) = 578.0 (100) $[M]^+$, 498.1 (20) $[M\text{-}Se]^+$.

IR (ATR,ῦ{cm^{-1}}): ῦ = 2998 (v), 2752.8 (m), 2654.0 (m), 1487.0 (s), 1289.1 (s), 1201.5 (s), 1098.2 (m), 964.0 (s).

^{1}H NMR (300.1 MHz, C_6D_6, 25 °C): δ = 0.8 (t, 12H, $^3J_{H,H}$ = 7.3 Hz, $NCH_2CH_2CH_2$*Me*), 1.3- 1.4 (m, 8H, NCH_2CH_2*CH_2*Me), 1.8- 1.9 (m, 8H, NCH_2*CH_2*CH_2Me), 4.4-4.5 (m, 8H, N*CH_2*CH_2CH_2Me).

^{13}C{^{1}H} NMR (75.5 MHz, C_6D_6, 25 °C): δ = 13.5 (s, $NCH_2CH_2CH_2$*Me*), 19.9 (s, NCH_2CH_2*CH_2*Me), 28.9 (t, $^3J_{P,C}$ = 1.6 Hz, NCH_2*CH_2*CH_2Me), 48.2 (t, $^3J_{P,C}$ = 4.6 Hz, NCH_2*CH_2*CH_2Me), 152.3 (t,$^1J_{P,C}$=23.1 Hz,P-*C*ofthemiddle ring), 168.3 (br, *C^2*).

^{31}P NMR (121.5 MHz, C_6D_6, 25 °C): δ = 78.2 (s).

^{77}SeNMR (57.28 MHz, $CDCl_3$): 178.6 (t, $^4J_{Se,P}$ = 12.1 Hz)

UV/vis λ_{max} [nm] (abs.): 296 (1.375), 383 (0.156), 554(0.139).

11.18. Double Se-methylation of tricyclic1,4-diphosphinine diselone 19

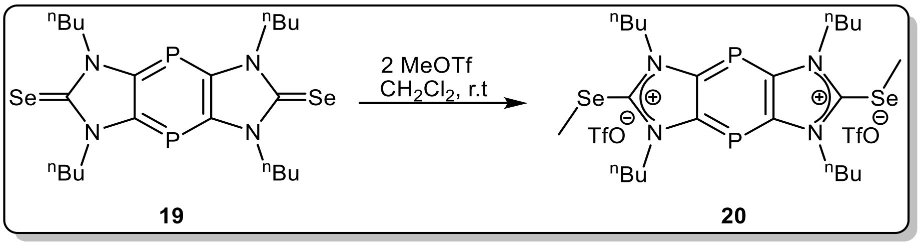

Trifluoromethanesulfonate was added toasolution of**19**inmethylene chloride, at room temperature.Thereactionmixturewasstirredfor 1 hours. Change in color was observed from violetto light yellow at the end of reaction.After concentrating the reaction mixture under reduced pressure, residue was washed with *n*-pentane/diethylether (1:1) (2 × 5 mL) to get pure light yellow colored solid.

11.18.1 {1,3,5,7-Tetra-*n*-butyl-[1,4]diphosphinine[2,3-d:5,6-d']bis(imidazole-2,6-selanylium)}bis(trifluoromethanesulfonate)(20)

Chemicals	Amounts(g or mL)	mmol
19	0.1g	0.17
MeOTf	0.04mL	0.34
CH_2Cl_2	5 mL	

<u>Reaction code</u>: NRN-412, NRN-463

<u>Yield</u>: 0.14 g (0.15 mmol) 91 %; light yellow solid

<u>Melting point</u>: 96 °C

<u>Elemental composition</u>: $C_{26}H_{46}F_6N_4O_6P_2S_2Se_2$

<u>Molecular weight</u>: 904.62 g/mol

Elemental analysis: for $C_{26}H_{46}F_6N_4O_6P_2S_2Se_2$:

Theor.	C	34.52	H	4.68	N	6.19
Exp.	C	34.11	H	4.63	N	5.97

Pos. ESI-MS: m/z = theor. (exp.) for $[C_{25}H_{42}F_3N_4O_3P_2S_2Se_2]^+$: 757.0728 (757.0750).

IR (ATR,ṽ{cm^{-1}}): ṽ = 3009 (v), 2992 (m), 2954 (m), 1623 (w), 1529 (w), 1461 (m), 1236 (m), 1201 (w), 1075 (m), 1032 (v), 974 (s).

^{1}H NMR (300.1 MHz, $CDCl_3$, 25 °C): δ = 1.04(t, 12H, $^3J_{H,H}$ = 7.4 Hz, $NCH_2CH_2CH_2$*Me*), 1.52-1.62 (m, 8H, NCH_2CH_2*CH_2*Me), 2.05- 2.15 (m, 8H, NCH_2*CH_2*CH_2Me),2.76 (s, 6H, Se*Me*) 4.89-4.94 (m, 8H, N*CH_2*CH_2CH_2Me).

^{13}C{^{1}H} NMR (75.5 MHz, $CDCl_3$, 25 °C): δ = 11.7 (s, Se*Me*), 13.4 (s, $NCH_2CH_2CH_2$*Me*), 20.1 (s, NCH_2CH_2*CH_2*Me), 30.7 (s, NCH_2*CH_2*CH_2Me), 52.2 (s, NCH_2*CH_2*CH_2Me), 148.8 (t, $^3J_{P,C}$ = 4.6 Hz Se-*C^2*),154.9 (t,$^1J_{P,C}$=26.1 Hz,P-*C*ofthemiddle ring).

^{31}P NMR (121.5 MHz, $CDCl_3$, 25 °C): δ = 119.9(s).

^{77}SeNMR (57.28 MHz, $CDCl_3$): 138.8 (s)

11.19 Reductive deselenization of double Se-methylated salt 20

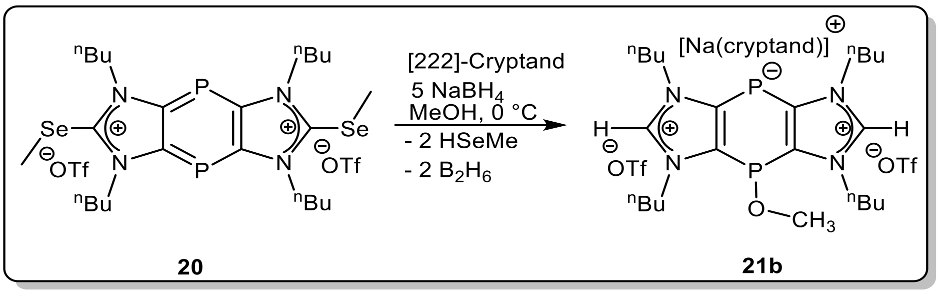

To a methanolic solution of **20** an excess of sodium tetraborohydrideand one equivalent of [2.2.2]-cryptand was added as solid at 0 °C. The reaction mixture turned from light yellow to orange-red and astrong odour was recognized indicating the liberation of methylselane (HSeMe). The solution was then concentrated *in vacuo* (2×10^{-2} mbar) after 30 minutes stirring.Extraction was done with methylene chloride followed by washing with diethyl ether (2 × 5 mL) to get a pure orange-red solid.

11.19.1. Sodium([2.2.2]-cryptand){4-methoxy-8-phosphan-1-ide-1,3,5,7-tetra-*n*-butyl-[2,3-d:5,6-d']bis(imidazole-2,6-ium}bis(trifluoromethanesulfonate) (21b)

Chemicals	Amounts(g or mL)	mmol
20	1.0g	0.9
$NaBH_4$	0.17 g	4.7
[2.2.2]-cryptand	0.34 g	0.9
MeOH	30mL	

Reaction code: NRN-533

Yield: 0.65 g (0.56 mmol) 63 %; orange-red solid

Melting point: 142 °C

Elemental composition: $[C_{25}H_{41}F_6N_4O_7P_2S_2]^-[Na(C_{18}N_2H_{36}O_6)]^+$

Molecular weight: 1149.26 g/mol

Elemental analysis: for $C_{43}H_{77}F_6NaN_6O_{13}P_2S_2$:

Theor.	C	44.94	H	6.75	N	7.31	S	5.58
Exp.	C	43.27	H	6.63	N	6.48	S	5.49

Pos. ESI-MS: *m/z* (%) = 451.3 (100) $[M]^{\cdot+}$, 399.1 (97) $[Na(C_{18}N_2H_{36}O_6)]^{\cdot+}$

HRMS: $[C_{23}H_{41}N_4OP_2]^+$ calcd (found) 451.2750 (451.2754).

IR (ATR,ῦ{cm⁻¹}): ῦ = 2984 (v), 2921 (m), 2894 (m), 1542 (w), 1498 (w), 1423 (m), 1246 (m), 1206 (w), 1012 (m), 968 (s).

^{1}H NMR (300.1 MHz, CD_2Cl_2, 25 °C): δ = 1.0 (t, 12H, $^3J_{H,H}$ = 7.3 Hz, $NCH_2CH_2CH_2$*Me*), 1.3- 1.5 (m, 8H, NCH_2CH_2*CH_2*Me), 1.9- 2.1 (m, 8H, NCH_2*CH_2*CH_2Me),2.4 (d, 3H, $^3J_{P,H}$ = 7.3 Hz, O-

Me)2.6 (t, 12H, cryptand), 3.6 (t, 12H, cryptand), 3.7 (s, 12H, cryptand), 4.1-4.6 (m, 8H, N*CH₂*CH₂CH₂Me), 8.9 (t, 2H, $^4J_{P,H}$ = 1.7 Hz, C^2-*H*).

$^{13}C\{^1H\}$ NMR (75.5 MHz, CD_2Cl_2, 25 °C): δ = 13.2 (s, $NCH_2CH_2CH_2$*Me*), 19.6 (s, NCH_2CH_2*CH_2*Me), 30.2 (s, NCH_2*CH_2*CH_2Me), 47.8 (s, N*CH_2*CH_2CH_2Me), 67.5 (s, Cryptand), 68.5 (s, Cryptand), 120.9 (d, $^2J_{P,C}$= 7.3 Hz, O-*CH_3*), 121.7 (q, $^1J_{P,F}$ = 321.0 Hz, *C*F_3), 137.2 (d, $^3J_{P,C}$ = 4.5 Hz H-*C^2*), 155.5 (ddd,$^{1/2}J_{P,C}$ = 47.0 Hz,*$C^{4/5}$*).

^{31}P NMR (121.5 MHz, CD_2Cl_2, 25 °C):δ = 19.8(s), - 67.3(s).

11.20 Synthesis of tricyclic P-functional anionic bis(NHC) 22b

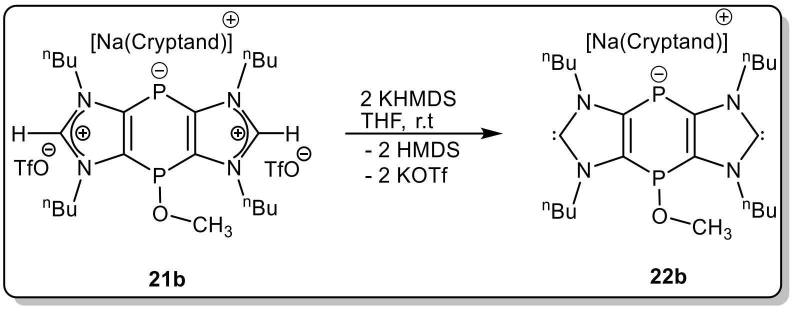

A solution of potassium hexamethyldisilazide (KHMDS) in 5mL of THF was added dropwise to a solution of **21b** in 10 mL of THF at -78 °C. After 1 h, all volatiles were removed in *vacuo* (2×10^{-2} mbar). Residue was washed (twice) with diethyl ether followed by extraction with mixture of THF and diethyl ether to remove potassium triflate. After concentrating extracted solution, a dark orange solid was obtained.

11.20.1 Sodium([222]-cryptand)[4-methoxy-8-phosphan-1-ide-1,3,5,7-tetra-*n*-butyl-[2,3-d:5,6-d']bis(imidazole-2,6-ylidene)] (22b)

Chemicals	Amounts(g or mL)	mmol
21b	2 g	1.7
KHMDS	0.67 g	3.4
THF	40 mL	

Reaction code: NRN-483

Yield: 1.1 g (1.3 mmol) 76 %; orange brown solid

Melting point: 126°C

Elemental composition: $C_{41}H_{75}N_6O_7P_2S_2Na$

Neg. ESI-MS: *m/z* (%) = 449.261 (15) $[M]^{+\cdot}$

HRMS: $[C_{23}H_{39}N_4OP_2]^-$ calcd (found) 449.2605 (449.2608).

IR (ATR,ṽ{cm^{-1}}): ṽ = 3191.2 (w), 3045.0 (m), 2975.7 (m), 1623.4 (m), 1436.3 (m), 1375.3 (m), 1245.7 (s), 1184.8 (s), 1016.5 (S), 968.5 (s)

^{1}H NMR (300.1 MHz, THF-d$_8$, 25 °C): δ = 0.9 (t, 12H, $^3J_{H,H}$ = 6.5 Hz, $NCH_2CH_2CH_2\underline{Me}$), 1.2-1.3 (m, 8H, $NCH_2CH_2\underline{CH_2}Me$), 1.8- 1.9 (m, 8H, $NCH_2\underline{CH_2}CH_2Me$),2.1 (d, 3H, $^4J_{P,H}$ = 6.3 Hz, O-$\underline{Me}$)2.5 (t, 12H, cryptand), 3.5 (t, 12H, cryptand), 3.6 (s, 12H, cryptand), 3.8-4.5 (m, 8H, $N\underline{CH_2}CH_2CH_2Me$).

^{13}C{^{1}H} NMR (75.5 MHz, THF-d$_8$, 25 °C):δ = 13.5 (s, $NCH_2CH_2CH_2\underline{Me}$), 20.1 (s, $NCH_2CH_2\underline{CH_2}Me$), 32.3 (s, $NCH_2\underline{CH_2}CH_2Me$), 47.5 (s, $N\underline{CH_2}CH_2CH_2Me$), 67.6 (s, Cryptand), 70.4 (s, Cryptand),120.2 (d, $^2J_{P,C}$= 7.5 Hz, O-$\underline{CH_3}$), 154.2 (d,$^{1/2}J_{P,C}$ = 43.9 Hz,$\underline{C^{4/5}}$), 215.5(d, $J_{P,C}$ = 2.7, $\underline{C^2}$).

^{31}P NMR (500.0 MHz, THF-d$_8$, 25 °C): δ = 23.9 (s), - 75.8(s).

UV-vis (THF): λ_{max}[nm] (abs.): 407(0.517)

11.21. Reaction of anionic bis(imidazolium) salt with CH_3I

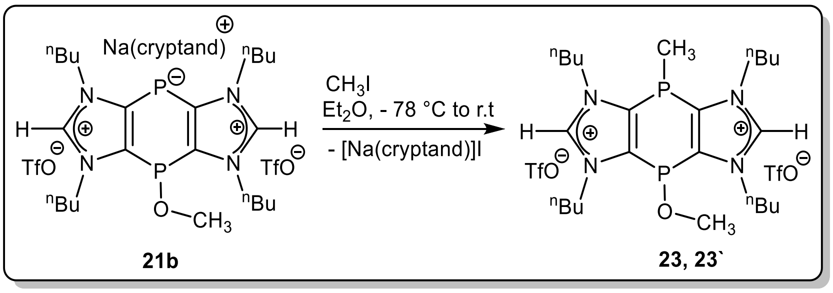

To a suspension solution of **21b** (NRN-533) in diethyl ether, methyl iodide was added dropwise at -78 °C. Reaction mixture was stirred for 18 h and warmed to room temperature. All volatiles were removed in *vacuo* (2×10^{-2} mbar). Residue was extracted with methylene chloride followed by washing (twice) with 20 mL of diethyl ether. Solvent was removed under *vacuo* (2×10^{-2} mbar) and resulted in a pure white oily product.

11.21.1. 4-Methyl-8-methoxy-1,3,5,7-tetra-*n*-butyl-4,8-dihydro[1,4]diphosphinine[2,3-d:5,6d'] bis(imidazole-2,6-ium)}bis(trifluoromethane sulfonate) (23, 23′)

Chemicals	Amounts(g or mL)	mmol
21b	2.5 g	2.1
CH_3I	1.35 mL	2.1
Et_2O	50 mL	

Reaction code: NRN-534

Yield: 1.2 g (1.6 mmol) 75 %; colorless liquid

Elemental composition: $C_{26}H_{44}F_6N_4O_7P_2S_2$

Molecular weight: 764.2 g/mol

Elemental analysis: for $C_{26}H_{44}F_6N_4O_7P_2S_2$:

Theor.	C	40.84	H	5.80	N	7.33
Exp.	C	39.95	H	6.00	N	7.41

Pos. ESI-MS: *m/z* (%) = 615.251 (54) $[M\text{-}TfO]^{+\cdot}$

HRMS: $[C_{25}H_{44}F_3N_4O_4P_2S_2]^{+\cdot}$ calcd (found) 615.2505 (615.2511).

IR (ATR,ṽ{cm^{-1}}): ṽ = 3204 (m), 3145 (m), 2975 (w), 2768 (m), 1534 (w), 1445 (s), 1317 (m), 1206 (m), 1046 (m), 1009 (s), 921 (s).

^{1}H NMR (300.1 MHz, CD_2Cl_2, 25 °C): δ = 1.1 (t, 12H, $^3J_{H,H}$ = 7.4 Hz, $NCH_2CH_2CH_2$*Me*), 1.4-1.5 (m, 8H, PCH_2CH_2*CH_2*Me), 1.7 (d, $^2J_{P,H}$ = 5.2 Hz, *P-Me*), 1.8 (d, $^2J_{P,H}$ = 6.8 Hz, *O-Me*), 1.9-2.1 (m, 8H, $NCH_2\underline{CH_2}CH_2Me$, 4.3-4.6 (m, 8H, $N\underline{CH_2}CH_2CH_2Me$), 9.5(t, 2H, $^3J_{P,H}$ = 3.03 Hz, C^2-$\underline{H}$), 9.6 (br, C^2-$\underline{H}$; 2nd isomer).

$^{13}C\{^1H\}$ NMR (75.5 MHz, CD_2Cl_2, 25 °C): δ = 13.1 (s, $NCH_2CH_2CH_2\underline{Me}$), 19.5 (br,*P-Me*), 19.7 (s, $NCH_2CH_2\underline{CH_2}Me$), 29.7 (br, $NCH_2\underline{CH_2}CH_2Me$), 31.8 (d, $^3J_{P,C}$ = 2.6 Hz, $NCH_2\underline{CH_2}CH_2Me$), 32.2 (d, $^3J_{P,C}$ = 2.4 Hz, $NCH_2\underline{CH_2}CH_2Me$; 2nd isomer), 49.1(ddd, $^3J_{P,C}$ = 9.1 Hz, $N\underline{CH_2}CH_2CH_2Me$), 49.9 (ddd, $^3J_{P,C}$ = 8.2Hz, $N\underline{CH_2}CH_2CH_2Me$; 2nd isomer), 122.8 (q, $^1J_{P,F}$ = 319.5 Hz, $\underline{C}F_3$), 131.5 (d, $^2J_{P,C}$= 9.5 Hz, O-$\underline{CH_3}$), 135.4 (ddd, $^{1/2}J_{P,C}$ = 3.7 Hz, *P-C*of the middle ring), 135.7 (t, $^{1/2}J_{P,C}$ = 3.0 Hz, *P-C*of the middle ring; 2ndisomer), 142.4 (br, H-$\underline{C^2}$), 143.4 (br, H-$\underline{C^2}$; 2nd isomer).

^{31}P NMR (500.0 MHz, CD_2Cl_2, 25 °C): δ = -71.6(d, $^3J_{P,H}$ = 5.2 Hz, *P-Me*),- 66.2(d, $^3J_{P,H}$= 4.9Hz, *P-Me*; 2nd isomer), 39.7 (br, *P-OMe*), 43.7 (br, *P- OMe*;2nd isomer).

Isomer ratio: 1: 0.3

11.22 Synthesis of {*P*-Me}-/{*P*-OMe}-bridged bis(NHC) 24,24′

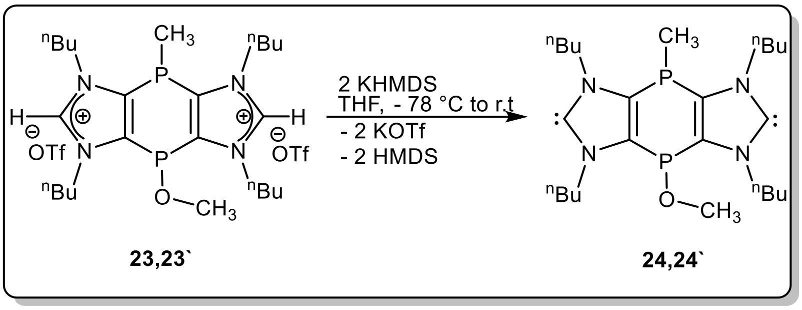

A pre-cooled solution (-78°C) of potassium hexamethyldisilazide (KHMDS) in 5 mL of THF was added dropwise to a solution of **23, 23`**in 10 mL of THF at - 78 °C. After 1 h, all volatiles were removed in *vacuo* (2×10^{-2} mbar). Residue was extracted with diethyl ether to remove potassium triflate using filtering cannulation. After extraction with *n*-pentane, removal of the solvent in *vacuo* (2×10^{-2} mbar), a yellow liquid was obtained.

11.22.1 4-Methyl-8-methoxy-1,3,5,7-tetra-*n*-butyl-4,8-dihydro[1,4]diphosphinine[2,3-d:5,6d']bis(imidazole-2,6-ylidene) (24, 24′)

Chemicals	Amounts(g or mL)	mmol
23,23′	0.078g	0.1
KHMDS	0.043 g	0.2
THF	4 mL	

Reaction code: NRN-347, NRN-503, NRN-487

Yield: 0.035 g (0.075 mmol) 75 %; yellow liquid

Elemental composition: $C_{24}H_{42}N_4OP_2$

Molecular weight: 464.3 g/mol

Pos. ESI-MS: m/z (%) = 465.290 (12) $[M+H]^{\cdot+}$

HRMS: $[C_{24}H_{43}N_4OP_2]^+$ calcd (found) 465.2907 (465.2909).

IR (ATR,ṽ{cm⁻¹}): ṽ = 3204.7 (m), 3145 (m), 2975.5 (w), 2768.8 (m), 1534.3 (w), 1445.3 (s), 1317.7 (m), 1206.8 (m), 1046.9 (m), 1009.5 (s), 921.5 (s).

^{1}H NMR (500.1 MHz, THF-d$_8$, 25 °C): δ = 0.8, 1.1 (t, 12H, $^3J_{H,H}$ = 7.1 Hz, $NCH_2CH_2CH_2$*Me*),1.2 (d, $^2J_{P,H}$ = 5.3 Hz, *P-Me*), 1.2-1.4 (m, 8H, PCH_2CH_2*CH_2*Me), 1.9-2.1 (m, 8H, NCH_2*CH_2*CH_2Me), 2.7 (d, $^2J_{P,H}$ = 7.2 Hz, *O-Me*), 3.9-4.2 (m, 8H, N*CH_2*CH_2CH_2Me), 4.3-4.5 (m, 8H, N*CH_2*CH_2CH_2Me; 2nd isomer).

^{13}C{^{1}H} NMR (125.75 MHz, THF-d$_8$, 25 °C): δ = 12.9,12.8 (s, $NCH_2CH_2CH_2$*Me*of two isomers), 19.9 (s,*P-Me*), 23.7 (s, NCH_2CH_2*CH_2*Me), 25.7 (s, NCH_2*CH_2*CH_2Me), 32.8 (d, $^3J_{P,C}$ = 2.1 Hz, NCH_2*CH_2*CH_2Me), 32.9 (d, $^3J_{P,C}$ = 2.2 Hz, NCH_2*CH_2*CH_2Me; 2ndisomer), 48.5(ddd, $^3J_{P,C}$ = 9.6 Hz, N*CH_2*CH_2CH_2Me), 49.6 (ddd, $^3J_{P,C}$ = 8.3 Hz, N*CH_2*CH_2CH_2Me; 2nd isomer), , 118.5 (d, $^2J_{P,C}$= 9.2 Hz, O-*CH_3*), 131.4 (br, *P-C*of the middle ring), 132. 2 (d, $^{1/2}J_{P,C}$ = 2.5 Hz, *P-C*of the middle ring; 2nd isomer), 223.4 (t, $^3J_{P,C}$ = 2.7 Hz,*C^2*), 224.2(t, $^3J_{P,C}$ = 2.7 Hz, *C^2*; 2nd isomer).

<u>^{31}P NMR (500.0 MHz, THF-d_8, 25 °C)</u>: δ = 41.3 (d, *J* = 3.8 Hz, *P-OMe*), 37.2(d, *J* = 4.6.Hz, *P-OMe;* 2nd isomer), -68.6 (d, *J* = 3.7 Hz, *P-Me*),-74.0 (d, *J* = 4.8 Hz, *P-Me*; 2nd isomer)

<u>Ratio of two isomers</u>: 1: 0.3

11.23 Oxidation of tricyclic *P*-OMe-bridged anionic bis(NHC) 22a with selenium

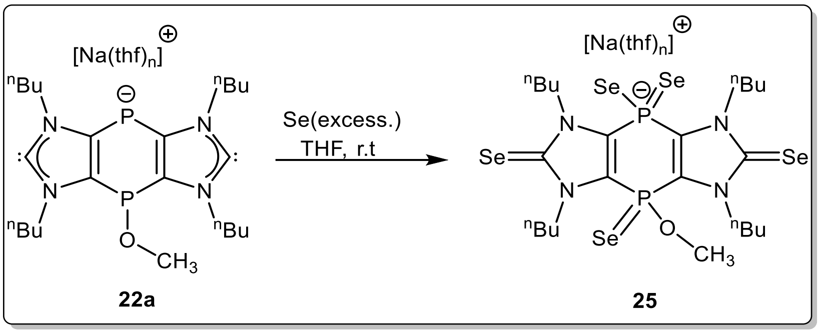

To a THF solution of **22a**, seleniumgrey was added as solid inexcess. Reaction mixture was stirred for 3 hours at room temperature. After completion of reaction, the solutionhad turned toyellow. It was filtered using double-ended canulla to remove unreacted selenium. All volatiles were removed in *vacuo* (6 × 10^{-3} mbar). The residue was washed (twice) with 6 mL of *n*-pentane resulted in a pure yellow solid.

11.23.1 Sodium(thf)$_n$[1,3,5,7-tetra-*n*-butyl-4,8-dihydro[1,4]diphosphinine[2,3-d:5,6-d']bis(imidazole-2,6-selone)-4-methoxy-4-selenide-8-diselenide] (25)

Chemicals	Amounts(g or mL)	mmol
22a	1.0 g	1.2
Se	0.51 g	6.4
THF	20 mL	

<u>Reaction code</u>: NRN-541

<u>Yield:</u> yellow solid

<u>Melting point:</u> 186 °C

<u>Elemental composition:</u>[$C_{23}H_{39}N_4NaOP_2Se_5$]$^-$[without solvent molecules]

Neg. ESI-MS: *m/z* (%) = 844.846 (100) $[M]^{+\cdot}$

HRMS: $[C_{23}H_{39}N_4OP_2Se_5]^-$ calcd (found) 844.8464 (844.8461).

IR (ATR,ῦ{cm⁻¹}): ῦ = 2895 (v), 2823 (m), 2765 (m), 1564 (w), 1499 (w), 1412 (m), 1206 (m), 1175 (w), 1123 (m), 1075 (v), 952 (s).

^{1}H NMR (300.1 MHz, THF, 25 °C): δ = 1.1 (t, 12H, $^3J_{H,H}$ = 7.2 Hz, $NCH_2CH_2CH_2$*Me*), 1.5 (m, 8H, NCH_2CH_2*CH_2*Me), 2.1 (m, 8H, NCH_2*CH_2*CH_2Me),2.4 (d, 3H, $^4J_{P,H}$ = 7.1 Hz, O-*Me*), 4.8 (m, 8H, N*CH_2*CH_2CH_2Me).

^{13}C{^{1}H} NMR (75.5 MHz, THF-d$_8$, 25 °C): δ = 13.1 (s, $NCH_2CH_2CH_2$*Me*), 19.8 (s, NCH_2CH_2*CH_2*Me), 29.3 (s, NCH_2*CH_2*CH_2Me), 48.4 (s, N*CH_2*CH_2CH_2Me), 112.5 (d, $^2J_{P,C}$ = 7.1 Hz, O-*CH_3*), 135.6 (d, $^{1/2}J_{P,C}$=20.1 Hz,P-*C*ofthemiddle ring), 164.4 (br, *C^2*=Se).

^{31}P NMR (121.15 MHz, THF-d$_8$, 25 °C): δ = - 43:1 ($^1J_{Se,P}$ = 681 Hz), 30.4 ($^1J_{Se,P}$ = 851 Hz)

^{77}Se NMR (57.28 MHz, THF-d$_8$): δ = - 154.4 (d, $^1J_{Se,P}$ = 681 Hz, (MeO)P=*Se*), 81 (s, C=*Se*), 105.2 (d, $^1J_{Se,P}$ = 690 Hz, Se-P=*Se*), 132.7 (d, $^1J_{Se,P}$ = 690 Hz, *Se*-P=Se)

11.24. Synthesis of anionic tricyclic rhodium (I) complex 26

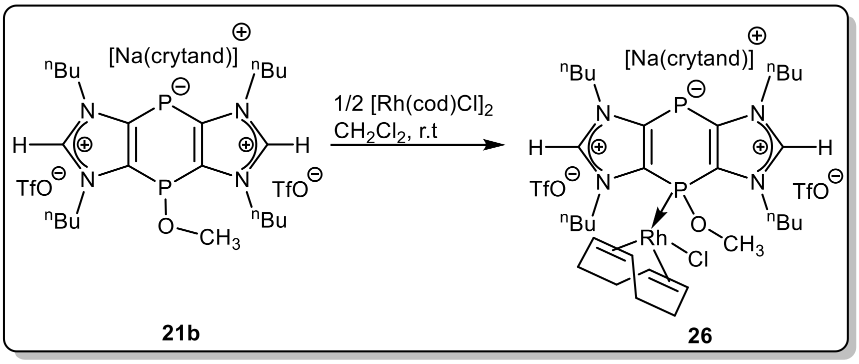

To a solution of **21b**, synthesized according to NRN-533, in methylene chloride, a half equivalent of $[Rh(cod)Cl]_2$ was added as solid at ambient temperature. Reaction mixture was stirred for 6 hours, then all volatiles removed in *vacuo* (2×10^{-2} mbar), and the residue was washed (twice) with 10 mL of diethyl ether. Subsequent drying in *vacuo* (2×10^{-2} mbar) afforded an orange solid.

11.24.1. Sodium([2.2.2]-cryptand)[1,3,5,7-tetra-*n*-butyl-4,8-dihydro-1,4-diphosphinine[2,3-d:5,6-d']bis(imidazole-2,6-ium)-8-ide-4-methoxy-4-[{(1,2,5,6-η^4)-1,5-cyclooctadiene)chlororhodium(I)] (26)

Chemicals	Amounts(g or mL)	mmol
21b	2 g	1.7
$[Rh(cod)Cl]_2$	0.43 g	0.87
CH_2Cl_2	20 mL	

Reaction code: NRN-526

Yield: 2.1 g (1.5 mmol) 88 %; Orange brown solid

Melting point: 82 °C

Elemental composition: $C_{51}H_{89}ClF_6N_6NaO_{13}P_2RhS_2$

Elemental analysis: for $C_{51}H_{89}ClF_6N_6O_{13}NaP_2S_2Rh$:

Theor.	C	43.89	H	6.43	N	6.02	S	4.59
Exp.	C	43.70	H	6.71	N	6.10	S	4.28

Neg. ESI MS: *m/z* (%) = 995.151 (29) $[M]^{\cdot+}$

HRMS: $[C_{33}H_{53}ClF_3N_4O_7P_2RhS_2F_6]^+$ calcd (found) 995.1473 (995.1494).

IR (ATR,ῦ{cm^{-1}}): ῦ = 2975.2 (m), 2931.4 (m), 2840.1 (w), 1511.4 (s), 1480.4 (m), 1398.1 (m), 1247.8(s), 1175.5 (m), 1129.8 (m), 1007.1 (s), 910.2 (s)

^{1}H NMR (300.1 MHz, CD_2Cl_2, 25 °C): δ = 0.9 (t, 12H, $^3J_{H,H}$ = 7.2 Hz, $NCH_2CH_2CH_2$*Me*), 1.2- 1.5 (m, 8H, NCH_2CH_2*CH_2*Me), 1.9 (m, 4H, cod), 1.9- 2.2 (m, 8H, NCH_2*CH_2*CH_2Me), 2.6 (br, 12H, cryptand),2.3 (m, 4H, cod), 2.5 (d, 8H, $^3J_{P,H}$ = 10.2 Hz, O-*CH_3*), 3.6 (br, 24H, cryptand), 3.8 (br, 2H, cod), 4.0- 4.2 (m, 8H, N*CH_2*CH_2CH_2Me), 5.3 (m, 2H, cod), 8.9(br, C^2-*H*).

<u>$^{13}C\{^1H\}$ NMR (75.5 MHz, CD_2Cl_2, 25 °C)</u>: δ = 13.4 (s, $NCH_2CH_2CH_2$*<u>Me</u>*), 19.9 (s, NCH_2CH_2*<u>CH_2</u>*Me), 28.5 (s, cod), 30.1 (br, NCH_2*<u>CH_2</u>*CH_2Me), 33.2(s, cod), 49.5 ((d, $^3J_{P,C}$ = 7.2 Hz, N*<u>CH_2</u>*CH_2CH_2Me), 69.6 (br, cod), 73.2 (d, $^1J_{Rh,C}$ = 11.2 Hz, cod), 122.1 (q, $^1J_{P,F}$ = 322.8 Hz, <u>C</u>F_3), 108.68 (d, $^2J_{P,C}$= 11.1 Hz, O-*<u>CH_3</u>*), 155.9 (br, <u>*P-C*</u>of the middle ring), 156.3 (d, $^{1/2}J_{P,C}$ = 44.2 Hz, <u>*P-C*</u>of the middle ring), 137.9 (br, H-*<u>C^2</u>*).

<u>^{31}P NMR (500.0 MHz, CD_2Cl_2, 25 °C)</u>: δ = -70.6 (s), 47. 5(d, $^1J_{Rh,P}$= 188.2Hz)

11.25 Synthesis of anionic, tricyclic trinuclear rhodium(I) NHC complex 27, 27`

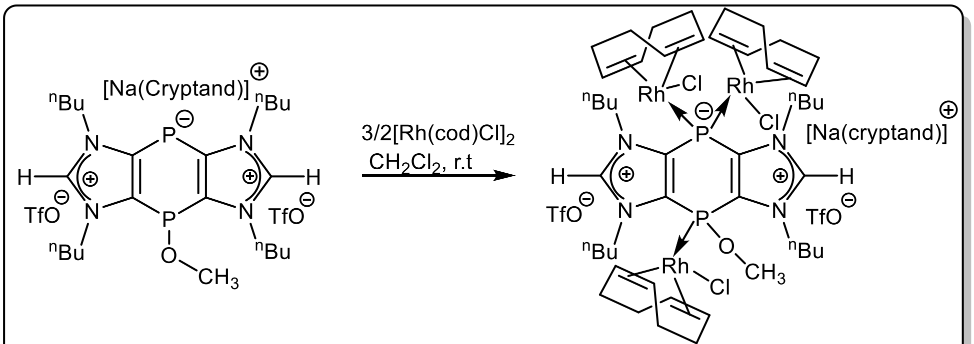

21b **27, 27`**

To a solution of **21b**, synthesized according to NRN-533, in methylene chloride, 1.5 equivalent of $[Rh(cod)Cl]_2$ was added as solid at ambient temperature. The reaction mixture was stirred at ambient temperature for 12 h. Then the solvent was removed in *vacuo* (2×10^{-2} mbar) and the residue washed (twice) with 10 mL of diethyl ether.Subsequent drying in *vacuo* (2×10^{-2} mbar) furnished a dark orange solid.

11.25.1. Sodium([2.2.2]cryptand)[1,3,5,7-Tetra-*n*-butyl--4,8-dihydro-1,4-diphosphinine [2,3-d:5,6-d']bis(imidazole-2,6-ium)-8-ide-4-methoxy-4,8-[tri-(1,2,5,6-*η*)-1,5-cyclooctadiene]chlororhodium(I)] (27, 27`)

Chemicals	Amounts(g or mL)	mmol
21b	1.5 g	1.3
$[Rh(cod)Cl]_2$	0.97 g	1.9
CH_2Cl_2	20 mL	

<u>Reaction code</u>: NRN-502

<u>Yield</u>: 1.7 g (0.9 mmol) 69%; dark orange solid

<u>Melting point</u>: 102 °C

<u>Elemental composition</u>: $C_{67}H_{113}Cl_3F_6N_6NaO_{13}P_2S_2Rh_3$

<u>Elemental analysis</u>: for $C_{67}H_{113}Cl_3F_6NaN_6O_{13}P_2S_2Rh_3$:

Theor.	C	42.61	H	6.03	N	4.45	S	3.40
Exp.	C	41.18	H	5.85	N	4.22	S	3.74

<u>Pos. ESI-MS</u>: *m/z* (%) = 1153.205 (36) $[M\text{-}Cl\text{-}2TfO]^+$.

<u>HR-MS</u>: $[C_{47}H_{76}Cl_2N_4OP_2Rh_3]^+$ calcd (found) 1153.2031 (1153.2043).

<u>IR (ATR,ῦ{cm^{-1}})</u>: ῦ = 2984 (m), 2971 (m), 2861 (w), 1545 (s), 1491 (m), 1421 (m), 1327 (s), 1265 (m), 1129 (w), 1069 (s), 978 (s).

<u>^{1}H NMR (500.1 MHz, CD_2Cl_2, 25 °C)</u>: δ = 1.1- 1.2 (t, 12H, $^3J_{H,H}$ = 7.0 Hz, $NCH_2CH_2CH_2$<u>*Me*</u>), 1.5- 1.7 (m, 8H, NCH_2CH_2<u>*CH_2*</u>Me), 2.2-2.4 (m, 24H, cod), 2.5- 2.6 (m, 8H, NCH_2<u>*CH_2*</u>CH_2Me), 2.9, 3.0 (d, 3H, $^3J_{P,H}$ = 12.4 Hz, O-<u>*CH_3*</u>), 3.9 (m, 6H, cod), 4.2 (br, 8H, N<u>*CH_2*</u>CH_2CH_2Me), 5.2 (m, 6H, cod), 9.5 (br , C^2-<u>*H*</u>), 9.7 (br , C^2-<u>*H*</u>).

<u>^{13}C{^{1}H} NMR (125.75 MHz, CD_2Cl_2, 25 °C)</u>: δ = 13.5, 13.8(s, $NCH_2CH_2CH_2$<u>*Me*</u>) two isomers, 19.9, 20.1 (s, NCH_2CH_2<u>*CH_2*</u>Me) two isomers, 28.4 (s, cod), 31.3 (br, NCH_2<u>*CH_2*</u>CH_2Me), 32.7 (s, cod), 49.9 (d, $^3J_{P,C}$ = 6.3 Hz, N<u>*CH_2*</u>CH_2CH_2Me), 49.9 (br, N<u>*CH_2*</u>CH_2CH_2Me), 72.0 (d, $^1J_{Rh,C}$ = 13.0 Hz, cod), 72.6 (d, $^1J_{Rh,C}$ = 13.0 Hz, cod), 73.21 (d, $^1J_{Rh,C}$ = 13.1 Hz, cod), 74.2 (d, $^1J_{Rh,C}$ = 13.2 Hz, cod), 74.6 (d, $^1J_{Rh,C}$ = 13.0 Hz, cod), 75.4 (d, $^1J_{Rh,C}$ = 13.1 Hz, cod), 113.4 (d, $^2J_{P,C}$ = 9.5 Hz, O-<u>*CH_3*</u>), 121.1 (q, $^1J_{P,F}$ = 332.7 Hz, <u>*C*</u>F_3), 131.9 (br, <u>*P-C*</u>of the middle ring), 133.3 (d, $^{1/2}J_{P,C}$ = 45.2 Hz, <u>*P-C*</u>of the middle ring), 141.9 (br, H-<u>*C^2*</u>), 142.4 (br, H-<u>*C^2*</u>; 2nd isomer).

<u>^{31}P NMR (500.0 MHz, CD_2Cl_2, 25 °C)</u>: δ = -123.4 (t, $^1J_{Rh,P}$ = 123.2 Hz), -120.3 (t, $^1J_{Rh,P}$ = 123.2 Hz) (s), 65.0 (d, $^1J_{Rh,P}$= 199.2Hz),64.0(d, $^1J_{Rh,P}$= 196.4Hz).

11.26. Synthesis of 1,4-diphosphabarrelenediselone 28

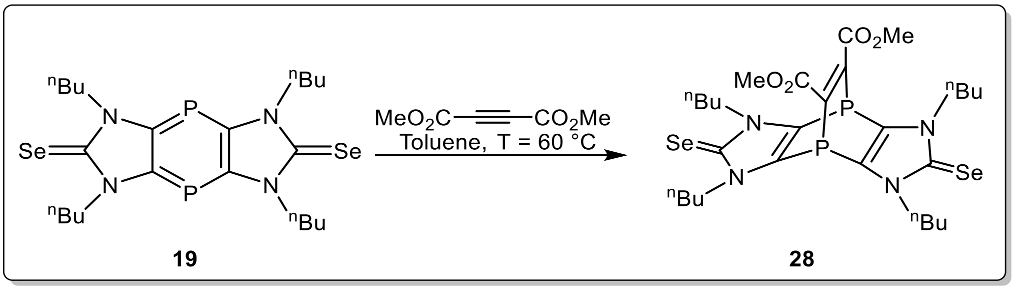

In a Schlenk tube asolutionof **19** in toluene was heated at 60 °C with dimethyl acetylene dicarboxylate for 1 h. The color of the reaction mixture turned into dark reddish-orange. After removal of the solvent *in vacuo* (2×10^{-2} mbar), the residue was washed with *n*-pentane (thrice5 mL) and then dried in*vacuo* (2×10^{-2} mbar) to get a pure (orange red) solid.

11.26.1. 7,8-Bis(methoxycarbonyl)-[2,3-d:5,6-d']bis(1,3-*n*-butyl-imidazole-2-selone)-1,4-diphospha-bicyclo[2.2.2]octa-2,5,7-triene (28)

Chemicals	**Amounts(g or mL)**	**mmol**
19	0.1 g	0.17
DMAD	0.021 mL	0.17
Toluene	5 mL	

<u>Reaction code</u>: NRN-418

<u>Yield</u>: 0.115 g (0.16 mmol) 94 %; Orange red.

<u>Melting point</u>: 127 °C

<u>Elemental composition</u>: $C_{28}H_{42}N_4O_4P_2Se_2$

<u>Molecular weight</u>: 718.53 g/mol

<u>Elemental analysis</u>: for $C_{28}H_{42}N_4O_4P_2Se_2$:

Theoretical	C	46.80	H	5.89	N	7.79
Experimental	C	47.16	H	5.80	N	6.24

Pos. ESI-MS: 720.0(42) $[M]^{+\cdot}$, 578(100) $[M-2CO_2Me]^{+\cdot}$

HRMS: $C_{28}H_{42}N_4O_4P_2Se_2$ theor.(exp.) 720.1012(720.1010)

IR (ATR,ῦ{cm^{-1}}): ῦ=2978 (w), 2942 (w), 2821 (w), 1745 (m), 1532. (w), 1479 (w), 1252 (vs), 1208 (m), 1067 (m), 698 (m).

^{1}H NMR (300.1 MHz, $CDCl_3$, 25 °C): δ= 0.9 (t, 12H, $^3J_{H,H}$ = 7.1 Hz, $NCH_2CH_2CH_2$*Me*), 1.3-1.4(m, 8H, NCH_2CH_2*CH_2*Me), 1.6-1.9 (m, 8H, NCH_2*CH_2*CH_2Me), 3.8 (s,6H, -CO_2*Me*), 4.3 (t, 8H, $^3J_{H,H}$ = 7.6 Hz N*CH_2*CH_2CH_2Me).

^{13}C{^{1}H} NMR (75.5 MHz, $CDCl_3$, 25 °C): δ = 13.8 (s, $NCH_2CH_2CH_2$*Me*), 20.1 (s, NCH_2CH_2*CH_2*Me), 31.9 (s, NCH_2*CH_2*CH_2Me), 49.7 (bs, N*CH_2*CH_2CH_2Me), 53.2 (s, -CO_2*Me*), 128.7 (d, $^1J_{P,C}$ = 58.9 Hz, P-CO_2Me), 144.7 (dd, $^{1/2}J_{P,C}$ = 4.1 Hz *P-C* of the middle ring), 160.3 (dd, $^2J_{P,C}$ = 12.4 Hz, ^2JP,C = 12.1 Hz, Me-CO_2) 164.3 (s, C^2=Se), 166.1 (dd, $^2J_{P,C}$ = 16.4 Hz, Me-CO_2)

^{31}P NMR (121.5 MHz, $CDCl_3$, 25 °C): δ = - 86.6 (s)

^{77}SeNMR (57.28 MHz, $CDCl_3$): 38.8(s)

10.27. Reaction of compound 28 with MeOTf

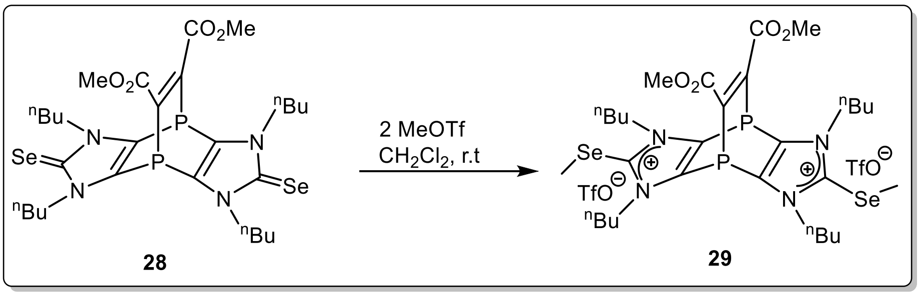

Trifluoromethane sulfonate was added to a solution of **28** in methylene chloride at room temperature. The reaction mixture was stirred for 2 hours, a change in color was observed from reddish-orange to orange at the end of reaction. After removal of the solvent *in vacuo* (2×10^{-2} mbar), the residue was washed with *n*-pentane (twice 10 x mL) to get the product as pure orange solid.

11.27.1. [7,8-Bis(methoxycarbonyl)-[2,3-d:5,6-d']bis(1,3-^{n}butyl-imidazole-2,6-bis{(methylselanylium}-1,4-diphospha-bicyclo[2.2.2]octa-2,5,7-triene]bis(trifluoromethane sulfonate) (29)

Chemicals	Amounts(g or mL)	mmol
28	1.0 g	1.4
MeOTf	0.32 mL	2.8
CH_2Cl_2	20 mL	

Reaction code: NRN-425

Yield: 1.40 g (1.3 mmol) 96 %; Orange.

Melting point: 52 °C

Elemental composition: $C_{32}H_{48}F_6N_4O_{10}P_2S_2Se_2$

Molecular weight: 1046.73 g/mol

Elemental analysis: for $C_{32}H_{48}F_6N_4O_{10}P_2S_2Se_2$:

Theor.	C 36.72	H 4.62	N 5.35	S 6.12
Exp.	C 37.35	H 4.43	N 4.62	S 5.69

Pos. ESI-MS: m/z (%) = 899.1(72) $[M]^{+\cdot}$

HRMS: $[C_{31}H_{48}F_3N_4O_7P_2SSe_2]$ theor.(exp.) 899.1002 (899.1011)

IR (ATR,ῦ{cm^{-1}}): ῦ= 3102 (w), 2960.4 (m), 2320 (m), 2049 (m), 1692 (m), 1501 (w), 1312 (s), 1223 (s), 1046 (s), 1018.5 (S), 612 (vs).

^{1}H NMR (300.1 MHz, $CDCl_3$, 25 °C): δ= 0.9 (t, 12H, $^{3}J_{H,H}$ = 7.3 Hz, $NCH_2CH_2CH_2$*Me*), 1.3-1.4 (m, 8H, NCH_2CH_2*CH_2*Me), 1.8-1.9 (m, 8H, NCH_2*CH_2*CH_2Me), 2.5 (s, 6H, Se-*Me*), 3.8 (s,6H, -CO_2*Me*), 4.5 (t, 8H, $^{3}J_{H,H}$ = 7.7 Hz N*CH_2*CH_2CH_2Me).

$^{13}C\{^1H\}$ NMR (75.5 MHz, $CDCl_3$, 25 °C): δ = 11.4 (s, Se-*Me*), 13.5 (s, $NCH_2CH_2CH_2$*Me*), 19.9 (s, NCH_2CH_2*CH_2*Me), 33.5 (t, $^4J_{P,C}$ = 2.1 Hz, NCH_2*CH_2*CH_2Me), 51.5 (bs, N*CH_2*CH_2CH_2Me), 53.5 (s, -CO_2*Me*), 120.6 (q, $^1J_{P,F}$ = 318.2 Hz, *C*F_3), 136.3(br, P-*C*O_2Me), 149.2(dd, $^{1/2}J_{P,C}$ = 6.9 Hz, $^{1/2}J_{P,C}$ = 6.7 Hz, *P-C*of the middle ring), 160.4 (s, *C*=Se), 166.1 (dd, $^2J_{P,C}$ = 16.8 Hz, -*C*O_2Me).

^{31}P NMR (500.1 MHz, $CDCl_3$, 25 °C): δ = - 90.0 (s)

^{77}SeNMR (57.28 MHz, $CDCl_3$): 113.1(s)

11.28. Synthesis of dianionic phosphanido type 1,4 diphosphinine 30

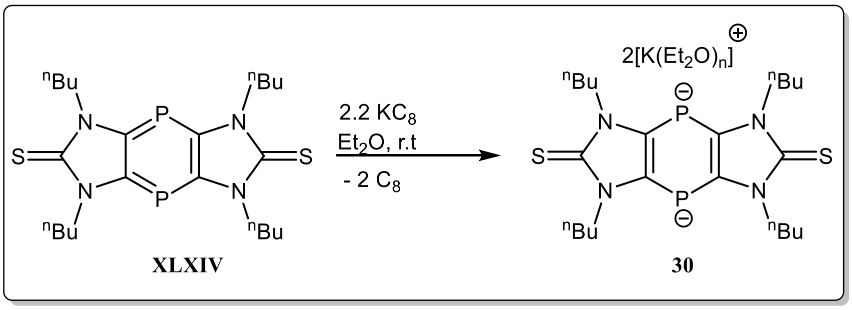

To an ethereal solution of **XLXIV**, 2.2 equivelent of $KC_8$was added as solids and stirred for 24 hours. Dark reddish-brown precipitate was formed which was filtered off using glass filter paper. Afterwards the precipitate was dissolved in THF and again filtered to get rid of unreacted KC_8 and graphite formed. After removal of the solvent*in vacuo* (2×10^{-2} mbar), a dark reddish-brown powder was obtained.

11.28.1 Dipotassium(thf)$_n$[1,3,5,7-tetra-*n*-butyl-4,8-dihydro-1,4-diphosphinine[2,3-d:5,6-d']bis(imidazole-2,6-dithione)-4,8-diide](30)

Chemicals	Amounts(g or mL)	mmol
XLXIV	0.5 g	1.0
KC_8	0.28 g	2.1
Et_2O	10 mL	

Reaction code: NRN-496, NRN-520

Melting point: 307 °C

Elemental composition: $[C_{22}H_{36}N_4P_2S_2]^{-2}$ (without $[K(Et_2O)_n]^{+2}$ cations)

^{1}H NMR (500 MHz, THF-d$_8$, 25 °C): δ = 1.1 (t, 12H, $^3J_{H,H}$ = 7.7 Hz, $NCH_2CH_2CH_2$*Me*), 1.4-1.5(m, 8H, NCH_2CH_2*CH$_2$*Me), 1.7 (m, 8H, NCH_2*CH$_2$*CH_2Me), 3.9 (br, 8H, N*CH$_2$*CH_2CH_2Me).

^{13}C{^{1}H} NMR (75.5 MHz, THF-d$_8$, 25 °C): δ = 13.4 (s, $NCH_2CH_2CH_2$*Me*), 20.0 (s, NCH_2CH_2*CH$_2$*Me), 31.3 (s, NCH_2*CH$_2$*CH_2Me), 44.9 (br, N*CH$_2$*CH_2CH_2Me), 128.1 (br, *P-C* of the middle ring), 159.9 (br, *C^2*=S).

^{31}P NMR (500.1 MHz, THF-d$_8$, 25 °C): δ = - 114.9 (s)

IR (ATR,ῦ{cm^{-1}}): ῦ= 2945 (m), 2930 (m), 2878 (m), 1469 (s), 1462 (w), 1426 (w), 1195 (m), 1060 (m), 1042 (m), 765 (w).

Neg. ESI-MS: m/z(%) = 482.1864 (32) $[M]^-$, 483.1936(30) $[M+H]^-$

HRMS: $[C_{22}H_{36}N_4P_2S]^{-2}$ theor.(exp.) 482.1862 (482.1864)
$[C_{22}H_{36}N_4P_2SH]^-$theor.(exp.) 483.1940 (483.1936)

UV-vis (THF):λ_{max} [nm] (abs.): 565 (0.09).

11.29. Synthesis of dianionic, tricyclic tetranuclear rhodium(I) complex 31

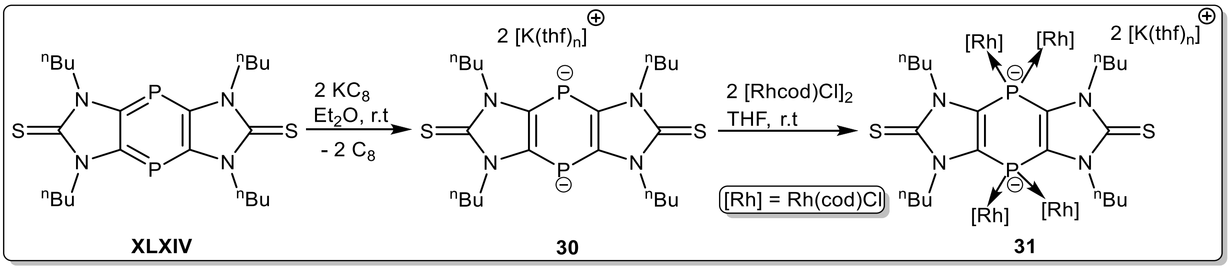

To an ethereal solution of **XLXIV**, 2 equivalent of KC_8 was added as solid and stirred for 24 hours. A dark reddish brown precipitate was formed, which was then filtered using glass filter paper. Afterwards, the precipitate was dissolved in THF and again filtered to get rid of unreacted graphite. Removal of all volatiles *in vacuo* (2×10^{-2} mbar) afforded a dark reddish brown powder. This was dissolved in THF, and this freshly prepared solution of **19** was then treated with 2 equivalent of $[Rh(cod)Cl]_2$ at room temperature. The reaction mixture was stirred for 2 hours, then all volatiles removed *invacuo* (2×10^{-2} mbar) to get a dark brown powder which was washed twice with 5mL of *diethyl ether*, but still contained some minor impurities.

11.29.1. Di(potassium(thf)$_n$)[1,3,5,7-tetra-*n*-butyl-4,8-dihydro-1,4-diphosphinine[2,3-d:5,6-d']bis(imidazole-2,6-dithione)-4,8-diide-*κ*P-,*κ*P-]tetrakis[{(1,2,5,6-*η*)-1,5-cyclooctadiene}-chlororhodium(I)}] (31)

Chemicals	Amounts(g or mL)	mmol
XLXIV	0.25 g	0.5
KC_8	0.14 g	1.0
$[Rh(cod)Cl]_2$	0.52 g	1.0
THF	5 mL	

Reaction code: NRN-492

Yield: Blackish brown.

Elemental composition: $[C_{54}H_{84}N_4Cl_4P_2Rh_4S_2]^{2-}$ (without counter cations $[K(thf)_n]^{2+}$)

^{1}H NMR (500 MHz, CD_2Cl_2, 25 °C): δ = 0.9 (br, 12H, $NCH_2CH_2CH_2$*Me*), 1.5 (m, 8H, NCH_2CH_2*CH_2*Me), 2.2 (m, 32H, cod), 2.3 (m, 8H, NCH_2*CH_2*CH_2Me), 3.3 (m, 8H, cod), 4.6 (br, 8H, N*CH_2*CH_2CH_2Me), 5.7 (m, 8H, cod).

^{13}C{^{1}H} NMR (75.5 MHz, CD_2Cl_2, 25 °C): δ = 13.8 (s, $NCH_2CH_2CH_2$*Me*), 20.2 (s, NCH_2CH_2*CH_2*Me), 28.2 (s, cod), 31.2 (br, NCH_2*CH_2*CH_2Me), 32.1 (s, cod), 49.3 (d, $^3J_{P,C}$ = 6.1 Hz, N*CH_2*CH_2CH_2Me), 71.6 (d, $^1J_{Rh,C}$ = 16.4 Hz, cod), 125.8 (br, *P-C* of the middle ring), 131.9(s, *C^2*=S).

^{31}P NMR (121.51 MHz, CD_2Cl_2, 25 °C): δ = - 112.3 (t, $^1J_{Rh,P}$ = 128.7 Hz)

IR (ATR,ῦ{cm^{-1}}): ῦ= ῦ = 2974 (m), 2921 (m), 2811 (w), 1505 (s), 1461 (m), 1401 (m), 1317 (s), 1295 (m), 1159 (w), 1029 (s), 889 (s).

Neg. ESI-MS: $[C_{54}H_{84}Cl_3N_4P_2Rh_4S_2]^{-2}$ theor.(exp.) 1433.0888 (1433.0875).

11.30 Synthesis of dianionic bis(NHC) 32

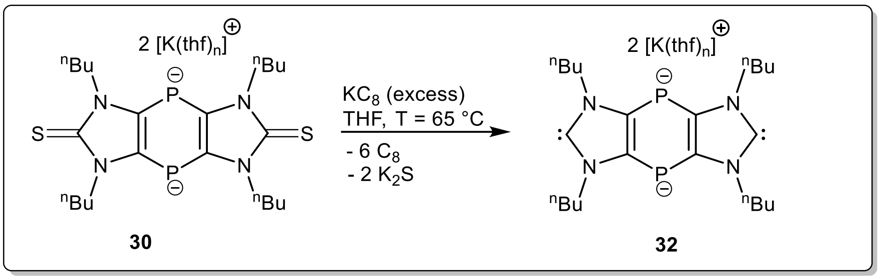

To a THFsolution of **30**, 4 equivalent of KC_8 was added as solid and stirred at 65 °C for 48 h. All volatiles were then removed *invacuo* (2× 10^{-2} mbar). The solution was filtered to remove potassium sulfide and graphite. All volatiles were then removed from the filtrate *invacuo* (2× 10^{-2} mbar) to get a solid which was washed with 15 mL of diethyl ether and *n*-pentane mixture (1:1) (twice). This resulted in a dark brown powder.

11.30.1 dipotassium(thf)$_n$[1,3,5,7-tetra-*n*-butyl-4,8-dihydro-1,4-diphosphinine[2,3-d:5,6-d']bis(imidazole-2,6-diylidene)-4,8-diide](32)

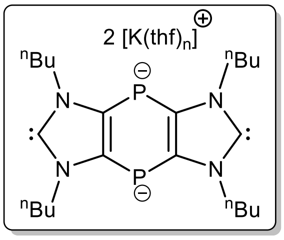

Chemicals	Amounts(g or mL)	mmol
30	0.5 g	1.0
KC_8	Excess	
THF	10 mL	

Reaction code: NRN-474, NRN-535

Elemental composition: [$C_{22}H_{36}N_4P_2$]$^-$ (without K(thf)$_n$ cations)

^{1}H NMR (500 MHz, THF-d$_8$, 25 °C): δ = 0.8 (t, 12H, $^3J_{H,H}$ = 6.8 Hz, NCH$_2$CH$_2$CH$_2$*Me*), 1.2 (br, 8H, NCH$_2$CH$_2$*CH$_2$*Me), 1.6 (br, 8H, NCH$_2$*CH$_2$*CH$_2$Me), 3.9 (br, 8H, N*CH$_2$*CH$_2$CH$_2$Me).

$^{13}C\{^1H\}$ NMR (125.78 MHz, THF-d_8, 25 °C): δ = 13.5 (s, $NCH_2CH_2CH_2$*Me*), 19.9 (s, NCH_2CH_2*CH₂*Me), 35.2 (s, NCH_2*CH₂*CH_2Me), 48.0 (br, N*CH₂*CH_2CH_2Me), 130.2 (d, $^1J_{P,C}$ = 39.2 Hz, *P-C* of the middle ring), 207.5(br, *C^2*).

^{31}P NMR (500.1 MHz, THF-d_8, 25 °C): δ = - 117.7 (s), -120.6 (s)

LIFDI-MS: m/z(%) = 422.2 (11) $[M+3H]^{\bullet+}$

11.31. Synthesis of tricyclic {P(O)OH}-bridgedbis(imidazolium) salt 34, 34′

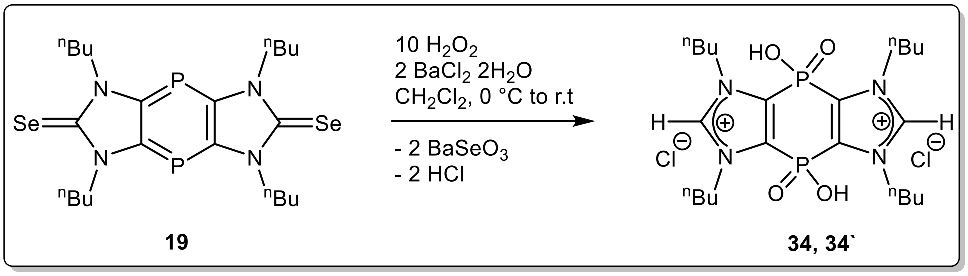

To a methylene chloridesolution of **19**, H_2O_2 (35 % in water) was added at 0 °C using ice bath. The reaction mixture was stirred at 0 °C for 30 min, then at ambient temperature for 1 h. The reaction solution turned to colorless showing thus completion (^{31}P NMR control). An aqueous solution of $BaCl_2{\cdot}2H_2O$ was added and the mixture stirred for an additional hour. The reaction mixture was then filtered over a frit equipped with a layer of celite® to remove barium selenite. The filtrate was concentrated *in vacuo* (6 × 10^{-3} mbar) and, hence, resulted in a white coloured solid which was washed with *n*-pentane (2 × 5mL) and dried *in vacuo*.

11.31.1. {1,3,5,7-Tetra-*n*-butyl-4,8-dihydro-1,4-diphosphinine[2,3-d:5,6-d']bis(imidazole-2,6-ium)-4,8-dioxo-4,8-dihydroxo} dichloride (34, 34′)

Chemicals	Amounts(g or mL)	mmol
19	0.08 g	0.14
H_2O_2	0.134 mL	1.4
$BaCl_2.2H_2O$	0.7g	0.28
CH_2Cl_2	5 mL	

Reaction code: NRN-428, NRN-469

Yield: 0.057 g (0.102 mmol) 72 %; white solid.

Melting point: 168 °C

Elemental composition: $C_{22}H_{42}Cl_2N_4O_4P_2$

Molecular weight: 558.48 g/mol

^{1}H NMR (300.1 MHz, CH_3OH-d_4, 25 °C): δ = 0.9 (t, 12H, $^3J_{H,H}$ = 7.3 Hz, $NCH_2CH_2CH_2$*Me*), 1.3-1.4 (m, 8H, NCH_2CH_2*CH_2*Me), 2.0-2.1 (m, 8H, NCH_2*CH_2*CH_2Me), 4.4 (t, 8H, $^3J_{H,H}$ = 7.7 Hz, N*CH_2*CH_2CH_2Me), 9.3 (br, 1H, C^2-*H*).

^{13}C{^{1}H} NMR (75.5 MHz, CH_3OH-d_4, 25 °C): δ = 12.5 (s, $NCH_2CH_2CH_2$*Me*), 19.4 (s, NCH_2CH_2*CH_2*Me), 31.9 (s, NCH_2*CH_2*CH_2Me), 41.5 (br, N*CH_2*CH_2CH_2Me), 131.8 (d, $^{1/2}J_{P,C}$ = 20.3 Hz *P-C* of the middle ring), 133.2 (d, $^1J_{P,C}$ = 20.3 Hz, *P-C* of the middle ring), 139.3 (t,$^3J_{P,C}$ = 6.3 Hz,H-*C^2*).

^{31}P NMR (121.5 MHz, CH_3OH-d_4, 25 °C): δ = -14.1 (s)

IR (ATR,ṽ{cm^{-1}}): ṽ = 2864 (m), 2821 (m), 2741 (w), 1605 (s), 1531 (s), 1375 (m), 1265 (s), 1225 (m), 1059 (w), 1001 (s), 841 (s).

pos. ESI-MS: $[C_{22}H_{39}N_4O_4P_2]^+$theor.(exp.) 485.244 (485.247).

11.32. Synthesis of tricyclic bis(phosphinic acid)-bridgedbis(NHC) 35, 35′

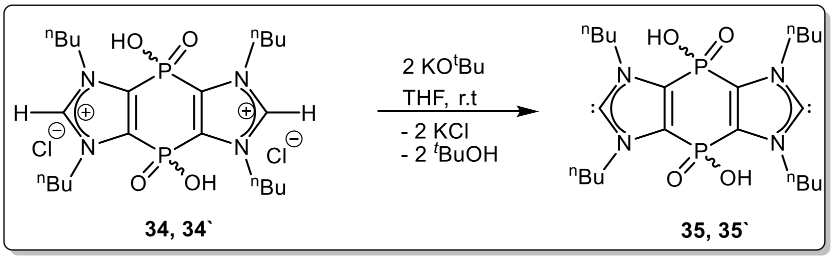

A solution of KO^{t}Bu in THF was added dropwise to a solution of bis(imidazolium) salts **33, 33′** in THF through a double-ended needle over 10 minutes at ambient temperaturewith continuous stirring. The reaction mixture was then stirred for an additional 3 hours. The THF was removed *in vacuo* (2× 10^{-2}mbar), and the residue was dissolved with 10 mL of diethyl ether and the solid potassium chloride was removed via cannulation. The solvent was then was removed *in vacuo* (2×10^{-2}mbar) and the residue dried *in vacuo* (2×10^{-2}mbar) to get **35, 35`** as pure solid.

11.32.1. {1,3,5,7-Tetra-*n*-butyl-4,8-dihydro-1,4-diphosphinine[2,3-d:5,6-d']bis(imidazole-2,6-diylidene)-4,8-dioxo-4,8-dihydroxo} (35, 35`)

Chemicals	Amounts(g or mL)	mmol
33	0.5 g	0.90
KO^{t}Bu	0.40 g	1.9
THF	10 mL	

Reaction code: NRN-422

Yield: 0.32 g (0.66 mmol) 73 %; light yellow solid.

Elemental composition: $C_{22}H_{38}N_4O_4P_2$

Molecular weight: 484.52 g/mol

^{1}H NMR (300.1 MHz, CDCl$_3$, 25 °C): δ = 0.9 (t, 12H, $^3J_{H,H}$ = 7.4 Hz, NCH$_2$CH$_2$CH$_2$*Me*), 1.3 - 1.4 (m, 8H, NCH$_2$CH$_2$*CH$_2$*Me), 1.9 - 2.1 (m, 8H, NCH$_2$*CH$_2$*CH$_2$Me), 4.5 (t, 8H, $^3J_{H,H}$ = 7.3 Hz, N*CH$_2$*CH$_2$CH$_2$Me); the OH resonance signal was not observed.

^{13}C{^{1}H} NMR (75.5 MHz, CDCl$_3$, 25 °C): δ = 13.5 (s, NCH$_2$CH$_2$CH$_2$*Me*), 19.6 (s, NCH$_2$CH$_2$*CH$_2$*Me), 32.2 (s, NCH$_2$*CH$_2$*CH$_2$Me), 49.9 (br, N*CH$_2$*CH$_2$CH$_2$Me), 133.5 (d, $^{1/2}J_{P,C}$ = 18.5 Hz *P-C* of the middle ring), 135.6 (d, $^1J_{P,C}$ = 18.5 Hz, *P-C* of the middle ring); the carbene atom resonance could not be detected.

^{31}P NMR (121.5 MHz, CH$_3$OH-d$_4$, 25 °C): δ = -15.3 (s)

11.33. Synthesis of tricyclic bis(phosphinic acid)-bridged bis(NHC) silver(I) complexes 36,36′

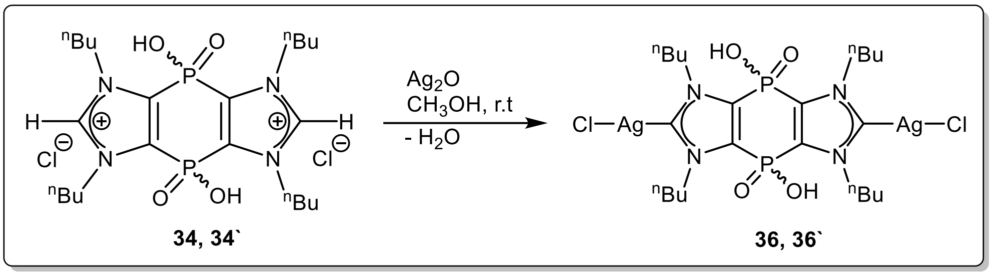

To a stirred solution of bis(imidazolium) salts **33, 33′** in methanol, containing molecular sieve (3Å)(to adsorb H_2O),Ag(I) oxide was added as solid at once at room temperature. The reaction mixture was then stirred in darkness for 12 h, and the solvent removed*in vacuo* (2× 10^{-2} mbar) to dryness. It was then subjected to filtration over silica using methanol and methylene chloride mixture (1:1) to get a clear solution. The solvent was then evaporated *in vacuo* (2 × 10^{-2} mbar) followed by washing with *n*-pentane (2 × 5 mL) to get a white solid.

11.33.1. {1,3,5,7-Tetra-*n*-butyl-4,8-dihydro-1,4-diphosphinine[2,3-d:5,6-d']bis(imidazole-2,6-ylidene-*κ*C-,*κ*C-)-4,8-dioxo-4,8-dihydroxo}di{chlorosilver(I)} (36,36′)

Chemicals	Amounts(g or mL)	mmol
34, 34′	1.0 g	1.8
Ag_2O	0.83 g	3.6
MeOH	20 mL	

Reaction code: NRN-537

Yield: 1.05 g (1.3 mmol) 75 %; white solid.

Elemental composition: $C_{22}H_{40}Ag_2Cl_2N_4O_4P_2$

Molecular weight: 773.16 g/mol

^{1}H NMR (500.1 MHz, CH_3OH-d_4, 25 °C): δ = 1.0 (br, $NCH_2CH_2CH_2$*Me*), 1.5 (br, 8H, NCH_2CH_2*CH_2*Me), 2.1 (br, 8H, NCH_2*CH_2*CH_2Me), 4.5 (br, N*CH_2*CH_2CH_2Me).

$^{13}C\{^{1}H\}$ NMR (125.78 MHz, CH_3OH-d_4, 25 °C): δ = 12.5 (s, $NCH_2CH_2CH_2$*Me*), 14.8 (s, $NCH_2CH_2CH_2$*Me*; 2nd isomer), 19.4 (s, NCH_2CH_2*CH_2*Me), 20.0 (s, NCH_2CH_2*CH_2*Me; 2nd isomer), 33.2 (s, NCH_2*CH_2*CH_2Me),34.2 (s, NCH_2*CH_2*CH_2Me; 2nd isomer),45.6 (br, N*CH_2*CH_2CH_2Me), 51.2 (br, N*CH_2*CH_2CH_2Me; 2nd isomer), 132.5 (d, $^{1/2}J_{P,C}$ = 21.7 Hz *P-C* of the middle ring), 134.5 (d, $^{1/2}J_{P,C}$ = 18.5 Hz, *P-C* of the middle ring; 2nd isomer), 183.4 (br,*C^2*), 184.3 (br, *C^2*; 2nd isomer).

^{31}P NMR (202.48 MHz, CH_3OH-d_4, 25 °C): δ = - 11.5 (s), -9.4 (s)

Isomer ratio: 1: 0.3

12. References

[1] a) M. Hermann, *Justus Liebigs Ann. Chem.*, **1855**, *95*, 211–225; b) D. J. Cardin, B. Cetinkaya, M. F. Lappert, *Chem. Rev.*, **1972**, *72*, *5*, 545–574; c) A. Gautier, F. Cisnetti, *Metallomics*, **2012**, *4*, 23–32; d) M. A. Sierra, *Chem. Rev.*, **2000**, *100*, *10*, 3591–3638.

[2] D. Bourissou, O. Guerret, F. P. Gabbaï, G. Bertrand, *Chem. Rev.*, **1999**, *100*, 39–92

[3] E. O. Fischer, A. Maasböl, *Angew. Chem.*, *Int. Ed. Engl.*, **1964**, *3*, 580–581

[4] a) R. Breslow, *J. Am. Chem. Soc.*, **1957**, *79*, 1762–1763; b) R. Breslow, *J. Am. Chem. Soc.*, **1958**, *80*, 3719–3726; c) H. W. Wanzlick, E. Schikora, *Angew. Chem.* **1960**, *72*, 494–494; d) H. W. Wanzlick, H. J. Kleiner, *Angew. Chem.* **1961**, *73*, 493–493; e) P. Haake, L. P. Bausher, W. B. Miller, *J. Am. Chem. Soc.*, **1969**, *91*, 1113–1119; f) P. Haake, W. B. Miller, *J. Am. Chem. Soc.*, **1963**, *85*, 4044–4045; g) P. Haake, L. P. Bausher, J. P. McNeal, *J. Am. Chem. Soc.*, **1971**, *93*, 7045–7049.

[5] W. M. Butler, J. H. Enemark, *Inorg. Chem.*, **1971**, *10*, 2416–2419.

[6] H. W. Wanzlick, *Angew. Chem. Int. Ed. Engl.* **1962**, *1*, 75–80.

[7] K. Öfele, *J. Organomet. Chem.* **1968**, *12*, 42–43.

[8] H. W. Wanzlick, H. J. Schönherr, *Angew. Chem.*, *Int. Ed. Engl.* **1968**, *7*, 141–142.

[9] A. Igau, H. Grützmacher, A. Baceiredo, G. Bertrand, *J. Am. Chem. Soc.*, **1988**, *110*, 6463–6466.

[10] a) A. J. Arduengo III, R. L. Harlow, M. Kline, *J. Am. Chem. Soc.* **1991**, *113*, 361–363; b) a) T. Dröge, F. Glorius, *Angew. Chem.* **2010**, *122*, 7094–7107; *Angew. Chem. Int. Ed.* **2010**, *49*, 6940–6952; c) H. Clavier, S. P. Nolan, *Chem. Commun.* **2010**, *46*,841–861; d) O. Kühl, Coord. *Chem. Rev.* **2009**, *253*, 2481–2492; e) S. Diez-Gonzalez, S. P. Nolan, Coord. *Chem. Rev.* **2007**, *251*, 874–883; f) L. Cavallo, A.Correa, C. Costabile, H. Jacobsen, *J. Organomet. Chem.* **2005**, *690*, 5407–5413; g) M. Poyatos, J. A. Mata, E. Peris, *Chem. Rev.* **2009**, *109*, 3677–3707; h) J. C. Y. Lin, R. T. W. Huang, C. S. Lee, A. Bhattacharyya, W. S. Hwang, I. J. B. Lin, *Chem. Rev.* **2009**, *109*, 3561–4598; i) P. L. Arnold, I. J. Casely, *Chem. Rev.* **2009**,*109*, 3599–3611; j) C. M. Crudden, D. P. Allen, Coord. *Chem. Rev.* **2004**, *248*, 2247–2273.

[11] N. Kuhn, T. Kratz, *Synthesis*, **1993**, 561–562.

[12] M. K. Denk, A. Hezarkhani, F.-L. Zheng, *Eur. J. Inorg. Chem.* **2007**, 3527–3534.

[13] G. W. Nyce, S. Csihony, R. M. Waymouth, J. L. Hedrick, *Chem.Eur. J.* **2004**, *10*, 4073–4079.

[14] B. Bantu, G. M. Pawar, U. Decker, K. Wurst, A. M. Schmidt, M. R. Buchmeiser, *Chem.Eur. J.* **2009**, *15*, 3103–3109.

[15] M. Otto, S. Conejero, Y. Canac, V. D. Romanenko, V. Rudzevitch, G. Bertrand, *J. Am. Chem. Soc.* **2004**, *126*, 1016–1017.

[16] J. S. Warner, *J. Org. Chem.* **1963**, *28*, 1642–1644.

[17] a) F. Bigoli, A. M. Pellinghelli, P. Deplano, F. A. Devillanova, V. Lippolis, M. L. Mercuri, E. F. Trogu, *Gazz. Chim. Ital.* **1994**, *124*, 445–454; b) H. Küçükbay, R. Durmaz, E. Orhan, S. Günal, *IL Farmaco* **2003**, *58*, 431–437; c) A. P. Marchenko, H. N. Koidan, A. N. Hurieva, I. I. Pervak, S. V. Shishkina, O. V. Shishkin, A. N. Kostyuk, *Eur. J. Org. Chem.* **2012**, 4018–4033; d) A. Sathyanarayana, K. Srinivas, A. Mandal, S. Gharami, G. Prabusankar, *J. Chem. Sci*. **2014**, *126*, 1589–1595; e) M. Jonek, A. Makhloufi, P. Rech, W. Frank, C. Ganter, *J. Organomet. Chem.* **2014**, *750*, 140–149.

[18] a) O. Kose, S. Saito, *Org. Biomol.Chem.* **2010**, *8*, 896–900; b) A.K. Verma, J. Singh, V.K. Sankar, R. Chaudhary, R. Chandra, *Tetrahedron Lett.* **2007**, *48*, 4207–42010.

[19] F. E. Hahn, M. C. Jahnke, T. Pape, *Organometallics* **2007**, *26*, 150–154.

[20] F. E. Hahn, M. C. Jahnke, *Angew. Chem., Int. Ed.* **2008**, *47*, 3122–3172.

[21] D. J. Nelson, A. Collado, S. Manzini, S. Meiries, A. M. Z. Slawin, D. B. Cordes, S. P. Nolan, *Organometallics* **2014**, *33*,2048–2058.

[22] Y. Rong, A. Al-Harbi, B. Kriegel, G. Parkin, *Inorg. Chem.* **2013**, *52*, 7172–7182.

[23] B. M. Powell, B. H. Torrie, *Acta Crystallogr., Sect. C* **1983**, *39*, 963–965.

[24] Fantasia, J. L. Petersen, H. Jacobsen, L. Cavallo, S.P. Nolan, *Organometallics* **2007**, *26*, 5880–5889.

[25] a) A. C. Hillier, W. J. Sommer, B. S. Yong, J. L. Petersen, L. Cavallo, S. P. Nolan, *Organometallics* **2003**, *22*, 4322–4326; b) A. B. P. Lever, *Inorg. Chem.* **1990**, *29*, 1271–1285; c) A. B. P. Lever, *Inorg. Chem.***1991**, *30*, 1980–1985; d) S. S. Fielder, M. C. Osborne, A. B. P. Lever, W. J. Pietro, *J. Am. Chem. Soc.* **1995**, *117*, 6990–6993.

[26] A. Decken, C. J. Carmalt, J. A. C. Clyburne, A. H. Cowley, *Inorg. Chem.* **1997**, *36*, 3741–3744.

[27] A. Liske, K. Verlinden, H. Buhl, K. Schaper, C. Ganter, *Organometallics* **2013**, *32*, 5269–5272

[28] S.K. Shih, S. D. Peyerimhoff, R. J. Buenker, M. Perić, *Chem. Phys. Lett.* **1978**, *55*, 206–212

[29] O. Back, M. Henry-Ellinger, C. D. Martin, D. Martin, G. Bertrand, *Angew. Chem., Int. Ed.* **2013**, *52*, 2939–2943.

[30] R. W. Alder, P. R. Allen, M. Murray, A. G. Orpen, *Angew. Chem., Int. Ed. Engl.* **1996**, *35*, 1121–1123.

[31] M. Braun, W. Frank, G. J. Reiß, C. Ganter, *Organometallics* **2010**, *29*, 4418–4420

[32] M. Braun, W. Frank, C. Ganter, *Organometallics* **2012**, *31*, 1927–1934

[33] a)D. J. Nelson, A. Collado, S. Manzini, S. Meiries, A. M. Z. Slawin, D. B. Cordes, S. P. Nolan, *Organometallics*, **2014**, *33*, 2048–2058; b) A. Decken, C. J. Carmalt, J. A. C. Clyburne, A. H. Cowley, Inorg. Chem. **1997**, *36*, 3741–3744; c)M. Regitz, O. J. Scherer, *Multiple Bonds and Low Coordination in Phosphorus Chemistry*, Georg Thieme, Stuttgart and New York, **1990**.d) R. Appel, F. Knoll, I. Ruppert, *Angew. Chem*. **1981**, *93*, 771–784.

[34] a) D. J. Nelson, F. Nahra, S. R. Patrick, D. B. Cordes, A. M. Z. Slawin, S. P.Nolan, *Organometallics***2014**, *33*, 3640–3645; b) S. V. C. Vummaleti, D. J. Nelson, A. Poater, A. Gómez-Suárez, D. B. Cordes, A. M. Z. Slawin, S. P. Nolan, L. Cavallo, *Chem. Sci.* **2015**, *6*, 1895–1904.

[35] a) W. A. Herrmann, B. Cornils, *Angew. Chem. Int. Ed. Engl.* **1997**, *36*, 2162-2187; b) D. Bourissou, O. Guerret, F. P. Gabbai, G. Bertrand, *Chem. Rev.***2000**, *100*, 39–92; c) Y. Ryu, G. Ahumada, C. W. Bielawski, *Chem. Commun.***2019**,*55*, 4451–4466.

[36] a) M. Poyatos, J. A. Mata, E. Peris, *Chem. Rev.***2009**, *109*, 3677–3707; b) J. C. Y. Lin, R. T. W. Huang, C. S. Lee, A. Bhattacharyya, W. S. Hwang, I. J. B. Lin, *Chem. Rev*.**2009**, *109*, 3561–4598; c) P. L. Arnold, I. J. Casely, *Chem. Rev*.**2009**, *109*, 3599–3611; d) C. M. Crudden, D. P. Allen, *Coord. Chem. Rev.* **2004**, *248*, 2247–2273; e) P. C. Purba, S Bhattacharyya, M. Maity, S. Mukhopadhyay, P. Howlader and P. S. Mukherjee, *Chem. Commun.*, 2019, **55**, 8309–8312; f) S. Gonell, E. Peris, M. Poyatos, *Eur. J. Inorg. Chem.* **2019**, 3776–3781.

[37] a) W. A. Herrmann, L. J. Goossen, C. Köcher, G. R. J. Artus, *Angew. Chem. Int. Ed. Engl.***1996**, *35*, 2805–2807; b) S. Diez- Gonzalez, N. Marion, S. P. Nolan, *Chem. Rev.***2009**, *109*, 3612–3676; c) N. E. Kamber, W. Jeong, R. M. Waymouth, R. C. Pratt, B. G. G. Lohmeijer, J. L. Hedrick, *Chem. Rev.* **2007**, *107*, 5813–5840; d) D. Enders, O. Niemeier, A. Henseler, *Chem. Rev.***2007**, *107*, 5606–5655.

[38] a) K. M. Hindi, M. J. Panzner, C. A. Tessier, C. L. Cannon, W. J. Youngs, *Chem. Rev.***2009**, *109*, 3859–2884; b) L. Mercs, M. Albrecht, *Chem. Soc. Rev.* **2010**, *39*, 1903–1912; c) L. Mercs, A. Neels, H. Stoeckli-Evans, M. Albrecht, *Dalton Trans.* **2009**, 7168–7178.

[39] a) A. J. Arduengo, L. I. Iconaru, *Dalton Trans.* **2009**, 6903-6914; b) S. Saravanakumar, M. K. Kindermann, J. Heinicke, M. Kockerling, *Chem. Commun.* **2006**, 640–642.

[40] H. V. Huynh, *Coord. Chem. Rev.***2018**, *118*, 9457–9492.

[41] D. M. Khramov, V. M. Lynch, C. W. Bielawski, *Organometallics,***2007**, *26*, 6042– 6049

[42] A. J. Arduengo, F. Davidson, H. V. R. Dias, J. R. Goerlich, D. Khasnis, W. J. Marshall, T. K. Prakasha, *J. Am. Chem. Soc.* **1997**, *119*, 12742–12749

[43] a) K. R. Grundy, W. R. Roper, *J. Organomet. Chem.* **1975**, *91*, 61–64; b) Z. Kelemen, O. Hollóczki, J. Oláh, L. Nyulászi, *RSC Adv.* **2013**, *3*, 7970–7978.

[44] D. Enders, T. Balensiefer, *Acc. Chem. Res.* **2004**, *37*, 534–541

[45] R. S. Ghadwal, H. W. Roesky, M. Granitzka, D. Stalke, *J. Am. Chem. Soc.* **2010**, *132*, 10018–10020.

[46] K. E. Krahulic, G. D. Enright, M. Parvez, R. Roesler, *J. Am. Chem. Soc.* **2005**, *127*, 4142–4143.

[47] J. I. Bates, P. Kennepohl, D. P. Gates, *Angew. Chem. Int. Ed.* **2009**, *48*, 9844–9847.

[48] D. Mendoza-Espinosa, B. Donnadieu, G. Bertrand, *J. Am. Chem. Soc.* **2010**, *132*, 7264–7265.

[49] P. K. Majhi, PhD thesis, University of Bonn, **2014**.

[50] P. K. Majhi, S. C. Serin, G. Schnakenburg, D. P. Gates, R. Streubel, *Eur. J. Inorg. Chem.* **2014**, 4975–4983.

[51] S. Gaillard, J.-L. Renaud, *Dalton Trans.* **2013**, *42*, 7255–7270.

[52] J. Rauiz, A. F. Mesa, *Chem. Eur. J.* **2012**, *18*, 4485–4488.

[53] D. M. Espinosa, B. Donnadieu, G. Bertrand, *Chem. Asian J.* **2011**, *6*, 1099–1103

[54] R. E. Douthwaite, D. Haüssinger, M. L. H. Green, P. J. Silcock, P. T. Gomes, A. M. Martins, A. A. Danopoulos, *Organometallics* **1999**, *18*, 4584–4590.

[55] W. A. Herrmann, J. Schwarz, M. G. Gardiner, *Organometallics* **1999**, *18*, 4082–4089.

[56] J. A. Mata, A. R. Chianese, J. R. Miecznikowski, M. Poyatos, E. Peris, J. W. Faller, R. H. Crabtree, *Organometallics* **2004**, *23*, 1253–1263.

[57] J. R. Miecznikowski, R. H. Crabtree, *Organometallics* **2004**, *23*, 629–631.

[58] S. Ahrens, E. Herdtweck, S. Goutal, T. Strassner, *Eur. J. Inorg. Chem.* **2006**, 1268–1274.

[57] J. W. Wang, Q. S. Li, F. B. Xu, H. B. Song, Z. Z. Zhang, *Eur. J. Org. Chem.* **2006**, 1310–1316.

[58] M. Slivarichova, E. Reading, M. F. Haddow, H. Othman, G. R. Owen, *Organometallics* **2012**, *31*, 6595–6607.

[59] M. Slivarichova, M. F. Haddow, H. Othman, G. R. Owen, *Eur. J. Inorg. Chem.* **2013**, 2782–2788.

[60] S. Saha, T. Ghatak, B. Saha, H. Doucet, J. K. Bera, *Organometallics* **2012**, *31*, 5500–5505.

[61] S. Zlatogorsky, C. A. Muryn, F. Tuna, D. J. Evans, M. J. Ingleson, *Organometallics* **2011**, *30*, 4974–4982.

[62] J. A. Cabeza, M. Damonte, P. Garcia-Alvarez, E. Perez-Carreno, *Organometallics* **2013**, *32*, 4382–4390.

[63] M. Micksch, T. Strassner, *Eur. J. Inorg. Chem.* **2012**, 5872–5880.

[64] Z. Shi, R. P. Thummel, *J. Org. Chem.* **1995**, *60*, 5935–5945.

[65] W. W. H. Wong, M. S. Vickers, A. R. Cowley, R. L. Paul, P. D. Beer, *Org. Biomol. Chem.* **2005**, *3*, 4201–4208.

[66] C. H. Suresh, M. J. Ajitha, *J. Org. Chem.* **2013**, *78*, 3918–3924.

[67] H. M. Bass, S. A. Cramer, A. S. McCullough, K. J. Bernstein, C. R. Murdock, D. M. Jenkins, *Organometallics* **2013**, *32*, 2160–2167.

[68] H. M. Bass, S. A. Cramer, J. L. Price, D. M. Jenkins, *Organometallics* **2010**, *29*, 3235–3238.

[69] F. E. Hahn, V. Langenhahn, T. Lügger, T. Pape, D. Le Van, *Angew. Chem.* **2005**, *117*, 3825–3829; *Angew. Chem. Int. Ed.* **2005**, *44*, 3759–3763.

[70] R. McKie, J. A. Murphy, S. R. Park, M. D. Spicer, S.-Z. Zhou, *Angew. Chem.* **2007**, *119*, 6645-6648; *Angew. Chem. Int. Ed.* **2007**, *46*, 6525–6528.

[71] D. Pugh, A. A. Danopoulos, *Coord. Chem. Rev.* **2007**, *251*, 610–641.

[72] A. J. Huckaba, T. K. Hollis, T. O. Howell, H. U. Valle, Y. Wu, *Organometallics* **2013**, *32*, 63–69.

[73] X. Zhang, A. M. Wright, N. J. DeYonker, T. K. Hollis, N. I. Hammer, C. E. Webster, E. J. Valente, *Organometallics* **2012**, *31*, 1664–1672.

[74] a) N. Darmawan, C. H. Yang, M. Mauro, M. Raynal, S. Heun, J. Pan, H. Buchholz, P. Braunstein, L. De Cola, *Inorg. Chem.* **2013**, *52*, 10756–10765; b) X. Hu, I. Castro-Rodriguez, K. Meyer, *Organometallics* **2003**, *22*, 3016–3018.

[75] Y. Wang, Y. Xie, M. Y. Abraham, P. Wei, H. F. Schaefer, P.v. R. Schleyer, G. H. Robinson, *J. Am. Chem. Soc*. **2010**, *132*, 14370–14372

[76] D. M. Khramov, A. J. Boydston and C. W. Bielawski, *Angew. Chem. Int. Ed.* **2006**, *45*, 6186 – 6189.

[77] A. J. Boydston, K. A. Williams, C. W. Bielawski, *J. Am. Chem. Soc.* **2005**, *127*, 12496–12497.

[78] J. W. Kamplain, C. W. Bielawski, *Chem. Commun.* **2006**, 1727–1729.

[79] A. J. Boydston, C. W. Bielawski, *Dalton Trans.* **2006**, 4073–4077.

[80] A. J. Boydston, J. D. Rice, M. D. Sanderson, O. L. Dykhno, C. W. Bielawski, *Organometallics* **2006**, *25*, 6087–6098.

[81] A. G. Tennyson, R. J. Ono, T. W. Hudnall, D. M. Khramov, J. A. V. Er, J. W. Kamplain, V. M. Lynch, J. L. Sessler, C. W. Bielawski, *Chem. Eur. J.* **2010**, *16*, 304−315.

[82] A. Prades, E. Peris, M. Alcarazo, *Organometallics* 2012, **31**, 4623−4626.

[83] a) E. Peris, *Chem. Rev.***2018**, *118*, 9988–10031; b) M. Böhmer, G. Guisado-Barrios, F. Kampert, F. Roelfes, Tan, T. Tsai Yuan, E. Peris and E. Hahn, *Organometallics* **2019,** *38*, 2120−213.

[84] M. Schmidtendorf, C. Schulte to Brinke, F. E. Hahn, *Organometallics* **2014**, *751*, 620–627.

[85] D.P. Allen, C. M. Crudden, L. A. Calhoun, R. Wang, *Organometallics* **2004**, *689*, 3203– 3209.

[86] P. K. Majhi, G. Schnakenburg, R. Streubel, *Dalton Trans.* **2014**, *43*, 16673–16679.

[87] F. Bonati, A. Burini, B. R. Pietroni, B. Bovio, *Organometallics* **1989**, *375*, 147–160.

[88] J. A. Mata, F. E. Hahn, E. Peris, Heterometallic Complexes, Tandem Catalysis and Catalytic Cooperativity. *Chem. Sci.* **2014**, *5*, 1723–1732.

[89] R. Bertani, M. Mozzon, R. A. Michelin, F. Benetollo, G. Bombieri, T. J. Castilho, A. J. L. Pombeiro; *Inorg. Chim. Acta* **1991**, *189*, 175– 187.

[90] L. Xiang, J. Xiao, L. Deng; *Organometallics* **2011**, *30*, 2018–2025.

[91] S. E. Flowers, M. B. Cossairt, *Organometallics* **2014**, *33*, 4341–4344.

[92] a) S. Conde-Guadano, M. Hanton, R. P. Tooze, A. A. Danopoulos, P. Braunstein, *Dalton Trans*. **2012**, *41*, 12558–12567; b) S. Conde-Guadano, A. A. Danopoulos, R. Pattacini, M. Hanton, R. P. Tooze, *Organometallics* **2012**, *31*, 1643–1652.

[93] L. Benhamou, V. César, H. Gornitzka, N. Lugan, Guy Lavigne, *Chem. Commun*., **2009**, 4720–4722.

[94] S. Kronig, E. Theuergarten, C. G. Daniliuc, P. G. Jones, Matthias Tamm, *Angew. Chem. Int. Ed.* **2012**, *51*, 3240 –3244.

[95] A. A. Danopoulos, K. Y. Monakhov, P. Braunstein, *Chem. Eur. J*. **2013**, *19*, 450–455.

[96] P. K. Majhi, G. Schnakenburg, Z. Kelemen, L. Nyulászi, D. P. Gates, R. Streubel, *Angew. Chem*. **2013**, *125*, 10264–10267; *Angew. Chem. Int. Ed.* **2013**, *52*, 10080–10083.

[97] Y. Kobayashi, J. Kumadaki, A. Ohsawa, W. Hamana, Tetrahedron Lett. **1976**, *41*, 3715–3716.

[98] Y. Kobayashi, H. Hamana, S. Fujino, A. Ohsawa, I. Kumadaki, *J. Am. Chem. Soc.* **1980**, *102*, 252–255.

[99] a) I. M. Downie, J. B. Lee, M. F. S. Matough, *Chem. Commun.* **1968**, 1350–1351; b) T. Kalisch, Z. Kelemen, L. Nyulászi, R. Streubel, to be published.

[100] Y. Kobayashi, S. Fujino, J. Kumadaki, *J. Am. Chem. Soc.* **1981**, *103*, 2465–2466.

[101] A. Koner, G. Pfeifer, Z. Kelemen, G. Schnakenburg, L. Nyulászi, T. Sasamori, R. Streubel, *Angew. Chem. Int. Ed.* **2017**, *56*, 9231–9235.

[102] A. Koner, Z. Kelemen, G. Schnakenburg, L. Nyulászi, R. Streubel, *Chem. Commun.* **2018**, *54*, 1182–1184.

[103] A. Koner, PhD Thesis, University of Bonn, **2017**.

[104] I. Begum, G. Schnakenburg, Z. Kelemen, L. Nyulászi, R. T. Boeré and R. Streubel, *Chem. Commun*. **2018**, *54*, 13555–13558.

[105] I. Begum, PhD Thesis, University of Bonn, **2019**.

[106] D. M. Wolfe, P. R. Schreiner, *Eur. J. Org. Chem.* **2007**, 2825–2838.

[107] (a) B. L. Benac, E. M. Burgess, A. J. Arduengo III, *Org. Synth.* **1986**, *64*, 92–94. (b) D. J. Williams, S. K. Tata, M. C. Koether, V. L. H. Bevilaqua, B. E. Huck, R. E. Hart, *Chem. Educ.* **2002**, *7*, 167–172. (c) J. Kister, G. Assef, G. Mille, J. Metzger, *Can. J. Chem.* **1979**, *57*, 813–821. (d) H. R. Kim, I. G. Jung, K. Yoo, K. Jang, E. S. Lee, J. Yun, S. U. Son, *Chem.Commun.* **2010**, *46*, 758–760. (e) S. Sauerbrey, P. K. Majhi, J. Daniels, G. Schnakenburg, G. M. Brändle, K. Scherer, R. Streubel, *Inorg. Chem.* **2011**, *50*, 793–799.

[108] S. Sauerbrey, PhD thesis, University of Bonn, **2010.**

[109] P. K. Majhi, A. Koner, G. Schnakenburg, Z. Kelemen, L. Nyulászi, R. Streubel, *Eur. J. Inorg. Chem.* **2016**, 3559–3573.

[110] M. Davis, F. G. Mann, *J. Chem. Soc.* **1964**, 3770–3785.

[111] G. Märkl, W. Weber, W. Weiß, *Chem. Ber.***1985**, *118*, 2365–2395.

[112] N. Avarvari, M. Fourmigué, *Chem. Commun*. **2004**, 2794–2795.

[113] D. Fenske, E. Langer, M. Heymann, H. J. Becher, *Chem. Ber.* **1976**, *109*, 359–362.

[114] A. N. Huryeva, A. P. Marchenko, G. N. Koidan, A. A. Yurchenko, E. V. Zarudnitskii, A. M. Pinchuk, A. N. Kostyuk, *Heteroat. Chem*., **2010**, *21*, 103–118.

[115] a) A. Koner, S. Sauerbrey, G. Schnakenburg, A. Bauzá, A. Frontera, R. Streubel, *Eur. J. Inorg. Chem.*, **2018**, 904–916; b) A. Koner, M. Kunz, G. Schnakenburg, R. Streubel, *Eur. J. Inorg. Chem*., **2018**, 3778–3784.

[116] I. Begum, G. Schnakenburg, Z. Kelemen, L. Nyulaszi, R. T. Boere, R. Streubel, *Chem. Commun.* **2018**, *54*, 13555–1355.

[117] A. Gese, PhD thesis, University of Bonn, **2020.**

[118] N. R. Naz, G. Schnakenburg, A. Mikeházi, Z. Kelemen, L. Nyulászi, R. T. Boeré, R. Streubel, *Chem. Commun.* **2020**, *56*, 2646–2649.

[119] a) M. Banerjee, G. Roy, *Inorg. Chem*. **2017**, *56*, 12739−12750; b) G. Roy, P. N. Jayaram, G.Mugesh, *Chem. Asian J*. **2013**, *8*, 1910 – 1921.

[120] N. C. Payne, A Geissler, A. Button, A. R. Sasuclark, A. L. Schroll, E. L. Ruggles, V. N. Gladyshev, R. J. Hondal, *Free Rad Bio and Medicine*, **2017**, *104*, 249–261.

[121] a) P. K. Majhi, S. Sauerbrey, G. Schnakenburg, A. J. Arduengo III, R. Streubel, *Inorg. Chem*. **2012**, *51*, 10408–10416; b) P. K. Majhi, S. C. Serin, G. Schnakenburg, D. P. Gates, R. Streubel, *Eur. J. Inorg. Chem*., **2014**, 4975–4983.

[122] U. Fleischer, W. Kutzelnigg, A. Bleiber, J. Sauer, *J. Am. Chem. Soc*., **1993**, *115*, 7833–7838.

[123] B. Bildstein, M. Malaun, H. Kopacka, K. H. Ongania, K. Wurst, *J. Organomet. Chem.* **1998**, *552*, 45–61.

[124] P. W. Codding, K. A. Kerr, *Acta Cryst*. **1978**, *34*, 3785–3787.

[125] K. Al-Farhan, *J. Cryst. Spectr. Res*. **1992**, *22*, 687–689.

[126] a) S. Saravanakumar, A. I. Oprea, M. K. Kindermann, P. G.Jones, J. Heinicke, *Chem. Eur. J.* **2006**, *12*, 3143–3154; b) F. E. Hahn, M. C. Jahnke, V. Gomez-Benitez, D. Morales-Morales, T. Pape, *Organometallics,* **2005**, *24*, 6458–6463.

[127] a) F. E. Hahn, L. Wittenbecher, R. Boose, D. Bläser, *Chem. Eur. J.* **1999**, *5*, 1931-1935; b) F. M. Rivas, U. Riaz, A. Giessert, J. A. Smulik, S. T. Diver, *Org. Lett.* **2001**, *3*, 2673–2676.

[128] G. T. S. Andavan, E. B. Bauer, C. S. Letko, T. K. Hollis, F. S. Tham, *Journal of Organometallic*, **2005**, *690*, 5938–5947.

[129] a) A. J. Arduengo III, J. R. Goerlick, W. J. Marshall, *J. Am. Chem. Soc.* **1995**, *117*, 11027–11028; b) M. K. Denk, A. Thadani, K. Hatano, A. J. Lough, *Angew. Chem.* **1997**, *109*, 2719–2721; *Angew. Chem. Int. Ed.* **1997**, *36*, 2067; c) F. E. Hahn, M. Paas,D. L. Van, T. Lügger, *Angew. Chem.* **2003**, *115*, 5402; *Angew. Chem. Int. Ed.* **2003**, *42*, 5243.

[130] Gaussian 09, Revision B.01, M. J. Frisch, G. W. Trucks, H. B. Schlegel, G. E. Scuseria, M. A. Robb, J. R. Cheeseman, G. Scalmani, V. Barone, B. Mennucci, G. A. Petersson, H. Nakatsuji, M. Caricato, X. Li, H. P. Hratchian, A. F. Izmaylov, J. Bloino, G. Zheng, J. L. Sonnenberg, M. Hada, M. Ehara, K. Toyota, R. Fukuda, J. Hasegawa, M. Ishida, T. Nakajima, Y. Honda, O. Kitao, H. Nakai, T. Vreven, J. A. Montgomery, Jr., J. E. Peralta, F. Ogliaro, M. Bearpark, J. J. Heyd, E. Brothers, K. N. Kudin, V. N. Staroverov, T. Keith, R. Kobayashi, J. Normand, K. Raghavachari, A. Rendell, J. C. Burant, S. S. Iyengar, J. Tomasi, M. Cossi, N. Rega, J. M. Millam, M. Klene, J. E. Knox, J. B. Cross, V. Bakken, C. Adamo, J. Jaramillo, R. Gomperts, R. E. Stratmann, O. Yazyev, A. J. Austin, R. Cammi, C. Pomelli, J. W. Ochterski, R. L. Martin, K. Morokuma, V. G. Zakrzewski, G. A. Voth, P. Salvador, J. J. Dannenberg, S. Dapprich, A. D. Daniels, O. Farkas, J. B. Foresman, J. V. Ortiz, J. Cioslowski, D. J. Fox, Gaussian Inc., Wallingford CT, **2010.**

[131] G. Schaftenaar, J. H. Noordik, *J. Comput. Aided Mol. Design,* **2000**, *14*, 123–134.

[132] **9′***cis/trans*, **10a′** = compounds with methyl substituents.

[133] L. Nyulászi, A. Forró, T. Veszprémi, PCCP, **2000**, *2,* 3127–3129.

[134] K. Verlinden, H. Buhl, W. Frank, C. Ganter, *Eur. J. Inorg. Chem.* **2015**, 2416–2425.

[135] F. Diness, D. P. Fairlie, *Angew. Chem. Inter. Ed*. **2012**, *51*, 8012–8016.

[136] J. H. M. Wang, I. J. B. Lin, *Organometallics,* **1998**, *17*, 972–975.

[137] J. C. Garrison, W. J. Youngs, *Chem. Rev*. **2005**, *105*, 3978–4008.

[138] P. de Fre´mont, N. M. Scott, E. D. Stevens, S. P. Nolan, *Organometallics* **2005**, *24,* 2411–2418.

[139] M. R. L. Furst, C. S. J. Cazin, *Chem. Commun.*, **2010**, *46*, 6924–6925

[140] H. M. J. Wang, C. S. Vasam, T. Y. R. Tsai, S.-H. Chen, A. H. H. Chang, I. J. B. Lin, *Organometallics*, **2005**, *24*, 486–493.

[141] M. V. Baker, P. J. Barnard, S. J. Berners-Price, S. K. Brayshaw, J. L. Hickey, B.

W. Skelton, A. H. White, *Organometallics* **2005**, *690*, 5625–5635.

[142] E. Schuh, C. Pfluger, A. Citta, A. Folda, M. P. Rigobello, A. Bindoli, A. Casini, F. Mohr, *J. Med. Chem*. **2012**, *55*, 5518–5528.

[143] G. T. S. Andavan, E. B. Bauer, C. S. Letko, T. K. Hollis, F. S. Tham, *Journal of Organometallic* **2005**, *690*, 5938–5947.

[144] J. I. Bates, P. Kennepohl, D. P. Gates, *Angew. Chem.* **2009**, *121*, 10028–10031; *Angew. Chem. Int. Ed.* **2009**, *48*, 9844-9847.

[145] J. I. Bates, D. P. Gates, *Organometallics* **2012**, *31*, 4529–4536.

[146] F. Wudl, M. Kaplan, E. Hufnagel, E. Southwick Jr, *J. Org. Chem.* **1974**, *39*, 3608–3609.

[147] D. M. Khramov, Phd thesis, Texas. **2008**.

[148] (a) K. C. Nicolaou, R. L. Magolda, Sipio, W. E. Barnette, Z. Lysenko, M. Joullie, *J. Am.Chem. Soc.* **1980**, *102*, 3784–3793. (b) D. H. R. Barton, M. R. Britten-Kelly, D. Ferreira, *J. Chem. Soc.*, **1978**, 1682–1692. (c) D. L. J. Clive, G. Chittattu, C. K.C. Wong, *J. Chem*. **1977**, *55*, 3894. (d) K. C. Nicolaou, Z. Lysenko, *J. Am. Chem. Soc*. **1977**, *99*, 3185–3187. (e) S. V. Ley, P. J. Murray, *Chem. Commun*. **1982**, 1252–1253; (f) M. Sevrin, D. E. Van, A. Krief, *Tetrahedron Lett.* **1976**, 2643–2646. (g) B. Danieli, G. Lesma, G. Palmisano, S. Tollari, *J. Chem. Soc.*, **1984**, 1237–1240.

[149] R. O. Hutchins, K. Learn, *J. Org. Chem*. **1982**, *47*, 4380–4382.

[150] a) E. J. Corey, H. L. Pearce, I. Székely, M. Ishiguro, *Tetrahedron Lett.* **1978**, 1023. (b) K. C. Nicolaou, W. E. Barnette, R. L. Magolda, P. A. Grieco, W. Owens, C. L. J. Wang, J. B. Smith, M. Ogletree, A. M. Lefer, *Prostaglandins*, **1978**, *16*, 789–794. (c) K. C. Nicolaou, D. A. Claremon, W. E. Barnette, S. P. Seitz, *J. Am. Chem. Soc.* **1979**, *101*, 3704–3706.

[151] a) D. L. J. Clive, G. Chittattu, C. K. Wong, *Chem. Commun.***1978**, *41*, 441–442; (b) D. L. J. Clive, G. J. Chittattu, V. Farina,W. A. Kiel, S.M. Menchen, C. G. Russell, A. Singh, C. K. Wong, N. J. Curtis, *J. Am. Chem. Soc*. **1980**, *102*, 4438–4447.

[152] T. G. Back, S. Collins, U. Gokhale, K. W. Law, *J. Org. Chem.* **1983**, *48*, 4776–4779.

[153] T. G. Back, *Chem. Commun.***1984**, 1417–1418.

[154] U. Fleischer, W. Kutzelnigg, A. Bleiber, J. Sauer, *J. Am. Chem. Soc.***1993**, *115*, 7833–7838.

[155] D. M. Khramov, Phd thesis, Texas. **2008**.

[156] A. Prades, E Peris, M Alcarazo, *Organometallics* **2012**, *31*, 4623−4626.

[157] P. L. Arnold, M. Rodden, C. Wilson, *Chem. Commun.* **2005,** 1743–1745; b) S. P. Downing, A. A. Danopoulos, Organometallics **2006**, *25*, 1337–1340; c) P. L. Arnold, S. T. Liddle, Organometallics **2006**, *25*, 1485–1491; d) M. S. Hill, G. K. Kçhn, D. J. MacDougall, *Inorg. Chem*. **2011**, *50*, 5234–5241; e) R. A. Musgrave, R. S. P. Turbervill, M. Irwin, J. M. Goicoechea, *Angew. Chem*. **2012**, *124,* 10990–10993; *Angew. Chem. Int. Ed.***2012**, *51*, 10832–10835.

[158] P. K. Majhi, G. Schnakenburg, Z. Kelemen, L. Nyulaszi, D. P. Gates, R. Streubel, *Angew. Chem. Int. Ed.*, **2013**, *52*, 10080–10083.

[159] L. Nyulászi, O. Hollóczki, C. Lescop, M. Hissler, R. Réau, *Org. Biomol. Chem.* **2006**, *4*, 996–998.

[160] C. Hay, M. Hissler, C. Fischmeister, J. Rault-Berthelot, L. Toupet, L. Nyulászi, R. Reau, *Chem. Eur. J.* **2001**, *7*, 4222–4236.

[161] K. Verlinden, H. Buhl, W. Frank, C. Ganter, *Eur. J. Inorg. Chem.* 2015, 2416–2425.

[162] M. Feroci, I. Chiarotto, F. D'Anna, F. Gala, R. Noto, L. Ornano, G. Zollo, A. Inesi, *Chem Electro Chem*. **2016**, *3*, 1133–1141.

[163] T. Ramnial, I. McKenzie, B. Gorodetsky, E. M. W. Tsang, J. A. C. Clyburne, *Chem. Commun.*, **2004**, 1054–1055.

[164] L. Mercs, A. Neels, M. Albrecht, *Dalton Trans.* **2008**, 5570–5576.

[165] J. C. Garrison, W. J. Youngs, *Chem. Rev*. **2005**, *105*, 3978–4008.

[166] A. J. Arduengo III, C. J. Carmalt, J. A. C. Clyburne, A. H. Cowley, R. Pyati, *Chem. Commun*. 1997, 981–982.

[167] a) P. Le Floch, *Coord. Chem. Rev.* **2006**, *250*, 627–681;b) C.Müller, L. E. E. Broeckx, I. de Krom, J. J. M. Weemers, *Eur. J. Inorg. Chem.* **2013**, 187–202.

[168] a) R. L. Falconer, C. A. Russell, *Coord. Chem. Rev.* **2015**, *297*, 146–167;b) R. Gleiter, H. Lange, P. Binger, J. Stannek, C. Krügger, J. Bruckmann, U. Zenneck, S. Kummer, *Eur. J. Inorg. Chem.* **1998**, 1619–1621.

169] S. Gundersen, S. Samdal, T. G. Strand, H. V. Volden, *J. Mol. Struct.* **2007**, *832*, 164–171.

[170] K. T. Potts, S. J. Chen, *J. Org. Chem.* **1977**, *42*, 1639–1644.

[171] a) R. Riemschneider, S. Georgi, *Mh. Chem.* **1960**, *91*, 623–629; b) F. Cristiani, F. A. Devillanova, A.Diaz, G. Verani, *Phosphorus and sulfur* **1984**, *20*, 231–240.

[172] F. Wudl, M. Kaplan, E. Hufnagel, E. Southwick Jr, *J. Org. Chem.* **1974**, *39*, 3608–3609.

[173] N. H. T. Huy, B. Donnadieu, G. Bertrand, F. Mathey, *Chem. Asian J.* 2009, 4, 1225–1228.

[174] A. M. Geer , Á. L. Serrano, B.de Bruin, M. A. Ciriano, C. Tejel, *Angew. Chem. Int. Ed*. **2015**, *54*, 472–475.

[175] S. Welfelé, N. Mézailles, N. Maigrot, L. Ricard, F. Mathey, P. Le Floch, *New. J. Chem.* **2001**, *25*, 1264–1268.

[176] T. Kalisch, *Msc.* Thesis, University of Bonn, **2019**.

[177] a) K. Dimroth, W. Steuber, *Angew. Chem. Int. Ed. Engl.* **1967**, *6*, 445–446; b) F. Gerson, G. Plattner, A. J. Ashe III, G. Märkl, *Mol. Phys.* **1974**, *28*, 601–615; c) H. Plato, W. Lubitz, K. Möbius, *J. Phys.Chem.* **1981**, *85*, 1202–1219.

[178] F. Gerson, P. Merstetter, S. Pfenninger, G. Märkl, *Magn. Reson. Chem.* **1997**, *35*, 384–388.

[179] N. Kuhn, T. Kratz, *Synthesis* **1993**, 561–562.

[180] A. Hettche, K. Dimroth, *Chem. Ber.* **1973**, *106*, 1001–1011.

[181] P. K. Majhi, G. Schnakenburg, A. J. Arduengo, R. Streubel, *Aust. J. Chem.* **2015**, *68*,1282–1292.

[182] G. A. Wiley, W. R. Stine, *Tetrahedron Lett.* **1967**, *8*, 2321–2324.

[183] B. Punji, J. T. Mague, M. S. Balakrishna, *Inorg. Chem*. **2007**, *46*, 10268–10275.

[184] M. T. Reetz, W. F. Maier, *Liebigs Ann. Chem*. **1980**, 1471–1473.

13. Appendix

13.1 Crystal data and structure refinement for 6*cis* (NRN-142).

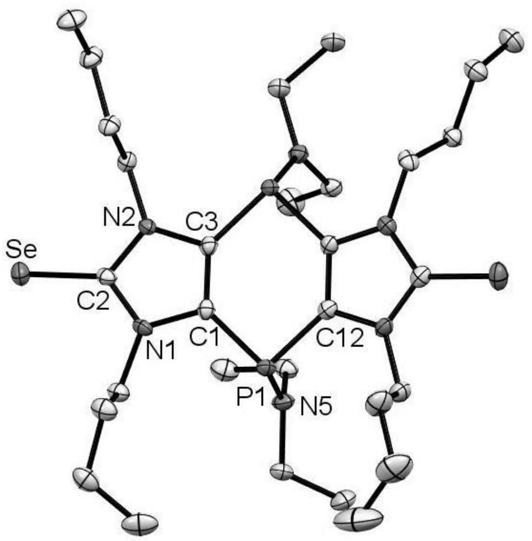

Table 13.1. Crystal data and structure refinement for **6***cis*

Identification code	GSTR592// GXray5366
Crystal Habitus	clear colourless plate
Device Type	Bruker D8-Venture
Empirical formula	$C_{30}H_{56}N_6P_2Se_2$
Moiety formula	C30 H56 N6 P2 Se2
Formula weight	720.66
Temperature/K	123
Crystal system	Triclinic
Space group	P-1
a/Å	9.2393(5)
b/Å	13.1195(7)
c/Å	16.0254(7)
α/°	74.256(4)
β/°	75.947(4)
γ/°	74.656(4)
Volume/Å^3	1772.13(17)
Z	2
ρ_{calc}g/cm^3	1.351
μ/mm^{-1}	2.205

F(000)	752.0
Crystal size/mm^3	0.12 × 0.1 × 0.03
Absorption correction	Integration
Tmin; Tmax	0.5308; 0.8344
Radiation	MoKα (λ = 0.71073)
2Θ range for data collection/°	5.374 to 51.992°
Completeness to theta	0.982
Index ranges	-11 ≤ h ≤ 11, -15 ≤ k ≤ 16, -19 ≤ l ≤ 19
Reflections collected	13026
Independent reflections	6846 [R_{int} = 0.0368, R_{sigma} = 0.0634]
Data/restraints/parameters	6846/0/369
Goodness-of-fit on F^2	1.098
Final R indexes [I>=2σ (I)]	R_1 = 0.0493, wR_2 = 0.1090
Final R indexes [all data]	R_1 = 0.0742, wR_2 = 0.1142
Largest diff. peak/hole / e Å^{-3}	1.00/-0.54

Table 13.2. Bond Lengths for **6*^{cis}***.

Atom	Atom	Length/Å	Atom	Atom	Length/Å
Se1	C2	1.835(5)	N5	C25	1.461(6)
Se2	C13	1.845(5)	N6	C27	1.480(6)
P1	N5	1.679(4)	N6	C29	1.472(6)
P1	C1	1.815(4)	C1	C3	1.370(6)
P1	C12	1.822(5)	C4	C5	1.523(7)
P2	N6	1.677(4)	C5	C6	1.539(7)
P2	C3	1.836(5)	C6	C7	1.520(7)
P2	C14	1.809(4)	C8	C9	1.520(6)
N1	C1	1.403(6)	C9	C10	1.531(6)
N1	C2	1.354(6)	C10	C11	1.519(7)
N1	C4	1.471(6)	C12	C14	1.375(6)
N2	C2	1.367(6)	C15	C16	1.526(7)
N2	C3	1.381(5)	C16	C17	1.509(7)
N2	C8	1.471(5)	C17	C18	1.482(11)
N3	C12	1.391(6)	C19	C20	1.523(6)
N3	C13	1.351(6)	C20	C21	1.525(6)
N3	C15	1.471(6)	C21	C22	1.520(7)
N4	C13	1.359(6)	C23	C24	1.516(7)
N4	C14	1.397(6)	C25	C26	1.531(7)
N4	C19	1.471(6)	C27	C28	1.509(7)
N5	C23	1.486(6)	C29	C30	1.511(7)

Table 13.3. Bond Angles for $\mathbf{6}^{cis}$.

Atom	Atom	Atom	Angle/°	Atom	Atom	Atom	Angle/°
N5	P1	C1	104.3(2)	N2	C2	Se1	126.7(3)
N5	P1	C12	106.4(2)	N2	C3	P2	120.3(3)
C1	P1	C12	94.5(2)	C1	C3	P2	130.7(3)
N6	P2	C3	111.2(2)	C1	C3	N2	106.5(4)
N6	P2	C14	104.23(19)	N1	C4	C5	112.3(4)
C14	P2	C3	95.4(2)	C4	C5	C6	111.2(4)
C1	N1	C4	125.2(4)	C7	C6	C5	113.4(4)
C2	N1	C1	110.3(4)	N2	C8	C9	112.2(4)
C2	N1	C4	124.5(4)	C8	C9	C10	110.7(4)
C2	N2	C3	111.1(4)	C11	C10	C9	112.7(4)
C2	N2	C8	123.2(4)	N3	C12	P1	120.4(3)
C3	N2	C8	125.7(4)	C14	C12	P1	132.9(3)
C12	N3	C15	125.0(4)	C14	C12	N3	106.2(4)
C13	N3	C12	111.1(4)	N3	C13	Se2	127.1(3)
C13	N3	C15	123.7(4)	N3	C13	N4	105.9(4)
C13	N4	C14	110.2(4)	N4	C13	Se2	126.9(4)
C13	N4	C19	122.6(4)	N4	C14	P2	120.6(3)
C14	N4	C19	127.1(4)	C12	C14	P2	132.1(4)
C23	N5	P1	117.4(3)	C12	C14	N4	106.7(4)
C25	N5	P1	124.9(3)	N3	C15	C16	110.5(4)
C25	N5	C23	116.3(4)	C17	C16	C15	114.1(5)
C27	N6	P2	117.4(3)	C18	C17	C16	113.9(6)
C29	N6	P2	125.2(3)	N4	C19	C20	113.6(4)
C29	N6	C27	116.5(4)	C19	C20	C21	110.1(4)
N1	C1	P1	120.4(3)	C22	C21	C20	112.3(4)
C3	C1	P1	133.0(3)	N5	C23	C24	113.2(4)
C3	C1	N1	106.7(4)	N5	C25	C26	114.6(4)
N1	C2	Se1	127.8(3)	N6	C27	C28	114.8(4)
N1	C2	N2	105.4(4)	N6	C29	C30	114.1(4)

13.2 Crystal data and structure refinement for 7^{cis} (NRN-157).

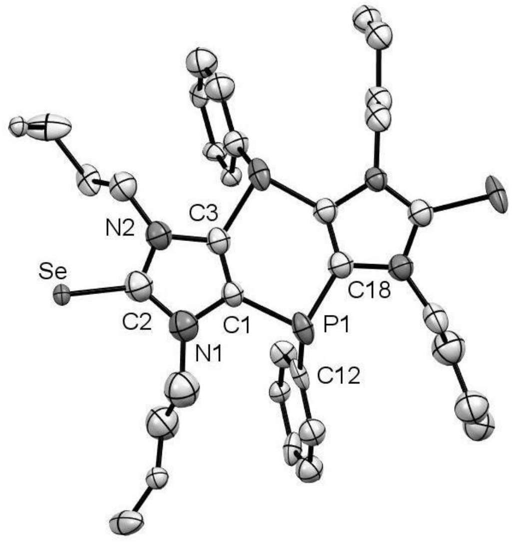

Table 13.4. Crystal data and structure refinement for $\mathbf{7}^{cis}$

Identification code	GSTR602// GXray5474_0m0
Crystal Habitus	clear colourless block
Device Type	Bruker X8-KappaApexII
Empirical formula	$C_{34}H_{46}N_4P_2Se_2$
Moiety formula	C34 H46 N4 P2 Se2
Formula weight	730.61
Temperature/K	100
Crystal system	Monoclinic
Space group	$P2_1/c$
a/Å	18.3842(15)
b/Å	17.5919(15)
c/Å	22.8537(18)
α/°	90
β/°	110.672(4)
γ/°	90
Volume/Å^3	6915.3(10)
Z	8
ρ_{calc}g/cm^3	1.403
μ/mm^{-1}	2.260
F(000)	3008.0
Crystal size/mm^3	0.18 × 0.1 × 0.09
Absorption correction	Empirical
Tmin; Tmax	0.318422; 0.745907

Radiation	MoKα (λ = 0.71073)
2Θ range for data collection/°	2.368 to 56°
Completeness to theta	1.000
Index ranges	$-24 \leq h \leq 22, 0 \leq k \leq 23, 0 \leq l \leq 30$
Reflections collected	58121
Independent reflections	16702 [R_{int} = 0.3241, R_{sigma} = 0.2110]
Data/restraints/parameters	16702/478/866
Goodness-of-fit on F^2	1.067
Final R indexes [I>=2σ (I)]	R_1 = 0.1626, wR_2 = 0.3642
Final R indexes [all data]	R_1 = 0.2772, wR_2 = 0.4240
Largest diff. peak/hole / e $Å^{-3}$	1.88/-1.39

Table 13.5. Bond Lengths for **7*cis***

Atom	Atom	Length/Å	Atom	Atom	Length/Å
Se1	C2	1.857(13)	P2'	C3'	1.802(11)
Se2	C20	1.857(12)	P2'	C19'	1.848(10)
P1	C1	1.836(11)	P2'	C29'	1.832(9)
P1	C12	1.820(12)	N1'	C1'	1.423(14)
P1	C18	1.814(12)	N1'	C2'	1.356(13)
P2	C3	1.834(12)	N1'	C4'	1.506(18)
P2	C19	1.818(12)	N2'	C2'	1.341(14)
P2	C29	1.827(11)	N2'	C3'	1.412(13)
N1	C1	1.411(15)	N2'	C8'	1.490(14)
N1	C2	1.405(17)	N3'	C18'	1.433(12)
N1	C4	1.501(19)	N3'	C20'	1.346(13)
N2	C2	1.316(16)	N3'	C21'	1.441(12)
N2	C3	1.434(15)	N4'	C19'	1.413(13)
N2	C8	1.415(15)	N4'	C20'	1.379(13)
N3	C18	1.420(14)	N4'	C25'	1.470(15)
N3	C20	1.380(15)	C1'	C3'	1.305(14)
N3	C21	1.439(15)	C4'	C5'	1.46(2)
N4	C19	1.417(14)	C5'	C6'	1.58(3)
N4	C20	1.310(14)	C5'	C6T	1.58(3)
N4	C25	1.461(15)	C6'	C7'	1.53(3)
C1	C3	1.291(16)	C7T	C6T	1.503(9)
C2	Se1S	1.902(13)	C8'	C9'	1.505(17)
C4	C5	1.52(2)	C9'	C10'	1.552(17)
C5	C6	1.490(9)	C10'	C11'	1.518(9)
C5	C6S	1.679(19)	C10'	C11T	1.513(9)
C6	C7	1.495(9)	C12'	C13'	1.409(15)
C8	C9	1.519(15)	C12'	C17'	1.373(13)
C9	C10	1.557(17)	C13'	C14'	1.384(15)

C10	C11	1.51(3)	C14'	C15'	1.358(15)
C10	C11S	1.513(9)	C15'	C16'	1.390(15)
C12	C13	1.392(16)	C16'	C17'	1.343(13)
C12	C17	1.436(13)	C18'	C19'	1.321(13)
C13	C14	1.383(17)	C20'	Se2T	1.759(11)
C14	C15	1.391(15)	C21'	C22'	1.537(13)
C15	C16	1.386(15)	C22'	C23'	1.543(13)
C16	C17	1.365(14)	C23'	C24'	1.487(9)
C18	C19	1.316(16)	C23'	C24T	1.514(9)
C25	C26	1.540(16)	C25'	C26'	1.512(17)
C26	C27	1.535(16)	C26'	C27'	1.535(19)
C27	C28	1.513(6)	C27'	C28'	1.500(9)
C27	C28S	1.515(9)	C29'	C30'	1.395(11)
C29	C30	1.432(15)	C29'	C34'	1.426(14)
C29	C34	1.375(17)	C30'	C31'	1.366(14)
C30	C31	1.350(13)	C31'	C32'	1.385(15)
C31	C32	1.377(15)	C32'	C33'	1.389(15)
C32	C33	1.415(18)	C33'	C34'	1.373(15)
C33	C34	1.341(17)	C7S	C6S	1.503(9)
Se1'	C2'	1.825(11)	C21	C22	1.561(18)
Se2'	C20'	1.904(10)	C22	C23	1.503(9)
P1'	C1'	1.838(11)	C23	C24	1.510(9)
P1'	C12'	1.832(10)	C23	C24S	1.520(9)
P1'	C18'	1.792(10)			

Table 13.6. Bond Angles for **7**^{cis}.

Atom	**Atom**	**Atom**	**Angle/°**	**Atom**	**Atom**	**Atom**	**Angle/°**
C12	P1	C1	101.8(5)	C29'	P2'	C19'	102.3(4)
C18	P1	C1	94.3(5)	C1'	N1'	C4'	127.6(10)
C18	P1	C12	104.8(5)	C2'	N1'	C1'	109.0(9)
C19	P2	C3	93.6(5)	C2'	N1'	C4'	123.2(10)
C19	P2	C29	104.2(5)	C2'	N2'	C3'	112.9(9)
C29	P2	C3	103.9(5)	C2'	N2'	C8'	123.5(9)
C1	N1	C4	125.7(11)	C3'	N2'	C8'	123.4(9)
C2	N1	C1	106.4(10)	C18'	N3'	C21'	125.2(8)
C2	N1	C4	127.9(12)	C20'	N3'	C18'	110.7(8)
C2	N2	C3	108.4(10)	C20'	N3'	C21'	124.1(8)
C2	N2	C8	121.8(11)	C19'	N4'	C25'	128.7(9)
C8	N2	C3	129.8(10)	C20'	N4'	C19'	108.0(8)
C18	N3	C21	126.0(10)	C20'	N4'	C25'	123.2(9)
C20	N3	C18	108.5(9)	N1'	C1'	P1'	118.3(8)

C20	N3	C21	125.5(10)	C3'	C1'	P1'	131.8(9)
C19	N4	C25	125.0(9)	C3'	C1'	N1'	109.2(9)
C20	N4	C19	110.7(9)	N1'	C2'	Se1'	127.5(8)
C20	N4	C25	124.2(10)	N2'	C2'	Se1'	128.2(8)
N1	C1	P1	119.6(8)	N2'	C2'	N1'	104.2(9)
C3	C1	P1	130.7(9)	N2'	C3'	P2'	121.6(7)
C3	C1	N1	109.0(10)	C1'	C3'	P2'	132.8(8)
N1	C2	Se1	113.8(9)	C1'	C3'	N2'	104.6(9)
N1	C2	Se1S	131.8(10)	C5'	C4'	N1'	114.0(13)
N2	C2	Se1	137.9(10)	C4'	C5'	C6'	128.4(16)
N2	C2	N1	107.9(11)	C4'	C5'	C6T	94.2(13)
N2	C2	Se1S	120.2(10)	C7'	C6'	C5'	107.5(16)
N2	C3	P2	116.6(8)	N2'	C8'	C9'	112.9(9)
C1	C3	P2	133.6(9)	C8'	C9'	C10'	113.6(10)
C1	C3	N2	108.3(10)	C11'	C10'	C9'	102.8(10)
N1	C4	C5	113.0(11)	C11T	C10'	C9'	112.0(12)
C4	C5	C6S	121.3(11)	C13'	C12'	P1'	116.8(7)
C6	C5	C4	94.5(10)	C17'	C12'	P1'	125.3(8)
C5	C6	C7	127.7(13)	C17'	C12'	C13'	117.8(9)
N2	C8	C9	114.9(10)	C14'	C13'	C12'	120.5(10)
C8	C9	C10	113.5(9)	C15'	C14'	C13'	119.3(10)
C11	C10	C9	107.0(12)	C14'	C15'	C16'	120.6(10)
C11S	C10	C9	110.8(13)	C17'	C16'	C15'	119.9(10)
C13	C12	P1	118.3(8)	C16'	C17'	C12'	121.9(10)
C13	C12	C17	118.3(10)	N3'	C18'	P1'	121.0(7)
C17	C12	P1	123.5(9)	C19'	C18'	P1'	132.9(8)
C14	C13	C12	120.4(11)	C19'	C18'	N3'	105.4(8)
C13	C14	C15	120.4(12)	N4'	C19'	P2'	118.5(7)
C16	C15	C14	120.2(11)	C18'	C19'	P2'	131.1(8)
C17	C16	C15	120.3(9)	C18'	C19'	N4'	109.7(9)
C16	C17	C12	120.5(10)	N3'	C20'	Se2'	132.4(7)
N3	C18	P1	119.1(8)	N3'	C20'	N4'	106.1(8)
C19	C18	P1	133.4(10)	N3'	C20'	Se2T	120.8(8)
C19	C18	N3	107.0(10)	N4'	C20'	Se2'	121.4(8)
N4	C19	P2	120.3(8)	N4'	C20'	Se2T	132.4(8)
C18	C19	P2	130.8(9)	N3'	C21'	C22'	113.0(8)
C18	C19	N4	107.3(10)	C21'	C22'	C23'	113.7(8)
N3	C20	Se2	124.6(8)	C24'	C23'	C22'	114.6(10)
N4	C20	Se2	128.9(9)	C24T	C23'	C22'	110.4(12)
N4	C20	N3	106.4(10)	N4'	C25'	C26'	112.5(9)
N4	C25	C26	114.9(9)	C25'	C26'	C27'	111.1(9)

C27	C26	C25	113.9(9)	C28'	C27'	C26'	110.9(12)
C28	C27	C26	112.7(10)	C30'	C29'	P2'	124.8(8)
C28S	C27	C26	100.8(10)	C30'	C29'	C34'	118.9(8)
C30	C29	P2	123.4(9)	C34'	C29'	P2'	116.3(6)
C34	C29	P2	120.6(9)	C31'	C30'	C29'	120.6(9)
C34	C29	C30	116.0(10)	C30'	C31'	C32'	120.4(9)
C31	C30	C29	121.3(10)	C31'	C32'	C33'	120.3(10)
C30	C31	C32	121.1(10)	C34'	C33'	C32'	120.3(10)
C31	C32	C33	118.1(11)	C33'	C34'	C29'	119.5(8)
C34	C33	C32	120.1(13)	C7S	C6S	C5	109.3(13)
C33	C34	C29	123.3(13)	C7T	C6T	C5'	121.5(16)
C12'	P1'	C1'	105.3(5)	N3	C21	C22	115.4(9)
C18'	P1'	C1'	94.2(5)	C23	C22	C21	111.5(10)
C18'	P1'	C12'	101.8(4)	C22	C23	C24	98.9(12)
C3'	P2'	C19'	94.0(5)	C22	C23	C24S	125.7(14)
C3'	P2'	C29'	103.8(4)				

13.3 Crystal data and structure refinement for 9*trans*

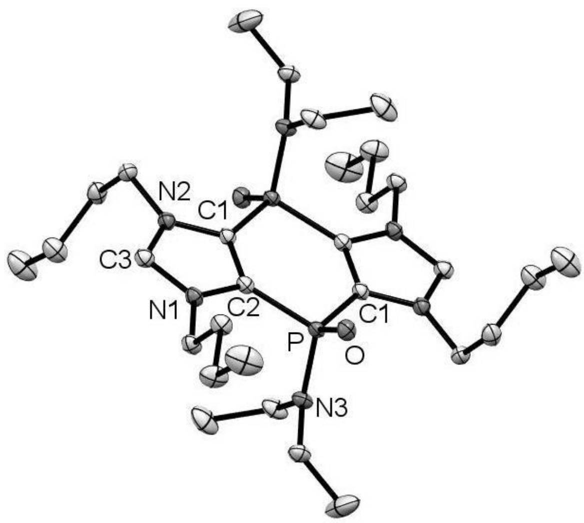

Table 13.7. Crystal data and structure refinement for **9***trans*.

Identification code	GSTR619// GXray5630f
Crystal Habitus	clear light yellow block
Device Type	Bruker X8-KappaApexII
Empirical formula	$C_{30}H_{56}N_6O_2P_2$
Moiety formula	C30 H56 N6 O2 P2
Formula weight	594.74

Temperature/K	100
Crystal system	monoclinic
Space group	$P2_1/c$
a/Å	8.6880(5)
b/Å	20.2501(11)
c/Å	9.9593(5)
α/°	90
β/°	104.166(2)
γ/°	90
Volume/Å^3	1698.89(16)
Z	2
ρ_{calc}g/cm^3	1.163
μ/mm^{-1}	0.163
F(000)	648.0
Crystal size/mm^3	0.22 × 0.21 × 0.16
Absorption correction	empirical
Tmin; Tmax	0.6810; 0.7462
Radiation	MoKα (λ = 0.71073)
2Θ range for data collection/°	5.238 to 55.996°
Completeness to theta	0.998
Index ranges	$-11 \le h \le 11$, $-26 \le k \le 26$, $-13 \le l \le 13$
Reflections collected	52094
Independent reflections	4102 [R_{int} = 0.0322, R_{sigma} = 0.0161]
Data/restraints/parameters	4102/0/185
Goodness-of-fit on F^2	1.111
Final R indexes [I>=2σ (I)]	R_1 = 0.0387, wR_2 = 0.0943
Final R indexes [all data]	R_1 = 0.0417, wR_2 = 0.0966
Largest diff. peak/hole / e Å^{-3}	0.34/-0.30

Table 13.8. Bond Lengths for **9**^{trans}

Atom	Atom	Length/Å	Atom	Atom	Length/Å
P	O	1.4769(9)	N3	C14	1.4709(16)
P	N3	1.6448(11)	C1	C2	1.3688(17)
P	C1	1.7921(13)	C2	P^1	1.8000(13)
P	C2^1	1.8000(13)	C4	C5	1.5234(17)
N1	C2	1.3966(16)	C5	C6	1.5262(18)
N1	C3	1.3686(17)	C6	C7	1.519(2)
N1	C4	1.4695(16)	C8	C9	1.5245(19)
N2	C1	1.3971(16)	C9	C10	1.5220(19)
N2	C3	1.3674(17)	C10	C11	1.525(2)

N2	C8	1.4715(16)	C12	C13	1.511(2)
N3	C12	1.4734(16)	C14	C15	1.523(2)

Table 13.9. Bond Angles for **9*trans***

Atom	**Atom**	**Atom**	**Angle/°**	**Atom**	**Atom**	**Atom**	**Angle/°**
O	P	N3	112.46(5)	N2	C1	P	125.34(9)
O	P	C1	115.25(6)	C2	C1	P	128.57(10)
O	P	C2[1]	112.77(6)	C2	C1	N2	106.09(11)
N3	P	C1	105.66(6)	N1	C2	P[1]	124.04(9)
N3	P	C2[1]	108.74(6)	C1	C2	P[1]	130.28(10)
C1	P	C2[1]	101.11(6)	C1	C2	N1	105.62(11)
C2	N1	C4	125.52(11)	N2	C3	N1	102.40(11)
C3	N1	C2	113.08(10)	N1	C4	C5	114.40(11)
C3	N1	C4	121.39(11)	C4	C5	C6	110.28(11)
C1	N2	C8	125.53(11)	C7	C6	C5	113.04(13)
C3	N2	C1	112.80(11)	N2	C8	C9	113.60(11)
C3	N2	C8	121.63(11)	C10	C9	C8	114.42(11)
C12	N3	P	120.28(9)	C9	C10	C11	111.59(12)
C14	N3	P	120.25(9)	N3	C12	C13	112.80(12)
C14	N3	C12	117.17(10)	N3	C14	C15	113.84(12)

13.4 Crystal data and structure refinement for 10c*trans*.

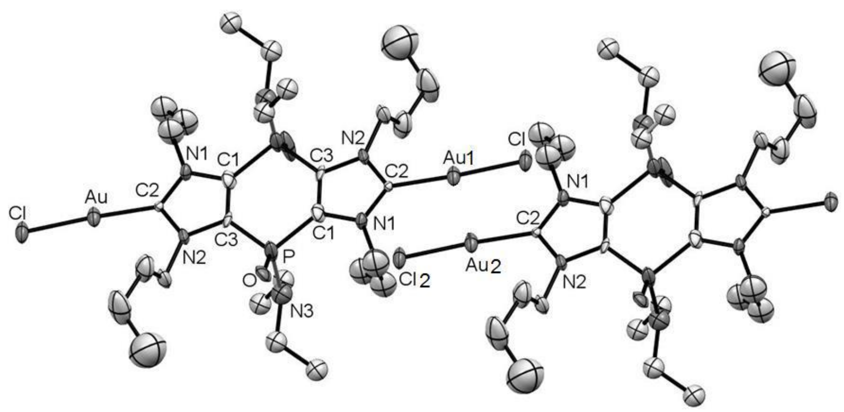

Table 13.10. Crystal data and structure refinement for **10c*trans***.

Identification code	GSTR670// GXray5974h
Crystal Habitus	clear colourless plank
Device Type	Bruker APEX-II CCD
Empirical formula	$C_{32}H_{60}N_6O_2P_2Cl_6Au_2$

Moiety formula	C30 H56 Au2 Cl2 N6 O2 P2, 2(C H2 Cl2)
Formula weight	1229.43
Temperature/K	100
Crystal system	Triclinic
Space group	P-1
a/Å	10.0790(10)
b/Å	10.7792(11)
c/Å	34.650(4)
α/°	87.642(3)
β/°	87.059(3)
γ/°	64.781(3)
Volume/Å^3	3400.4(6)
Z	3
ρ_{calc}g/cm^3	1.801
μ/mm^{-1}	6.924
F(000)	1800.0
Crystal size/mm^3	0.28 × 0.18 × 0.14
Absorption correction	Empirical
Tmin; Tmax	0.0057; 0.1854
Radiation	MoKα (λ = 0.71073)
2Θ range for data collection/°	1.178 to 50.5°
Completeness to theta	0.999
Index ranges	-12 ≤ h ≤ 12, -12 ≤ k ≤ 12, -41 ≤ l ≤ 41
Reflections collected	72074
Independent reflections	12268 [R_{int} = 0.1066, R_{sigma} = 0.0747]
Data/restraints/parameters	12268/81/689
Goodness-of-fit on F^2	1.244
Final R indexes [I>=2σ (I)]	R_1 = 0.0892, wR_2 = 0.1809
Final R indexes [all data]	R_1 = 0.1015, wR_2 = 0.1861
Largest diff. peak/hole / e Å^{-3}	4.79/-7.94

Table 13.11. Bond Lengths for **10c*trans***.

Atom	Atom	Length/Å	Atom	Atom	Length/Å
Au1	Au2[1]	3.2600(9)	C17	C18	1.51(3)
Au1	Cl1	2.278(4)	C19	C20	1.52(3)
Au1	C2	1.996(15)	C20	C21	1.50(2)
Au2	Cl2	2.286(4)	C21	C22	1.55(3)
Au2	C13	1.966(17)	C23	C24	1.52(2)
P1	O1	1.474(12)	C25	C26	1.51(2)
P1	N5	1.604(15)	C27	C28	1.47(3)

P1	C1	1.801(16)	C29	C30	1.55(3)
P1	C12	1.775(14)	Au3	Au3[2]	3.1601(13)
P2	O2	1.454(13)	Au3	Cl3	2.287(4)
P2	N6	1.643(19)	Au3	C32	1.984(17)
P2	C3	1.789(15)	P3	O3	1.453(12)
P2	C14	1.801(16)	P3	N9	1.624(16)
N1	C1	1.389(19)	P3	C31	1.788(16)
N1	C2	1.345(19)	P3	C33[3]	1.784(16)
N1	C4	1.45(2)	N7	C31	1.400(19)
N2	C2	1.349(19)	N7	C32	1.35(2)
N2	C3	1.38(2)	N7	C34	1.47(2)
N2	C8	1.45(2)	N8	C32	1.35(2)
N3	C12	1.415(19)	N8	C33	1.39(2)
N3	C13	1.38(2)	N8	C38	1.48(2)
N3	C15	1.481(19)	N9	C42	1.47(2)
N4	C13	1.34(2)	N9	C44	1.49(2)
N4	C14	1.367(19)	C31	C33	1.39(2)
N4	C19	1.471(19)	C34	C35	1.48(3)
N5	C23	1.50(2)	C35	C36	1.44(3)
N5	C25	1.45(2)	C36	C37	1.52(3)
N6	C27	1.49(3)	C38	C39	1.51(2)
N6	C29	1.45(2)	C39	C40	1.50(3)
C1	C3	1.36(2)	C40	C41	1.51(3)
C4	C5	1.53(3)	C42	C43	1.53(2)
C5	C6	1.52(2)	C44	C45	1.51(3)
C6	C7	1.50(3)	Cl4	C46	1.745(19)
C8	C9	1.56(3)	Cl5	C46	1.771(18)
C9	C10	1.48(3)	Cl6	C47	1.81(2)
C10	C11	1.58(4)	Cl7	C47	1.76(2)
C12	C14	1.38(2)	Cl8	C48	1.76(2)
C15	C16	1.51(2)	Cl9	C48	1.74(3)
C16	C17	1.54(2)			

[1]-1+X,1+Y,+Z; [2]1-X,1-Y,1-Z; [3]-X,2-Y,1-Z

Table 13.12. Bond Angles for **10c***trans*.

Atom	**Atom**	**Atom**	**Angle/°**	**Atom**	**Atom**	**Atom**	**Angle/°**
Cl1	Au1	Au2[1]	100.77(11)	N3	C13	Au2	126.7(12)
C2	Au1	Au2[1]	83.6(5)	N4	C13	Au2	128.8(12)
C2	Au1	Cl1	175.6(5)	N4	C13	N3	104.2(14)

Cl2	Au2	Au1^{2}	101.05(11)	N4	C14	P2	123.9(12)
C13	Au2	Au1^{2}	82.0(5)	N4	C14	C12	108.3(13)
C13	Au2	Cl2	176.8(5)	C12	C14	P2	127.8(11)
O1	P1	N5	113.4(7)	N3	C15	C16	110.0(13)
O1	P1	C1	11<2.6(7)	C15	C16	C17	111.9(15)
O1	P1	C12	110.1(7)	C18	C17	C16	113.8(15)
N5	P1	C1	108.5(7)	N4	C19	C20	111.8(15)
N5	P1	C12	112.1(7)	C21	C20	C19	110.5(18)
C12	P1	C1	99.3(7)	C20	C21	C22	110.2(18)
O2	P2	N6	114.5(8)	N5	C23	C24	113.2(14)
O2	P2	C3	116.3(7)	N5	C25	C26	114.4(15)
O2	P2	C14	112.8(7)	C28	C27	N6	113.1(15)
N6	P2	C3	104.8(8)	N6	C29	C30	113(2)
N6	P2	C14	106.7(7)	Cl3	Au3	Au3^{3}	101.22(11)
C3	P2	C14	100.3(7)	C32	Au3	Au3^{3}	83.1(5)
C1	N1	C4	126.3(13)	C32	Au3	Cl3	175.4(5)
C2	N1	C1	110.1(12)	O3	P3	N9	114.7(7)
C2	N1	C4	123.2(13)	O3	P3	C31	113.5(7)
C2	N2	C3	110.1(13)	O3	P3	C33^{4}	114.8(7)
C2	N2	C8	122.9(13)	N9	P3	C31	107.5(7)
C3	N2	C8	126.9(13)	N9	P3	C33^{4}	104.6(7)
C12	N3	C15	125.6(12)	C33^{4}	P3	C31	100.2(7)
C13	N3	C12	111.4(12)	C31	N7	C34	125.9(13)
C13	N3	C15	122.6(13)	C32	N7	C31	111.1(13)
C13	N4	C14	112.3(14)	C32	N7	C34	122.8(13)
C13	N4	C19	122.4(13)	C32	N8	C33	111.5(14)
C14	N4	C19	125.2(13)	C32	N8	C38	122.9(13)
C23	N5	P1	121.0(12)	C33	N8	C38	125.3(13)
C25	N5	P1	121.1(11)	C42	N9	P3	121.9(12)
C25	N5	C23	117.5(14)	C42	N9	C44	117.3(16)
C27	N6	P2	119.7(12)	C44	N9	P3	119.7(13)
C29	N6	P2	120.6(17)	N7	C31	P3	125.1(11)
C29	N6	C27	119.1(19)	C33	C31	P3	128.9(12)
N1	C1	P1	123.5(11)	C33	C31	N7	106.0(13)
C3	C1	P1	129.8(12)	N7	C32	Au3	129.2(12)
C3	C1	N1	106.6(13)	N7	C32	N8	105.5(14)
N1	C2	Au1	127.0(11)	N8	C32	Au3	125.3(12)
N1	C2	N2	106.4(13)	N8	C33	P3^{4}	123.3(12)
N2	C2	Au1	126.6(11)	C31	C33	P3^{4}	130.7(13)
N2	C3	P2	122.6(11)	C31	C33	N8	105.8(13)
C1	C3	P2	129.6(12)	N7	C34	C35	115.2(19)

C1	C3	N2	106.9(13)	C36	C35	C34	125(3)
N1	C4	C5	110.0(15)	C35	C36	C37	113(3)
C6	C5	C4	112.8(17)	N8	C38	C39	111.3(13)
C7	C6	C5	113.1(18)	C40	C39	C38	114.4(17)
N2	C8	C9	110.3(15)	C39	C40	C41	114.2(17)
C10	C9	C8	114(2)	N9	C42	C43	115.2(14)
C9	C10	C11	108(2)	N9	C44	C45	113.4(18)
N3	C12	P1	124.8(10)	Cl4	C46	Cl5	111.4(10)
C14	C12	P1	131.4(11)	Cl7	C47	Cl6	108.9(11)
C14	C12	N3	103.7(12)	Cl9	C48	Cl8	110.7(12)

^{1}-1+X,1+Y,+Z; ^{2}1+X,-1+Y,+Z; ^{3}1-X,1-Y,1-Z; ^{4}-X,2-Y,1-Z

13.5 Crystal data and structure refinement for 12*trans* (NRN-166).

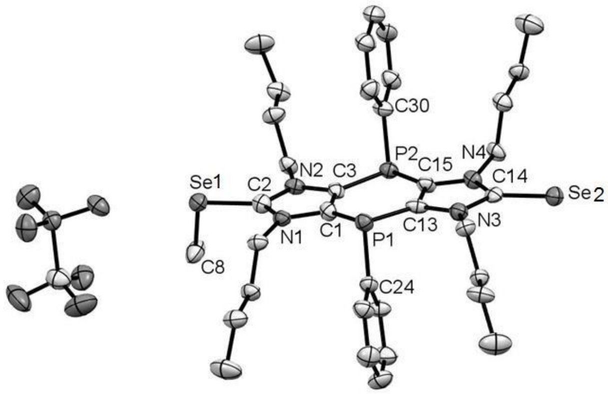

Table 13.13. Crystal data and structure refinement for **12*trans***.

Identification code	GSTR606// GXray5510
Crystal Habitus	clear colourless needle
Device Type	STOE IPDS-2T
Empirical formula	$C_{38}H_{53}Cl_4F_3N_4O_3P_2SSe_2$
Moiety formula	C35 H49 N4 P2 Se2, 2(C H2 Cl2), C F3 O3 S
Formula weight	1064.56
Temperature/K	123
Crystal system	monoclinic
Space group	Pc
a/Å	8.3944(4)
b/Å	14.2835(9)
c/Å	19.7123(9)

α/°	90
β/°	97.948(3)
γ/°	90
Volume/Å^3	2340.8(2)
Z	2
ρ_{calc}g/cm^3	1.510
μ/mm^{-1}	1.972
F(000)	1084.0
Crystal size/mm^3	0.4 × 0.03 × 0.02
Absorption correction	integration
Tmin; Tmax	0.3551; 0.8479
Radiation	MoKα (λ = 0.71073)
2Θ range for data collection/°	5.67 to 50.5°
Completeness to theta	0.999
Index ranges	-10 ≤ h ≤ 9, -17 ≤ k ≤ 17, -23 ≤ l ≤ 23
Reflections collected	14955
Independent reflections	7812 [R_{int} = 0.1102, R_{sigma} = 0.1094]
Data/restraints/parameters	7812/2/519
Goodness-of-fit on F^2	0.945
Final R indexes [I>=2σ (I)]	R_1 = 0.0587, wR_2 = 0.1312
Final R indexes [all data]	R_1 = 0.0794, wR_2 = 0.1399
Largest diff. peak/hole / e Å^{-3}	0.62/-1.08
Flack parameter	0.007(17)

Table 13.14. Bond Lengths for **12*trans***.

Atom	Atom	Length/Å	Atom	Atom	Length/Å
Se1	C2	1.888(13)	C16	C17	1.522(16)
Se1	C8	1.953(12)	C17	C18	1.511(16)
Se2	C14	1.818(13)	C18	C19	1.508(19)
P1	C1	1.801(13)	C20	C21	1.526(16)
P1	C13	1.815(13)	C21	C22	1.500(17)
P1	C24	1.819(11)	C22	C23	1.496(18)
P2	C3	1.823(12)	C24	C25	1.401(16)
P2	C15	1.832(12)	C24	C29	1.409(15)
P2	C30	1.830(11)	C25	C26	1.383(18)
N1	C1	1.381(16)	C26	C27	1.381(17)
N1	C2	1.345(16)	C27	C28	1.374(18)
N1	C4	1.491(14)	C28	C29	1.394(17)
N2	C2	1.331(15)	C30	C31	1.428(16)
N2	C3	1.377(16)	C30	C35	1.385(16)
N2	C9	1.500(14)	C31	C32	1.382(17)

N3	C14	1.396(15)	C32	C33	1.375(19)
N3	C13	1.386(16)	C33	C34	1.391(18)
N3	C16	1.459(15)	C34	C35	1.381(17)
N4	C14	1.344(16)	Cl1	C37	1.78(2)
N4	C15	1.366(16)	Cl2	C37	1.713(18)
N4	C20	1.491(14)	Cl4	C38	1.766(13)
C1	C3	1.373(16)	Cl14	C38	1.738(15)
C4	C5	1.497(15)	S	O1	1.452(8)
C5	C6	1.533(17)	S	O2	1.421(10)
C6	C7	1.531(19)	S	O3	1.445(9)
C9	C10	1.525(16)	S	C36	1.829(14)
C10	C11	1.513(16)	F1	C36	1.313(17)
C11	C12	1.495(18)	F2	C36	1.331(17)
C13	C15	1.371(15)	F3	C36	1.368(15)

Table 13.15. Bond Angles for **12**^{trans}.

Atom	**Atom**	**Atom**	**Angle/°**	**Atom**	**Atom**	**Atom**	**Angle/°**
C2	Se1	C8	97.7(5)	N4	C15	P2	121.7(8)
C1	P1	C13	95.7(5)	N4	C15	C13	107.3(10)
C1	P1	C24	101.6(5)	C13	C15	P2	130.7(10)
C13	P1	C24	100.5(5)	N3	C16	C17	114.3(9)
C3	P2	C15	96.4(5)	C18	C17	C16	112.5(9)
C3	P2	C30	100.9(5)	C19	C18	C17	113.8(10)
C30	P2	C15	100.5(5)	N4	C20	C21	112.5(9)
C1	N1	C4	123.7(10)	C22	C21	C20	112.5(9)
C2	N1	C1	111.3(10)	C23	C22	C21	112.5(10)
C2	N1	C4	124.9(10)	C25	C24	P1	118.7(8)
C2	N2	C3	110.2(10)	C25	C24	C29	118.5(10)
C2	N2	C9	124.9(10)	C29	C24	P1	122.8(8)
C3	N2	C9	124.8(10)	C26	C25	C24	120.9(11)
C14	N3	C16	123.4(10)	C27	C26	C25	120.5(12)
C13	N3	C14	109.8(10)	C28	C27	C26	119.3(12)
C13	N3	C16	126.5(10)	C27	C28	C29	121.7(11)
C14	N4	C15	111.9(9)	C28	C29	C24	119.1(11)
C14	N4	C20	122.8(10)	C31	C30	P2	121.9(9)
C15	N4	C20	124.2(10)	C35	C30	P2	118.5(8)
N1	C1	P1	121.9(8)	C35	C30	C31	119.6(10)
C3	C1	P1	132.8(10)	C32	C31	C30	118.5(11)
C3	C1	N1	104.8(10)	C33	C32	C31	121.1(11)
N1	C2	Se1	124.8(9)	C32	C33	C34	120.4(11)
N2	C2	Se1	128.6(9)	C35	C34	C33	119.8(11)

N2	C2	N1	106.2(11)	C34	C35	C30	120.5(10)
N3	C14	Se2	126.6(9)	Cl2	C37	Cl1	110.9(9)
N4	C14	Se2	128.7(9)	Cl14	C38	Cl4	109.9(7)
N4	C14	N3	104.7(10)	O1	S	C36	102.6(6)
N2	C3	P2	121.5(8)	O2	S	O1	115.8(6)
C1	C3	P2	131.0(10)	O2	S	O3	114.3(6)
C1	C3	N2	107.5(10)	O2	S	C36	104.1(6)
N1	C4	C5	111.8(8)	O3	S	O1	114.6(5)
C4	C5	C6	112.0(9)	O3	S	C36	103.0(6)
C7	C6	C5	112.3(10)	F1	C36	S	112.5(9)
N2	C9	C10	112.5(9)	F1	C36	F2	108.3(12)
C11	C10	C9	111.7(9)	F1	C36	F3	108.3(12)
C12	C11	C10	112.1(10)	F2	C36	S	112.1(10)
N3	C13	P1	121.0(8)	F2	C36	F3	105.6(11)
C15	C13	P1	132.4(10)	F3	C36	S	109.8(9)
C15	C13	N3	106.4(11)				

13.6. Crystal data and structure refinement for **14*trans*** (NRN-176).

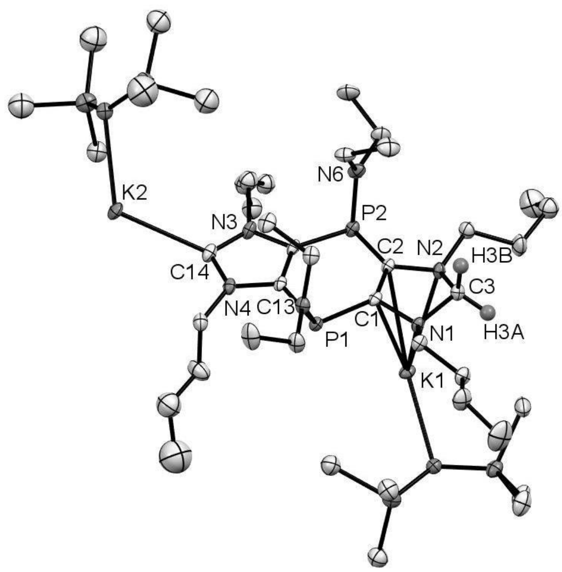

Table 13.16. Crystal data and structure refinement for **14*trans***.

Identification code	GSTR632// GXraycu_5761f
Crystal Habitus	clear colourless plate
Device Type	Bruker D8-Venture
Empirical formula	$C_{42}H_{94}K_2N_8P_2S_4$
Moiety formula	C42 H94 K2 N8 P2 S4

Formula weight	979.63
Temperature/K	150.0
Crystal system	Triclinic
Space group	P-1
a/Å	12.4708(4)
b/Å	12.6826(4)
c/Å	21.2636(7)
α/°	92.658(2)
β/°	93.180(2)
γ/°	117.487(2)
Volume/Å^3	2969.01(17)
Z	2
ρ_{calc}g/cm^3	1.096
μ/mm^{-1}	3.480
F(000)	1068.0
Crystal size/mm^3	0.17 × 0.09 × 0.04
Absorption correction	Empirical
Tmin; Tmax	0.4679; 0.7536
Radiation	CuKα (λ = 1.54178)
2Θ range for data collection/°	7.884 to 135.492°
Completeness to theta	0.998
Index ranges	-14 ≤ h ≤ 14, -15 ≤ k ≤ 15, -25 ≤ l ≤ 25
Reflections collected	98448
Independent reflections	10751 [R_{int} = 0.0940, R_{sigma} = 0.0440]
Data/restraints/parameters	10751/231/642
Goodness-of-fit on F^2	1.021
Final R indexes [I>=2σ (I)]	R_1 = 0.0826, wR_2 = 0.2259
Final R indexes [all data]	R_1 = 0.1082, wR_2 = 0.2489
Largest diff. peak/hole / e Å^{-3}	0.66/-0.94

Table 13.17. Bond Lengths for **14*trans***.

Atom	**Atom**	**Length/Å**	**Atom**	**Atom**	**Length/Å**
K1	S1^1	3.6556(17)	S4	C42S	1.784(2)
K1	S1	3.6170(17)	S4	C41S	1.782(2)
K1	S2^1	3.6580(17)	P1	N5	1.678(4)
K1	N1	3.032(4)	P1	C1	1.812(5)
K1	N2	3.124(4)	P1	C13	1.804(5)
K1	N7^1	2.861(4)	P2	N6	1.677(4)
K1	N7	2.727(4)	P2	C2	1.820(4)
K1	C1	3.173(4)	P2	C12	1.805(5)

K1	C2	3.244(4)	N1	C1	1.427(5)
K1	C3	3.505(5)	N1	C3	1.450(6)
K1	C32[1]	3.317(6)	N1	C4	1.474(6)
K1	C33	3.386(7)	N2	C2	1.418(5)
K2	K2[2]	3.636(2)	N2	C3	1.460(6)
K2	S3[2]	3.566(2)	N2	C8	1.453(6)
K2	S3	3.658(2)	N3	C12	1.396(6)
K2	S4	3.619(2)	N3	C14	1.355(7)
K2	S4[2]	3.7808(19)	N3	C15	1.416(11)
K2	N8	2.769(4)	N3	C15S	1.62(3)
K2	N8[2]	2.800(4)	N4	C13	1.394(6)
K2	C14	2.905(5)	N4	C14	1.357(6)
K2	C37	3.249(13)	N4	C19	1.459(7)
K2	C42	3.539(15)	N5	C23	1.467(6)
K2	C42S	3.174(17)	N5	C25	1.464(7)
S1	K1[1]	3.6555(17)	N6	C27	1.463(7)
S1	N7	1.665(4)	N6	C29	1.478(7)
S1	C31	1.875(7)	N7	K1[1]	2.861(4)
S1	C32	1.7926(10)	N8	K2[2]	2.800(4)
S1	C33	1.871(7)	C1	C2	1.354(6)
S2	K1[1]	3.6579(17)	C4	C5	1.512(7)
S2	N7	1.675(4)	C5	C6	1.527(8)
S2	C34	1.808(15)	C6	C7	1.455(11)
S2	C35	1.912(14)	C8	C9	1.528(8)
S2	C36	1.916(16)	C9	C10	1.490(9)
S2	C34S	1.893(15)	C10	C11	1.402(12)
S2	C35S	1.815(15)	C12	C13	1.366(7)
S2	C36S	1.873(16)	C15	C16	1.503(8)
S3	K2[2]	3.566(2)	C16	C17	1.515(14)
S3	N8	1.656(4)	C17	C18	1.432(12)
S3	C37	1.947(12)	C18	C17S	1.94(3)
S3	C38	1.7904(10)	C19	C20	1.495(9)
S3	C39	1.826(17)	C20	C21	1.484(12)
S3	C37S	1.7901(10)	C21	C22	1.4992(10)
S3	C38S	1.781(2)	C23	C24	1.507(8)
S3	C39S	1.74(3)	C25	C26	1.508(8)
S4	K2[2]	3.7808(19)	C27	C28	1.489(9)
S4	N8	1.675(4)	C29	C30	1.521(9)
S4	C40	1.932(12)	C32	K1[1]	3.317(6)
S4	C41	1.804(9)	C15S	C16S	1.58(3)
S4	C42	1.826(12)	C16S	C17S	1.53(3)
S4	C40S	1.87(3)			

[1]1-X,1-Y,1-Z; [2]1-X,-Y,-Z

Table 13.18. Bond Angles for **14**^{trans}.

Atom	Atom	Atom	Angle/°	Atom	Atom	Atom	Angle/°
S1	K1	S1[1]	117.51(3)	C35S	S2	K1[1]	162.6(6)
S1	K1	S2[1]	98.57(4)	C35S	S2	K1	101.9(7)
S1[1]	K1	S2[1]	48.89(4)	C35S	S2	C34S	108.7(8)
N1	K1	S1[1]	142.97(8)	C35S	S2	C36S	102.8(8)
N1	K1	S1	96.75(7)	C36S	S2	K1[1]	79.2(6)
N1	K1	S2[1]	143.44(8)	C36S	S2	K1	78.5(6)
N1	K1	N2	42.78(10)	C36S	S2	C34S	104.9(8)
N1	K1	C1	26.47(10)	K2[2]	S3	K2	60.43(4)
N1	K1	C2	42.08(10)	N8	S3	K2[2]	49.84(15)
N1	K1	C3	24.28(10)	N8	S3	K2	45.75(16)
N1	K1	C32[1]	114.09(8)	N8	S3	C37	107.9(4)
N1	K1	C33	81.03(15)	N8	S3	C38	113.8(4)
N2	K1	S1[1]	122.22(8)	N8	S3	C39	118.1(6)
N2	K1	S1	114.47(8)	N8	S3	C37S	117.9(10)
N2	K1	S2[1]	100.74(8)	N8	S3	C38S	115.4(10)
N2	K1	C1	41.65(11)	N8	S3	C39S	122.1(10)
N2	K1	C2	25.64(10)	C37	S3	K2[2]	94.3(4)
N2	K1	C3	24.60(10)	C37	S3	K2	62.3(4)
N2	K1	C32[1]	106.81(13)	C38	S3	K2[2]	68.8(4)
N2	K1	C33	85.15(14)	C38	S3	K2	122.3(4)
N7[1]	K1	S1[1]	26.15(8)	C38	S3	C37	97.9(6)
N7	K1	S1	25.90(9)	C38	S3	C39	113.6(7)
N7[1]	K1	S1	100.57(8)	C39	S3	K2	123.3(6)
N7	K1	S1[1]	102.35(9)	C39	S3	K2[2]	162.2(6)
N7	K1	S2[1]	104.86(9)	C39	S3	C37	102.6(7)
N7[1]	K1	S2[1]	26.33(8)	C37S	S3	K2[2]	71.4(10)
N7[1]	K1	N1	161.45(11)	C37S	S3	K2	92.0(11)
N7	K1	N1	103.38(11)	C38S	S3	K2	155.1(10)
N7[1]	K1	N2	122.01(11)	C38S	S3	K2[2]	124.3(10)
N7	K1	N2	135.08(11)	C38S	S3	C37S	112.8(15)
N7	K1	N7[1]	95.12(11)	C39S	S3	K2	87.2(11)
N7[1]	K1	C1	136.84(12)	C39S	S3	K2[2]	140.6(11)
N7	K1	C1	123.54(12)	C39S	S3	C37S	89.4(16)
N7	K1	C2	145.37(12)	C39S	S3	C38S	94.7(15)
N7[1]	K1	C2	119.38(11)	K2	S4	K2[2]	58.81(4)
N7[1]	K1	C3	145.15(12)	N8	S4	K2[2]	43.02(15)
N7	K1	C3	111.89(12)	N8	S4	K2	47.21(15)
N7	K1	C32[1]	115.64(15)	N8	S4	C40	114.9(4)

N7^{1}	K1	C32^{1}	54.76(9)	N8	S4	C41	116.5(4)
N7^{1}	K1	C33	111.09(16)	N8	S4	C42	117.7(5)
N7	K1	C33	56.24(15)	N8	S4	C40S	116.0(10)
C1	K1	S1	122.59(9)	N8	S4	C42S	108.4(6)
C1	K1	S1^{1}	116.76(8)	N8	S4	C41S	108.9(11)
C1	K1	S2^{1}	131.41(9)	C40	S4	K2	127.2(4)
C1	K1	C2	24.32(11)	C40	S4	K2^{2}	149.6(4)
C1	K1	C3	39.31(11)	C41	S4	K2	125.2(4)
C1	K1	C32^{1}	88.57(9)	C41	S4	K2^{2}	77.4(3)
C1	K1	C33	106.63(15)	C41	S4	C40	107.3(6)
C2	K1	S1	134.59(8)	C41	S4	C42	110.4(6)
C2	K1	S1^{1}	107.65(8)	C42	S4	K2	72.8(5)
C2	K1	S2^{1}	107.76(8)	C42	S4	K2^{2}	121.4(5)
C2	K1	C3	39.19(11)	C42	S4	C40	85.8(7)
C2	K1	C32^{1}	85.13(12)	C40S	S4	K2	158.0(10)
C2	K1	C33	108.54(14)	C40S	S4	K2^{2}	121.8(11)
C3	K1	S1^{1}	145.64(9)	C42S	S4	K2^{2}	103.8(6)
C3	K1	S1	95.51(9)	C42S	S4	K2	61.3(5)
C3	K1	S2^{1}	120.78(9)	C42S	S4	C40S	131.3(12)
C32^{1}	K1	S1^{1}	29.28(2)	C41S	S4	K2	101.3(13)
C32^{1}	K1	S1	138.71(11)	C41S	S4	K2^{2}	65.9(11)
C32^{1}	K1	S2^{1}	73.05(8)	C41S	S4	C40S	98.1(15)
C32^{1}	K1	C3	123.93(12)	C41S	S4	C42S	85.1(14)
C32^{1}	K1	C33	164.80(14)	N5	P1	C1	107.38(19)
C33	K1	S1^{1}	135.83(14)	N5	P1	C13	103.11(19)
C33	K1	S1	30.77(12)	C13	P1	C1	96.8(2)
C33	K1	S2^{1}	95.86(15)	N6	P2	C2	107.1(2)
C33	K1	C3	70.52(15)	N6	P2	C12	103.3(2)
K2^{2}	K2	S3	58.53(4)	C12	P2	C2	96.4(2)
K2^{2}	K2	S4^{2}	58.38(4)	C1	N1	K1	82.3(2)
S3^{2}	K2	K2^{2}	61.04(4)	C1	N1	C3	104.0(4)
S3^{2}	K2	S3	119.57(4)	C1	N1	C4	118.3(3)
S3^{2}	K2	S4	101.57(5)	C3	N1	K1	96.4(2)
S3	K2	S4^{2}	96.89(4)	C3	N1	C4	114.7(4)
S3^{2}	K2	S4^{2}	48.88(4)	C4	N1	K1	134.3(3)
S4	K2	K2^{2}	62.81(4)	C2	N2	K1	81.9(2)
S4	K2	S3	49.48(4)	C2	N2	C3	104.6(3)
S4	K2	S4^{2}	121.19(4)	C2	N2	C8	120.7(4)
N8	K2	K2^{2}	49.61(9)	C3	N2	K1	92.5(3)
N8^{2}	K2	K2^{2}	48.87(9)	C8	N2	K1	133.0(3)
N8^{2}	K2	S3^{2}	26.88(8)	C8	N2	C3	116.6(4)
N8	K2	S3	25.37(9)	C12	N3	C15	127.0(6)

$N8^2$	K2	S3	102.46(10)	C12	N3	C15S	120.2(11)
N8	K2	$S3^2$	105.44(10)	C14	N3	C12	113.3(4)
N8	K2	S4	26.35(8)	C14	N3	C15	119.0(6)
N8	K2	$S4^2$	103.57(9)	C14	N3	C15S	125.5(11)
$N8^2$	K2	$S4^2$	24.09(9)	C13	N4	C19	124.3(4)
$N8^2$	K2	S4	107.03(10)	C14	N4	C13	112.7(4)
N8	K2	$N8^2$	98.49(12)	C14	N4	C19	123.0(4)
$N8^2$	K2	C14	139.29(15)	C23	N5	P1	118.5(4)
N8	K2	C14	117.26(15)	C25	N5	P1	122.9(3)
$N8^2$	K2	C37	101.0(3)	C25	N5	C23	116.0(4)
N8	K2	C37	57.3(2)	C27	N6	P2	124.0(3)
N8	K2	C42	55.1(2)	C27	N6	C29	117.5(5)
$N8^2$	K2	C42	121.3(3)	C29	N6	P2	117.8(4)
$N8^2$	K2	C42S	114.2(3)	K1	N7	$K1^1$	84.88(11)
N8	K2	C42S	55.85(10)	S1	N7	$K1^1$	104.61(18)
C14	K2	$K2^2$	158.84(12)	S1	N7	K1	108.43(19)
C14	K2	S3	102.47(12)	S1	N7	S2	129.9(3)
C14	K2	$S3^2$	136.84(12)	S2	N7	$K1^1$	104.42(18)
C14	K2	S4	113.65(12)	S2	N7	K1	114.05(19)
C14	K2	$S4^2$	120.85(11)	K2	N8	$K2^2$	81.51(12)
C14	K2	C37	84.1(3)	S3	N8	$K2^2$	103.28(18)
C14	K2	C42	96.1(3)	S3	N8	K2	108.9(2)
C14	K2	C42S	102.3(3)	S3	N8	S4	132.2(3)
C37	K2	$K2^2$	74.7(2)	S4	N8	K2	106.44(19)
C37	K2	$S3^2$	126.9(2)	S4	N8	$K2^2$	112.9(2)
C37	K2	S3	32.0(2)	P1	C1	K1	100.28(17)
C37	K2	S4	80.9(2)	N1	C1	K1	71.3(2)
C37	K2	$S4^2$	84.1(2)	N1	C1	P1	118.2(3)
C37	K2	C42	102.7(3)	C2	C1	K1	80.7(2)
C42	K2	$K2^2$	87.9(2)	C2	C1	P1	130.7(3)
C42	K2	$S3^2$	103.4(2)	C2	C1	N1	108.8(4)
C42	K2	S3	74.8(2)	P2	C2	K1	109.02(17)
C42	K2	$S4^2$	143.0(2)	N2	C2	K1	72.5(2)
C42	K2	S4	29.52(19)	N2	C2	P2	119.0(3)
C42S	K2	$K2^2$	83.6(2)	C1	C2	K1	74.9(2)
C42S	K2	S3	77.54(11)	C1	C2	P2	132.1(3)
C42S	K2	$S3^2$	96.1(3)	C1	C2	N2	107.8(4)
C42S	K2	$S4^2$	136.5(3)	N1	C3	K1	59.3(2)
C42S	K2	S4	29.53(4)	N1	C3	N2	101.1(3)
K1	S1	$K1^1$	62.49(3)	N2	C3	K1	62.9(2)
N7	S1	K1	45.67(14)	N1	C4	C5	112.0(4)

N7	S1	K1^{1}	49.24(14)	C4	C5	C6	112.3(5)
N7	S1	C31	117.3(3)	C7	C6	C5	113.4(7)
N7	S1	C32	112.2(3)	N2	C8	C9	111.8(5)
N7	S1	C33	112.3(3)	C10	C9	C8	115.2(6)
C31	S1	K1	138.5(2)	C11	C10	C9	110.9(8)
C31	S1	K1^{1}	143.2(3)	N3	C12	P2	123.4(4)
C32	S1	K1^{1}	64.8(2)	C13	C12	P2	131.0(3)
C32	S1	K1	116.7(2)	C13	C12	N3	105.1(4)
C32	S1	C31	104.8(3)	N4	C13	P1	121.9(3)
C32	S1	C33	106.4(4)	C12	C13	P1	131.9(3)
C33	S1	K1	67.8(2)	C12	C13	N4	106.1(4)
C33	S1	K1^{1}	113.9(3)	N3	C14	K2	128.1(3)
C33	S1	C31	102.9(4)	N3	C14	N4	102.7(4)
K1^{1}	S2	K1	61.33(3)	N4	C14	K2	118.9(3)
N7	S2	K1^{1}	49.25(14)	N3	C15	C16	114.4(8)
N7	S2	K1	41.79(14)	C15	C16	C17	113.1(8)
N7	S2	C34	114.8(5)	C18	C17	C16	109.4(8)
N7	S2	C35	118.5(5)	N4	C19	C20	111.9(5)
N7	S2	C36	110.1(5)	C21	C20	C19	109.3(7)
N7	S2	C34S	111.7(5)	C20	C21	C22	111.9(10)
N7	S2	C35S	115.8(5)	N5	C23	C24	114.2(5)
N7	S2	C36S	112.1(5)	N5	C25	C26	113.7(4)
C34	S2	K1^{1}	75.2(6)	N6	C27	C28	115.3(5)
C34	S2	K1	134.9(6)	N6	C29	C30	113.5(5)
C34	S2	C35	105.1(7)	S1	C32	K1^{1}	85.9(2)
C34	S2	C36	104.2(8)	S1	C33	K1	81.5(2)
C35	S2	K1	120.0(6)	S3	C37	K2	85.6(4)
C35	S2	K1^{1}	162.6(6)	S4	C42	K2	77.7(5)
C35	S2	C36	102.5(8)	S4	C42S	K2	89.2(5)
C36	S2	K1^{1}	94.2(6)	C16S	C15S	N3	118.3(19)
C36	S2	K1	69.4(5)	C17S	C16S	C15S	103.9(17)
C34S	S2	K1	147.4(5)	C16S	C17S	C18	93.2(14)
C34S	S2	K1^{1}	87.1(6)				

13.7. Crystal data and structure refinement for 19 (NRN-174).

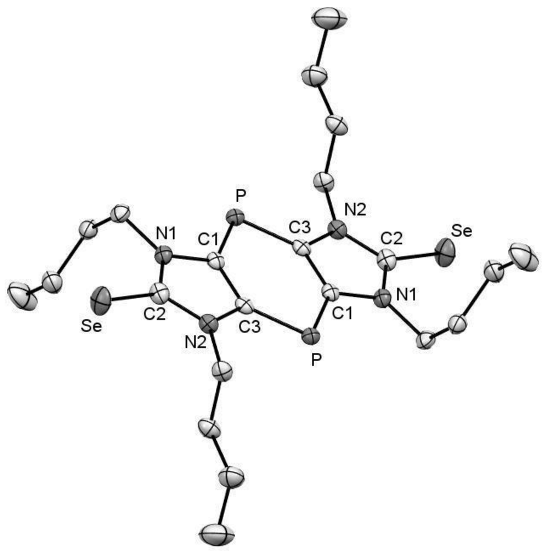

Table 13.19. Crystal data and structure refinement for **19**.

Identification code	GSTR687// GXray6186f
Crystal Habitus	clear red needle
Device Type	Bruker X8-KappaApexII
Empirical formula	$C_{22}H_{36}N_4P_2Se_2$
Moiety formula	2(C11 H18 N2 P Se)
Formula weight	576.41
Temperature/K	100
Crystal system	monoclinic
Space group	$P2_1/n$
a/Å	9.5787(5)
b/Å	24.9549(12)
c/Å	12.3331(6)
α/°	90
β/°	96.935(2)
γ/°	90
Volume/Å^3	2926.5(3)
Z	4
ρ_{calc}g/cm^3	1.308
μ/mm^{-1}	2.651
F(000)	1176.0
Crystal size/mm^3	0.3 × 0.1 × 0.06
Absorption correction	Empirical

Tmin; Tmax	0.4726; 0.7460
Radiation	MoKα (λ = 0.71073)
2Θ range for data collection/°	4.662 to 56°
Completeness to theta	0.998
Index ranges	-12 ≤ h ≤ 12, -32 ≤ k ≤ 32, -16 ≤ l ≤ 16
Reflections collected	53791
Independent reflections	7062 [R_{int} = 0.0582, R_{sigma} = 0.0358]
Data/restraints/parameters	7062/0/275
Goodness-of-fit on F^2	1.014
Final R indexes [I>=2σ (I)]	R_1 = 0.0314, wR_2 = 0.0707
Final R indexes [all data]	R_1 = 0.0472, wR_2 = 0.0758
Largest diff. peak/hole / e $Å^{-3}$	0.54/-0.40

Table 13.20. Bond Lengths for **19**.

Atom	**Atom**	**Length/Å**	**Atom**	**Atom**	**Length/Å**
Se	C2	1.829(2)	Se'	C2'	1.829(2)
P	C1	1.744(2)	P'	C1'	1.744(2)
P	$C3^1$	1.742(2)	P'	$C3'^2$	1.746(2)
N1	C1	1.397(3)	N1'	C1'	1.395(3)
N1	C2	1.366(3)	N1'	C2'	1.364(3)
N1	C4	1.462(3)	N1'	C4'	1.470(3)
N2	C2	1.362(3)	N2'	C2'	1.362(3)
N2	C3	1.395(3)	N2'	C3'	1.394(3)
N2	C8	1.466(3)	N2'	C8'	1.465(3)
C1	C3	1.408(3)	C1'	C3'	1.401(3)
C3	P^1	1.742(2)	C3'	P'^2	1.746(2)
C4	C5	1.527(3)	C4'	C5'	1.529(3)
C5	C6	1.514(3)	C5'	C6'	1.518(4)
C6	C7	1.523(4)	C6'	C7'	1.526(3)
C8	C9	1.518(3)	C8'	C9'	1.524(3)
C9	C10	1.517(3)	C9'	C10'	1.487(4)
C10	C11	1.519(4)	C10'	C11'	1.526(4)

^{1}2-X,1-Y,1-Z; ^{2}1-X,1-Y,1-Z

Table 13.21. Bond Angles for **19**.

Atom	**Atom**	**Atom**	**Angle/°**	**Atom**	**Atom**	**Atom**	**Angle/°**
$C3^1$	P	C1	96.92(10)	C1'	P'	$C3'^2$	96.93(10)
C1	N1	C4	123.96(18)	C1'	N1'	C4'	123.99(18)
C2	N1	C1	110.47(18)	C2'	N1'	C1'	110.97(18)
C2	N1	C4	125.57(18)	C2'	N1'	C4'	124.88(19)

C2	N2	C3	111.13(18)	C2'	N2'	C3'	111.12(18)
C2	N2	C8	125.40(18)	C2'	N2'	C8'	125.14(19)
C3	N2	C8	123.42(18)	C3'	N2'	C8'	123.43(18)
N1	C1	P	122.26(16)	N1'	C1'	P'	122.91(16)
N1	C1	C3	106.39(18)	N1'	C1'	C3'	106.10(19)
C3	C1	P	131.35(17)	C3'	C1'	P'	130.99(17)
N1	C2	Se	127.11(17)	N1'	C2'	Se'	128.04(17)
N2	C2	Se	126.64(17)	N2'	C2'	Se'	126.19(17)
N2	C2	N1	106.20(18)	N2'	C2'	N1'	105.75(19)
N2	C3	P^1	122.47(16)	N2'	C3'	P'^2	121.87(16)
N2	C3	C1	105.79(18)	N2'	C3'	C1'	106.05(18)
C1	C3	P^1	131.73(16)	C1'	C3'	P'^2	132.08(17)
N1	C4	C5	112.92(18)	N1'	C4'	C5'	112.17(18)
C6	C5	C4	114.3(2)	C6'	C5'	C4'	114.7(2)
C5	C6	C7	111.6(2)	C5'	C6'	C7'	112.2(2)
N2	C8	C9	111.94(18)	N2'	C8'	C9'	110.75(18)
C10	C9	C8	112.0(2)	C10'	C9'	C8'	114.1(2)
C9	C10	C11	112.4(2)	C9'	C10'	C11'	111.8(3)

^{1}2-X,1-Y,1-Z; ^{2}1-X,1-Y,1-Z

13.8. Crystal data and structure refinement for 20 (NRN-272).

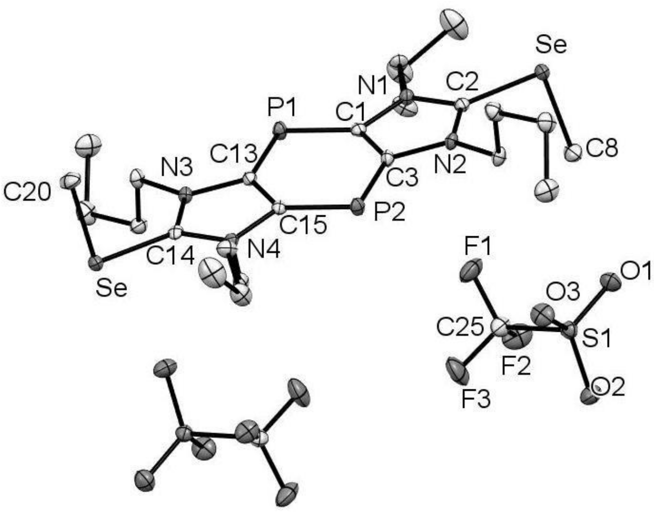

Table 13.21. Crystal data and structure refinement for **20**.

Identification code	GSTR674// GXray6000f
Crystal Habitus	clear light yellow block
Device Type	Bruker X8-KappaApexII
Empirical formula	$C_{26}H_{42}F_6N_4O_6P_2S_2Se_2$
Moiety formula	C24 H42 N4 P2 Se2, 2(C F3 O3 S)
Formula weight	904.61
Temperature/K	100
Crystal system	Orthorhombic
Space group	$Pca2_1$
a/Å	16.4677(7)
b/Å	9.3211(4)
c/Å	23.9930(9)
α/°	90
β/°	90
γ/°	90
Volume/Å^3	3682.9(3)
Z	4
ρ_{calc}g/cm^3	1.632
μ/mm^{-1}	2.282
F(000)	1832.0
Crystal size/mm^3	0.16 × 0.14 × 0.09
Absorption correction	Empirical
Tmin; Tmax	0.5453; 0.7461
Radiation	MoKα (λ = 0.71073)
2Θ range for data collection/°	1.698 to 56°
Completeness to theta	0.999
Index ranges	$-21 \leq h \leq 21$, $-12 \leq k \leq 12$, $-31 \leq l \leq 31$
Reflections collected	32863
Independent reflections	8876 [R_{int} = 0.0507, R_{sigma} = 0.0464]
Data/restraints/parameters	8876/1/440
Goodness-of-fit on F^2	1.028
Final R indexes [I>=2σ (I)]	R_1 = 0.0298, wR_2 = 0.0611
Final R indexes [all data]	R_1 = 0.0358, wR_2 = 0.0632
Largest diff. peak/hole / e Å^{-3}	0.59/-0.33
Flack parameter	0.003(4)

Table 13.22. Bond Lengths for **20**.

Atom	Atom	Length/Å	Atom	Atom	Length/Å
Se1	C2	1.896(4)	C9	C10	1.504(6)
Se1	C8	1.952(4)	C10	C11	1.518(7)
Se2	C14	1.896(4)	C11	C12	1.536(7)
Se2	C20	1.965(4)	C13	C15	1.407(6)
P1	C1	1.744(4)	C16	C17	1.522(6)
P1	C13	1.747(4)	C17	C18	1.519(6)
P2	C3	1.736(4)	C18	C19	1.529(7)
P2	C15	1.744(4)	C21	C22	1.515(6)
N1	C1	1.400(5)	C22	C23	1.533(6)
N1	C2	1.343(5)	C23	C24	1.522(6)
N1	C4	1.476(5)	S1	O1	1.441(3)
N2	C2	1.339(5)	S1	O2	1.448(3)
N2	C3	1.397(5)	S1	O3	1.443(3)
N2	C9	1.478(5)	S1	C25	1.828(5)
N3	C13	1.394(5)	F1	C25	1.338(5)
N3	C14	1.338(5)	F2	C25	1.335(5)
N3	C16	1.476(5)	F3	C25	1.336(5)
N4	C14	1.341(5)	S2	O4	1.433(3)
N4	C15	1.397(5)	S2	O5	1.446(3)
N4	C21	1.478(5)	S2	O6	1.444(3)
C1	C3	1.412(6)	S2	C26	1.829(5)
C4	C5	1.520(6)	F4	C26	1.321(5)
C5	C6	1.529(6)	F5	C26	1.345(5)
C6	C7	1.519(6)	F6	C26	1.340(5)

Table 13.23. Bond Angles for **20**.

Atom	Atom	Atom	Angle/°	Atom	Atom	Atom	Angle/°
C2	Se1	C8	94.78(18)	N3	C14	N4	108.7(3)
C14	Se2	C20	93.70(18)	N4	C14	Se2	125.1(3)
C1	P1	C13	96.3(2)	N4	C15	P2	122.0(3)
C3	P2	C15	96.3(2)	N4	C15	C13	105.8(3)
C1	N1	C4	125.0(3)	C13	C15	P2	132.2(3)
C2	N1	C1	109.5(3)	N3	C16	C17	110.8(3)
C2	N1	C4	125.4(3)	C18	C17	C16	112.1(4)
C2	N2	C3	109.8(3)	C17	C18	C19	114.0(4)
C2	N2	C9	125.7(3)	N4	C21	C22	114.0(3)
C3	N2	C9	124.3(3)	C21	C22	C23	109.6(4)
C13	N3	C16	124.7(3)	C24	C23	C22	112.9(4)
C14	N3	C13	109.6(4)	O1	S1	O2	115.2(2)
C14	N3	C16	125.5(3)	O1	S1	O3	114.66(19)

C14	N4	C15	109.6(3)	O1	S1	C25	102.9(2)
C14	N4	C21	125.2(3)	O2	S1	C25	102.2(2)
C15	N4	C21	125.1(3)	O3	S1	O2	115.78(19)
N1	C1	P1	122.2(3)	O3	S1	C25	103.5(2)
N1	C1	C3	106.0(3)	F1	C25	S1	112.1(3)
C3	C1	P1	131.9(3)	F2	C25	S1	111.6(3)
N1	C2	Se1	125.8(3)	F2	C25	F1	106.9(4)
N2	C2	Se1	125.3(3)	F2	C25	F3	107.8(4)
N2	C2	N1	108.8(3)	F3	C25	S1	110.8(3)
N2	C3	P2	122.2(3)	F3	C25	F1	107.4(4)
N2	C3	C1	105.9(3)	O4	S2	O5	115.1(2)
C1	C3	P2	131.9(3)	O4	S2	O6	115.62(19)
N1	C4	C5	111.7(3)	O4	S2	C26	103.9(2)
C4	C5	C6	112.6(4)	O5	S2	C26	102.9(2)
C7	C6	C5	113.7(4)	O6	S2	O5	114.9(2)
N2	C9	C10	111.7(3)	O6	S2	C26	101.8(2)
C9	C10	C11	112.8(4)	F4	C26	S2	112.0(3)
C10	C11	C12	113.5(4)	F4	C26	F5	108.5(4)
N3	C13	P1	122.4(3)	F4	C26	F6	107.5(4)
N3	C13	C15	106.3(4)	F5	C26	S2	111.5(3)
C15	C13	P1	131.4(3)	F6	C26	S2	111.3(3)
N3	C14	Se2	126.0(3)	F6	C26	F5	105.6(4)

13.9. Crystal data and structure refinement for 28

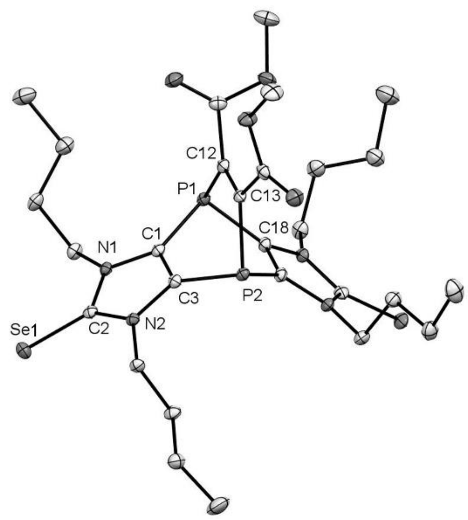

Table 13.25. Crystal data and structure refinement for **28**.

Identification code	GSTR685// GXray6160f
Crystal Habitus	clear red plank
Device Type	Bruker X8-KappaApexII
Empirical formula	$C_{29}H_{44}Cl_2N_4O_4P_2Se_2$
Moiety formula	C28 H42 N4 O4 P2 Se2, C H2 Cl2
Formula weight	803.44
Temperature/K	100
Crystal system	Triclinic
Space group	P-1
a/Å	11.8997(7)
b/Å	13.7366(9)
c/Å	13.7807(9)
α/°	61.210(2)
β/°	86.919(2)
γ/°	66.678(2)
Volume/Å^3	1786.4(2)
Z	2
ρ_{calc}g/cm^3	1.494
μ/mm^{-1}	2.347
F(000)	820.0
Crystal size/mm^3	0.24 × 0.12 × 0.1
Absorption correction	Empirical
Tmin; Tmax	0.5177; 0.7461
Radiation	MoKα (λ = 0.71073)
2Θ range for data collection/°	4.426 to 56°
Completeness to theta	0.998
Index ranges	-15 ≤ h ≤ 15, -18 ≤ k ≤ 18, -18 ≤ l ≤ 18
Reflections collected	66903
Independent reflections	8617 [R_{int} = 0.0483, R_{sigma} = 0.0272]
Data/restraints/parameters	8617/6/394
Goodness-of-fit on F^2	1.026
Final R indexes [I>=2σ (I)]	R_1 = 0.0263, wR_2 = 0.0608
Final R indexes [all data]	R_1 = 0.0355, wR_2 = 0.0647
Largest diff. peak/hole / e Å^{-3}	0.62/-0.69

Table 13.26. Bond Lengths for **28**

Atom	Atom	Length/Å	Atom	Atom	Length/Å
Se1	C2	1.8453(18)	N4	C19	1.366(2)
Se2	C19	1.8453(17)	N4	C20	1.383(2)
P1	C1	1.8181(18)	N4	C25	1.466(2)

P1	C12	1.8903(18)	C1	C3	1.351(2)
P1	C18	1.8225(18)	C4	C5	1.526(2)
P2	C3	1.8247(18)	C5	C6	1.518(3)
P2	C13	1.8707(18)	C6	C7	1.530(3)
P2	C20	1.8356(17)	C8	C9	1.521(2)
O1	C14	1.332(2)	C9	C10	1.522(2)
O1	C15	1.454(2)	C10	C11	1.522(3)
O2	C14	1.201(2)	C12	C13	1.335(2)
O3	C16	1.330(2)	C12	C14	1.498(2)
O3	C17	1.449(2)	C13	C16	1.494(2)
O4	C16	1.205(2)	C18	C20	1.351(2)
N1	C1	1.384(2)	C21	C22	1.522(3)
N1	C2	1.366(2)	C22	C23	1.521(3)
N1	C4	1.469(2)	C23	C24	1.520(3)
N2	C2	1.356(2)	C25	C26	1.521(3)
N2	C3	1.384(2)	C26	C27	1.523(3)
N2	C8	1.461(2)	C27	C28	1.520(3)
N3	C18	1.387(2)	Cl1	C29	1.757(2)
N3	C19	1.365(2)	Cl2	C29	1.764(2)
N3	C21	1.462(2)			

Table 13.27. Bond Angles for **28**.

Atom	**Atom**	**Atom**	**Angle/°**	**Atom**	**Atom**	**Atom**	**Angle/°**
C1	P1	C12	93.14(8)	N2	C8	C9	111.03(14)
C1	P1	C18	94.69(8)	C8	C9	C10	110.68(14)
C18	P1	C12	93.27(8)	C9	C10	C11	112.67(16)
C3	P2	C13	94.00(8)	C13	C12	P1	122.14(14)
C3	P2	C20	93.20(8)	C13	C12	C14	124.48(16)
C20	P2	C13	92.68(8)	C14	C12	P1	113.38(12)
C14	O1	C15	115.15(16)	C12	C13	P2	122.26(13)
C16	O3	C17	115.27(15)	C12	C13	C16	124.22(16)
C1	N1	C4	126.12(14)	C16	C13	P2	113.21(12)
C2	N1	C1	109.07(14)	O1	C14	C12	111.14(15)
C2	N1	C4	124.28(15)	O2	C14	O1	125.72(17)
C2	N2	C3	109.66(14)	O2	C14	C12	123.06(17)
C2	N2	C8	125.27(15)	O3	C16	C13	112.75(15)
C3	N2	C8	124.47(14)	O4	C16	O3	124.80(17)
C18	N3	C21	124.70(15)	O4	C16	C13	122.42(16)
C19	N3	C18	109.29(14)	N3	C18	P1	129.76(13)

C19	N3	C21	126.01(15)	C20	C18	P1	122.67(13)
C19	N4	C20	109.61(14)	C20	C18	N3	107.57(15)
C19	N4	C25	125.24(15)	N3	C19	Se2	127.00(13)
C20	N4	C25	124.55(14)	N3	C19	N4	106.15(14)
N1	C1	P1	129.85(13)	N4	C19	Se2	126.85(13)
C3	C1	P1	122.29(14)	N4	C20	P2	129.43(13)
C3	C1	N1	107.64(15)	C18	C20	P2	123.19(13)
N1	C2	Se1	126.53(13)	C18	C20	N4	107.37(15)
N2	C2	Se1	126.99(13)	N3	C21	C22	111.69(15)
N2	C2	N1	106.43(15)	C23	C22	C21	114.14(16)
N2	C3	P2	128.83(13)	C24	C23	C22	111.93(19)
C1	C3	P2	123.88(13)	N4	C25	C26	110.26(14)
C1	C3	N2	107.19(15)	C25	C26	C27	113.43(16)
N1	C4	C5	114.83(14)	C28	C27	C26	111.27(17)
C6	C5	C4	114.30(16)	Cl1	C29	Cl2	111.33(12)
C5	C6	C7	112.93(17)				

13.10. Crystal data and structure refinement for 30

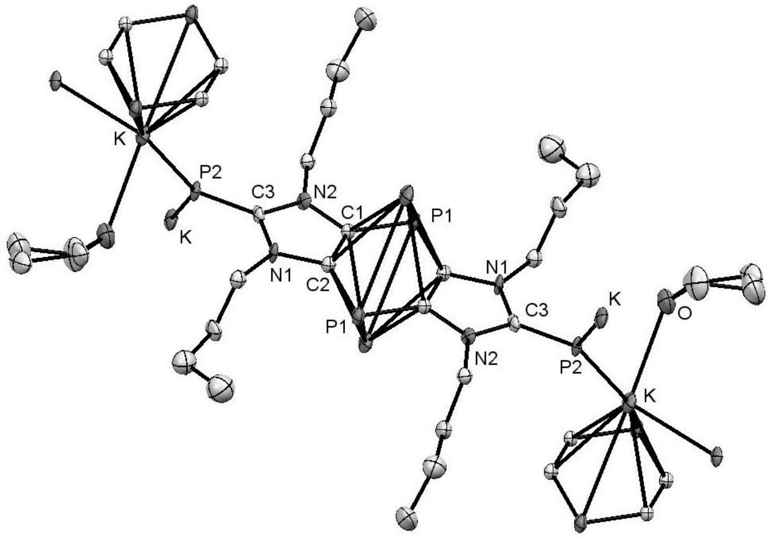

Table 3.28. Crystal data and structure refinement for **30**.

Identification code	GSTR690// GXray6218f_pl
Crystal Habitus	clear dark red block
Device Type	Bruker X8-KappaApexII
Empirical formula	$C_{15}H_{26}KN_2OPS$
Moiety formula	C15 H26 K N2 O P S
Formula weight	352.51
Temperature/K	100
Crystal system	monoclinic
Space group	$P2_1/c$
a/Å	14.195(5)
b/Å	15.726(6)
c/Å	8.514(3)
α/°	90
β/°	97.619(10)
γ/°	90
Volume/Å^3	1883.8(12)
Z	4
ρ_{calc}g/cm^3	1.243
μ/mm^{-1}	0.478
F(000)	752.0
Crystal size/mm^3	0.25 × 0.24 × 0.22
Absorption correction	Empirical
Tmin; Tmax	0.4084; 0.7459
Radiation	MoKα (λ = 0.71073)
2Θ range for data collection/°	5.18 to 55.994°
Completeness to theta	0.996
Index ranges	-18 ≤ h ≤ 18, -20 ≤ k ≤ 20, -11 ≤ l ≤ 11
Reflections collected	23270
Independent reflections	4503 [R_{int} = 0.1778, R_{sigma} = 0.1633]
Data/restraints/parameters	4503/1/192
Goodness-of-fit on F^2	1.044
Final R indexes [I>=2σ (I)]	R_1 = 0.1147, wR_2 = 0.2952
Final R indexes [all data]	R_1 = 0.2048, wR_2 = 0.3512
Largest diff. peak/hole / e Å^{-3}	0.63/-1.08

Table 13.29. Bond Lengths for **30**.

Atom	Atom	Length/Å	Atom	Atom	Length/Å
K	S	3.190(2)	N1	C4	1.461(8)
K	S^1	3.242(3)	N2	C2	1.358(8)
K	P^2	3.327(3)	N2	C3	1.408(8)

K	P[3]	3.423(3)	N2	C8	1.457(9)
K	O	2.751(7)	C1	K[5]	3.160(6)
K	C1[3]	3.160(6)	C1	K[2]	3.103(7)
K	C1[2]	3.103(7)	C1	C3	1.376(10)
K	C3[2]	3.161(8)	C3	K[2]	3.161(7)
K	C3[3]	3.120(7)	C3	K[5]	3.120(7)
K	C12	3.459(14)	C3	P[6]	1.836(7)
S	K[4]	3.242(3)	C4	C5	1.518(11)
S	C2	1.715(7)	C5	C6	1.538(11)
P	K[5]	3.423(3)	C6	C7	1.506(15)
P	K[2]	3.327(3)	C8	C9	1.508(11)
P	C1	1.815(8)	C9	C10	1.546(12)
P	C3[6]	1.836(7)	C10	C11	1.455(15)
O	C12	1.401(13)	C12	C13	1.474(9)
O	C15	1.421(10)	C13	C14	1.467(16)
N1	C1	1.422(8)	C14	C15	1.534(13)
N1	C2	1.345(9)			

[1]+X,3/2-Y,1/2+Z; [2]-X,1-Y,1-Z; [3]+X,+Y,1+Z; [4]+X,3/2-Y,-1/2+Z; [5]+X,+Y,-1+Z; [6]-X,1-Y,-Z

Table 13.30. Bond Angles for **30**.

Atom	**Atom**	**Atom**	**Angle/°**	**Atom**	**Atom**	**Atom**	**Angle/°**
S	K	S[1]	89.31(5)	C1	P	K[2]	66.9(2)
S[1]	K	P[2]	89.29(7)	C1	P	K[5]	66.2(2)
S	K	P[3]	152.03(7)	C1	P	C3[6]	93.0(3)
S	K	P[2]	114.31(7)	C3[6]	P	K[5]	66.1(2)
S[1]	K	P[3]	118.63(7)	C3[6]	P	K[2]	67.4(2)
S	K	C12	70.66(19)	C12	O	K	108.4(7)
S[1]	K	C12	84.5(2)	C12	O	C15	109.3(8)
P[2]	K	P[3]	70.36(6)	C15	O	K	130.0(6)
P[2]	K	C12	172.1(2)	C1	N1	C4	122.7(6)
P[3]	K	C12	108.4(2)	C2	N1	C1	111.6(6)
O	K	S	83.06(14)	C2	N1	C4	125.7(5)
O	K	S[1]	103.72(15)	C2	N2	C3	110.0(6)
O	K	P[2]	158.72(15)	C2	N2	C8	125.2(6)
O	K	P[3]	88.54(15)	C3	N2	C8	124.8(5)
O	K	C1[3]	108.63(19)	K[2]	C1	K[5]	123.50(19)
O	K	C1[2]	130.2(2)	P	C1	K[5]	82.2(2)
O	K	C3[2]	106.2(2)	P	C1	K[2]	80.5(3)
O	K	C3[3]	133.06(19)	N1	C1	K[5]	116.8(4)

O	K	C12	22.6(3)	N1	C1	K^{2}	118.3(4)
$C1^{2}$	K	S^{1}	121.54(15)	N1	C1	P	120.6(5)
$C1^{3}$	K	S	168.18(14)	C3	C1	K^{5}	75.7(4)
$C1^{2}$	K	S	114.76(12)	C3	C1	K^{2}	79.7(4)
$C1^{3}$	K	S^{1}	89.56(14)	C3	C1	P	134.7(5)
$C1^{3}$	K	P^{3}	31.68(14)	C3	C1	N1	104.6(6)
$C1^{2}$	K	P^{3}	53.35(13)	N1	C2	S	127.1(5)
$C1^{2}$	K	P^{2}	32.55(14)	N1	C2	N2	106.2(5)
$C1^{3}$	K	P^{2}	53.90(13)	N2	C2	S	126.7(5)
$C1^{2}$	K	$C1^{3}$	56.50(19)	K^{5}	C3	K^{2}	122.9(2)
$C1^{2}$	K	$C3^{2}$	25.36(18)	P^{6}	C3	K^{2}	81.9(3)
$C1^{3}$	K	$C3^{2}$	49.51(17)	P^{6}	C3	K^{5}	79.8(2)
$C1^{2}$	K	$C3^{3}$	50.35(17)	N2	C3	K^{2}	119.8(4)
$C1^{2}$	K	C12	152.4(3)	N2	C3	K^{5}	116.2(4)
$C1^{3}$	K	C12	120.9(2)	N2	C3	P^{6}	120.1(5)
$C3^{3}$	K	S	143.50(15)	C1	C3	K^{5}	79.0(4)
$C3^{2}$	K	S	126.60(13)	C1	C3	K^{2}	75.0(4)
$C3^{2}$	K	S^{1}	135.19(14)	C1	C3	P^{6}	132.3(5)
$C3^{3}$	K	S^{1}	78.10(14)	C1	C3	N2	107.6(5)
$C3^{2}$	K	P^{2}	54.01(14)	N1	C4	C5	110.9(6)
$C3^{3}$	K	P^{2}	32.89(13)	C4	C5	C6	112.0(7)
$C3^{2}$	K	P^{3}	32.06(12)	C7	C6	C5	114.4(7)
$C3^{3}$	K	P^{3}	53.35(14)	N2	C8	C9	112.6(6)
$C3^{3}$	K	$C1^{3}$	25.31(18)	C8	C9	C10	110.8(7)
$C3^{3}$	K	$C3^{2}$	57.1(2)	C11	C10	C9	115.8(10)
$C3^{2}$	K	C12	128.8(3)	O	C12	K	49.0(5)
$C3^{3}$	K	C12	140.1(2)	O	C12	C13	107.4(10)
K	S	K^{4}	141.01(7)	C13	C12	K	124.2(10)
C2	S	K^{4}	104.6(2)	C14	C13	C12	106.4(10)
C2	S	K	114.3(2)	C13	C14	C15	105.9(8)
K^{2}	P	K^{5}	109.64(6)	O	C15	C14	104.4(8)

[1]+X,3/2-Y,1/2+Z; [2]-X,1-Y,1-Z; [3]+X,+Y,1+Z; [4]+X,3/2-Y,-1/2+Z; [5]+X,+Y,-1+Z; [6]-X,1-Y,-Z

Table 13.31. Torsion Angles for **30**.

A	**B**	**C**	**D**	**Angle/°**	**A**	**B**	**C**	**D**	**Angle/°**
K	S	C2	N1	-62.4(7)	C2	N1	C1	P	177.5(5)
K^{1}	S	C2	N1	119.5(6)	C2	N1	C1	C3	-0.6(8)
K^{1}	S	C2	N2	-58.8(7)	C2	N1	C4	C5	-92.2(8)
K	S	C2	N2	119.3(6)	C2	N2	C3	K^{2}	-86.0(6)
K^{2}	P	C1	K^{3}	126.00(15)	C2	N2	C3	K^{3}	82.6(6)

K^{3}	P	C1	K^{2}	-126.00(15)	C2	N2	C3	P^{4}	-179.2(5)
K^{3}	P	C1	N1	117.4(6)	C2	N2	C3	C1	0.2(8)
K^{2}	P	C1	N1	-116.6(6)	C2	N2	C8	C9	-100.2(8)
K^{3}	P	C1	C3	-65.1(7)	$C3^{4}$	P	C1	K^{3}	63.8(2)
K^{2}	P	C1	C3	60.9(7)	$C3^{4}$	P	C1	K^{2}	-62.2(3)
K	O	C12	C13	120.6(11)	$C3^{4}$	P	C1	N1	-178.8(6)
K	O	C15	C14	-111.6(8)	$C3^{4}$	P	C1	C3	-1.3(9)
K^{3}	C1	C3	K^{2}	-128.71(16)	C3	N2	C2	S	178.0(5)
K^{2}	C1	C3	K^{3}	128.71(16)	C3	N2	C2	N1	-0.5(8)
K^{3}	C1	C3	P^{4}	-63.7(6)	C3	N2	C8	C9	79.5(8)
K^{2}	C1	C3	P^{4}	65.0(6)	C4	N1	C1	K^{2}	-100.1(6)
K^{3}	C1	C3	N2	117.1(5)	C4	N1	C1	K^{3}	92.7(7)
K^{2}	C1	C3	N2	-114.2(5)	C4	N1	C1	P	-3.1(9)
K	C12	C13	C14	67.0(16)	C4	N1	C1	C3	178.7(6)
P	C1	C3	K^{3}	65.5(7)	C4	N1	C2	S	2.8(11)
P	C1	C3	K^{2}	-63.3(7)	C4	N1	C2	N2	-178.6(6)
P	C1	C3	P^{4}	1.8(12)	C4	C5	C6	C7	70.8(10)
P	C1	C3	N2	-177.5(6)	C8	N2	C2	S	-2.2(10)
O	C12	C13	C14	15.1(18)	C8	N2	C2	N1	179.2(6)
N1	C1	C3	K^{2}	114.5(5)	C8	N2	C3	K^{2}	94.3(7)
N1	C1	C3	K^{3}	-116.8(5)	C8	N2	C3	K^{3}	-97.2(7)
N1	C1	C3	P^{4}	179.5(6)	C8	N2	C3	P^{4}	1.1(9)
N1	C1	C3	N2	0.2(7)	C8	N2	C3	C1	-179.5(6)
N1	C4	C5	C6	-170.5(6)	C8	C9	C10	C11	170.8(9)
N2	C8	C9	C10	-172.3(6)	C12	O	C15	C14	25.3(11)
C1	N1	C2	S	-177.9(5)	C12	C13	C14	C15	0.2(17)
C1	N1	C2	N2	0.7(8)	C13	C14	C15	O	-15.1(13)
C1	N1	C4	C5	88.5(8)	C15	O	C12	K	-146.5(8)
C2	N1	C1	K^{2}	80.5(6)	C15	O	C12	C13	-26.0(15)
C2	N1	C1	K^{3}	-86.6(6)					

^{1}+X,3/2-Y,-1/2+Z; ^{2}+X,+Y,-1+Z; ^{3}-X,1-Y,1-Z; ^{4}-X,1-Y,-Z